이학박사 학위논문

New Olefin Metathesis Polymerizations for Cycloalkene-based Monomers: Cascade and Multiple Olefin Metathesis Polymerizations

시클로 알켄을 포함하는 단량체를 이용한 새로운 올레핀 복분해 고분자 중합법의 개발

2018년 8월

서울대학교 대학원

화학부 유기화학 전공

이 호 근

Abstract

The focus of the research presented in this thesis is a development of new olefin metathesis polymerization methodologies and their polymer synthesis of the precise and well-controlled microstructure using monomer which has cycloalkene moieties.

A brief overview of metathesis, as well as metathesis polymerization, is discussed in introductory Chapter 1.

Chapter 2 describes cascade ring-opening/ring-closing metathesis (RO/RCM) polymerization of monomers containing two cycloalkenes. Cascade metathesis polymerization is a more advanced metathesis polymerization system. Previously, most examples of metathesis polymerization methodologies rely on just one of the three types of olefin metathesis reactions to make simple polymer structures. In order to synthesize well-defined polymers with complex microstructures, cascade polymerization, where more than two types of olefin metathesis transformations were combined in one-shot or one-pot, was successfully developed analogous to cascade reactions in organic synthesis.

Chapter 3 describes the unusual superior activity of the first generation Grubbs catalyst in cascade olefin metathesis polymerization. It is about unique Grubbs catalyst selectivity for the cascade polymerization. The cascade ring-opening/ring-closing metathesis polymerization of monomers containing two cyclopentene moieties using the first-generation Grubbs catalyst to give well-defined polymers containing new rings via a rearrangement reaction. Normally, more reactive catalyst gave better polymerization results in polymer synthesis. However, one surprising and puzzling feature was that the intrinsically less active the first-generation Grubbs catalyst outperformed than more active the third-generation Grubbs catalyst which should be generally more active.

Chapter 4 describes multiple olefin metathesis polymerization which produced well-

defined A,B-alternating copolymers using the same monomers. This is the first example of metathesis polymerization that all three types of olefin metathesis trans-formations (ring-opening, ring-closing, and cross metathesis) were combined in an orderly manner to produce just one uniform polymer microstructure via precisely controlled pathways.

Finally, the Last Chapter describes sequence controlled olefin metathesis Polymerization. Using alkyne selectivity of the third-generation Grubbs catalyst, unique monomer structure which contains alkyne and two cycloalkene moiety could be polymerized to sequence controlled polymer following cascade manner.

Table of contents

Chapter 1. Introduction to Olefin Metathesis and Metathesis Polymerization……..……1

Olefin Metathesis and Metathesis Polymerization…….……...2

Thesis Research……..…….....9

References……..…….....10

Chapter 2. Cascade Ring-Opening/Ring-Closing Metathesis Polymerization……16

Abstract……...17

Introduction…….....18

Results and Discussion……...20

Conclusion…….....40

Experimental section...……...41

References……102

Chapter 3. Unusual Superior Activity of the First Generation Grubbs Catalyst in Cascade Olefin Metathesis Polymerization…..……..…106

Abstract…….....……...107

Introduction…….....107

Results and Discussion……..……...109

Conclusion…….……117

Experimental section.....…….....117

References……...……..138

Chapter 4. Multiple Olefin Metathesis Polymerization…….....145

Abstract……..……...146

Introduction……..….. …….....146

Results and Discussion……..……. .. ……..149

Conclusion…….……. . ……160

Experimental section…….……. …….160

References…….…….……. . ……...174

Chapter 5. Sequence Specific Olefin Metathesis Polymerization…..... . ……..177

Abstract…….……... . ……..178

Introduction.……..….. . ……..178

Result and Discussion……..……. . …….180

Conclusion…….……. . ……183

References…….....……. . ……...183

Chapter 1:

Introduction to Olefin Metathesis and Metathesis Polymerization

Olefin Metathesis and Metathesis polymerization

1.1 Olefin metathesis

Organic chemists could achieve various organic synthesis to make almost any molecule that can be drawn on a paper. The construction of these molecules occurs by making and breaking chemical bonds in discrete chemical reactions. In organic chemistry, the carbon-carbon double bond (C=C) is the basis for a large number of chemical transformations. In particular, metathesis using carbon double bonds is a very useful and powerful organic synthesis method. During the last two decades, this olefin metathesis reaction has been widely used as an efficient method to synthesize various molecules by forming new carbon–carbon double bonds.[1] Olefin metathesis transformation can be carried out by three main types metathesis: ring-opening metathesis (ROM)[2], ring-closing metathesis (RCM)[3], and cross metathesis (CM)[4]; these metathesis transformations have become versatile tools in organic synthesis. These processes are proceeded by a metal carbene catalyst as shown in Figure 1.1. Upon binding of an olefin to the metal carbene catalyst, formation of a metallocyclobutane occurs.

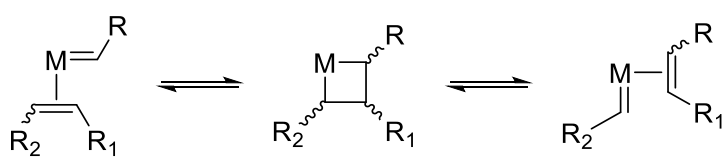

Figure 1.1. A simplified view of olefin metathesis reaction

This active species can form a new olefin and metal carbene or revert to the original olefin in a non-productive metathesis event. Many useful transformations can be carried out via olefin metathesis as depicted in **Figure 1.2.**

In detail, a diene molecule can go through a ring-closing metathesis (RCM) (**Figure 1.2)** A simplified view of olefin metathesis. a cyclic olefin, or, under conditions of very high concentration, may form a linear polymer through a process referred to as acyclic diene

metathesis polymerization (ADMET).[5] The driving force behind both RCM and ADMET is the loss of a small molecule, ethylene. In a process known as ring-opening metathesis polymerization (ROMP)[6], cyclic olefins can be transformed into high molecular weight linear polymer. In contrast to RCM and ADMET, ROMP is driven by the release of ring strain inherent in cyclic olefin monomers. It is important to realize that all of these transformations are reversible and are controlled by a thermodynamic equilibrium.

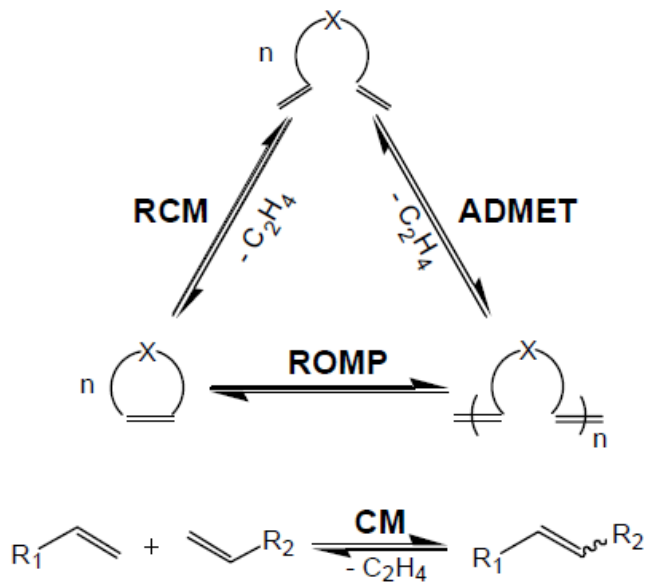

Figure 1.2. Chemical transformations by olefin metathesis

The utility of the olefin metathesis reaction was further broadened when organic chemists discovered tandem olefin metathesis reactions in which two or more olefin metathesis transformations occur simultaneously in a single step. This cascade reaction allowed chemists to efficiently synthesize various complex organic molecules.[7] Various examples of natural product total synthesis using this cascade reaction method as a key strategy for the formation of the core skeletons have been reported, demonstrating the versatility of these tandem olefin metathesis reactions.[8]

1.2 Olefin metathesis catalyst

Grubbs catalysts are series of Ru-based olefin metathesis catalysts. Before discussing these Ru-based Grubbs catalysts, let's look briefly at other olefin metathesis catalysts. Ill-defined traditional catalytic systems, for example, $WCl_6/BuSn_4$ or $WCl_6/CtAlCl_2$ and well-defined W, Mo, Ti- based alkylidenes are olefin metathesis catalyst using the early transition metal.[9] These catalysts had been developed and widely used because of their

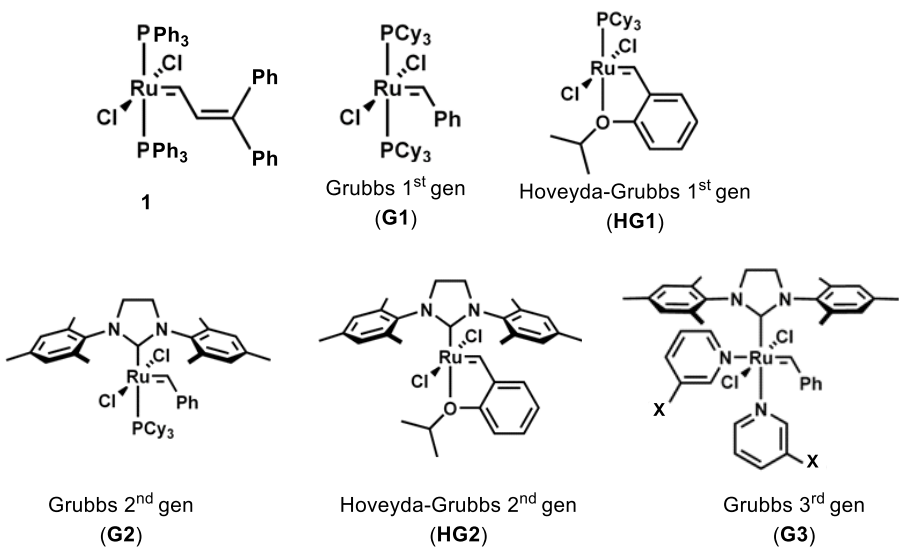

Figure 1.3. Ru-based Grubbs catalyst for the olefin metathesis reaction.

high activity and versatility that can be used variously. However, like double-edged swords, high reactivity caused high sensitivity. Thus, these catalysts are vulnerable to moisture, oxygen, and low functional group tolerance. Therefore, in spite of good reactivity, its use was limited in many cases. In contrast to these W- or Mo-based catalysts, Ru metal-based catalysts have inherent stability due to low oxophilicity, while at the same time, they have high reactivity and selectivity. Thus, the Ru-based olefin metathesis catalyst, Grubbs catalysts[10], could be used substantially in the synthesis of molecules and polymers of very

complex structures. The first Ru-based catalyst was $RuCl_2(PPh_3)_3$ and a diphenylcyclopropene which were developed by Grubbs. This catalyst was used for ROMP of norbornene and has the functional group tolerance for alcohol and water. It has more basic PCy_3 instead of PPh_3 to enhance the catalytic activity. Next, the Ru-based catalyst was alternative benzylidene catalyst, known as the first generation Grubbs catalyst (**G1**). It gave better initiation rate than previous diphenylvinyl derivative. To increase catalyst reactivity, *N*-heterocyclic carbene ligand was replaced PCy_3 ligand of **G1**. As a result, the second generation Grubbs catalyst (**G2**) was developed. More particularly, it was possible to modify to get the Hoveya-Grubbs catalyst (**HG2**), a phosphine-free catalyst, from **G2**. These catalysts are reusable and are resistant to heat due to isopropoxy groups. In the case of these catalysts with an NHC ligand, it was possible to increase the catalyst reactivity of the catalyst to be comparable to other early transition metal catalysts. This is possible with the strong sigma donor ability of NHC ligands over phosphine ligands. Thus, the utilization of Grubbs catalyst could be much broadened by the success of various difficult and challenging reactions.

1.3 Metathesis polymerization

Olefin metathesis polymerizations have led to a remarkable expansion of the field of synthetic polymer chemistry. the olefin metathesis reaction has been applied to various polymerizations such as ring-opening metathesis polymerization (ROMP), cyclopolymerization derived from RCM, and acyclic diene metathesis (ADMET) polymerization derived from CM. These polymerizations have produced various polymers, including both conjugated and nonconjugated polymers, and in some cases, living polymerization is also possible.

First, ring-opening metathesis polymerization (ROMP)[11] is achieved by using metathesis catalysts to synthesize polymers from cyclic olefins like cycloalkene. Since the relief of

ring strain is a major driving force of the polymerization, ROMP is most effective on strained cyclic olefins like cyclooctene and norbornenes. The highly strained cycloalkene monomers are excellent monomers for ROMP. So ring-strain free cyclohexene is very hard to polymerize any significant polymeric structure. In contrast to cyclohexne, norbornenes are most widely used monomers for ROMP, as a wide range of monomer functionalities are easily available through Diels-Alder reactions.

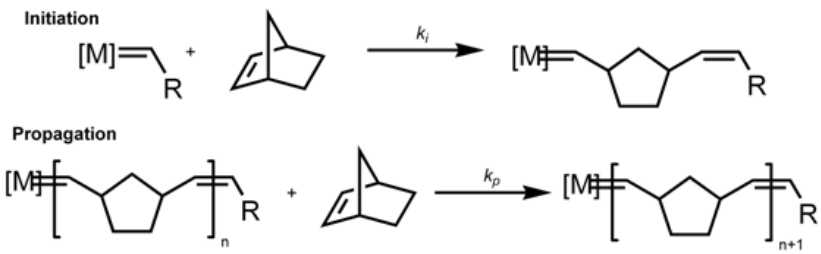

Figure 1.4 Ring-opening metathesis polymerization

To get the desired polymer structure using ROMP, the balance of catalyst, monomer, and other factors should be controlled carefully. When it comes to homogeneous catalysts, tungsten and molybdenum catalysts (Schrock catalysts) have very fast initiation rates. They are also able to produce living polymerizations with narrow polydispersity and chain tacticities, however, the low level of the functional group tolerance made limitations of the available monomers.[9] In contrast to tungsten and molybdenum catalyst, ruthenium-based metathesis catalysts[10] (Grubbs catalysts) tend to give slower initiation rates for the polymerization, leading to higher polydispersities. However, Ru-based catalysts have much better air stability and greater functional group tolerance than W- Mo- based catalyst. These features make them as a “user friendly” catalyst and are able to use for a wide range of functional monomers.

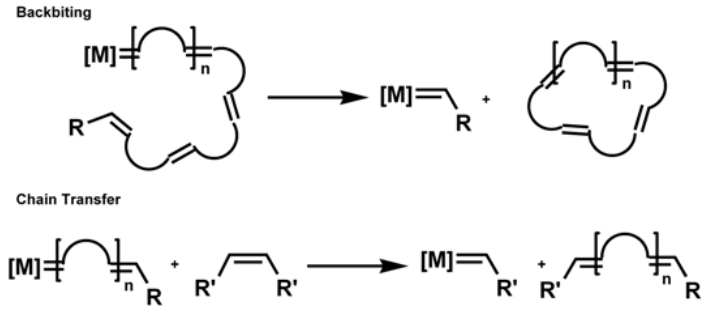

Figure1.5. Secondary metathesis reactions

Even though, secondary metathesis reactions also affect the product distribution as a side reaction. These are controlled by catalyst choice and reaction conditions. So if we control the catalyst type and appropriate reaction condition, these are avoidable. The first secondary metathesis reaction is backbiting, which is occurred by recoordination of an alkene on the growing polymer chain with the catalyst. This secondary metathesis reaction is able to lead to form a cyclic oligomer. Next secondary metathesis reaction is chain transfer between a growing polymer and an adjacent polymer alkene. Actually, this process is kind of cross metathesis. This also leads to broadened polymer molecular weights and polydispersity. The chain transfer can also be used to improve the process of the resulting polymer–addition of chain-transfer agent is able to make the limitation of chain molecular weights and introduction of terminal functional groups.

Next metathesis polymerization is cyclopolymerization(CP). Cyclopolymerization (CP) of diyne derivatives,[12] along with alkyne polymerization[13] via olefin metathesis reaction, is one of the most powerful and efficient methods for synthesizing conjugated polyenes. Initially, ill-defined catalysts, such as Ziegler-type,[14] $MoCl_5$, and WCl_6, were used.[9] Then, the development of homogeneous Schrock catalysts provided the first groundbreaking contribution to the understanding of the mechanism of CP and the structural information for the resulting conjugated polyenes.[15–19] Recently, the scope of CP was greatly expanded

with the development of Ru-based Grubbs catalysts and modified Grubbs catalysts because they were highly active, very user-friendly, and tolerant to air, moisture, and many functional groups.[20–24]

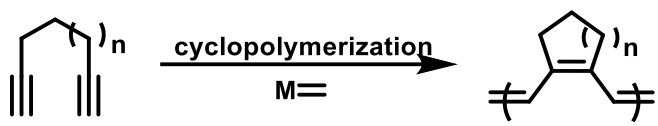

Scheme 1.1. Cyclopolymerization of Heptadiyne derivatives.

Final representative metathesis polymerization is Acyclic Diene Metathes is (ADMET)[26]. This polymerization is conducted by metathesis of terminal dienes to synthesize linear polymers and release ethylene. Since ADMET is kind of cross-metathesis, the process could be reversible, so ethylene must be released and removed from reaction to drive the complete polymerization. These polymers increased by step-growth kinetics, in contrast, to ROMP, which is increased by the chain propagation kinetics, so high-purity monomers are necessary definitely to get high MW polymer. These ADMET reactions are normally proceeded highly concentrated or neat condition, sometimes vacuum condition. both facilitating that drive the polymerization equilibrium and suppressing undesired cyclic oligomers formation by backbiting as a ring-closing metathesis mechanism.

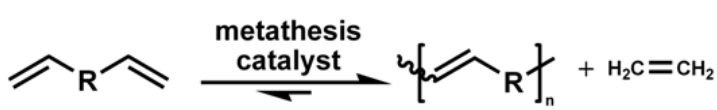

Figure 1.5. ADMET polymerization.

ADMET polymerization has been used to generate a wide range of polymers with very specific structure – if the α,ω-olefin monomer can be synthesized, it can be converted into a strictly linear polymer with precise control of backbone functionalities. The Wagener group, in particular, has developed ADMET methodology to explore systems as diverse as the effects of branching on polyethylene properties, to the polymerization of chiral monomers.

1.2 Thesis Research

Chapter 2 describes cascade ring-opening/ring-closing metathesis (RO/RCM) polymerization of monomers containing two cycloalkenes. Cascade metathesis polymerization is a more advanced metathesis polymerization system. Previously, most examples of metathesis polymerization methodologies rely on just one of the three types of olefin metathesis reactions to make simple polymer structures. In order to synthesize well-defined polymers with complex microstructures, cascade polymerization, where more than two types of olefin metathesis transformations were combined in one-shot or one-pot, was successfully developed analogous to cascade reactions in organic synthesis.

Chapter 3 describes multiple olefin metathesis polymerization which produced well-defined A,B-alternating copolymers using the same monomers. This is the first example of metathesis polymerization that all three types of olefin metathesis trans-formations (ring-opening, ring-closing, and cross metathesis) were combined in an orderly manner to produce just one uniform polymer microstructure via precisely controlled pathways.

Chapter 4 describes the unusual superior activity of the first generation Grubbs catalyst in cascade olefin metathesis polymerization. It is about unique Grubbs catalyst selectivity for the cascade polymerization. The cascade ring-opening/ring-closing metathesis polymerization of monomers containing two cyclopentene moieties using the first-

generation Grubbs catalyst to give well-defined polymers containing new rings via a rearrangement reaction. Normally, more reactive catalyst gave better polymerization results in polymer synthesis. However, one surprising and puzzling feature was that the intrinsically less active the first-generation Grubbs catalyst outperformed than more active the third-generation Grubbs catalyst which should be generally more active.

Finally, the Last Chapter describes sequence controlled olefin metathesis Polymerization. Using alkyne selectivity of the third-generation Grubbs catalyst, unique monomer structure which contains alkyne and two cycloalkene moiety could be polymerized to sequence controlled polymer following cascade manner.

1.3 References

(1) (a) Grubbs, R. H.; Chang, S. *Tetrahedron* **1998**, *54*, 4413. (b) Fürstner, A. *Angew. Chem., Int. Ed*. **2000**, *39*, 3013. (c) Grubbs, R. H. *Handbook of Metathesis*, Wiley-VCH: Weinheim, **2003**, *1*, 2. (d) Grubbs, R. H. *Tetrahedron* **2004**, *60*, 7117.

(2) For reviews, see: (a) Novak, B. M.; Risse, W.; Grubbs, R. H. *Adv. Polym. Sci.* **1992**, *102*, 47-72. (b) Grubbs, R. H.; Khosaravi, E. *Material Science and Technology*, **1999**, *20*, 65. c) Buchmeiser, M. R. *Chem. Rev*. **2000**, *100*, 1565.

(3) For reviews, see: (a) Gruubs, R. H.; Miller, S. J.; Fu, G. C. *Acc. Chem. Res.* **1995**, *28*, 446. (b) Deiters, A.; Martin, S. F. *Chem. Rev*. **2004**, *104*, 2199. (c) Schmidt, B.; Hermanns, J. *Curr. Org. Chem*. **2006**, *10*, 1363.

(4) For recent reviews, see: (a) Schuster, M.; Blechert, S. *Angew. Chem. Int. Ed*. **1997**, *36*, 2036. (b) Connon, S. J.; Blechert, S. *Angew. Chem. Int. Ed.* **2003**, *42*, 1900. (c) Grubbs, R. H. *Handbook of Metathesis*, 2nd ed.; Wiley-VCH: Weinheim, **2015**; Vols. 2, 3.

(5) (a) Wagener, K. B.; Boncella, J. M.; Nel, J. G. *Macromolecules* **1991**, *24*, 2649. (b) Patton, J. T.; Boncella, J. M.; Wagener, K. B. *Macromolecules* **1992**, *25*, 3862. (c) Brzezinska, K.; Wolfe, P. S.; Watson, M. D.; Wagener, K. B. *Macromol. Chem. Phys.* **1996**, *197*, 2065. (d) Mutlu, H.; Montero de Espinosa, L.; Meier, M. A. R. *Chem. Soc. Rev.* **2011**, *40*, 1404.

(6) (a) Novak, B. M.; Grubbs, R. H. *J. Am. Chem. Soc*. **1988**, *110*, 960. (b) Schrock, R. R. *Acc. Chem. Res*. **1990**, *23*, 158. (c) Bielawski, C. W.; Grubbs, R. H. *Angew. Chem., Int. Ed*. **2000**, *39*, 2903.

(7) (a) Kim, H.-S.; Bowden, N.; Grubbs, R. H. *J. Am. Chem. Soc*.**1994**, *116*, 10801. (b) Zuercher, W. J.; Scholl, M.; Grubbs, R. H. *J.Org. Chem*. **1998**, *63*, 4291. (c) Choi, T.-L.; Grubbs, R. H. *Chem. Commun*. **2001**, 2648. (d) Boyer,F.-D.; Hanna, I. *Tetrahedron Lett*. **2002**, *43*, 7469. (e) Maifeld, S. A.; Miller, R. L.; Lee, D. *J. Am. Chem. Soc*. **2004**, *126*, 12228. (f) Park, H.; Hong, Y.-L.; Kim, Y.; Choi. T.-L. *Org. Lett*. **2010**, *12*, 3442. (g) Huang, J.; Xiong, H.; Hsung, R. P.; Rameshkumar, C.; Mulder, J. A.; Grebe, T. P. *Org. Lett*. **2002**, *4*, 2417.

(8) (a) Kinoshita, A.; Mori, M. *J. Org. Chem.* **1996**, *61*, 8356. (b) Kinoshita, A.; Mori, M. *Heterocycles* **1997**, *46*, 287. (c) Layton, M. E.; Morales, C. A.; Shair, M. D. *J. Am. Chem. Soc.* **2002**, *124*, 773. (d) Virolleaud, M.-A.; Bressy, C.; Piva, O. *Tetrahedron Lett.* **2003**, *44*, 8081. (e) Boyer, F.-D.; Hanna, I.; Ricard, L. *Org. Lett.* **2004**, *6*, 1817. (f) Quinn, K. J.; Isaacs, A. K.; Arvary, R. A. *Org. Lett*. **2004**, *6*, 4143. (g) Niethe, A.; Fischer, D.; Blechert, S. *J. Org. Chem*. **2008**, *73*, 3088. (h) Cros, F.; Pelotier, B.; Piva, O. Eur. *J. Org. Chem*. **2010**, 5063.

(9) (a) Kim, Y.-H.; Gal, Y.-S.; Kim, U.-Y.; Choi, S.-K. *Macromolecules* **1988**, *21*, 1991. (b) Ryoo, M.-S.; Lee, W.-C.; Choi, S.-K. *Macromolecules* **1990**, *23*, 3029−3031. (c) Jang, M.-S.; Kwon, S.-K.; Choi, S.-K. *Macromolecules* **1990**, *23*, 4135−4140. (d) Koo, K.-M.; Han, S.-H.; Kang, Y.-S.; Kim, U.-Y.; Choi, S.-K. *Macromolecules* **1993**, *26*, 2485− 2488. (e)

Kang, K.-L.; Kim, S.-H.; Cho, H.-N.; Choi, K.-Y.; Choi, S.-K. *Macromolecules* **1993**, *26*, 4539−4543. (f) Kim, S.-H.; Kim, Y.-H.; Cho, H.-N.; Kwon, S.-K.; Kim, H.-K.; Choi, S.-K. *Macromolecules* **1996**, *29*, 5422−5426. (g) Gal, Y. S.; Jin, S. H.; Park, J. W.; Lee, W. C.; Lee, H. S.; Kim, S. Y. *J. Polym. Sci., Part A: Polym. Chem.* **2001**, *39*, 4101−4109. (h) Gal, Y. S.; Lee, W. C.; Gui, T. L.; Jin, S. H.; Koh, K.; Kim, S. H.; Kim, D. W.; Ko, J. M.; Chun, J. H. *Korea Polym. J.* **2001**, *9*, 220−227. (i) Gal, Y. S.; Jin, S. H.; Choi, S. K. *J. Mol. Catal. A: Chem.* **2004**, *213*,115−121. (j) Gal, Y. S.; Lee, I.-S.; Chang, E.-H.; Jeong, Y.-C.; Kwak, Y.-W. *Bull. Korean Chem. Soc.* **2007**, *28*, 1305−1310. (k) Gui, T. L.; Qiu, J.-L.; Wang, Y.; Shim, S.-Y.; Jin, S.-H.; Park, J.-W.; Lim, K. T.; Gal, Y. S. *Mol. Cryst. Liq. Cryst.* **2009**, *498*, 175−182.

(10) (a) Kanaoka, S.; Grubbs, R. H. *Macromolecules* **1995**, 28, 4707. (b) Weck, M.; Schwab, P.; Grubbs, R. H. *Macromolecules* **1996**, 29, 1789.

(17) Garber, S. B.; Kingsbury, J. S.; Gray, B. L.; Hoveyda, A. H. *J. Am. Chem. Soc*. **2000**, 122, 8168.

(11) (a) Novak, B. M.; Grubbs, R. H. *J. Am. Chem. Soc*. **1988**, *110*, 960. (b) Schrock, R. R. *Acc. Chem. Res*. **1990**, *23*, 158. (c) Bielawski, C. W.; Grubbs, R. H. *Angew. Chem., Int. Ed*. **2000**, *39*, 2903.

(12) Choi, S.-K.; Gal, Y.-S.; Jin, S.-H.; Kim, H. K. *Chem. Rev.* **2000**, *100*, 1645−1682.

(13) (a) Schuehler, D. E.; Williams, J. E.; Sponsler, M. B. *Macromolecules* **2004**, *37*, 6255−6257. (b) Sanda, F.; Nakai, T.; Kobayashi, N.; Masuda, T. *Macromolecules* **2004**, *37*, 2703−2708. (c) Masuda, T. *J. Polym. Sci., Part A: Polym. Chem.* **2007**, *45*, 165−180. (d) Katsumata, T.; Shiotsuki, M.; Sanda, F.; Sauvage, X.; Delaude, L.; Masuda, T. *Macromol. Chem. Phys.* **2009**, *210*, 1891−1902. (e) Liu, J. Z.; Lam, J. W. Y.; Tang, B. Z. *Chem. Rev.* **2009**, *109*, 5799−5867. (f) Shiotsuki, M.; Sanda, F.; Masuda, T. *Polym. Chem.* **2011**, *2*, 1044− 1058.

(14) (a) Stille, J. K.; Frey, D. A. *J. Am. Chem. Soc.* **1961**, *83*, 1697− 1701. (b) Gibson, H.

W.; Bailey, F. C.; Epstein, A. J.; Rommelmann, H.; Pochan, J. M. J. *Chem. Soc., Chem. Commun.* **1980**, 426a−426a. (c) Gibson, H. W.; Epstein, A. J.; Rommelmann, H.; Tanner, D. B.; Yang, X.-Q.; Pochan, J. M. *J. Phys. (Paris) Colloq.* **1983**, *44*, 651−656. (d) Gibson, H. W.; Bailey, F. C.; Epstein, A. J.; Rommelmann, H.; Kaplan, S.; Harbour, J.; Yang, X.-Q; Tanner, D. B.; Pochan, J. M. *J. Am. Chem. Soc.* **1983**, *105*, 4417−4431.

(15) Fox, H. H.; Schrock, R. R. *Organometallics* **1992**, *11*, 2763−2765.

(16) Fox, H. H.; Wolf, M. O.; O'Dell, R.; Lin, B. L.; Schrock, R. R.; Wrighton, M. S. *J. Am. Chem. Soc.* **1994**, *116*, 2827−2843.

(17) (a) Schattenmann, F. J.; Schrock, R. R.; Davis, W. M. *J. Am. Chem. Soc.* **1996**, *118,* 3295−3296. (b) Schattenmann, F. J.; Schrock, R. *Macromolecules* **1996**, *29*, 8990−8991. (c) Buchmeiser, M. R.; Schmidt, C.; Wang, D. *Macromol. Chem. Phys.* **2011**, *212*, 1999−2008.

(18) (a) Anders, U.; Nuyken, O.; Buchmeiser, M. R.; Wurst, K. *Angew. Chem., Int. Ed.* **2002**, *41*, 4044−4047. (b) Anders, U.; Nuyken, O.; Buchmeiser, M. R.; Wurst, K. *Macromolecules* **2002**, *35*, 9029−9038.

(c) Anders, U.; Wagner, M.; Nuyken, O.; Buchmeiser, M. R. *Macromolecules* **2003**, *36*, 2668−2673. (d) Sudheendran, M.; Horecha, M.; Kiriy, A.; Gevorgyan, S. A.; Krebs, F. C.; Buchmeiser, M.R. *Polym. Chem.* **2013**, *4*, 1590−1599. (e) Buchmeiser, M. R.; Sen, S.; Unold, J.; Frey, W. *Angew. Chem., Int. Ed.* **2014**, *53*, 9384−9388. (f) Herz, K.; Unold, J.; Hanle¨, J.; Schowner, R.; Frey, W.; Buchmeiser, M.R.; Sen, S. *Macromolecules* **2015**, *48*, 4768−4778.

(19) Schrock, R. R.; Tonzetich, Z. J.; Lichtscheidl, A. G.; Muller, P.; Schattenmann, F. J. *Organometallics* **2008**, *27*, 3986−3995.

(20) (a) Krause, J. O.; Zarka, M. T.; Anders, U.; Weberskirch, R.; Nuyken, O.; Buchmeiser, M. R. *Angew. Chem., Int. Ed.* **2003**, *42*, 5965−5969. (b) Krause, J. O.; Nuyken, O.; Buchmeiser, M. R. *Chem. - Eur. J.* **2004**, *10*, 2029−2035. (c) Halbach, T. S.; Krause, J. O.;

Nuyken, O.; Buchmeiser, M. R. *Macromol. Rapid Commun.* **2005**, *26*, 784−790. (d) Mayershofer, M. G.; Nuyken, O.; Buchmeiser, M. R. *Macromolecules* **2006**, *39*, 3484−3493. (e) Vygodskii, Y. S.; Shaplov, A. S.; Lozinskaya, E. I.; Vlasov, P. S.; Malyshkina, I. A.; Gavrilova, N. D.; Kumar, P. S.; Buchmeiser, M. R. *Macromolecules* **2008**, *41*, 1919−1928.

(f) Kumar, P. S.; Wurst, K.; Buchmeiser, M. R. *J. Am. Chem. Soc*. **2009**, *131*, 387−395. (g) Autenrieth, B.; Anderson, E. B.; Wang, D.; Buchmeiser, M. R. *Macromol. Chem. Phys.* **2013**, *214*, 33−40.

(21) (a) Kang, E.-H.; Lee, I. S.; Choi, T.-L. *J. Am. Chem. Soc.* **2011**, *133*, 11904−11907. (b) Kim, J.; Kang, E.-H.; Choi, T.-L. *ACS Macro Lett.* **2012**, *1*, 1090−1093. (c) Kang, E.-H.; Lee, I.-H.; Choi, T.-L. *ACS Macro Lett.* **2012**, *1*, 1098−1102. (d) Kang, E.-H.; Choi, T.-L. *ACS Macro Lett.* **2013**, *2*, 780−784. (e) Kang, E.-H.; Yu, S. Y.; Lee, I. S.; Park, S. E.; Choi, T.-L. *J. Am. Chem. Soc.* **2014**, *136*, 10508−10514.

(22) (a) Lee, I. S.; Kang, E.-H.; Park, H.; Choi, T.-L. *Chem. Sci.* **2012**, *3*, 761−765. (b) Park, H.; Lee, H.-K.; Choi, T.-L. *Polym. Chem.* **2013**, *4*, 4676−4681. (c) Song, J.-A.; Park, S. E.; Kim, T.-S.; Choi, T.-L. *ACS Macro Lett.* **2014**, *3*, 795−798. (d) Park, H.; Lee, H.-K.; Kang, E.-H.; Choi, T.-L. *J. Polym. Sci., Part A: Polym. Chem.* **2015**, *53*, 274−279.

(24) (a) Song, W.; Han, H.; Liao, X.; Sun, R.; Wu, J.; Xie, M. *Macromolecules* **2014**, *47*, 6181−6188. (b) Song, W.; Han, H.; Wu, J.; Xie, M. *Chem. Commun.* **2014**, *50*, 12899−12902. (c) Song, W.; Han, H.; Wu, J.; Xie, M. *Polym. Chem.* **2015**, *6*, 1118−1126. (d) Guo, M.; Sun, R.; Han, H.; Wu, J.; Xie, M.; Liao, X. *Macromolecules* **2015**, *48*, 2378−2387. (e) Liu, W.; Liao, X.; Li, Y.; Zhao, Q.; Xie, M.; Sun, R. *Chem. Commun.* **2015**, *51*, 15320−15323.

(23) (a) Wagener, K. B.; Boncella, J. M.; Nel, J. G. *Macromolecules* **1991**, *24*, 2649. (b) Patton, J. T.; Boncella, J. M.; Wagener, K. B. *Macromolecules* **1992**, *25*, 3862. (c) Brzezinska, K.; Wolfe, P. S.; Watson, M. D.; Wagener, K. B. *Macromol. Chem. Phys.* **1996**,

197, 2065. (d) Mutlu, H.; Montero de Espinosa, L.; Meier, M. A. R. *Chem. Soc. Rev.* **2011**, *40*, 1404.

Chapter 2: Cascade Ring-Opening/Ring-Closing Metathesis Polymerization

2.1 ABSTRACT

We demonstrated cascade ring-opening/ring-closing metathesis (RO/RCM) polymerization of monomers containing two cyclopentene moieties and post-modification via insertion polymerization. In this system, well-defined polymers were efficiently formed by tandem cascade ring-opening/ring-closing metathesis reaction pathway. Furthermore, these polymers could be transformed into new A,B-alternating copolymers via a sequential cross metathesis reaction with a diacrylate. Additionally, we demonstrated the concept of multiple olefin metathesis polymerization in which the dicyclopentene and diacrylate monomers underwent all three olefin metathesis transformations (ring-opening, ring-closing, and cross metathesis) in one shot to produce A,B-alternating copolymer. These polymerization methods yielded well-defined polymers via a combination of ring-opening and ring-closing metathesis (cascade polymerization). However, cascade polymerization gave some limitation such as low polymerization efficiency (maximum turnover number(TON) of 250) and narrow monomer scope. To overcome these problems, we designed various new monomers containing cyclopentene and even more challenging ring-strain free cyclohexene moieties, so that polymerization would produce a thermodynamically favored six-membered ring backbone repeat unit. With this enhanced driving force for polymerization, these new monomers successfully underwent cascade polymerization with a high polymerization efficiency leading to a maximum TON of 1940 and maximum number average molecular weight(M_n) up to 343 kDa. This was possible because the new monomer design with excellent thermodynamic and kinetic preference suppressed undesired polymerization pathways and lowering defects in polymer microstructures. In short, we present our strategies to achieve superior cascade polymerization from these new monomers.

2.2 Introduction

Olefin metathesis reaction is a powerful method to prepare various molecules by exchanging carbon–carbon double bonds.[1] This field has rapidly advanced over two decades with the development of highly active Grubbs[2] and Schrock catalysts.[3] Organic chemists have developed ring-opening metathesis (ROM)[4], ring-closing metathesis (RCM)[5], and cross-metathesis (CM)[6] to synthesize complex organic compounds such as natural products and drugs. Furthermore, polymer chemists developed polymerizations, such as ring-opening metathesis polymerization (ROMP)[7], cyclopolymerization (CP)[8], and acyclic diene metathesis polymerization (ADMET)[9] using CM reactions. However, most examples of metathesis polymerization methodologies rely on just one of the three types of olefin metathesis reactions to make simple polymer structures. In order to synthesize well-defined polymers with complex microstructures, tandem polymerization, where more than two types of olefin metathesis transformations were combined in one-shot or one-pot, was successfully developed analogous to cascade reactions in organic synthesis.[10-15]

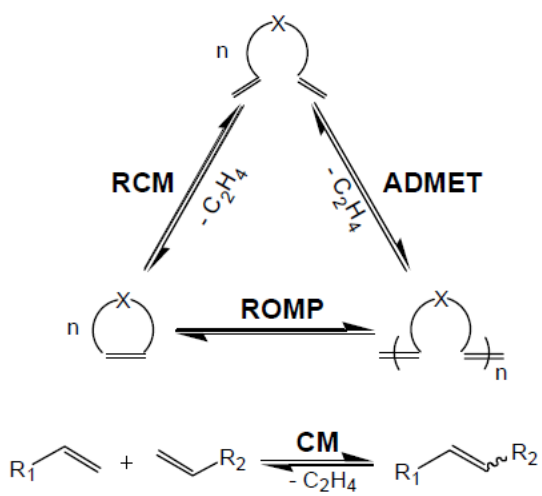

Figure 2.1. Chemical transformations by olefin metathesis

The first representative example of using more than two types of olefin metathesis process was ring-opening-insertion metathesis polymerization (ROIMP) using the second-generation Grubbs catalyst, which was used to synthesize well-defined A,B-alternating copolymers in the one-shot method.[10] The high alternation of this copolymer was due to enthalpically driven selective CM to form α,β-unsaturated carbonyl olefin with the in-situ generated polymers via fast ROMP of cycloalkene using the second-generation Grubbs catalyst. Another example is the two-pot polymerization using two olefin metathesis reactions sequentially (first ROMP and then ADMET) to produce branched polymers in an independent manner.[11] Recently, a new concept of cascade polymerization via tandem ring-opening/ring-closing polymerization of monomers containing cycloalkene and terminal alkyne moieties[12] attracted much attention because this selective cascade polymerization proceeded in a living manner using the fast-initiating third generation Grubbs catalyst to produce even sequence specific polymers.[13] The most recently reported living polymerization combining olefin metathesis and metallotropic shift occurring in a perfectly alternating cascade manner to produce unique conjugated polyeneynes was also demonstrated.[14] Lastly, our group reported cascade ring-opening/ring-closing polymerization using monomers containing two cyclopentene moieties[15a] (**Scheme 2.1a**). Although these two types of polymerization methods were mechanistically unique, maximum turnover number (TON) of 250 was relatively lower than the well-investigated ROMP. To further improve reactivity and selectivity for the cascade polymerization and to expand the polymerization scope of these two polymerizations, one needs to investigate the origin of low reactivity and narrow monomer scope and to develop a new strategy to overcome the limitation. Herein, we report a new design of bis-cycloalkene monomers to achieve highly efficient cascade polymerization with broad monomer scopes resulting in maximum TON up to 1940 and maximum number average molecular weight (M_n) of 343 kDa. Since these polymerizations from the new-design produced kinetically and

thermodynamically preferred six-membered ring backbone structures, we could broaden the monomer scope, not only for the cascade polymerization.

2.3 Results & Discussion.

Scheme 2.1. Cascade Ring-Opening/Ring-Closing Metathesis Polymerization and MOMP with M1 derivatives

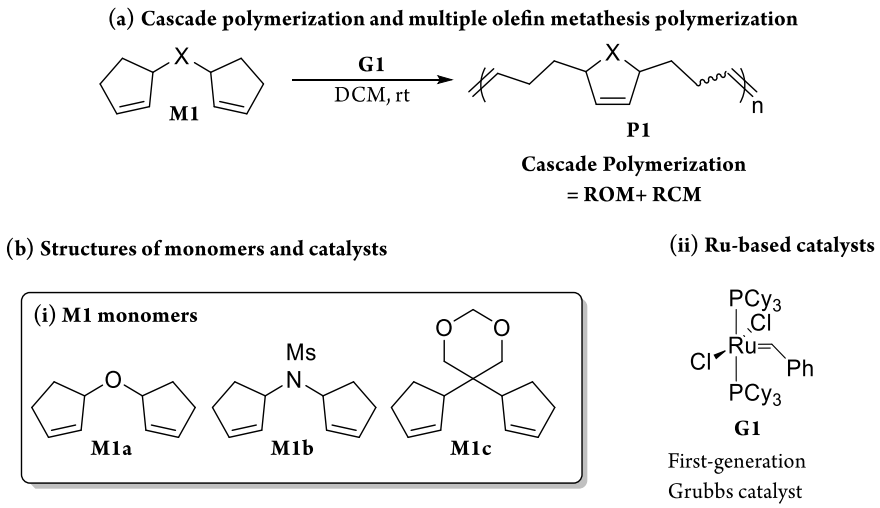

Herein, we report a new cascade olefin metathesis polymerization methodology via a cascade RO/RCM polymerization of monomers containing two cyclopentenes. To achieve cascade RO/RCM polymerization, we designed novel monomers containing cyclopentene moieties, because monomers should be able to undergo both ring-opening and ring-closing metathesis reactions simultaneously. Consequently, we synthesized three monomers **M1a-c**; in each, two cyclopentene moieties were connected by oxygen, nitrogen, or carbon linkers, respectively. (**Scheme 2.1(b))**

However, two issues need to be first overcome in order to achieve selective cascade RO/RCM polymerization from these new monomers containing two polymerizable cyclopentene moieties. The first issue was to determine whether these monomers having 3-

substituted cyclopentene moieties would polymerize at all. The Grubbs group reported that the ROMP of 3-substituted cyclopentene derivatives always failed,[11] because the substituent at the 3-position increased the steric hindrance and decreased the ring strain, thereby preventing the ROMP. The second issue was to determine how to control the competing ROM and RCM equilibrium of the cyclopentene moieties in the monomer so that the desired, structurally well-defined polymers would be produced selectively (**Scheme 2.2**). For example, if the ROMP became dominant, a cross-linked gel was produced. Even if the cascade RO/RCM reaction did occur, there were two possible pathways depending on the orientation of the approached catalyst. Only Pathway A was a productive pathway for the tandem polymerization because the second RCM step was favored due to the proximity effect. On the other hand, in Pathway B, a new carbene underwent RCM back to the monomer (**Scheme 2.2**). Thus, optimizing the polymerization condition to control the competing equilibrium between ROM and RCM was the key to the successful cascade polymerization.

Scheme 2.2. Reaction scheme of the cascade RO/RCM polymerization and proposed polymerization pathway for the selective formation of five-membered ring repeat units.

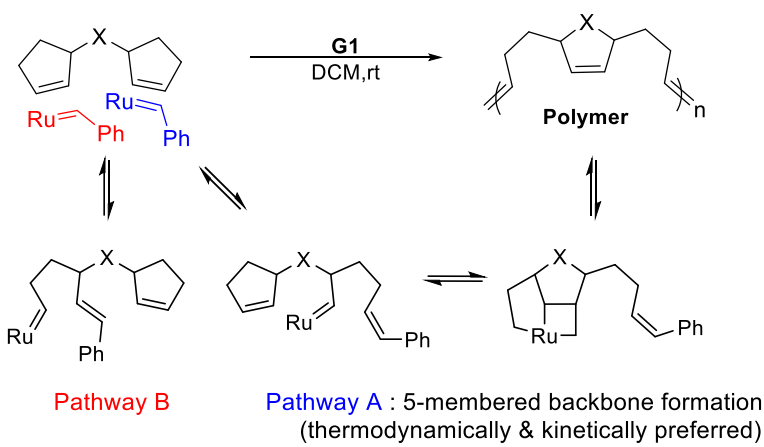

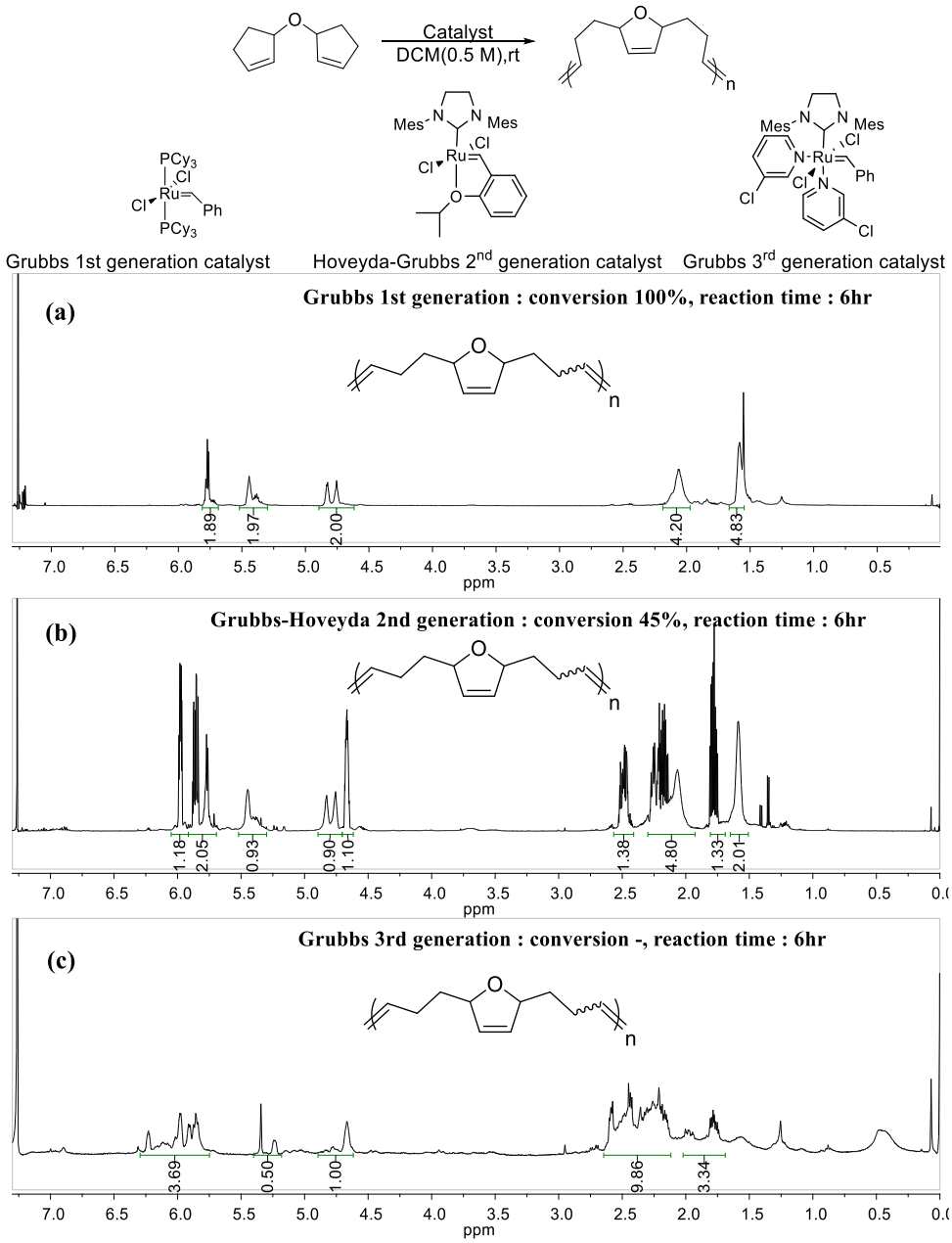

Figure 2.2. Catalyst reactivity comparison for Tandem RO/RCM polymerization (a) Grubbs 1st generation catalyst (b) Hoveyda-Grubbs 2nd generation catalyst (c) Grubbs 3rd generation catalyst

Initially, to search for the most suitable catalyst, we screened various catalysts for the cascade RO/RCM polymerization of **M1a**. Generally, a first-generation Grubbs catalyst (**G1**) has lower activity than do second- or third-generation Grubbs catalysts. In our system, however, **G1** showed the best performance when comparing the monomer consumptions via ^{1}H NMR (**Figure 2.2**). Next, we screened the reaction concentration to determine the effect of the polymerization. At 0.1 M, **M1a** with a monomer:catalyst ratio (M:C) of 50:1 was successfully polymerized into poly(2,5-disubstituted-2,5-dihydrofuran) with 87 % conversion after 24 h. To shorten the reaction time, we increased the concentration up to 1 M, but an insoluble cross-linked gel formed within 10 min, meaning that the concentration reached its critical concentration at which the ROMP of the cyclopentene moiety became dominant. This finding was somewhat expected because the critical monomer concentration for the ROMP of the cyclopentene is 0.8 M at 25 ℃.[12] On the other hand, at 0.5 M, full conversion was obtained after 12 h without any cross-linking, and simple precipitation in methanol produced a rubbery polymer with moderate yields. When decreasing the catalyst loading or increasing the M:C ratio to 150:1 and even 250:1, we achieved quantitative conversion under optimized conditions, producing **P1a** with Mn of 13.8 kDa–52.3 kDa in proportion to the M:C ratio (**Table 2.1**, **Entries 1-3**).

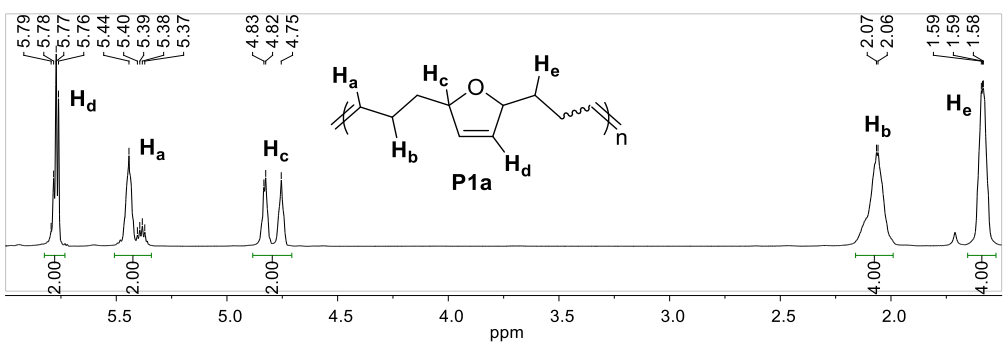

Figure 2.3. ^{1}H NMR spectrum of P1a

The structure of purified **P1a** was characterized with NMR (**Figure 1**, **Figure S2**), which clearly confirmed the formation of a low ring-strained, five-membered, 2,5-dihydrofuran backbone. Also, an internal olefin with an *E*:*Z* ratio of 5:1 for the acyclic olefin was observed. Interestingly, **M1a** was polymerized at concentrations less than 0 .1 M despite possessing the low-strained cyclopentene and the substitution at the 3-position. This finding was in sharp contrast to the case of cyclopentene, which was seemingly a more reactive monomer but did not undergo ROMP at concentrations less than 0.8 M.[12] Instead, at concentrations below the critical monomer concentration for the ROMP, the cascade RO/RCM occurred to produce the polymer with a rearranged backbone with the 2,5-dihydrofuran moiety, implying that the 2,5-dihydrofuran backbone moiety in **P1a** was thermodynamically more stable than the cyclopentene in the monomer. Also, due to the substitutions at the 2- and 5-positions on dihydrofuran, the reverse reaction or depolymerizion would be slower than chain propagation.

Table 2.1. Cascade RO/RCM polymerizations of M1a-c

Entry	Monomer	M:C	Conc. (M)	Time (h)	M_n[a] (kDa)	PDI[a]	Conv[b] (%)
1	M1a	50:1	0.5	12	13.8	1.79	100
2	M1a	150:1	0.5	12	38.0	1.91	100
3	M1a	250:1	0.5	12	52.3	1.83	100
4	M1b	50:1	1.5	24	25.9	1.53	100
5	M1b	150:1	1.5	24	66.2	1.91	97
6	M1b	250:1	1.5	48	114.5	2.14	98
7	M1c	50:1	1.5	24	29.9	1.48	100
8	M1c	150:1	1.5	48	62.9	1.70	97
9	M1c	250:1	1.5	48	114.4	1.90	95

[a] Determined by THF SEC calibrated using polystyrene standards. [b] Conversion was determined by crude ^{1}H NMR analysis

To broaden the monomer scope, we investigated the tandem polymerization of **M1b** and **M1c** in which two cyclopentenes were connected by nitrogen and carbon, respectively. Unlike **M1a**, the analogous polymerizations of **M1b** and **M1c** at 0.5 M did not achieve full conversions, but qualitative tandem polymerization without any cross-linking occurred when the concentration increased to 1.5 M. It seems that the ring-strain and the competing equilibrium between ROM and RCM for **M1b** and **M1c** were slightly different than those for **M1a**. Regardless, both monomers efficiently underwent the tandem polymerization even with low catalyst loading with M:C ratios of 250:1, and the M_n value of the resulting **P1b** and **P1c** were roughly controlled and proportional to the M/C ratios (**Table 2.1.**, **Entries 4-9**) and structures of purified **P1b** and **P1c** were also characterized by NMR. However, in all three cases, the polydispersity index (PDI) values were broad due to chain transfer reactions.

Scheme 2.3. Concentration-dependent polymerization

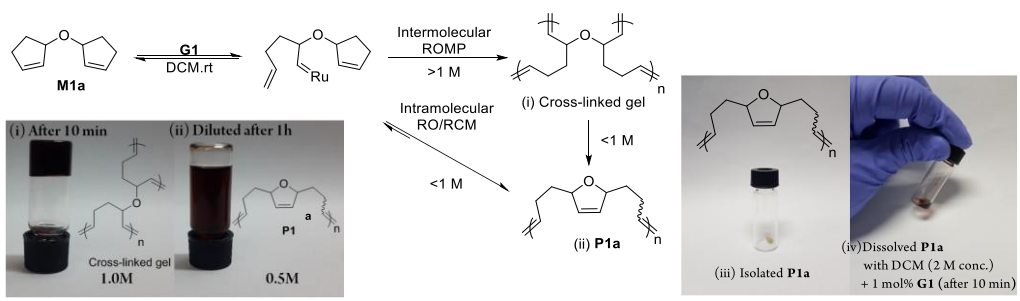

As we previously observed, the polymerization of **M1a** at concentrations over that of the critical monomer concentration produced cross-linked gel due to the dominant intermolecular ROMP process. However, by diluting the solution containing this cross-linked gel to 0.5 M, the gel completely disappeared after 6 h, mainly yielding a soluble polymer containing the same dihydrofuran backbone. This result was obtained because the dilution led to the reversible decross-linking via the intramolecular RO/RCM process to produce **P1a** (**Scheme 2.3.**). We also believe that the cross-linking occurs from the

independent ROMP of the monomers which fail to undergo selective RCM at high concentration. This is illustrated in **Scheme 2.3. (iii)** and (**iv)** by a control experiment which shows no further gelation occurring even when the isolated **P1a** in 2.0 M DCM was treated again with fresh **G1**. This indicates that further ROMP of the furanyl moiety in **P1a** (or cross-linking) does not occur.

Scheme 2.4. Depolymerization of P1a-c.

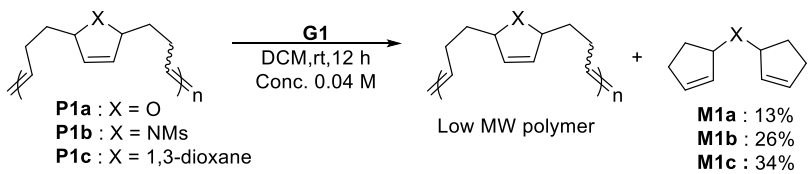

Since the entire polymerization was in thermodynamic equilibrium, the isolated polymers could also be depolymerized to the corresponding monomers via the reverse tandem intramolecular RO/RCM process. Each purified **P1a**, **P1b**, and **P1c** was redissolved into a 0.04 M CH_2Cl_2 solution, and fresh **G1** was added. After 12 h, 13 % of **M1a**, 26 % of **M1b**, and 34% of **M1c** were observed with ^{1}H NMR, implying that even depolymerization indeed occurred in dilute conditions (**Scheme 2.4**). These results demonstrated that by understanding the equilibrium, the direction of the ROMP or RO/RCM processes could be predicted depending on the concentration.

We have attempted to broaden further monomer scopes that completed and expanded the successful cascade polymerization like **M1a-c**. The new monomer synthesis of Ether and Amide and Carbon type linker, which has a different functional group which could affect different steric and electronic factor for the polymerization, was carried out and the following 15 monomers could be synthesized. In order to solve these problems, a new monomers having a different structure was synthesized.

Scheme 2.5. Various monomer scopes of cascade polymerization

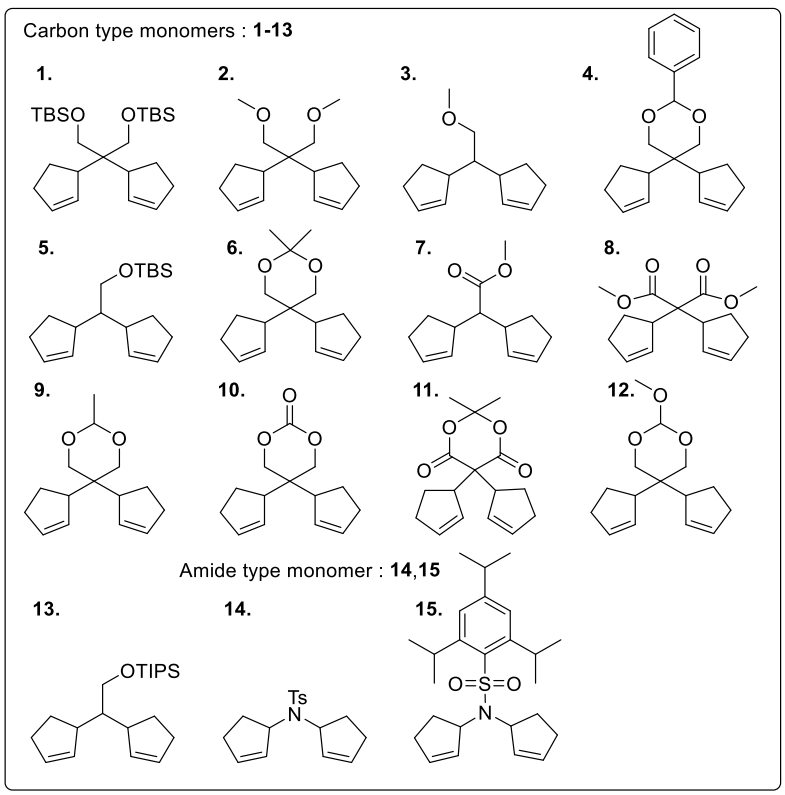

Unfortunately, the cascade polymerization results of these monomers show that the conversion itself is low or the coordination of the catalyst does not proceed so that the polymerization itself could not proceed at all. In detail, ester type monomer, **7**,**8**,**11** were not polymerized at all. Their polymerization conversions were 0% with **G1** and **HG2**. We thought these failures were due to the unexpected coordination of Ru metal in Grubbs catalyst and ester groups in monomer structure. Therefore, we tried to confirm this through polymerization of another monomer that has the different design. In the case of monomer **1**, cascade polymerization result was good conversion using M:C = 50:1. After increasing M:I ration up to 150:1, the conversion was decreased by 40%. So, we changed to sterically smaller group from sterically bulky silyl protection group in monomer structure. As a result,

Table 2.2. Cascade polymerization of M2 and M3 derivatives

Entry	Monomer	Monomer(M) : Catalyst(C)	Conc. (M)	Time (h)	Temp (°C)	Conv[a] (%)	M_n[b] (kDa)	PDI[b]
1	**1**	50:1	1.5	24	25	100	31	1.49
2	**2**	50:1	1.5	24	25	87	-	-
3	**3**	50:1	1.5	24	25	72	-	-
4	**4**	50:1	1.5	16	25	50	-	-
5	**4**	50:1	1.5	24	60	92	-	-
6	**5**	50:1	2.5	24	25	55	-	-
7	**6**	50:1	1.5	36	25	75	-	-
8	**7**	50:1	1.5	24	25	0	-	-
9	**8**	50:1	1.5	24	25	0	-	-
10	**9**	50:1	1.5	48	25	96	-	-
11	**10**	50:1	1.5	48	25	82	-	-
12	**11**	50:1	1.5	48	25	96	-	-
13	**11**	150:1	1.5	48	25	52	-	-
14	**12**	50:1	1.5	48	25	68	-	-
15	**13**	50:1	1.5	48	25	44	-	-
16	**14**	50:1	1.0	12	25	100	52	1.78
17	**14**	150:1	1.0	72	25	100	130	1.85
18	**14**	250:1	1.5	72	25	100	148	1.71
19	**14**	500:1	2.5	72	25	95	352	1.87
20	**14**	1000:1	2.5	72	25	75	495	1.75
21	**15**	50:1	2.5	72	25	82	-	-

[a] Determined by THF SEC calibrated using polystyrene standards. [b] Conversion was determined by crude ^{1}H NMR analysis

Monomer **2**,**3** were synthesized using simple organic synthesis reactions. The polymerization conversions were not completed after 48 hours with monomer **2**,**3**. So we changed methyl group to silyl protection group again like monomer **5,13**. However, unlike tandem ring-opening/ring-closing metathesis polymerization[12a,b], Thorpe-Ingold effect was not applied for this cascade polymerization. The conversion of each monomer was still low. Next protection groups were derivatives of acetal protection. In the case of monomer **4**, its polymerization conversion was increased at 60 °C, but the further increment of M:I ratio

was achieved. The others like **6**,**9**,**10** also could not achieve good cascade polymerization results at all. After checking carbon type centered monomer, we moved to polymerization of amide type monomer. With monomer **14,** we got quite nice results in terms of polymerization conversion and polymerization efficiency. But diastereomeric structure in polymer repeating unit made complicated proton NMR peaks, so it is hard to analyze them perfectly. We also intentionally changed the monomer structure to increase steric factor in monomer structure by changing tosyl to triisopropylbenzene sulfonyl group, but its results were also not good like **14**. So we chose **M1a-c** as best candidates for cascade polymerization.

Scheme 2.6. Cascade Polymerization of M2 and M3 monomers

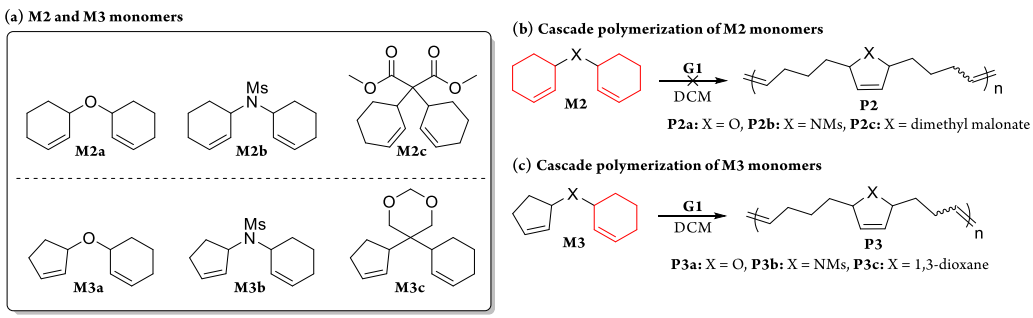

Now, we successfully synthesized well-defined polymers with a five-membered ring backbone in the repeat unit from monomers containing two cyclopentene moieties (**M1a-c)** and first-generation Grubbs catalyst (**G1**) (**Scheme 2.1.)**.[15a,16] We noticed that optimizing the polymerization concentration was important because, although polymerization at high concentration would promote higher conversion, some monomers containing bis-cycloalkene readily underwent cross-linking when polymerized at above critical concentration. To address these issues and to understand the factors that influence the polymerizations, we designed and synthesized three new monomers **M2a-c** (**Scheme 2.5.**) containing a challenging ring-strain-free cyclohexene (strain energy = 2.5 kcal/mol) moiety

instead of cyclopentene (strain energy = 6.8 kcal/mol)[18] present in **M1** derivatives. However, this challenging cascade polymerization of **M2** monomers all failed because the thermodynamics of cyclohexene favored the ring-closed state of the monomers over

cascade polymerization to give less stable membered ring structure on the polymer products (**Table 2.2, entries 1-3**).

Table 2.2. Cascade polymerization of M2 and M3 derivatives

Entry	Monomer	Monomer(M) : Catalyst(C)	Conc. (M)	Time (h)	Temp (°C)	Conv[a] (%)	M_n[b] (kDa)	PDI [b]
1	**M2a**	50:1	1.5	24	25	0	-	-
2	**M2b**	50:1	1.5	24	25	0	-	-
3	**M2c**	50:1	1.5	24	25	0	-	-
4	**M3a**	50:1	1.5	18	25	100	20.4	1.64
5	**M3a**	150:1	1.5	18	25	100	19.1	1.55
6	**M3b**	50:1	2.5	48	25	36	-	-
7	**M3b**	50:1	2.5	48	0	55	18.9	1.44
8	**M3c**	50:1	2.5	48	25	30	-	-
9	**M3c**	50:1	2.5	48	0	49	17.2	1.69

[a] Determined by THF SEC calibrated using polystyrene standards. [b] Conversion was determined by crude ^{1}H NMR analysis

Therefore, we designed other new monomers, **M3a-c** (**Scheme 2.5 a**) substituting one of the two cyclohexenes with a cyclopentene moiety, having the higher ring-strain energy to enhance the enthalpy gain. To our delight, polymerization using **M3a** at high concentration (1.5 M) successfully proceeded 100% conversion with monomer/catalyst (M/C) = 50 and 150 and the M_n of the resulting **P3a** was up to 20 kDa (**Scheme 2.5. c**, **Table 2.2, entries 4** and **5**). On the other hand, the polymerization of **M3b** containing an amide linker and

M3c containing a carbon linker at room temperature was less satisfactory with low conversions of 36% and 30%, respectively (**Table 2.2, entries 6** and **8**). To improve the polymerization conversion, we conducted polymerization at low temperature, 0 ^{o}C to increase the thermodynamic gain by decreasing the entropic factor ($\Delta G = \Delta H - T\Delta S$). As expected, their conversions increased by approximately 20% to give **P3b** and **P3c** with conversion up to 55% and M_n of 17–19 kDa (**Table 2.2, entries 7** and **9**). However, in all three cases, the polymerization efficiency was still low, implying that the driving force for the polymerization of **M3** derivatives was not sufficient because the polymer products still contained less stable five-membered rings compared to the monomers containing cyclohexene.

Scheme 2.6. A New Strategy for Improving Polymerization Efficiency and Selectivity of M4 derivatives by Forming a Six-membered Ring in the Polymer

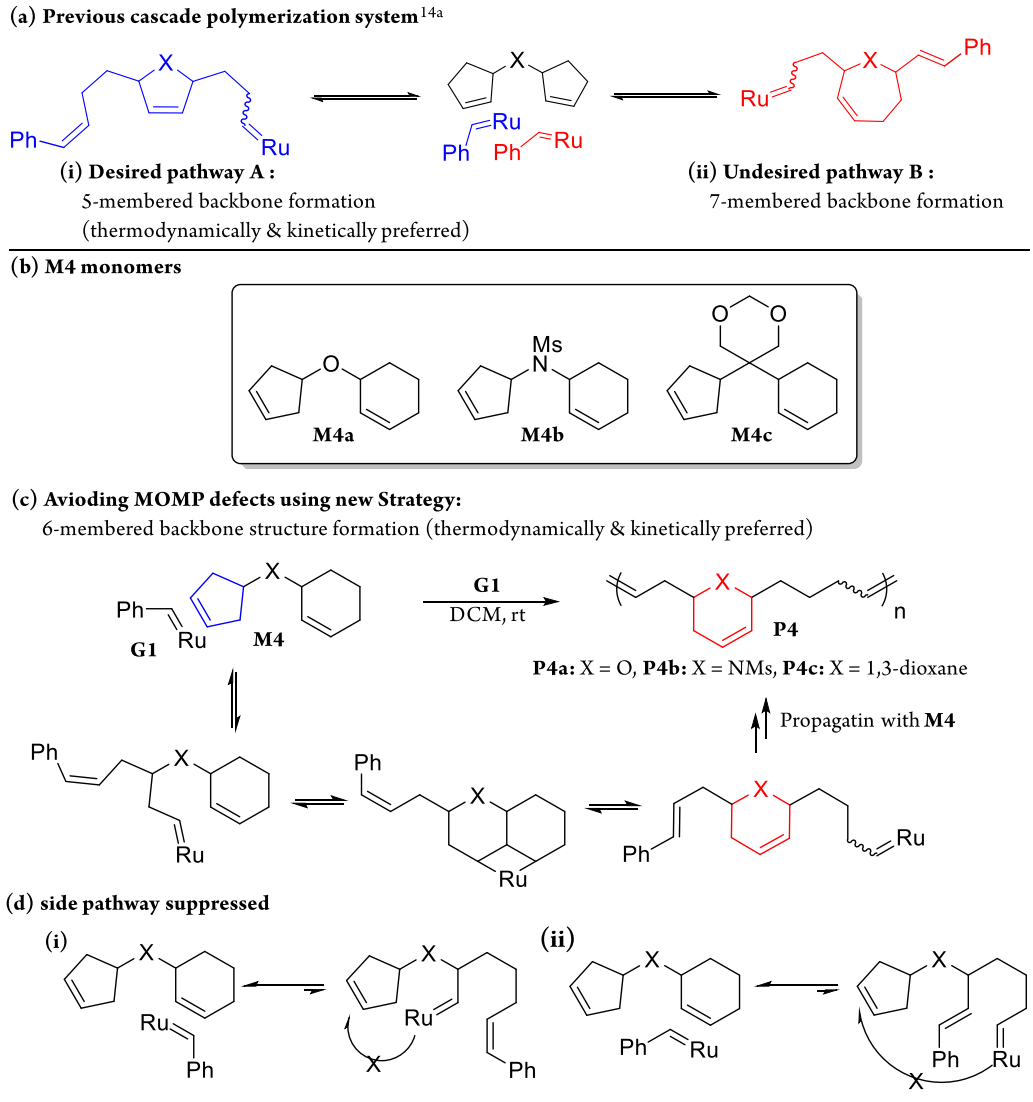

Based on the results of **M3**, we came up with a new strategy of monomer design to increase the thermodynamic gain by improving the stability of the polymer products.

Instead of forming five-membered ring repeat unit during the polymerization, the formation of the six-membered ring would enhance the driving force for the cascade polymerization. To test this, we synthesized new monomers, **M4** (**Scheme 2.6.b**) by using simple reactions such as S_N2 and Tsuji–Trost allylation to simply shift the position of olefin from the 3-position to the 4-position on the cyclopentene moiety in **M3**.[19]

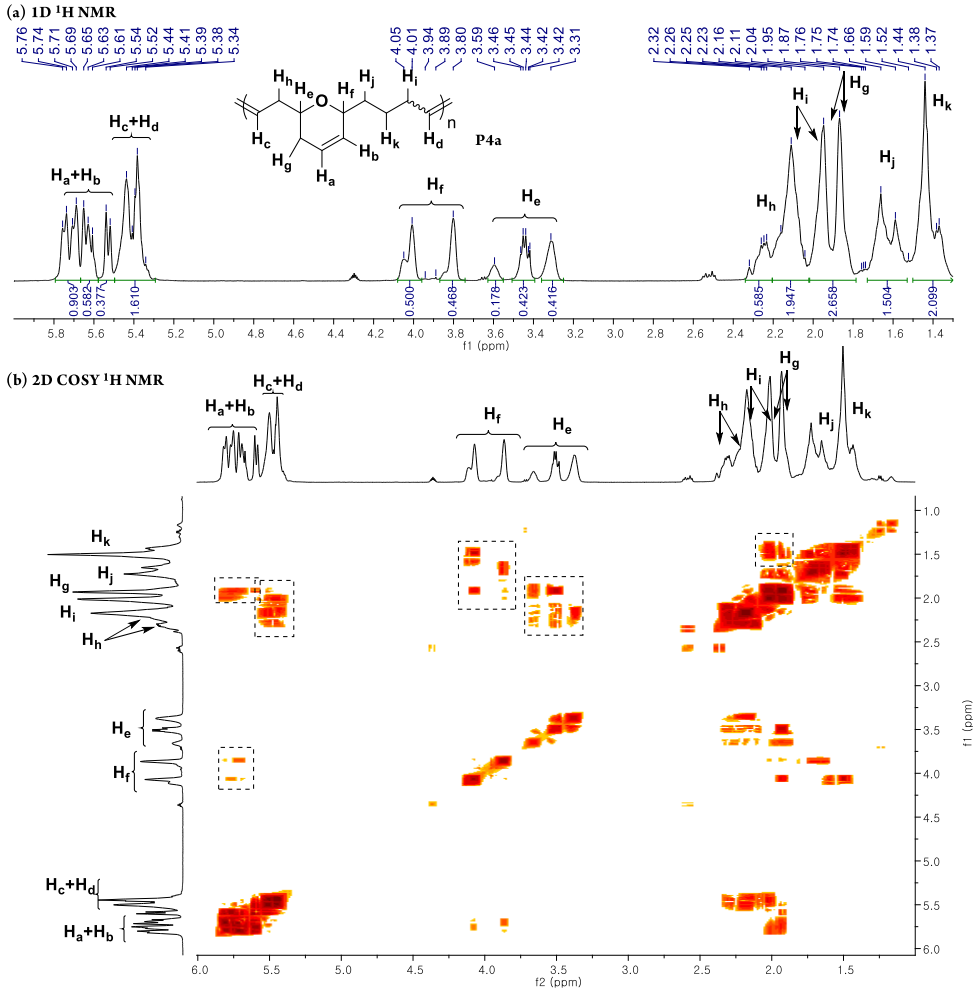

Figure 2.3. ^{1}H 1D and 2D COSY NMR spectra of P4a.

In addition to the strong enthalpic gain by the six-membered ring formation, in particularly, **M4** could achieve much faster and selective cascade polymerization because the catalyst would readily approach to the less sterically hindered 3-cyclopentene over the more sterically hindered 2-cyclohexene, thereby ring-opening the 3-cyclopentene first. Then, the resulting carbene would undergo ring-closing/opening reaction with the adjacent 2-cyclohexene (**Scheme 2.6.c**). The opposite sequence would be impossible not only because 2-cyclohexene were more crowded, but also the resulting carbene after the ring-opening would not reach to the neighboring 3-cyclopentene. Furthermore, even if it did reach the cyclopentene, eight-membered ring cyclization would be not kinetically and thermodynamically feasible (**Scheme 2.6.d**).

Table 2.3. Cascade polymerization of M4 monomers

Entry	Monomer	M:C	Conc. (M)	Time (h)	M_n[a] (kDa)	PDI[a]	Conv[b] (%)	Yield (%)
1	**M4a**	50:1	2.5	16	12.2	2.00	97	88
2	**M4a**	150:1	2.5	20	26.4	1.64	96	90
3	**M4a**	250:1	2.5	36	38.8	1.70	96	92
4	**M4a**	500:1	3.5	36	73.4	1.77	76	60
5	**M4b**	50:1	1.5	16	17.9	1.53	98	95
6	**M4b**	150:1	1.5	24	38.5	1.64	98	90
7	**M4b**	250:1	1.5	30	62.0	1.62	98	92
8	**M4b**	500:1	1.5	36	85.2	1.70	97	90
9	**M4b**	750:1	1.5	36	103.6	1.56	96	89
10	**M4b**	1000:1	3.5	36	121.0	1.69	70	63
11	**M4c**	50:1	1.5	18	20.3	1.68	95	91
12	**M4c**	150:1	1.5	20	52.7	1.72	97	93
13	**M4c**	250:1	1.5	24	67.0	1.75	97	90
14	**M4c**	500:1	1.5	36	85.0	1.93	96	88
15	**M4c**	750:1	1.5	36	127.5	1.81	96	92
16	**M4c**	1000:1	2.5	60	167.0	1.86	94	85

[a] Determined by THF SEC calibrated using polystyrene standards. [b] Conversion was determined by crude ^{1}H NMR analysis

To our delight, cascade polymerizations of **M4** derivatives produced well-defined **P4** with

high efficiency without any cross-linking even at higher concentration over 0.5 M. It is worth noting that ring-strain free cyclohexene moiety in **M4** which does not undergo ROMP by itself, would prevent cross-linking even at a high concentration over 2.5 M which is well above the critical concentration of cyclopentene. Particularly, cascade polymerization of **M4a** with M/C = 50-250 was successful with high efficiency and conversion over 96%, but the conversion dropped to 76% for the case of M/C = 500. The M_n of **P4a** increased from 12 kDa to 73 kDa according to the TON of 49 to 380 (**Table 2.3. Entries 1–4**). The structure of **P4a** was analyzed by ^{1}H NMR, ^{13}C NMR and MALDI-TOF (**Figure 2.3**, **Figure S29** and **Figure S63**). Although spectra of the **P4a** was complicated due to two stereogenic centers giving four diastereomers as well as *E*:*Z* mixture on the internal acyclic alkene, the detail polymer structure was confirmed by 2D COSY ^{1}H NMR (**Figure 2.3.b**) and MALDI showed clear mass difference corresponding to that of the monomer. The cascade polymerization of **M4b** with a methanesulfonyl amide linker also proceed well with excellent efficiency even with the M/C = 1000 and maximum TON of 700 and the M_n increased from 18 kDa to 121 kDa according to a TON of 48.5 to 700 (**Table 2.3. Entries 5–10**). Lastly, **M4c** containing the carbon linkage showed even higher efficiency where TON reached up to 940, and the resulting M_n increased from 20 kDa to 167 kDa under the optimized condition (M/C =50 to 1000, 2.5 M, for 60 h) (**Table 2.3. Entries 11–16**). These monomers (**M4a-c**) significant increase in polymerization efficiency compared to their analogous monomers such as **M3** and **M1** derivatives containing the same linker which only gave the maximum TON of 150 and 250, respectively. In short, forming the thermodynamically stable six-membered ring in the polymer backbone provided sufficient driving force for the successful cascade polymerization resulting in high molecular weights and high TON despite having low ring-strained cyclohexene moieties in the monomers.

Scheme 2.7. Superior Cascade Polymerization of M5 derivatives

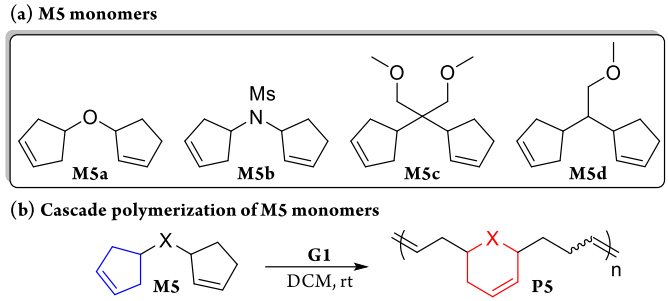

P5a: X = O, **P5b:** X = NMs ,**P5c:** X = 1,3-dimethoxypropane, **P5d:** X = methoxyethane

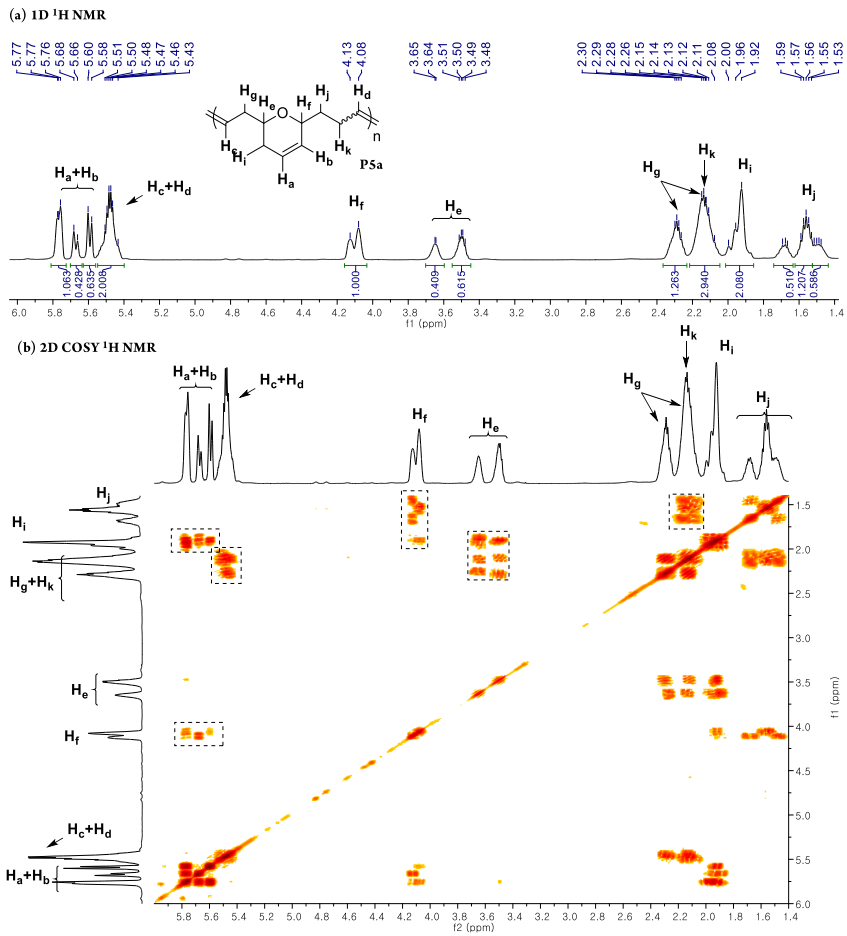

Figure 2.4. 1D and 2D COSY ¹H spectra of P5a.

Encouraged by the results on **M4** derivatives, we designed **M5a-d** by substituting the cyclohexene moieties on M4 with higher ring-strained cyclopentene moieties **(Scheme 2.7. a**). We anticipated that they would show even higher efficiency because ring-strain free six-membered rings would be formed from the monomer containing two cyclopentenes (**Scheme 2.7.b**). Firstly, we attempted polymerization of **M5a** containing an ether linkage at a high concentration over 1.0 M, but cross-linked gel was obtained just like **M1a**.[15a] In this case, two cyclopentenes with less steric congestion were likely to undergo faster ring-opening process leading to cross-linking, in contrast to the cases for **M4** derivatives. In other words, intermolecular ROMP of two cyclopentene moieties occurred dominantly at the high concentration condition instead of the desired sequential cascade polymerization. Fortunately, repeating the polymerization at low concentration of 0.5 M produced a well-defined P5a without any cross-linking over the wide range of the M/C = 50-1000 with a much shorter reaction time of 30 min. It is remarkable that the maximum TON up to 1000 was obtained in just 30 min to give **P5a** with M_n up to 101 kDa even at this low concentration (**Table 2.4**. **Entries 1**–**6**). Another monomer, **M5b** containing methanesulfonyl amide linker was successfully polymerized and in contrast to **M5a**, cross-linking did not occur even at the high concentration of 2.0 M. Presumably, it was due to steric hindrance of *N*-methanesulfonyl protecting group on **M5b** that suppressed the undesired independent ROMP of cyclopentene that would have led to cross-linking. At a relatively high concentration (1.0–2.0 M), **P5b** was produced with M_n from 14.6 kDa to 343 kDa and the TON up to 1940 (M/C = 50–2000, 2–4 hours) (**Table 2.4. Entries 7–13**). In particular, M_n of 343 kDa was the highest among all cascade polymerization attempted, testifying the power of this monomer design. Lastly, we polymerized **M5c** and **M5d** containing carbon linkages, at high concentration of over 1.0 M without cross-linking just like **M5b**. **P5c** containing two methoxyethane moieties was produced with the maximum

TON of 820 in 2–6 hours from the M/C= 50-1000 condition and its M_n increased from 14.2 kDa to 117 kDa (**Table 2.4**. **Entries 14**–**17**). A similar

monomer, **M5d** containing just one methoxyethane group showed significantly high reactivity under the condition of M/C = 50-2000 with a maximum TON of 1960. However, the M_n was relatively lower between 10.3 kDa and 42.6 kDa as compared to other monomers (**Table 2.4**. **Entries 18**–**22**). Using simple thermodynamic intuition, we successfully demonstrated cascade polymerization and provided some insight into what determined the efficiency of this cascade polymerization. Therefore, with proper monomer design, **M5** derivatives provided the highest driving force, thereby completing the cascade polymerization with either a short reaction time of 30 min or the maximum TON reaching to 1960 using just 0.05 mol% of the catalyst.

Since the cascade polymerization process was in thermodynamic equilibrium, even the isolated polymers could be depolymerized to the corresponding monomers via the reverse RO/RCM process. The degree of such depolymerization would reflect the thermodynamic preference of the monomer state over the polymer state or inverse of polymerization efficiency. The depolymerization experiment was conducted by adding fresh **G1** (2 mol%) to the each DCM solution of polymers in the low concentration of 0.04 M for 12 h. We previously reported depolymerization results that reverted 13% of **M1a**, 26% of **M1b**, and 34% of **M1c** as measured by ^{1}H NMR (**Scheme 2.7 a**).[15a] With these results in mind, the same experiments were repeated with **P3a**, **P4,** and **P5**. In case of **P3a**, which showed the lowest polymerization efficiency, the highest amount, 55% of

Table 2.4. Cascade polymerization of M5 monomers

Entry	Monomer	M:C	Conc.(M)	Time(h)	M_n [a] (kDa)	PDI[a]	Conv[b] (%)	Yield (%)
1	**M5a**	50:1	0.5	0.5	17.2	2.01	99	72
2	**M5a**	150:1	0.5	0.5	26.4	2.97	100	77
3	**M5a**	250:1	0.5	0.5	41.4	2.00	100	73
4	**M5a**	500:1	0.5	0.5	74.4	2.49	100	81
5	**M5a**	750:1	0.5	0.5	72.8	2.68	100	90
6	**M5a**	1000:1	0.5	0.5	100.7	2.51	100	87
7	**M5b**	50:1	2.0	2	14.6	1.61	97	63
8	**M5b**	150:1	2.0	2	26.8	2.02	97	76
9	**M5b**	250:1	2.0	2	55.0	1.50	97	92
10	**M5b**	500:1	2.0	4	103.9	1.69	98	90
11	**M5b**	750:1	2.0	4	153.0	2.04	98	88
12	**M5b**	1000:1	1.0	4	194.2	1.88	98	90
13	**M5b**	2000:1	1.0	4	343.4	1.50	97	91
14	**M5c**	50:1	1.0	2	14.2	1.58	99	80
15	**M5c**	250:1	2.0	2	61.8	1.65	100	90
16	**M5c**	500:1	2.0	4	82.7	1.79	97	87
17	**M5c**	1000:1	3.0	6	117.0	1.33	82	73
18	**M5d**	50:1	2.0	6	10.3	1.65	99	62
29	**M5d**	250:1	2.0	6	22.6	1.83	99	79
20	**M5d**	500:1	2.0	6	32.5	1.98	100	82
21	**M5d**	1000:1	2.0	6	38.1	2.01	100	84
22	**M5d**	2000:1	2.0	6	42.6	1.96	98	85

[a] Determined by THF SEC calibrated using polystyrene standards. [b] Conversion was determined by crude ^{1}H NMR analysis.

Scheme 2.7. Depolymerization of P1, P3, P4 and P5 derivatives

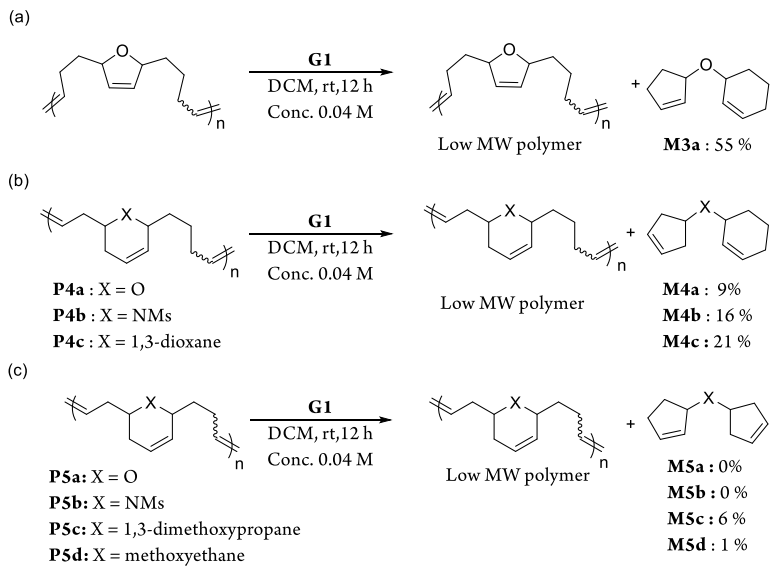

P3a, was depolymerized to **M3a** (**Scheme 2.7 b**). On the other hands, only 9% for **M4a**, 16% for **M4b**, and 21% for **M4c** were depolymerized, which are significantly lower than the analogous **P1** derivatives having the same linkers (**Scheme 2.7 c** vs **2.7 a**). Lastly, **P5** derivatives that were prepared with the best polymerization efficiency, indeed, produced the least amount of depolymerized monomer, 0 % for both **M5a** and **M5b** and just 6 and 1% for **M5c** and **M5d**, respectively (**Scheme 2.7 d**). These results matched with our original design and the polymerization data that the best cascade polymerization would be observed from the **M5** derivatives which produce six-membered rings from monomers containing two five-membered rings.

2.4. Conclusion

In conclusion, we investigated the cascade RO/RCM polymerization of monomers containing two polymerizable cyclopentene moieties with a first-generation Grubbs

catalyst. This tandem RO/RCM polymerization was carried out efficiently without side reactions such as cross-linking or depolymerization because, with the appropriate concentration, the precisely controlled cascade reaction occurred exclusively to produce a well-defined polymer microstructure. After then, we successfully expanded the monomer scope and greatly improved the efficiency or TON of the cascade polymerization by designing novel monomers. We could polymerize challenging monomers containing even low-strained cyclohexene by designing cascade polymerization to form a thermodynamically stable six-membered ring in the polymer backbone with a maximum TON of 940 and maximum M_n of 167 kDa. To further enhance the polymerization efficiency, another series of monomers containing two cyclopentene moieties produced enthalpically favored six-membered ring to give polymers exceeding M_n of 343 kDa with a maximum TON of 1940 in a much shorter time. This demonstrated an important lesson that novel monomer design based on understanding thermodynamic parameters, not only broadened the polymerization scope but also greatly improved the polymerization efficiency by up to eight-fold compared to the previous results.

2.5. Experimental Section

1. General experimental

All reagents which are commercially available were used without further purification. For polymerization, DCM was distilled from calcium hydride. DCM was degassed by Ar bubbling for 10 minutes before using on polymerization. Thin-layer chromatography (TLC) was carried out on MERCK TLC silica gel 60 F254 and flash column chromatography was performed using MERCK silica gel 60 (0.040~0.063 mm). ^{1}H-NMR was recorded by Varian/Oxford As-500 (500 MHz) spectrometers. THF SEC (size exclusion chromatography) was carried out at 1.0 mL/min. SEC for polymer analysis was carried out

with Waters system (1515 pump, 2414 refractive index detector) and Shodex GPC LF-804 column on samples diluted in 0.001-0.003 wt% by THF (HPLC grade, Honeywell Burdick & Jackson®) andfiltered with a 0.2-μm PTFE filter. The columns were thermostatted at 35 ^{o}C.

2. Monomer preparation & characterization

Preparation of M1a

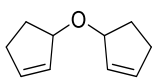

Ether formation from allylic alcohols catalyzed by samarium trichloride By Ouertani, Mohsen; Collin, Jacqueline; Kagan, Henri B. From *Tetrahedron* **1985**, 41(18), 3689-93.

^{1}H-NMR and ^{13}C-NMR analysis data are available in the same literature.

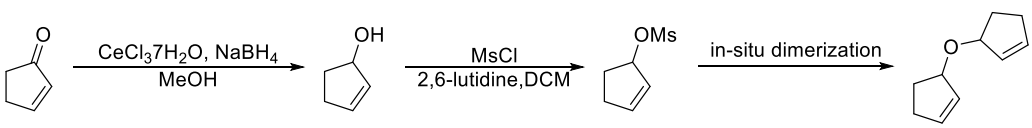

To a solution of 2-cyclopentenone (2.49 g, 30 mmol) and cerium trichloride heptahydrate(12.30 g, 33 mmol) in MeOH(60 ml), $NaBH_4$(2.0 g,36 mmol) was added slowly with an ice bath and stirred for 15 min. The reaction mixture was extracted with diethyl ether and water and dried with $MgSO_4$. Cyclopentenol is purified by silica gel column chromatography (Ethyl Acetate /Hexane = 1/1) to yield corresponding alcohol with 60-80 % yield. With cyclopentenol(0.87 g, 10 mmol) and DCM(25 ml) solution, 2,6-lutidine(1.3 ml, 12 mmol) was added to solution. After 5 mins, Mesyl chloride (0.41 ml, 5 mmol) is added slowly. During the reaction, not only Mesylate but also Monomer1 was synthesized by in-situ dimerization. The yield of Corresponding ether is 40 %.

Preparation of monomer M1b

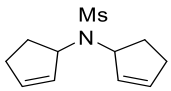

^{1}H NMR (500 MHz, $CDCl_3$, ppm) δ 6.0 (2H, m), 5.68(H, m), 5.62 (1H, m), 4.68 (1H, m), 2.88 (1H, s), 2.55 (2H, m), 2.29 (4H, m), 1.96 (2H, m)

^{13}C NMR (400 MHz, $CDCl_3$, ppm) δ 135.55, 135.13, 130.29, 129.58, 63.31, 63.28, 42.47, 42.11, 31.49, 31.45, 29.89, 29.49

HRMS (ESI) calcd.for $(C_{11}H_{17}NO_2S)^-$ Na^+ 250.0872 found, 250.0871

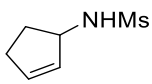

^{1}H NMR (500 MHz, $CDCl_3$, ppm) δ 5.96 (1H, m), 5.71 (1H, m), 4.53 (1H, m), 4.39 (1H, m), 2.97 (1H, s), 2.28-2.42 (3H, m), 1.71 (1H, m)

^{13}C NMR (400 MHz, $CDCl_3$, ppm) δ 136.24, 130.56, 59.89, 41.60, 32.09, 30.92

HRMS (ESI) calcd.for $(C_6H_{11}NO_2S)^-$ Na^+ 184.0403 found, 184.0402

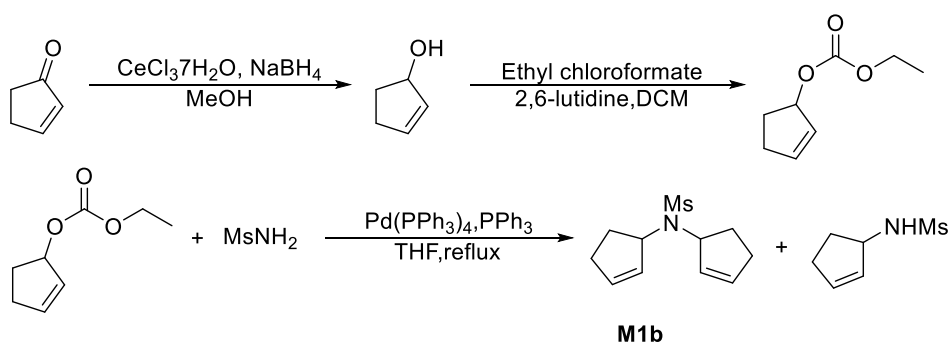

M1b

To a solution of 2-cyclopentenone (2.49 g, 30 mmol) and cerium trichloride heptahydrate (12.30 g,33 mmol) in MeOH (60 ml), $NaBH_4$ (2.0 g,36 mmol) was added slowly with an

ice bath and stirred for 15 min. The reaction mixture was extracted with diethyl ether and water and dried with $MgSO_4$. Cyclopentenol is purified by silica gel column chromatography (ethyl acetate /hexane = 1/1) to yield corresponding alcohol with 60-80 % yield.

With cyclopentenol (3 g, 35.7 mmol) and DCM solution, 2,6-lutidine (1.2 equiv) was added to solution. After 5mins, Ethyl chloroformate(1.1 equiv) is added slowly. Corresponding carboxylate is purified by silica gel column chromatography (ethyl acetate/hexane = 1/10) with 70 % yield

p-Mesylsulfonamide (570 mg, 5.5 mmol) was added to THF under argon at room temperature. The mixture was stirred for 10 min. To this was added $Pd(PPh)_4$ (0.65 g,0.55 mmol) and PPh_3 (290 mg,1,1 mmol), followed by cyclopent-2-enyl carboxylate (2.2 g,14 mmol). The resulting bright yellow solution was heated under reflux for 10 h. The mixture was then partitioned between diethyl ether and water. The organic layer was separated, and the aqueous extracted with diethyl ether. The organic extracts were combined, dried over $MgSO_4$ filtered and concentrated in vacuo. Purification of the resulting brown residue on silica gel (1:10 ethly acetate/ hexanes) gave **M2** (50 % yield).

Preparation of M1c

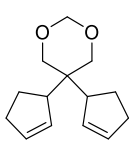

^{1}H NMR (500MHz, $CDCl_3$, ppm) δ 5.8 (4H, m), 3.75 (4H, t), 3.04 (2H, m), 2.28 (4H, m), 1.91 (2H, s), 1.78 (2H, m)

^{13}C NMR (400MHz, $CDCl_3$, ppm) δ 132.02, 131.73, 131.31, 131.14, 94.09, 93.93, 72.21, 71.55, 70.93, 48.40, 48.36, 32.00, 31.86, 25.14, 24.93

HRMS (CI+) calcd.for $C_{14}H_{21}O_2^+$ 222.1541 found, 222.1537

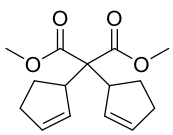

^{1}H NMR (500MHz, $CDCl_3$, ppm) δ 5.72 (4H, m), 3.62 (6H, m), 3.43 (2H, broad), 2.21 (4H, broad), 2.00 (2H, m), 1.77(1H, m), 1.65 (1H, m)

^{13}C NMR (400MHz, $CDCl_3$, ppm) δ 171.12, 170.86, 170.69, 132.12, 131.74, 131.28, 131.07, 65.16, 64.83, 51.86, 51.60, 51.48, 49.58, 49.52, 31.65, 31.51, 25.66, 25.35

HRMS (ESI) calcd.for $(C_{15}H_{20}O_4)^-$ Na^+ 287.1254 found, 287.1254

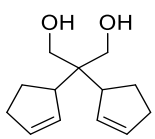

^{1}H NMR (500MHz, $CDCl_3$, ppm) δ 5.90 (2H, m), 5.81 (2H, m), 3.78 (2H, m), 3.68 (2H, m), 2.99 (2H, m), 2.35 (6H, m), 1.92(2H, m), 1.80 (2H, m)

^{13}C NMR (400MHz, $CDCl_3$, ppm) δ 132.56, 132.43, 131.86, 131.72, 66.64, 66.44, 66.23, 48.30, 48.28, 46.30, 46.08, 32.09, 31.91, 24.70, 24.67

HRMS (CI+) calcd.for $C_{13}H_{21}O_2^+$ 209.1542 found, 209.1541

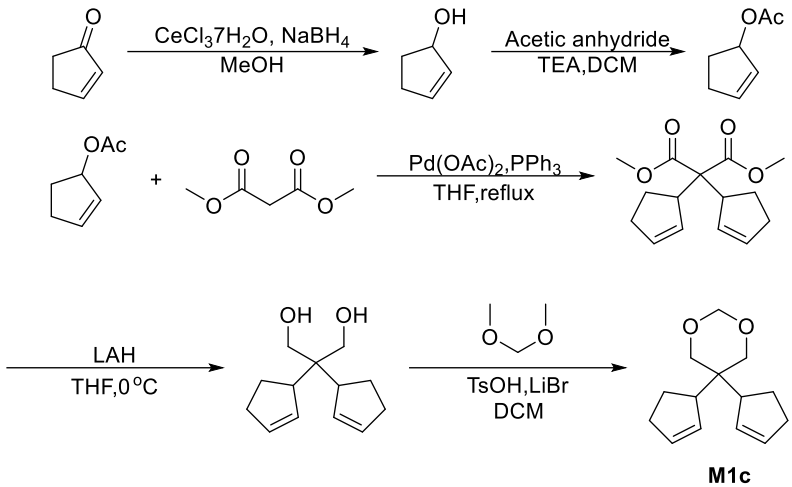

M1c

To a solution of 2-cyclopentenone and cerium trichloride heptahydrate in MeOH, $NaBH_4$ was added slowly with an ice bath and stirred for 15 min. The reaction mixture was extracted with diethyl ether and water and dried with $MgSO_4$. Cyclopentenol is purified by silica gel column chromatography (ethyl acetate /hexane = 1/1) to yield corresponding alcohol with 60-80 % yield.

With cyclopentenol (3.0 g, 35 mmol) and DCM solution, TEA (4.55 ml, 45 mmol) & DMAP (0.43 g, 3.57 mmol) was added to solution. After 5mins, acetic anhydride (3.9 ml, 40 mmol) is added slowly. Corresponding acetate derivative is purified by silica gel column chromatography (ethyl acetate/hexane = 1/10) with 80 % yield

To a suspension of NaH (1.0 g, 42 mmol) in THF under argon at room temperature was added dimethylmalonate (1.9 ml, 12 mmol). The mixture was stirred for 10 min. To this was added $Pd(OAc)_2$ (0.27 g, 1.2 mmol) and PPh_3 (0.64 g, 2.5 mmol), followed by cyclopent-2-enyl acetate (3.23 g, 25 mmol). The resulting bright yellow-green solution was heated under reflux for 10 h. The mixture was then partitioned between diethyl ether and water. The organic layer was separated, and the aqueous extracted with diethyl ether. The

organic extracts were combined, dried over $MgSO_4$ filtered and concentrated in vacuum. Purification of the resulting brown residue on silica gel (1:10 Ethly acetate/ hexanes) gave dimethyl 2,2-di(cyclopent-2-en-1-yl)malonate (50 % yield).

dimethyl 2,2-di(cyclopent-2-en-1-yl)malonate(0.81 g, 3 mmol) was added to Ar-purged flask and dissolved in THF. The solution was cooled to 0°C and lithium aluminum hydride (230 mg, 6 mmol) was added slowly. The reaction mixture was stirred for 2 hours until all ester groups were converted to alcohol. The resulting mixture was quenched by successive addition of water (1 ml per 1 g of LAH) in an ice bath, 10 % NaOH solution (2 ml per 1 g of LAH), and water (3ml per 1g of LAH). The resulting mixture was filtered through celite pad and ecaporated under reduced pressure. Diol was purified by silica gel column chromatography (ethyl acetate/hexane = 1/3) to yield over 90 %

2,2-di(cyclopent-2-en-1-yl)propane-1,3-diol(624mg,3mmol) was added to flask and dissolved in DCM(6 ml). Toluenesulfonyl acid (171 mg, 0.9 mmol) and Lithium bromid e(52 mg,0.6 mmol) is added to solution and methoxypropane (0.4 ml, 4.5 mmol) is added to solution. The reaction mixture was extracted with dichloromethane and water and dried with $MgSO_4$. M3 is purified by silica gel column chromatography (ethyl acetate/hexane = 1/5) to yield corresponding alcohol with 90 % yield.

Preparation of **M2a**

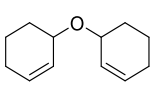

Direct synthesis of ethers via zinc chloride-mediated etherification of alcohols in DCM by Kim, S; Chung, K-N; and Yang, S-B. *J. Org. Chem*., **1987**, *52* (17), pp 3917

^{1}H-NMR and ^{13}C-NMR analysis data are also available in the same literature.

In-situ dimerization: To a solution of 2-cyclohexenone (2.49 g, 30 mmol) and cerium trichloride heptahydrate (12.30 g, 33 mmol) in MeOH (60 ml), $NaBH_4$ (2.0 g, 36 mmol) was added slowly with an ice bath and stirred for 15min. The reaction mixture was extracted with diethyl ether and water and dried with $MgSO_4$. Cyclohexenol is purified by silica gel column chromatography (ethyl acetate/hexane = 1/1) to yield corresponding alcohol with 70-80% yield. With this 2-cyclohexen-1-ol (0.87 g, 10 mmol) and DCM (25 ml) solution, 2,6-lutidine (1.3 ml, 12 mmol) was added to solution. After 5mins, Mesyl chloride (0.41 ml, 5 mmol) is added slowly. During the reaction, not only Mesylate but also **M2** was synthesized by *in-situ* dimerization. The yield of Corresponding ether, **M2a** is 40%.

Preparation of **M2b**

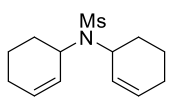

^{1}H NMR (500 MHz, $CDCl_3$, ppm) δ 5.84 (2H, d), 5.59 (2H, s), 4.86(1H, s), 4.15(2H, s) 2.93(3H, s), 2.06(2H, s), 1.98(6H, s), 1.84(2H, m), 1.62(2H, m)

^{13}C NMR (500MHz, CDCl3, ppm) δ 130.81, 130.60, 129.34, 129.04, 55.07, 55.05, 43.10, 43.05, 30.07, 29.26, 24.29, 24.27, 22.28, 22.27

HRMS (ESI) calcd.for $(C_{13}H_{21}NO_2S)^-Na^+$ 278.3861 found, 278.3863

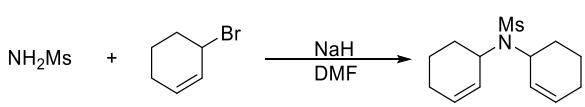

SN2 reaction: To a suspension of NaH (240 mg, 6 mmol) in DMF under argon at room temperature was added methanesulfonamide (280 mg, 3.0 mmol). The mixture was stirred

for 10 min. To this was added 3-bromocyclohexene (0.24 ml, 0.8 mmol) The resulting brown solution was heated under room temperature. The mixture was then partitioned between diethyl ether and water. The organic layer was separated, and the aqueous extracted with diethyl ether. The organic extracts were combined, dried over $MgSO_4$ filtered and concentrated in vacuum. Purification of the resulting brown residue on silica gel (ethly acetate/ hexane = 1/5) gave **M2b** (85% yield).

Preparation of **M2c**

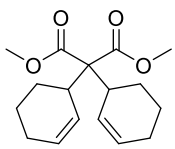

^{1}H NMR (500 MHz, $CDCl_3$, ppm) δ 5.71 (2H, d), 5.54 (2H, s), 3.68(6H, d), 3.15(2H, d), 2.04(2H, s), 1.92(5H, m), 1.63(4H, d), 1.24(3H, s)

^{13}C NMR (500MHz, CDCl3, ppm) δ 165.73, 165.58, 165.27, 124.13, 124.07, 122.61, 122.26, 60.60, 60.29, 46.85, 46.70, 46.61, 32.91, 20.22, 20.07, 19.81, 18.87, 17.65, 17.62

HRMS (ESI) calcd.for $(C_{17}H_{24}O_4)^-Na^+$ 315.3598 found, 315.3596

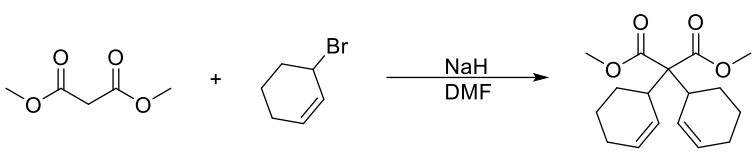

SN2 reaction: To a suspension of NaH (240 mg, 6 mmol) in DMF under argon at room temperature was added dimethylmalonate (400 mg, 3.0 mmol). The mixture was stirred for 10 min. To this was added 3-bromocyclohexene (2.4 ml, 8 mmol) The resulting brown solution was heated under room temperature. The mixture was then partitioned between diethyl ether and water. The organic layer was separated, and the aqueous extracted with diethyl ether. The organic extracts were combined, dried over $MgSO_4$ filtered and

concentrated in vacuum. Purification of the resulting brown residue on silica gel (ethly acetate/hexane = 1/10) gave **M2c** (73% yield).

Preparation of **M3a**

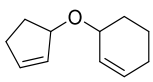

^{1}H NMR (500 MHz, $CDCl_3$, ppm) δ 5.83(2H, m), 5.75 (2H, m), 4.00 (2H, d), 2.01 (2H, d), 1.95 (2H, d),1.81 (4H, m),1.68 (2H, m), 1.54 (2H, m)

^{13}C NMR (500MHz, CDCl3, ppm) δ 130.37,130.29,128.84,128.70,70.58,70.53,29.64,29.19,35.19,19.52,19.25

HRMS (ESI) calcd.for $(C_{11}H_{16}O)^-$ Na^+ 187.1093 found, 187.1091

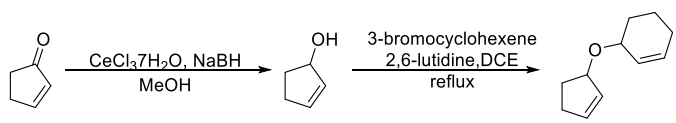

Etherification: To a solution of 2-cyclopentenone (2.63 g, 30 mmol) and cerium trichloride heptahydrate (12.30 g, 33 mmol) in MeOH (60 ml), $NaBH_4$ (2.0g, 36 mmol) was added slowly with an ice bath and stirred for 15min. The reaction mixture was extracted with diethyl ether and water and dried with $MgSO_4$. The resulting cyclopentenol in crude solution is purified by silica gel column chromatography (ethyl acetate/hexane = 1/1) to yield corresponding alcohol with 70-80% yield. With purified 2-cyclopenten-1-ol (1.64 g, 20 mmol) and DCE (25 ml) solution, 2,6-lutidine (2.6 ml, 24 mmol) was added to solution. After 5mins, 3-bromocyclohexene (0.64 ml, 5 mmol) is added slowly. After 6hr, the yield of Corresponding ether, **M3a** is 60-70%

Preparation of **M3b**

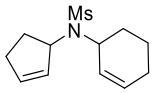

^{1}H NMR (500 MHz, $CDCl_3$, ppm) δ 5.99(1H, m), 5.85 (1H, t), 5.66 (1H, m) 5.55(1H, dd), 4.58-4.68 (2H, m), 4.18 (1H, m), 2.89(3h, d), 2.59(1H, m), 2.24(2H, m), 1.95(2H, m),1.86(2H, m), 1.60 (2H, m)

^{13}C NMR (500MHz, CDCl3, ppm) δ 131.42, 130.57, 130.48, 129.49, 128.81, 63.52, 62.19, 55.23, 54.86, 42.99, 42.69, 31.43, 30.48, 30.05, 29.62, 29.22, 24.37, 24.27, 22.18

HRMS (ESI) calcd.for $(C_{12}H_{19}NO_2S)^-Na^+$ 264.1030 found, 264.1029

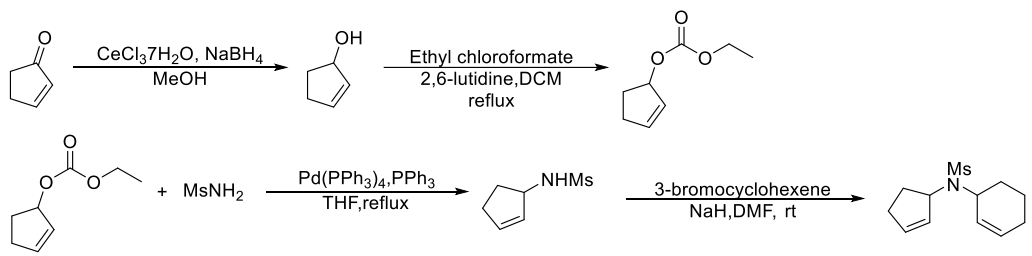

1. Preparing substrate for Tsuji-Trost allylation: To a solution of 2-cyclopentenone (2.49 g, 30 mmol) and cerium trichloride heptahydrate (12.30 g, 33 mmol) in MeOH (60 ml), $NaBH_4$ (2.0 g, 36 mmol) was added slowly with an ice bath and stirred for 15 min. The resulting reaction mixture was extracted with diethyl ether and water and dried with $MgSO_4$. 2-cyclopenten-1-ol is purified from a crude solution by silica gel column chromatography (ethyl acetate/hexane = 1/1) to yield corresponding alcohol with 70-80% yield. With 2-cyclopenten-1-ol (3 g, 35.7 mmol) and DCM solution, 2,6-lutidine (1.2 equiv) was added to solution. After 5mins, Ethyl chloroformate (1.5 equiv) is added slowly with an ice bath. After finishing addition of Ethyl chloroformate, this RBF was a move to reflux condition for 6 hours. Cyclopent-2-enyl carboxylate is purified by silica gel column chromatography (ethyl acetate/hexane = 1/10) with 70% yield.

2. Tsuji-Trost allylation: *p*-Mesylsulfonamide (570 mg, 5.5 mmol) was added to THF under argon at room temperature. The mixture was stirred for 10 min. To this was added $Pd(PPh)_4$ (0.65 g, 0.55 mmol) and PPh_3 (290 mg, 1.1 mmol), followed by cyclopent-2-enyl carboxylate (2.2 g, 14 mmol). The resulting bright yellow solution was heated under reflux for 10 hours. The mixture was then partitioned between diethyl ether and water. The organic layer was separated, and the aqueous extracted with diethyl ether. The organic extracts were combined, dried over $MgSO_4$ filtered and concentrated in vacuo. Purification of the resulting brown residue on silica gel (ethly acetate/hexane = 1/10) gave *N*-(cyclopent-2-en-1-yl)methanesulfonamide (50% yield).

3. SN2 reaction: To a suspension of NaH (40 g, 1 mmol) in DMF under argon at room temperature was added *N*-(cyclopent-2-en-1-yl)methanesulfonamide (0.5 g, 0.30 mmol) which was obtained from previous Tsuji-Trost allylation. The mixture was stirred for 10 min. To this was added 3-bromocyclohexene (0.12 ml, 0.4 mmol) The resulting brown solution was heated under room temperature. The mixture was then partitioned between diethyl ether and water. The organic layer was separated, and the aqueous extracted with diethyl ether. The organic extracts were combined, dried over $MgSO_4$ filtered and concentrated in vacuum. Purification of the resulting brown residue on silica gel (ethly acetate/hexane = 1:5) gave **M3b** (62% yield).

Preparation of M3c

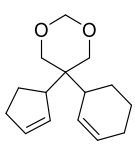

^1H NMR (500 MHz, $CDCl_3$, ppm) δ 5.84 (2H, d), 5.76 (2H, s), 4.86(1H, s), 4.71(1H, s), 3.90(2H, m), 3.64(2H, m), 2.86(1H, t), 2.74(1H, t), 2.24(2H, m), 1.98(1H, s), 1.84(4H, m),

1.69(2H, m), 1.49(2H, m)

^{13}C NMR (500MHz, CDCl3, ppm) δ 131.74, 128.21, 128.05, 93.99, 71.28, 71.19, 70.80, 70.65, 47.68, 39.85, 37.89, 37.78, 31.96, 26.19, 25.19, 24.47, 23.10

HRMS (ESI) calcd.for $(C_{15}H_{22}O_2)^-Na^+$ 257.1509 found, 257.1511

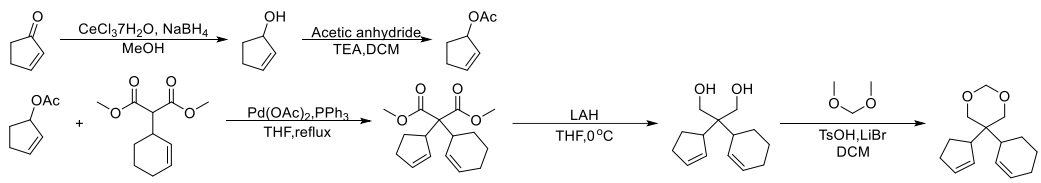

1. Preparing substrate for Tsuji-Trost allylation: To a solution of 2-cyclopentenone and cerium trichloride heptahydrate in MeOH, $NaBH_4$ was added slowly with an ice bath and stirred for 15 min. This reaction mixture was extracted with diethyl ether and water and dried with $MgSO_4$. 2-cyclopenten-1-ol is purified by silica gel column chromatography (ethyl acetate /hexane = 1/1) to yield with 70-80 % yield. With this cyclopentenol (3.0 g, 35 mmol) and DCM solution, TEA (4.55 ml, 45 mmol) & DMAP (0.43 g, 3.57 mmol) was added to solution. After 5mins, acetic anhydride (3.9 ml, 40 mmol) is added slowly. Corresponding acetate, cyclopent-2-en-1-yl acetate is purified by silica gel column chromatography (ethyl acetate/hexane = 1/10) with 80% yield.

2. SN2 reaction: To a suspension of NaH (1.0 g, 42 mmol) in DMF under argon at room temperature was added dimethylmalonate (1.9 ml, 12 mmol). The mixture was stirred for 10 min. To this was added 3-bromocyclohexene (1.2ml, 15 mmol) The resulting brown solution was heated under room temperature. The mixture was then partitioned between diethyl ether and water. The organic layer was separated, and the aqueous extracted with diethyl ether. The organic extracts were combined, dried over $MgSO_4$ filtered and concentrated in vacuum. Purification of the resulting brown residue on silica gel (ethly acetate/ hexane = 1/5) gave dimethyl 2-cyclohex-2-en-1-yl malonate (75% yield).

3. Tsuji-Trost allyalation: To a suspension of NaH (1.0 g, 42 mmol) in THF under argon at room temperature was dimethyl 2-cyclohex-2-en-1-yl malonate (1.9 ml, 12 mmol). The mixture was stirred for 10 min. To this RBR, $Pd(OAc)_2$ (0.27 g, 1.2 mmol) and PPh_3 (0.64 g, 2.5 mmol) were added and cyclopent-2-enyl acetate (3.23 g, 25 mmol) was also added after 5 min. The resulting bright yellow-green solution was heated under reflux for 10 h. The mixture was then partitioned between diethyl ether and water. The organic layer was separated, and the aqueous extracted with diethyl ether. The organic extracts were combined, dried over $MgSO_4$ filtered and concentrated in vacuum. Purification of the resulting brown residue on silica gel (ethly acetate/hexanes = 1/10) gave dimethyl dimethyl 2-(cyclohex-2-en-1-yl)-2-(cyclopent-2-en-1-yl)malonate (50% yield).

4. Reduction and Protection: The resulting dimethyl 2-(cyclohex-2-en-1-yl)-2-(cyclopent-2-en-1-yl)malonate (0.81 g, 3 mmol) was added to Ar-purged flask and dissolved in THF. The solution was cooled to 0°C and lithium aluminum hydride (230 mg, 6 mmol) was added slowly. The reaction mixture was stirred for 2 hours until all ester groups were converted to alcohol. The resulting mixture was quenched by successive addition of water (1 ml per 1 g of LAH) in an ice bath, 10 % NaOH solution (2 ml per 1 g of LAH), and water (3ml per 1g of LAH). The resulting mixture was filtered through celite pad and ecaporated under reduced pressure. Diol was purified by silica gel column chromatography (ethyl acetate/hexane = 1/3) to yield over 90%. 2-(cyclohex-2-en-1-yl)-2-(cyclopent-2-en-1-yl)propane-1,3-diol (624 mg, 3 mmol) was added to flask and dissolved in DCM(6 ml). Toluenesulfonyl acid (171 mg, 0.9 mmol) and Lithium bromide (52 mg, 0.6 mmol) are added to the solution and dimethoxy methane (0.4 ml, 4.5 mmol) is added to the solution. The reaction mixture was extracted with dichloromethane and water and dried with $MgSO_4$. **M3c** is purified by silica gel column chromatography (ethyl acetate/hexane = 1/5) with 90% yield.

Preparation of **M4a**

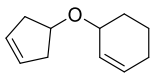

^{1}H NMR (500 MHz, $CDCl_3$, ppm) δ5.99(1H, σ), 5.85(2H, m), 5.77(1H, m), 4.72(1H, s), 3.98(1H, s), 2.53(1H, m),2.23(2H, m), 2.04-1.98(2H, dd),1.76(4H, d),1.69(1H, m),1.58(1H, m)

^{13}C NMR (500MHz, CDCl3, ppm)

δ 134.82,131.91,131.69,130.27,128.77,128.62,82.76,71.51,71.30,31.02,30.96,30.83,29.58 ,25.18,19.46,19.32

HRMS (ESI) calcd.for $(C_{11}H_{16}O)^{-}$ Na^{+} 187.1093 found, 187.096

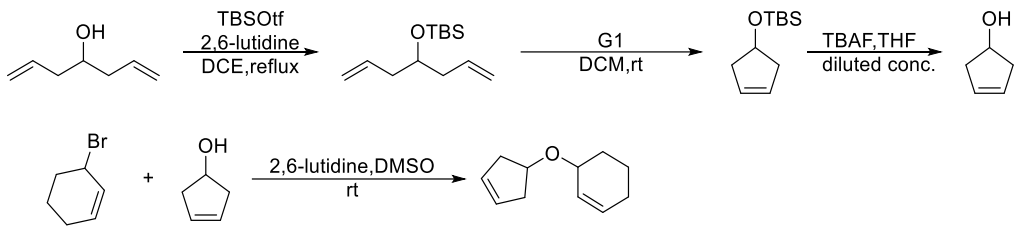

Etherification: Put 1,6-heptadien-4-ol, 2,6-Lutidine and DCM in the RBF. Then, place the RBF in an ice bath and slowly drop *tert*-butyl dimethyl silyl triflate. The reaction is carried out under reflux conditions for about 6 hours. The reaction mixture was extracted with DCM and water and dried with $MgSO_4$. Crude is purified by silica gel column chromatography (Ethyl Acetate/Hexane = 1/50) to yield *tert*-butyl(hepta-1,6-dien-4-yloxy)dimethylsilane with about 90% yield. This heptadiene is reacted with the Grubbs first generation catalyst (**G1**) to perform ring closing metathesis. The reaction proceeds at room temperature for about 12 hours, and the yield of the reaction is about 70-80%. After the ring closure product was diluted to 0.03 M in THF, TBAF was added at 0 ° C, and the reaction was allowed to proceed for about 1 hour, resulting in deprotected alcohol. The reaction crude can be obtained in an EA / Hexane 1: 1 condition immediately after removal

of the solvent to obtain a clean alcohol with a yield of 60-70%. With 3-cyclopentenol (1.64 g, 20 mmol) and DMSO (25 ml) solution, 2,6-lutidine (2.6 ml, 24 mmol) was added to solution. After 5mins, 3-bromocyclohexene (0.41 ml, 5 mmol) is added slowly with a reflux condition. After 12 hours, the yield of Corresponding ether, **M4a** is 40-50%

Preparation of M4b

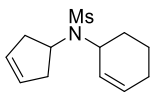

^{1}H NMR (500 MHz, $CDCl_3$, ppm) δ 5.91(1H, m), 5.70(2H, s), 5.53(1H, d), 4.24(1H, s), 4.07(1H, t), 2.91(3H, s), 2.79 (2H, m), 2.56 (2H, m), 2.02 (4H, s), 1.86 (1H, d), 1.77 (1H, dd), 1.62 (2H, dd)

^{13}C NMR (500MHz, CDCl3, ppm)

δ 131.86, 129.19, 120.00, 128.58, 56.25, 55.41, 42.62, 38.78, 37.46, 29.34, 24.33, 21.98

HRMS (ESI) calcd.for $(C_{12}H_{19}NO_2S)^{-}Na^{+}$ 264.1030 found, 264.1029

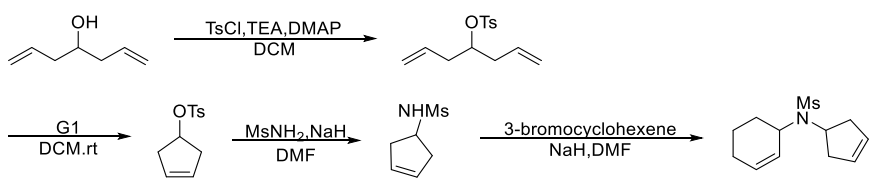

1. SN2 reaction: Put 1,6-heptadien-4-ol, Triethylamine (TEA) and DCM in the RBF. Then, place the RBF in an ice bath and put *p*-toluenesulfonic acid. The reaction is carried out under reflux conditions for about 12 hours. The reaction mixture was extracted with Ether and water and dried with $MgSO_4$. Crude is purified by silica gel column chromatography (ethyl acetate/hexane = 1/50) to yield hepta-1,6-dien-4-yl 4-methylbenzenesulfonate with about 80% yield.

2. Ring-closing metathesis: This heptadiene is reacted with the **G1** to perform ring closing

metathesis. The reaction proceeds at room temperature for about 12 hours, and the yield of the reaction is about 70-80%. cyclopent-3-en-1-yl 4-methylbenzenesulfonate is used for the next SN2 reaction with methanesulfonyl amide, NaH and DMF condition for 6 hours. The reaction mixture was extracted with Ether and water and dried with $MgSO_4$. This crude solution was purified by silica gel column chromatography (ethyl acetate/hexane = 1/30) to yield *N*-(cyclopent-3-en-1-yl)methanesulfonamide about 65% yield.

3. SN2 reaction: The resulting *N*-(cyclopent-3-en-1-yl)methanesulfonamide is dissolved in DMF and slowly added NaH with an ice bath. After 20 min, 3-bromocyclohexene was slowly injected and the reaction proceeds at reflux condition for 12 hours. The reaction mixture was extracted with Ether and water and dried with $MgSO_4$. The reaction crude was purified by silica gel column chromatography (ethyl acetate/hexane = 1/30) to yield the final monomer, *N*-(cyclohex-2-en-1-yl)-*N*-(cyclopent-3-en-1-yl)methanesulfonamide, **M4b** about 50% yield.

Preparation of **M4c**

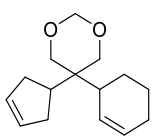

^{1}H NMR (500 MHz, $CDCl_3$, ppm) δ 5.74(1H, s), 5.68(1H, s), 4.92(1H, d), 4.72(1H, d), 3.96(2H, d), 3.66-3.74 (2H, dd), 2.83 (1H, m), 2.41 (1H,q), 2.26 (4H, d), 1.98 (2H, s), 1.87 (2H, t)

^{13}C NMR (500MHz, CDCl3, ppm)

δ 129.85, 128.05, 94.10, 70.87,70.72, 40.44, 39.06,37.84, 22.80,22.61, 25.19, 24.41,23.18

HRMS (ESI) calcd.for $(C_{15}H_{22}O_2)^-Na^+$ 257.1508 found, 257.1510

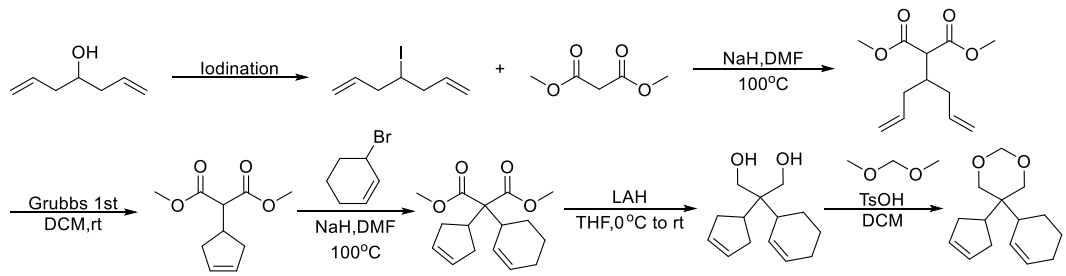

1. Iodination and S_N2 reaction: Put 1,6-heptadien-4-ol into DCM in RBF. Then, place the RBF in an ice bath and put Iodine and PPh_3. The reaction is carried out at room temperature for about 3 hours. The reaction mixture was extracted with DCM and water and dried with $MgSO_4$. Crude is purified by silica gel column chromatography (ethyl acetate/hexane = 1/100) to yield 4-iodohepta-1,6-diene about 70% yield.

2. Ring-closing metathesis: Dimethyl malonate and NaH was added to DMF solution. After 20 mins, 4-iodohepta-1,6-diene is added slowly. Corresponding malonate derivative is purified by silica gel column chromatography (ethyl acetate/hexane = 1/20) with a 75% yield. This heptadiene is reacted with the **G1** to perform ring closing metathesis. The reaction proceeds at room temperature for about 12 hours, and the yield of dimethyl 2-(cyclopent-3-en-1-yl)malonate is about 60%.

3. S_N2 reaction: Dimethyl 2-(cyclopent-3-en-1-yl)malonate was added to the Ar-purged flask and dissolved in DMF. The solution was cooled to 0°C and NaH was added slowly. After 20 min, 3-bromocyclohexene was added to solucition. The reaction mixture was stirred for 6 hours. The reaction mixture was extracted with Ether and water and dried with $MgSO_4$. Crude is purified by silica gel column chromatography (ethyl acetate/hexane = 1/30) to yield dimethyl 2-(cyclohex-2-en-1-yl)-2-(cyclopent-3-en-1-yl)malonate about 50% yield.

4. Reduction and protection: Dimethyl 2-(cyclohex-2-en-1-yl)-2-(cyclopent-3-en-1-

yl)malonate was added to Ar-purged flask and dissolved in THF. The solution was cooled to 0°C and lithium aluminum hydride (230 mg, 6 mmol) was added slowly. The reaction mixture was stirred for 2 hours until all ester groups were converted to alcohol. The resulting mixture was quenched by successive addition of water (1 ml per 1 g of LAH) in an ice bath, 10 % NaOH solution (2 ml per 1 g of LAH), and water (3ml per 1g of LAH). The resulting mixture was filtered through celite pad and ecaporated under reduced pressure. Diol was purified by silica gel column chromatography (ethyl acetate/hexane = 1/3) to yield over 90%. 2-(cyclohex-2-en-1-yl)-2-(cyclopent-3-en-1-yl)propane-1,3-diol (624mg,3mmol) was added to flask and dissolved in DCM(6 ml). Toluenesulfonyl acid (171 mg, 0.9 mmol) and Lithium bromide (52 mg,0.6 mmol) are added to the solution and dimethoxy methane (0.4 ml, 4.5 mmol) is added to the solution. The reaction mixture was extracted with dichloromethane and water and dried with $MgSO_4$. **M4c** is purified by silica gel column chromatography (ethyl acetate/hexane = 1/5) to yield corresponding alcohol with 90% yield

Preparation of **M5a**

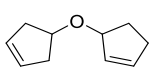

^{1}H NMR (500 MHz, $CDCl_3$, ppm) δ 5.98 (1H, s), 5.85 (1H, s), 4.62 (1H, s), 4.33(1H, s), 2.61, 2.37 (4H, dd), 2.46, 2.24 (2H, m), 2.17 (1H, m),1.76 (1H, m)

^{13}C NMR (500MHz, CDCl3, ppm)

δ 135.07, 131.38, 128.44, 128.36, 83.25, 39.81, 39.72, 30.94, 30.38

HRMS (ESI) calcd.for $(C_{10}H_{14}O)^-Na^+$ 173.0939 found, 173.0937

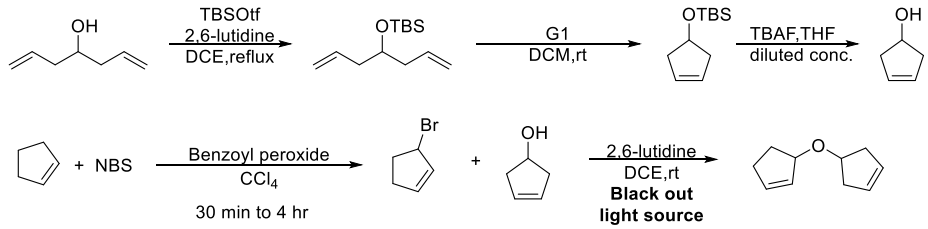

1. Silyl protection, ring-closing metathesis, and deprotection: 1,6-heptadien-4-ol, 2,6-Lutidine and DCM. Then, place the RBF in an ice bath and slowly drop *tert*-butyl dimethyl silyl triflate. The reaction is carried out under reflux conditions for about 6 hours. The reaction mixture was extracted with DCM and water and dried with $MgSO_4$. Crude is purified by silica gel column chromatography (ethyl acetate/hexane = 1/50) to yield *tert*-butyl(hepta-1,6-dien-4-yloxy)dimethylsilane with about 90% yield. This heptadiene is reacted with the Grubbs first generation catalyst to perform ring closing metathesis. The reaction proceeds at room temperature for about 12 hours, and the yield of the reaction is about 70 80%. After the ring closure product was diluted to 0.03 M in THF, TBAF was added at 0 ° C, and the reaction was allowed to proceed for about 1 hour, resulting in deprotected alcohol. The reaction crude can be obtained in an ethyl acetate/hexane = 1/1 condition immediately after removal of the solvent to obtain a clean alcohol with a yield of 60-70%.

2. Allylic bromination and etherification: 3-bromocyclopentene is prepared by bromination of cyclopentene. A mixture of cyclopentene, N-bromosuccinimide (30 g, 0.17 mol) and AIBN (100 mg) in carbon tetrachloride (300 mL) was heated and stirred at 80 °C. Additional NBS (90 g, 0.51 mol) was added in portions. After the addition of all NBS, the mixture was kept stirring under reflux for 1 h. The reaction was quenched by cooling the system to 0 °C and the precipitate was removed by celite filtration. After concentration of the solution, the resulting crude product was purified by vacuum distillation to afford 3-bromo-1-cyclooctene. With 3-cyclopentenol (1.64 g, 20 mmol) and DCE (25 ml) solution,

2,6-lutidine (2.6 ml, 24 mmol) was added to solution. After 5mins, 3-bromocyclopentene (0.41 ml, 5 mmol) is added slowly with blackout condition. After 12 hours, the yield of Corresponding ether, **M5a** is 30-40%

Preparation of **M5b**

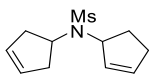

^{1}H NMR (500 MHz, $CDCl_3$, ppm) 5.69 (2H, s), 5.63(1H, m), 4.73(1H, d), 4.12(1H, p), 2.98(3H, s), 2.49-2.73(4H, m), 2.31(2H, m), 1.87(1H, m)

^{13}C NMR (500MHz, CDCl3, ppm)

δ 135.58, 129.79, 129.23, 129.05, 63.84, 55.76, 41.21, 38.23, 37.91, 31.47, 29.41

HRMS (ESI) calcd.for $(C_{11}H_{17}NO_2S)^-$ Na^+ 250.0873 found, 250.0872

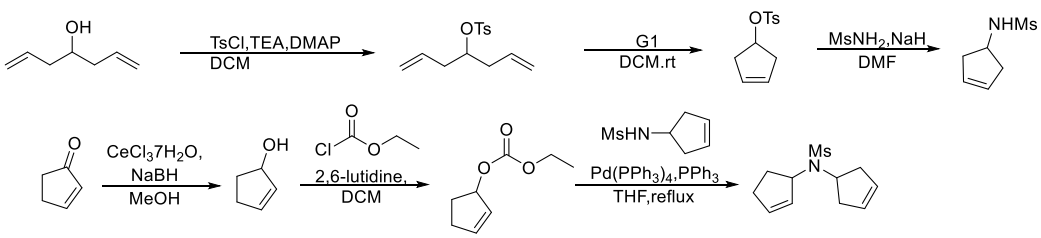

1. Tosylation and ring-closing metathesis: 1,6-heptadien-4-ol, Triethylamine(TEA) and DCM. Then, place the RBF in an ice bath and put *p*-toluenesulfonic acid. The reaction is carried out under reflux conditions for about 12 hours. The reaction mixture was extracted with Ether and water and dried with $MgSO_4$. Crude is purified by silica gel column chromatography (ethyl acetate/hexane = 1/50) to yield hepta-1,6-dien-4-yl 4-methylbenzenesulfonate with about 80% yield. This heptadiene is reacted with the Grubbs first generation catalyst to perform ring closing metathesis. The reaction proceeds at room temperature for about 12 hours, and the yield of the reaction is about 70-80%. cyclopent-3-en-1-yl 4-methylbenzenesulfonate is used for the next SN2 reaction with

methanesulfonyl amide, NaH and DMF condition for 6 hours. The reaction mixture was extracted with Ether and water and dried with $MgSO_4$. Crude is purified by silica gel column chromatography (Ethyl Acetate/Hexane = 1/30) to yield *N*-(cyclopent-3-en-1-yl)methanesulfonamidewith about 65% yield.

2. Substrate preparing for Tsuji-Trost allylation: Next step is preparing carboxylate substrate for Tsuji-Trost allylation. To a solution of 2-cyclopentenone (2.49 g, 30 mmol) and cerium trichloride heptahydrate (12.30 g, 33 mmol) in MeOH (60 ml), $NaBH_4$ (2.0 g, 36 mmol) was added slowly with an ice bath and stirred for 15 min. The reaction mixture was extracted with diethyl ether and water and dried with $MgSO_4$. 2-cyclopenten-1-ol is purified by silica gel column chromatography (ethyl acetate /hexane = 1/1) to yield corresponding alcohol with 70-80% yield. With cyclopentenol (3 g, 35.7 mmol) and DCM solution, 2,6-lutidine (1.2 equiv) was added to solution. After 5mins, Ethyl chloroformate (1.1 equiv) is added slowly. Corresponding carboxylate is purified by silica gel column chromatography (ethyl acetate/hexane = 1/10) with 70% yield.

3. Tsuji-Trost allylation: *N*-(cyclopent-3-en-1-yl)methanesulfonamide with (570 mg, 5.5 mmol) was added to THF under argon at room temperature. The mixture was stirred for 10 min. To this was added $Pd(PPh)_4$ (0.65 g, 0.55 mmol) and PPh_3 (290 mg,1,1 mmol), followed by cyclopent-2-enyl carboxylate (2.2 g, 14 mmol). The resulting bright yellow solution was heated under reflux for 10 h. The mixture was then partitioned between diethyl ether and water. The organic layer was separated, and the aqueous extracted with diethyl ether. The organic extracts were combined, dried over $MgSO_4$ filtered and concentrated in vacuo. Purification of the resulting brown residue on silica gel (ethly acetate/ hexane= 1/10) gave the final monomer, **M5b** (50% yield).

Preparation of **M5c**

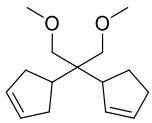

^{1}H NMR (500 MHz, $CDCl_3$, ppm) δ 5.74-5.80 (2H, d), 5.67 (2H, s), 3.37 (4H, m), 3.23 (6H,s), 2.98 (1H, m), 2.52 (1H, m), 2.36 (2H, m), 2.23 (4H, m), 1.86 (2H, m)

^{13}C NMR (500MHz, CDCl3, ppm) δ 129.85, 128.05, 94.10, 70.87,70.72, 40.44, 39.06, 37.84, 33.80,33.61, 25.19,24.41, 23.18

HRMS (ESI) calcd.for $(C_{15}H_{24}O_2)^{-}Na^{+}$ 259.1671 found, 259.1669

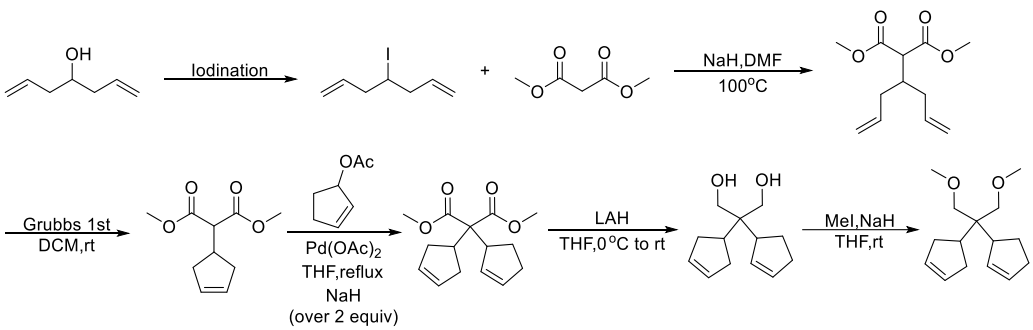

1. Iodination and SN2 reaction: Put 1,6-heptadien-4-ol into DCM in RBF. Then, place the RBF in an ice bath and put Iodine and PPh_3. The reaction is carried out at room temperature for about 3 hours. The reaction mixture was extracted with DCM and water and dried with $MgSO_4$. Crude is purified by silica gel column chromatography (ethyl acetate/hexane = 1/100) to yield 4-iodohepta-1,6-diene about 70% yield. Dimethyl malonate & NaH was added to DMF solution. After 20 mins, 4-iodohepta-1,6-diene is added slowly. Corresponding malonate derivative is purified by silica gel column chromatography (ethyl acetate/hexane = 1/20) with 75% yield.

2. Ring-closing metathesis: This heptadiene is reacted with the **G1** to perform ring closing metathesis. The reaction proceeds at room temperature for about 12 hours, and the yield of dimethyl 2-(cyclopent-3-en-1-yl)malonate is about 60%.

3. Tsuji-Trost allylation: Dimethyl 2-(cyclopent-3-en-1-yl)malonate was added to the Ar-purged flask and dissolved in THF. The solution was cooled to 0℃ and NaH was added slowly. After 10 min, cyclopent-2-en-1-yl acetate was added to solucition with $Pd(OAc)_2$. The reaction mixture was stirred for 6 hours. The reaction mixture was extracted with Ether and water and dried with $MgSO_4$. Crude is purified by silica gel column chromatography (ethyl acetate/hexane = 1/30) to yield dimethyl 2-(cyclopent-2-en-1-yl)-2-(cyclopent-3-en-1-yl)malonate about 50% yield.

4. Reduction: Dimethyl 2-(cyclopent-2-en-1-yl)-2-(cyclopent-3-en-1-yl)malonate was added to Ar-purged flask and dissolved in THF. The solution was cooled to 0℃ and lithium aluminum hydride (230 mg, 6 mmol) was added slowly. The reaction mixture was stirred for 2 hours until all ester groups were converted to alcohol. The resulting mixture was quenched by successive addition of water (1 ml per 1 g of LAH) in an ice bath, 10% NaOH solution (2 ml per 1 g of LAH), and water (3ml per 1g of LAH). The resulting mixture was filtered through celite pad and ecaporated under reduced pressure. Diol was purified by silica gel column chromatography (ethyl acetate/hexane = 1/3) to yield over 90%.

5. Methylation: dimethyl 2-(cyclopent-2-en-1-yl)-2-(cyclopent-3-en-1-yl)malonate-1,3-diol (624 mg, 3 mmol) was added to flask and dissolved in THF(6 ml). Iodomethane (0.14ml, 0.8 mmol) is added to solution and NaH (40mg, 1mmol) is added to solution. The reaction mixture was extracted with dichloromethane and water and dried with $MgSO_4$. **M5c** is purified by silica gel column chromatography (ethyl acetate/hexane = 1/1) to yield corresponding alcohol with 90% yield.

Preparation of **M5d**

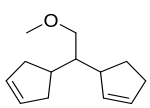

^{1}H NMR (500 MHz, $CDCl_3$, ppm) δ 5.67–5.75 (4H, μ), 3.34 (3H, s), 3.28 (3H, s), 2.90 (1H, s), 2.26-2.46 (5H, m), 1.92-2.17 (4H, m), 1.54-1.70 (2H, m)

^{13}C NMR (500MHz, CDCl3, ppm)

δ 131.96, 130.77, 130.46, 130.39, 129.87, 127.63, 127.59, 58.57, 56.06, 48.05, 48.03, 37.97, 37.76, 37.43, 36.88, 31.92, 29.69, 27.08, 25.39, 25.12.22.68, 22.65

HRMS (ESI) calcd.for $(C_{13}H_{20}O_2)^{-}Na^{+}$ 215.2870 found 215.2871

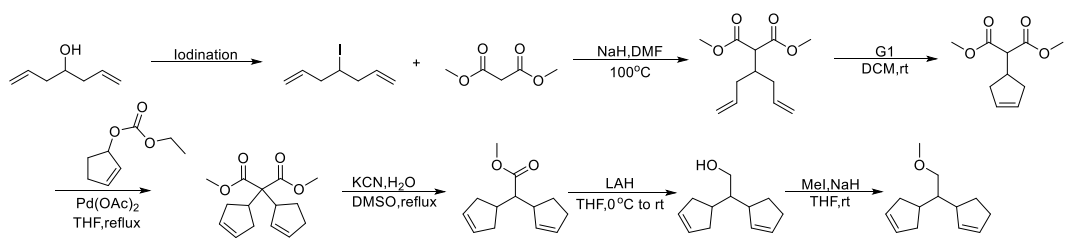

1. Iodination and SN2 reaction: Put 1,6-heptadien-4-ol into DCM in RBF. Then, place the RBF in an ice bath and put Iodine and PPh_3. The reaction is carried out at room temperature for about 3 hours. The reaction mixture was extracted with DCM and water and dried with $MgSO_4$. Crude is purified by silica gel column chromatography (ethyl acetate/hexane = 1/100) to yield 4-iodohepta-1,6-diene about 70% yield. Dimethyl malonate & NaH was added to DMF solution. After 20 mins, 4-iodohepta-1,6-diene is added slowly. Corresponding malonate derivative is purified by silica gel column chromatography (ethyl acetate/hexane = 1/20) with a 75% yield.

2. Ring-closing metathesis: This heptadiene is reacted with the **G1** to perform ring closing metathesis. The reaction proceeds at room temperature for about 12 hours, and the yield of dimethyl 2-(cyclopent-3-en-1-yl)malonate is about 60%.

3. Tsuji-Trost allylation: Dimethyl 2-(cyclopent-3-en-1-yl)malonate was added to the Ar-purged flask and dissolved in THF. The solution was cooled to 0°C and NaH was added

slowly. After 10 min, cyclopent-2-en-1-yl acetate was added to the solution with $Pd(OAc)_2$. The reaction mixture was stirred for 6 hours. The reaction mixture was extracted with Ether and water and dried with $MgSO_4$. Crude is purified by silica gel column chromatography (ethyl acetate/hexane = 1/30) to yield dimethyl 2-(cyclopent-2-en-1-yl)-2-(cyclopent-3-en-1-yl)malonate about 50% yield.

4. Decarboxylation: Dimethyl 2-(cyclopent-2-en-1-yl)-2-(cyclopent-3-en-1-yl)malonate was added to DMSO and 0.1 equiv of water. KCN was added to the solution and heated with reflux condition during 1-2 hour. (Krapcho decarboxylation condition) The reaction mixture was extracted with Ether and water and dried with $MgSO_4$. Resulting methyl 2-(cyclopent-2-en-1-yl)-2-(cyclopent-3-en-1-yl)acetate could be obtained from its crude. The crude is purified by silica gel column chromatography (ethyl acetate/hexane = 1/30) to yield methyl 2-(cyclopent-2-en-1-yl)-2-(cyclopent-3-en-1-yl)acetate 70% yield

5. Reduction: Methyl 2-(cyclopent-2-en-1-yl)-2-(cyclopent-3-en-1-yl)acetate was added to Ar-purged flask and dissolved in THF. The solution was cooled to 0℃ and lithium aluminum hydride (230 mg, 6 mmol) was added slowly. The reaction mixture was stirred for 2 hours until all ester groups were converted to alcohol. The resulting mixture was quenched by successive addition of water (1 ml per 1 g of LAH) in an ice bath, 10 % NaOH solution (2 ml per 1 g of LAH), and water (3ml per 1g of LAH). The resulting mixture was filtered through celite pad and evaporated under reduced pressure. alcohol was purified by silica gel column chromatography (ethyl acetate/hexane = 1/2) to yield over 95%.

6.Methylation: Methyl 2-(cyclopent-2-en-1-yl)-2-(cyclopent-3-en-1-yl)ethan-1-ol was added to flask and dissolved in THF. Iodomethane is added to the solution and NaH is added to the solution. The reaction mixture was extracted with dichloromethane and water and dried with $MgSO_4$. **M5d** is purified by silica gel column chromatography (ethyl acetate/hexane = 1/1) to yield corresponding alcohol with 90% yield

^{1}H-NMR & ^{13}C-NMR of Monomer

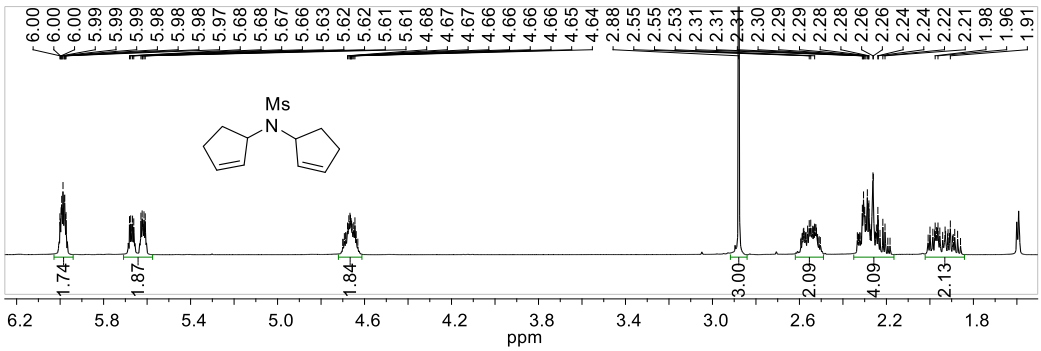

Figure S2.1-1 ^{1}H-NMR of **M1b**

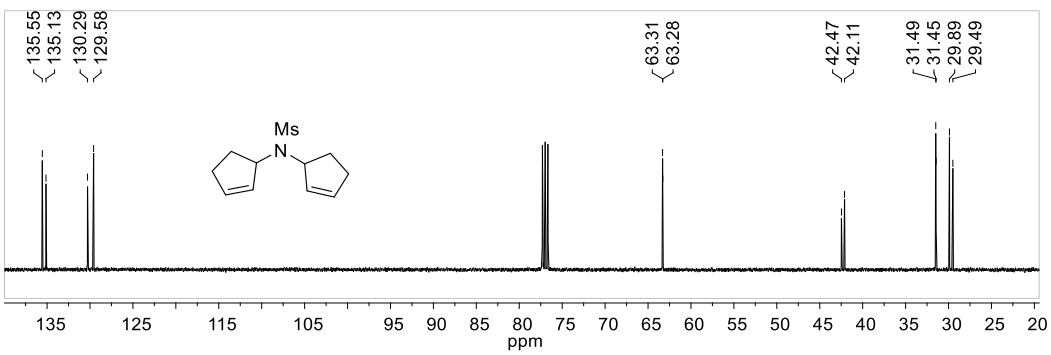

Figure S2.1-2 ^{13}C-NMR of **M1b**

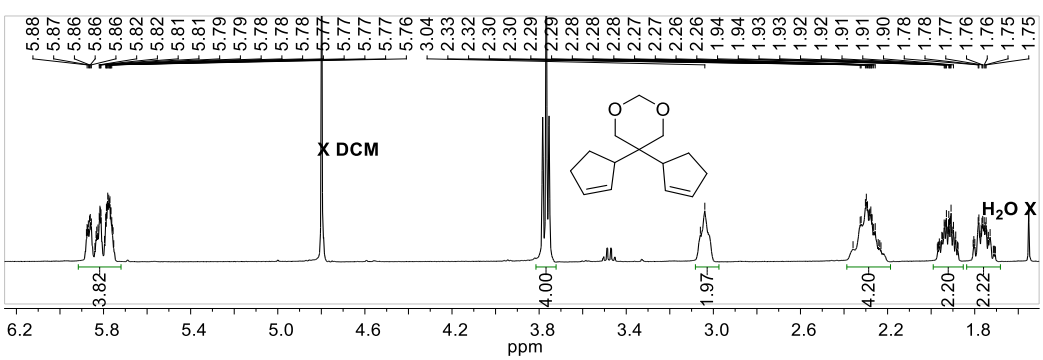

Figure S2.2-1 ^{1}H-NMR of **M1c**

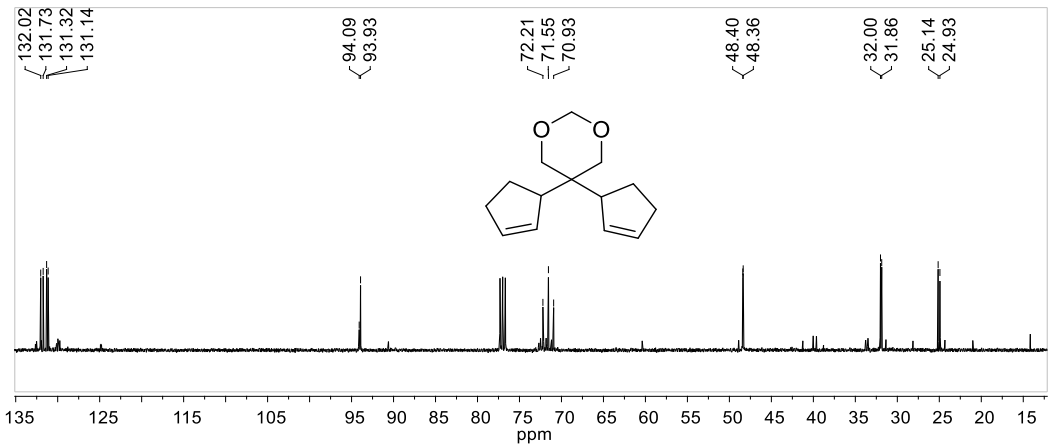

Figure S2.2-2 ^{13}C-NMR of **M1c**

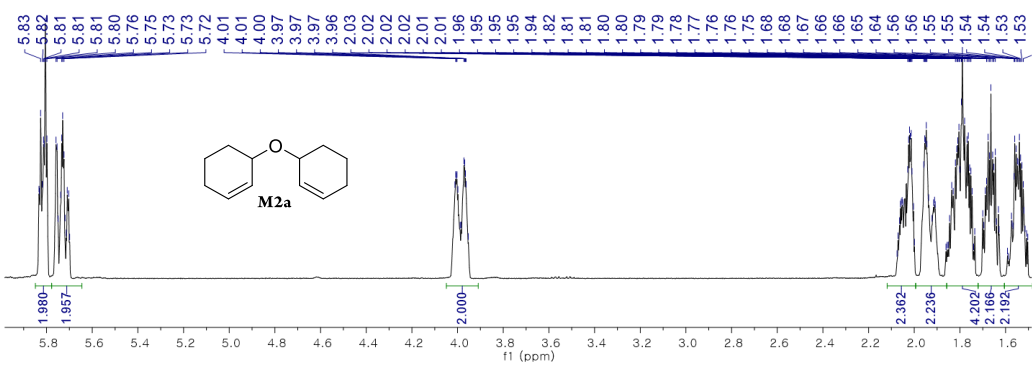

Figure S2.3-1. Proton NMR spectrum of **M2a**

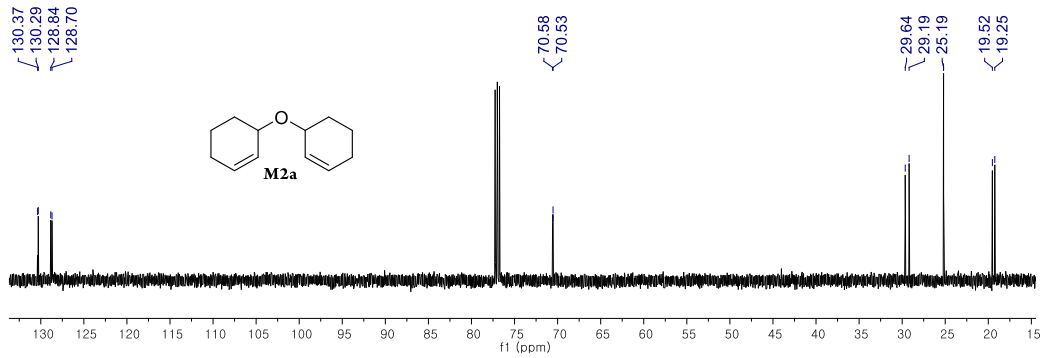

Figure S2.3-2. Carbon NMR spectrum of **M2a**

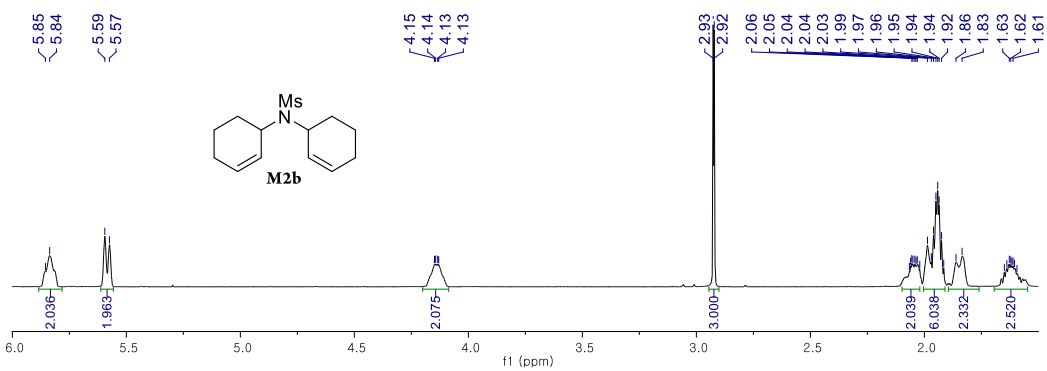

Figure S2.4-1. Proton NMR spectrum of **M2b**

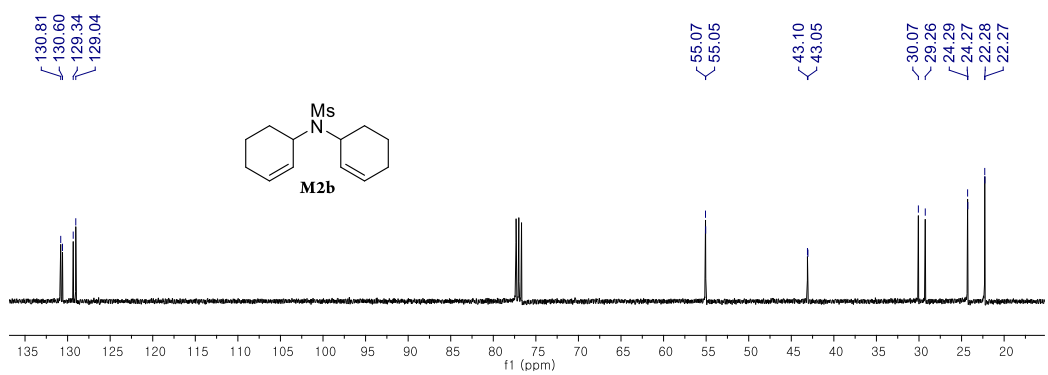

Figure S2.4-2. Carbon NMR spectrum of **M2b**

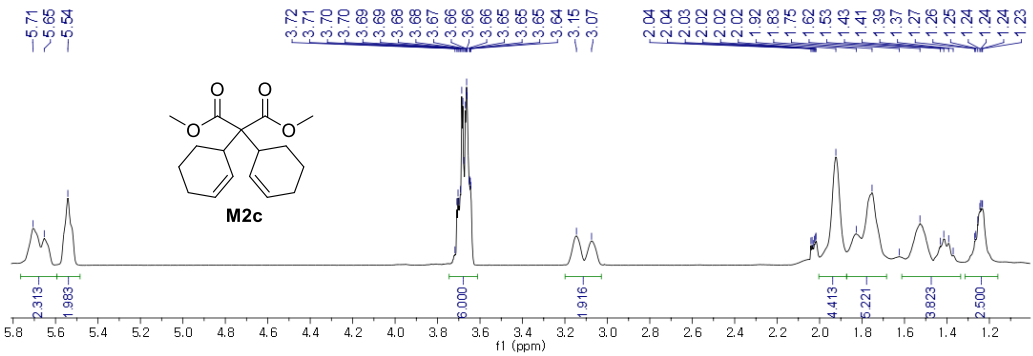

Figure S2.5-1. Proton NMR spectrum of **M2c**

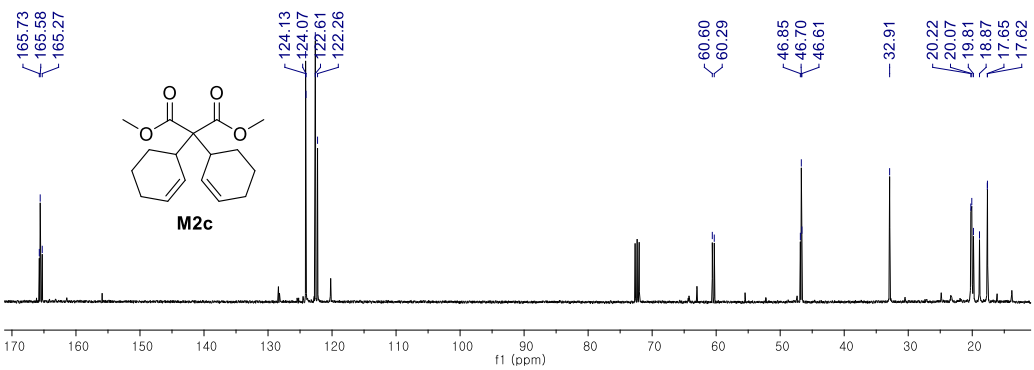

Figure S2.5-2. Carbon NMR spectrum of **M2c**

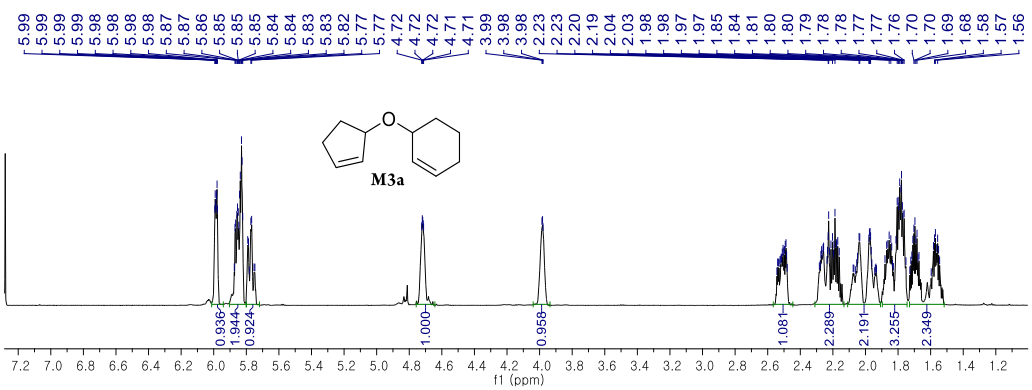

Figure S2.6-1. Proton NMR spectrum of **M3a**

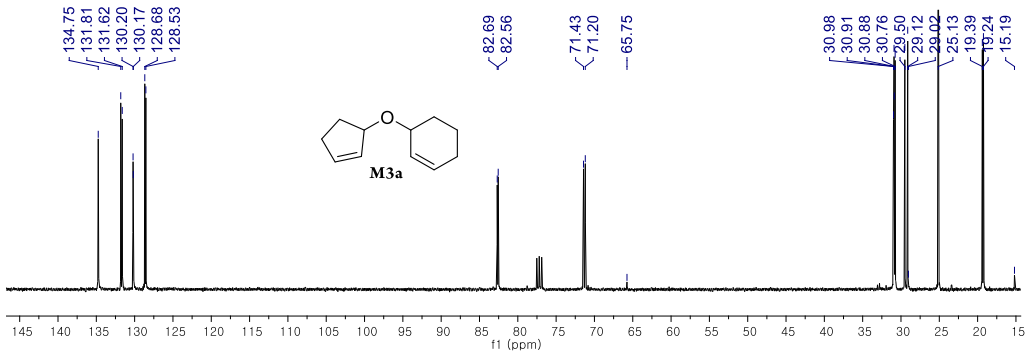

Figure S2.6-2. Carbon NMR spectrum of **M3a**

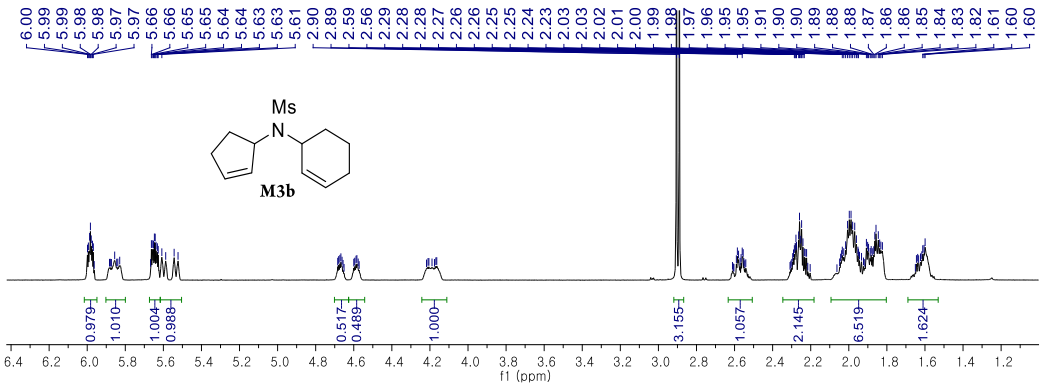

Figure S2.7-1. Proton NMR spectrum of **M3b**

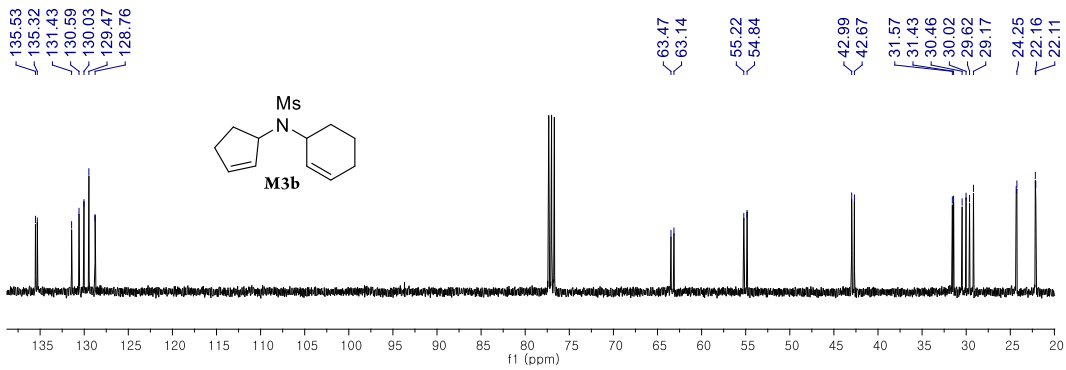

Figure S2.7-2. Carbon NMR spectrum of **M3b**

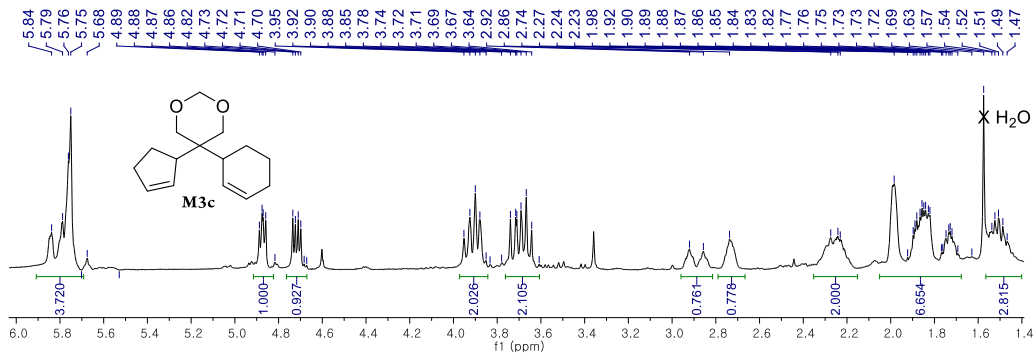

Figure S2.8-1. Proton NMR spectrum of **M3c**

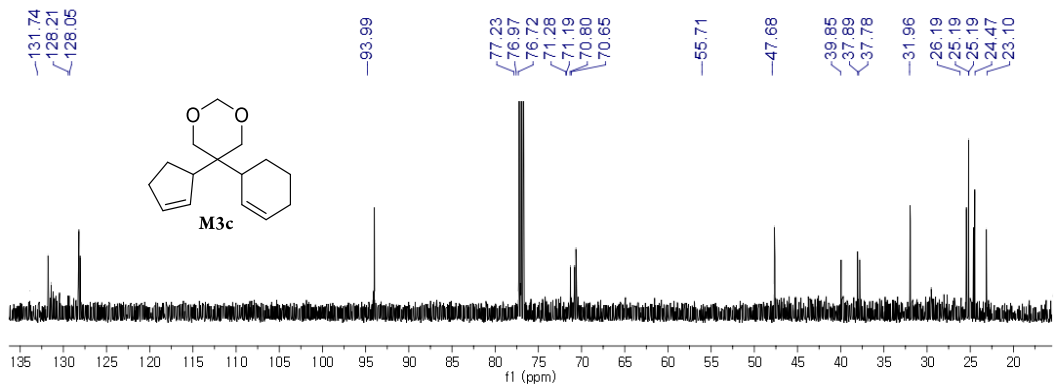

Figure S2.8-2. Carbon NMR spectrum of **M3c**

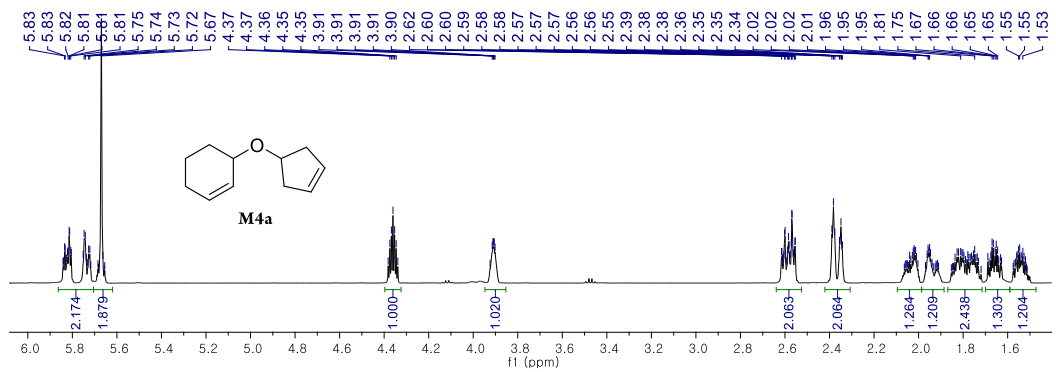

Figure S2.9-1. Proton NMR spectrum of **M4a**

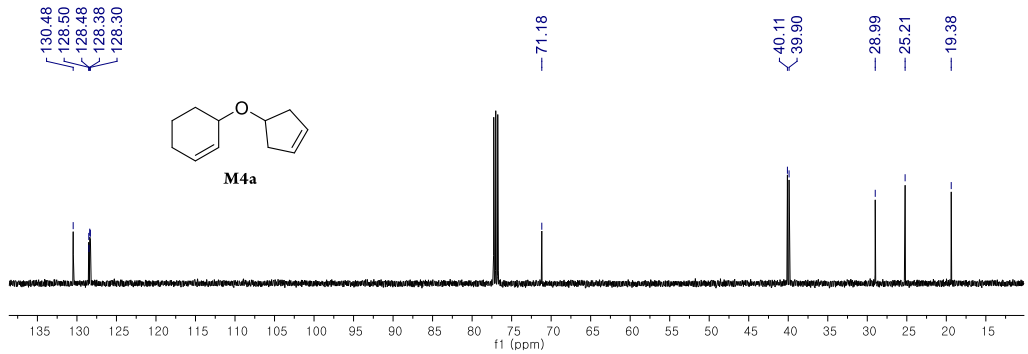

Figure S2.9-2. Carbon NMR spectrum of **M4a**

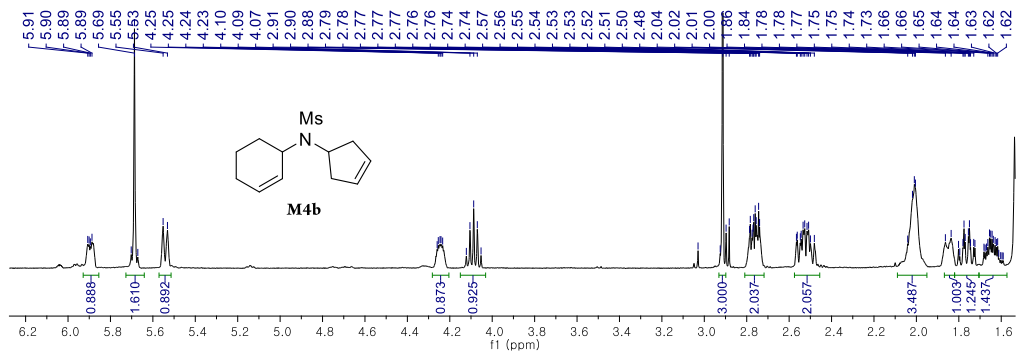

Figure S2.10-1. Proton NMR spectrum of **M4b**

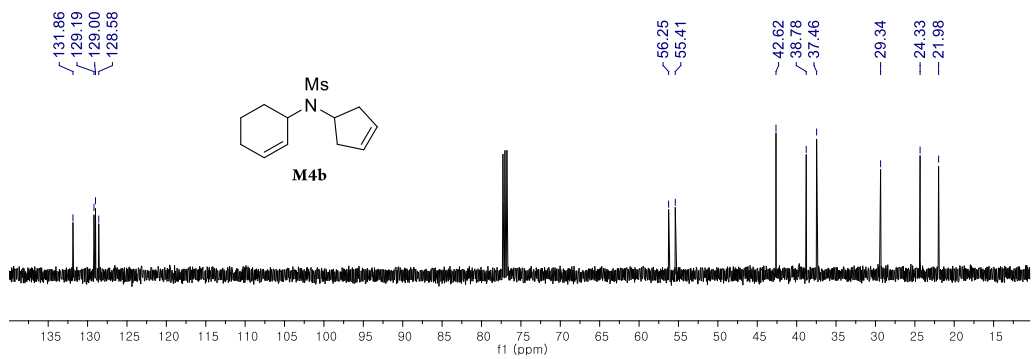

Figure S2.10-2. Carbon NMR spectrum of **M4b**

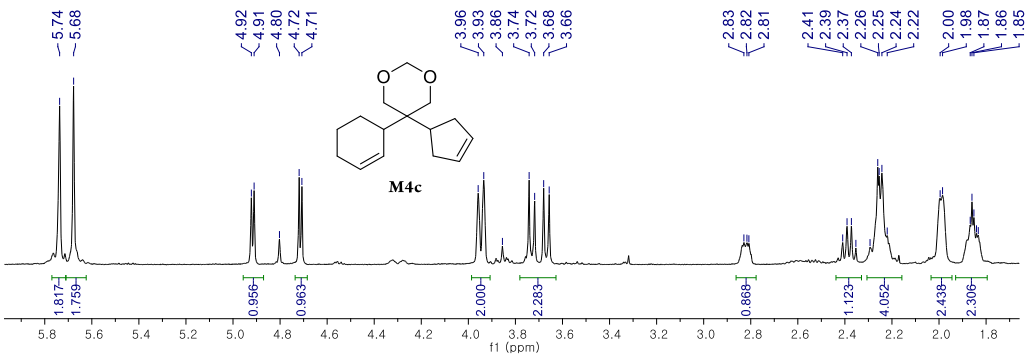

Figure S2.11-1. Proton NMR spectrum of **M4c**

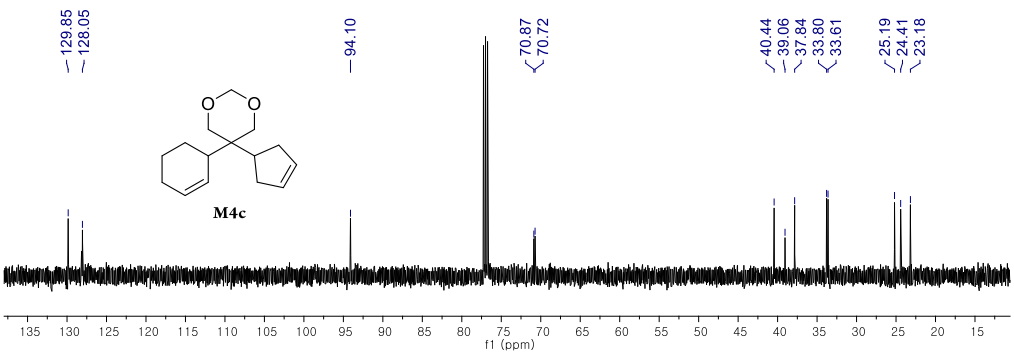

Figure S2.11-2. Carbon NMR spectrum of **M4c**

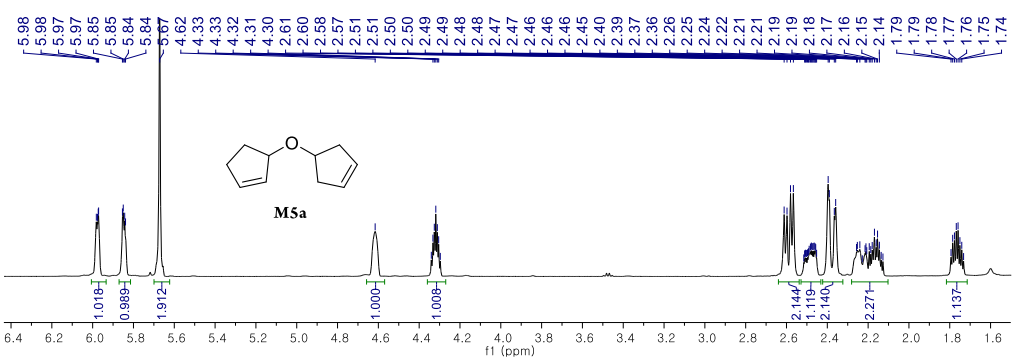

Figure S2.12-1. Proton NMR spectrum of **M5a**

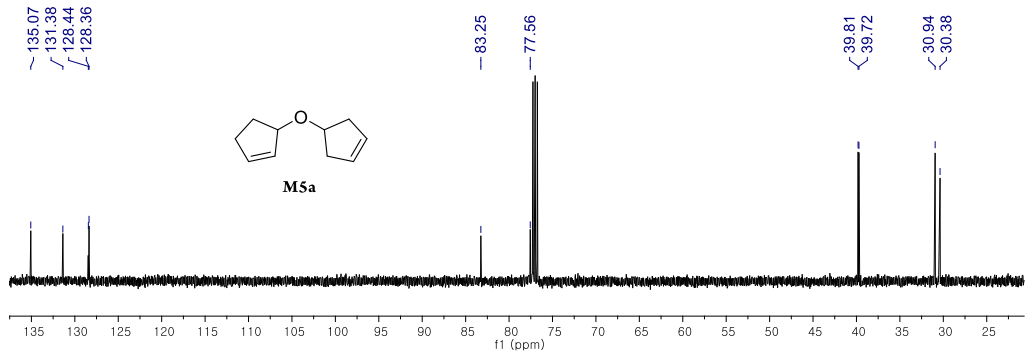

Figure S2.12-2. Carbon NMR spectrum of **M5a**

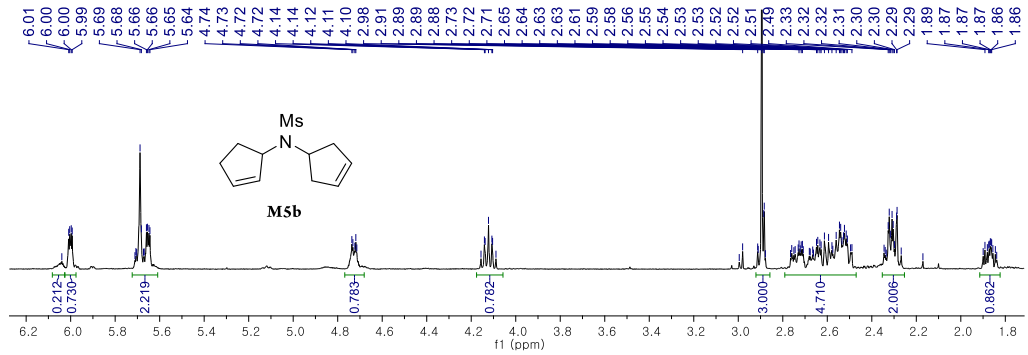

Figure S2.13-1. Proton NMR spectrum of **M5b**

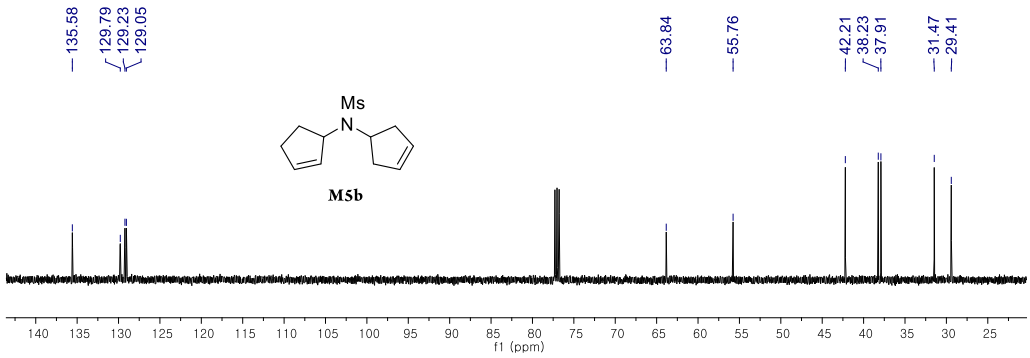

Figure S2.13-2. Carbon NMR spectrum of **M5b**

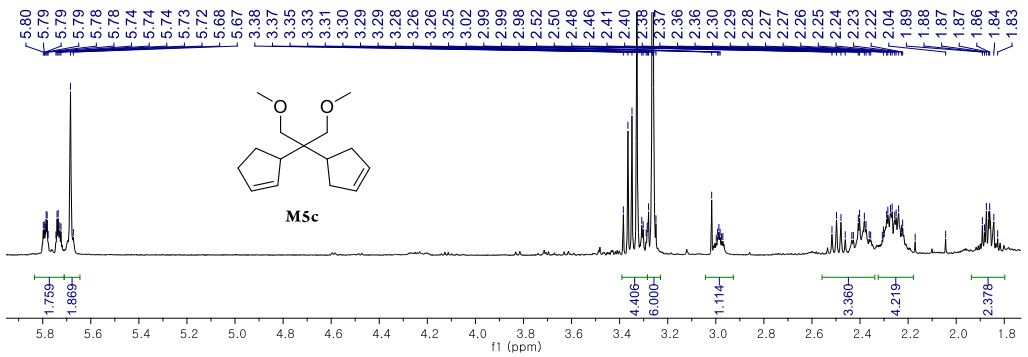

Figure S2.14-1. Proton NMR spectrum of **M5c**

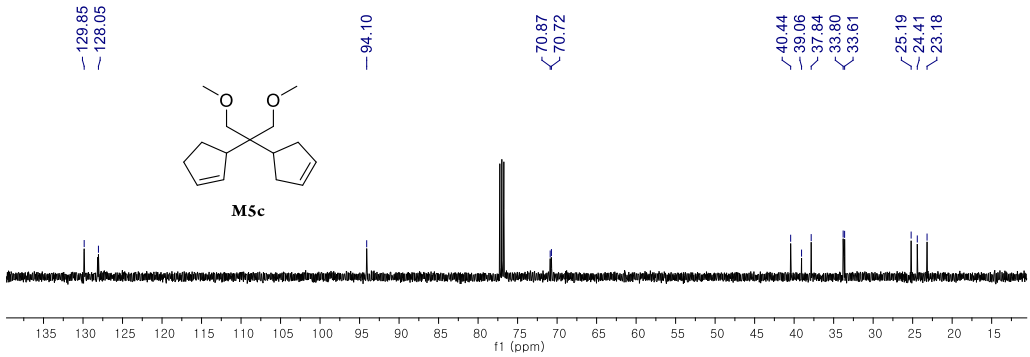

Figure S2.14-2. Carbon NMR spectrum of **M5c**

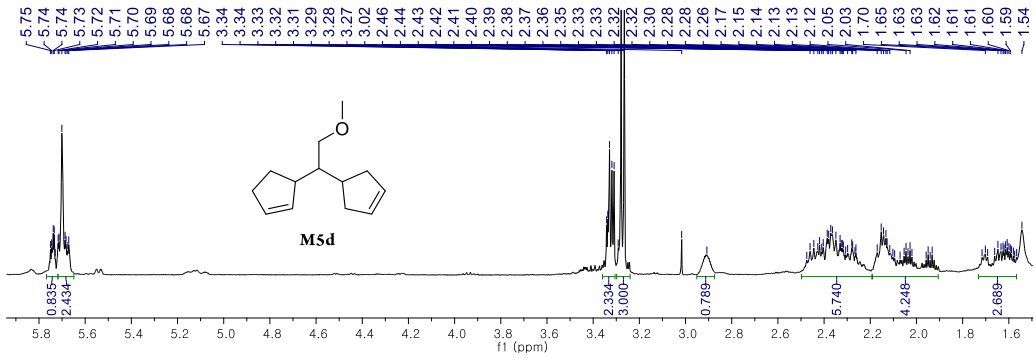

Figure S2.15-1. Proton NMR spectrum of **M5d**

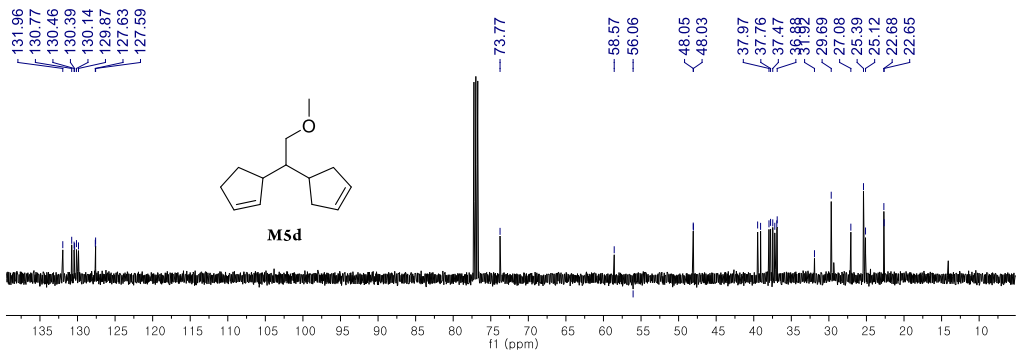

Figure S2.15-2. Carbon NMR spectrum of **M5d**

3. Polymer preparation & characterization

1) Cascade RO/RCM polymer

The general procedure of Cascade RO/RCM polymerization

The monomer (0.1 mmol) was put into a 2 mL sized vial with septum and purged with Ar-gas. Degassed DCM was added to the vial and stirred. A solution of metathesis catalyst in DCM was prepared in another Ar-purged vial with a septum, and the solution was added using a microsyringe rapidly. The conversion of polymerization was checked

by TLC and quantifed by crude ^{1}H-NMR after quenching by ethyl vinyl ether. The concentrated mixture was precipitated into cooled methanol.

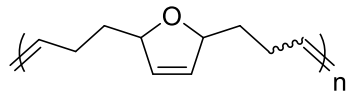

P1a

^{1}H NMR (500 MHz, $CDCl_3$, ppm) δ 5.78 (2H, m), 5.37 - 5.44 (2H, s), 4.82 (1H, s), 4.75 (1H, s), 2.06 (4H, broad), 1.58 (4H, s)

^{13}C NMR (400 MHz, $CDCl_3$, ppm) δ 131.46, 130.10, 130.05, 130.00, 129.96, 129.86, 129.79, 129.60, 129.54, 85.29, 85.18, 85.09, 36.72, 35.95, 35.87, 28.47, 28.21, 23.28, 22.97

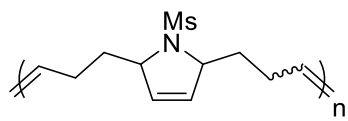

P1b

^{1}H NMR (500 MHz, $CDCl_3$, ppm) δ 5.78 (2H, d), 5.41-5.45 (2H, m), 4.53 (1H, s), 4.32 (1H, s), 2.93 (1.5H, s), 2.73 (1.5H, s), 2.04-2.10 (4H, br), 1.59-1.95 (4H, m)

^{13}C NMR (400 MHz, $CDCl_3$, ppm) δ 133.31, 133.16, 132.45, 132.04, 131.12, 130.24, 129.72, 94.01, 93.94, 71.54, 71.38, 69.72, 49.25, 48.94, 48.40, 45.60, 44.15, 32.23, 31.86,31.44, 31.04, 29.51, 26.11, 25.74, 24.93

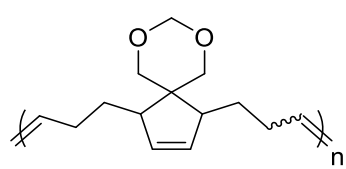

P1c

^{1}H NMR (500 MHz, $CDCl_3$, ppm) δ 5.83 (1H, m), 5.73 (1H, m), 4.82 (2H, m), 3.87 (1H,

s), 3.75 - 3.78(1H, d), 3.61 – 3.64 (1H, d), 3.47 (1H, s), 2.50 (1H, s), 2.33 (1H, s), 2.11 (2H, s), 1.98 (2H, s) , 1.66 (2H, s), 1.11 - 1.18 (2H, m)

^{13}C NMR (400 MHz, $CDCl_3$, ppm) δ 133.31, 133.16, 132.45, 132.04, 131.12, 130.24, 129.72, 94.01, 93.94, 71.54, 71.38, 69.72, 49.25, 48.94, 48.40, 45.60, 44.15, 32.23, 31.86,31.44, 31.04, 29.51, 26.11, 25.74, 24.93

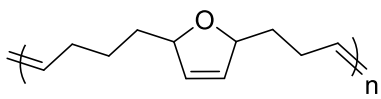

P3a

^{1}H NMR (500 MHz, $CDCl_3$, ppm) δ 5.76(2H,s), 5.34-5.60(2H,m), 4.75-4,82(1H,d), 3.70-3.85(1H,s), 1.73-2.05(4H,m), 1.38-1.74(6H,m)

^{13}C NMR (500 MHz, CDCl3, ppm) δ 132.53, 131.94, 130.21, 130.21, 130.06, 129.93, 129.71, 128.84, 85.64, 85.47, 85.13, 70.21,68.93, 36.79, 36.74,36.43, 35.96, 35.91, 32.63,32.51,32.28, 30.02, 28.73, 28.73, 28.60, 28.48, 28.21, 27.96, 25.39,25.25, 25.12, 25.08, 24.88, 19.85, 19.00

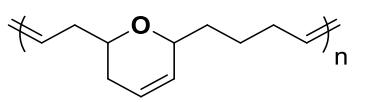

P4a

^{1}H NMR (500 MHz, $CDCl_3$, ppm) δ 5.52-5.76(2H, m), 5.34-5.44(2H,d), 3.80-4.05(1H,d), 3.31-3.59(1H, s*3), 2.11-2.32(3H,s), 1.87-2.04(2H,d), 1.52-1.76(2H,d), 1.37-1.44(2H,d)

^{13}C NMR (500MHz, $CDCl_3$, ppm) δ 132.57, 130.37, 128.42, 126.06, 124.51, 123.58, 74.77, 73.90, 73.81, 72.28, 71.17, 67.69, 40.39, 39.37, 38.58, 38.05, 35.12, 32.68, 30.86, 29.03, 25.69, 25.22, 25.01, 19.06

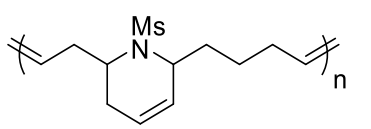

P4b

^{1}H NMR (500 MHz, $CDCl_3$, ppm) δ 5.72-5.81(2H,m), 5.30-5.55(2H,m), 4.04-4.26(1H,d), 3.49(1H,s), 2.81-2.93(3H,d), 2.04-2.47(5H,m), 1.59-1.81(2H,m), 1.16-1.24(1H,m)

^{13}C NMR (500MHz, CDCl3, ppm) δ 134.23, 132.15, 128.85, 127.92,125.60 122.11, 56.10, 53.98, 47.71, 42.50, 40.39, 40.20, 39.69, 36.61, 35.30, 33.56, 32.67, 32.42, 31.92, 30.41, 29.72, 28.86, 28.66

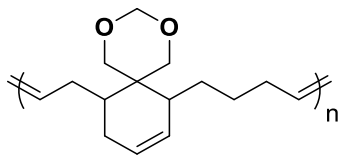

P5c

^{1}H NMR (500 MHz, $CDCl_3$, ppm) δ 5.58-5.74(2H,dd), 5.31-5.43(2H, d), 4.71-4.83(2H,d), 3.68-3.79(4H,s), 2.00-2.24(6H,m), 1.56-1.98(7H,m), 1.12-1.32(3H,m)

^{13}C NMR (500MHz, CDCl3, ppm) δ 131.85,128.96, 124.96, 94.16, 71.66, 71.21, 38.02, 37.05, 32.91, 32.46, 29.93, 27.79, 27.18

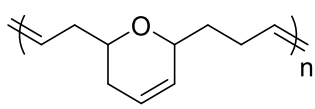

P5a

^{1}H NMR (500 MHz, CDCl3, ppm) δ 5.76-5.77(1H,s), 5.58-5.66(1H,s), 5.43-5.51(2H,s),4.08-4.13(1H,s), 3.48-3.68(1H,d), 2.30(1H,s), 2.15(3H,s), 1.92(2H,s), 1.45-1.68(1H,t)

^{13}C NMR (500 MHz, CDCl3, ppm) δ 132.39, 132.28, 132.21, 132.13, 131.01, 130.27, 129.73, 126.55, 126.34, 126.13, 124.67, 123.78, 74.20,73.85, 73.82, 71.81, 67.60, 39.37, 38.66, 35.31, 33.88, 33.75, 30.86, 30.29, 30.08, 29.69, 28.94, 28.24

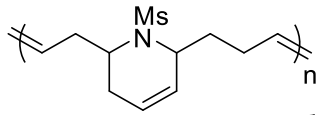

P5b

^{1}H NMR (500 MHz, $CDCl_3$, ppm) δ 5.73-5.78(2H,s), 5.35-5.47(2H,d), 3.48-4.28(2H), 2.79-2.91(3H,d), 2.03-2.35(6H,m), 1.50-1.73(4H,m)

^{13}C NMR (500MHz, CDCl3, ppm) δ 133.30, 127.26, 126.55, 122.02, 52.85, 50.50, 38.84, 38.67,36.90, 32.32, 32.17, 26.35, 25.70

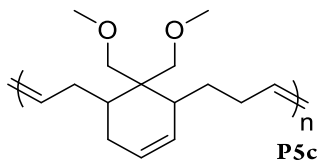

P5c

^{1}H NMR (500MHz, $CDCl_3$, ppm) δ 5.52-5.54(2H,s), 5.22-5.35(2H,t), 3.16-3.44(10H,m), 1.55-2.10(10H,m), 1.00-1.07(1H,s), 0.77(1H,s)

^{13}C NMR (500 MHz, $CDCl_3$, ppm) δ 131.43, 131.09, 130.49, 130.06, 129.29, 125.13, 75.47, 74.39, 72.34, 71.95, 59.19, 59.08, 59.04, 42.60, 42.29, 39.21, 38.21, 38.29, 37.37, 35.29, 33.46, 32.65, 31.36, 30.78, 30.38, 29.69, 29.69, 27.70

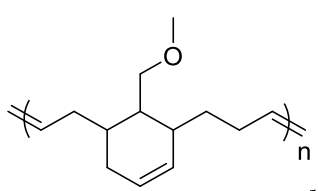

P5d

^{1}H NMR (500 MHz, $CDCl_3$, ppm) δ 5.48-5.54(2H,m), 5.35-5.45(2H,m), 3.13-3.37(5H,m), 1.47-2.17(10H,m), 1.30-1.36(2H,s), 1.19-1.24(3H,s)

^{13}C NMR (500 MHz, CDCl3, ppm)

δ 133.18,131.58,131.04,1130.33, 130.06, 129.76, 128.85, 125.65, 125.37, 73.98, 72.15, 5

8.70, 47.54, 39.97, 37.80, 36.39, 35.26, 32.27, 32.05, 30.40, 29.65, 28.30, 26.97, 26.88, 2
6.69, 26.36, 26.14, 14.05

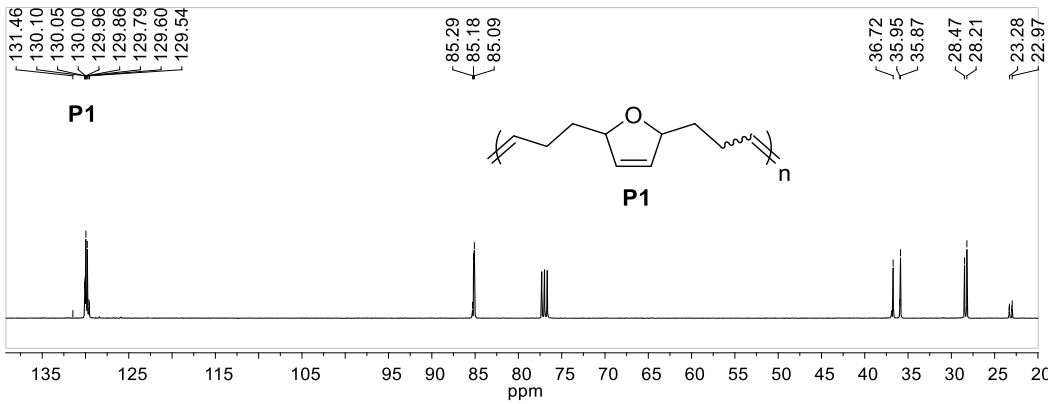

Figure S2.15. ^{13}C NMR of ether type tandem RO/RCM polymer

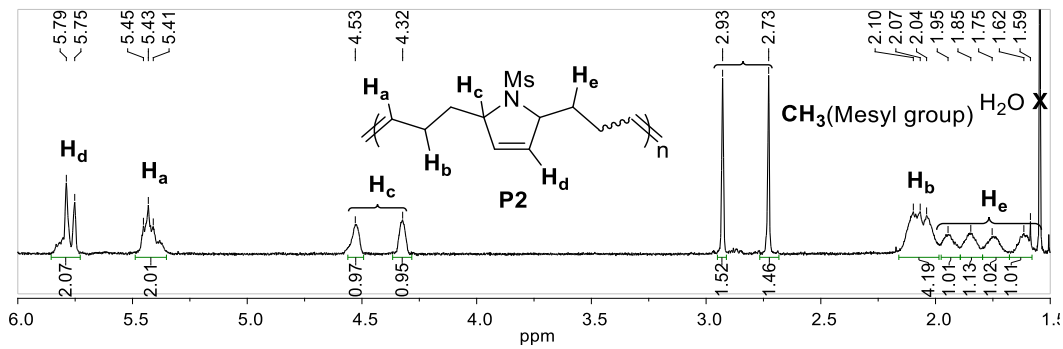

Figure S2.16-1. ^{1}H NMR of amide type tandem RO/RCM polymer

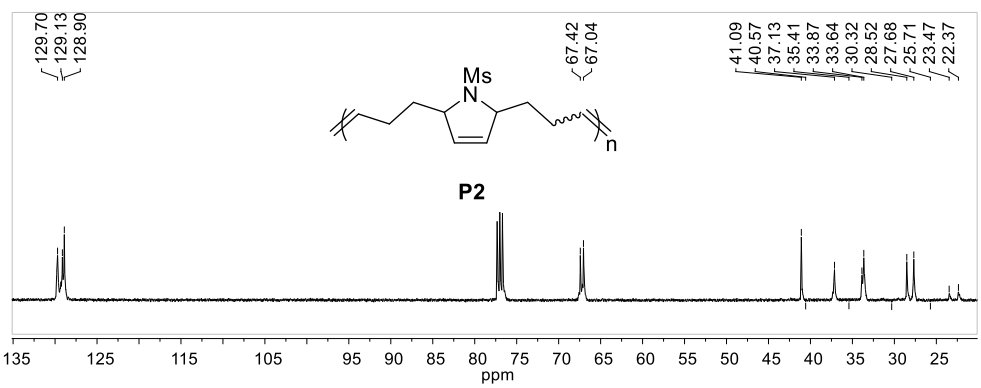

Figure S2.16-2. ^{13}C NMR of amide type tandem RO/RCM polymer

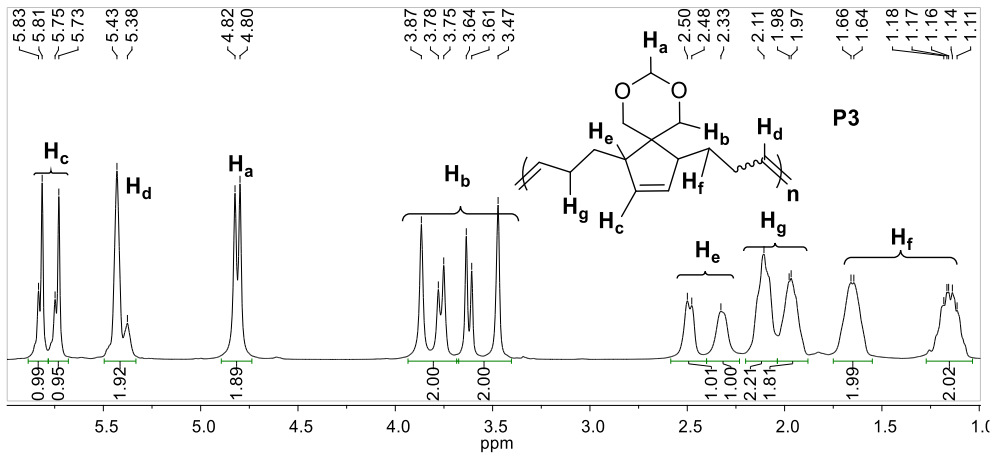

Figure S2.17-1. ^{1}H NMR of carbon type tandem RO/RCM polymer

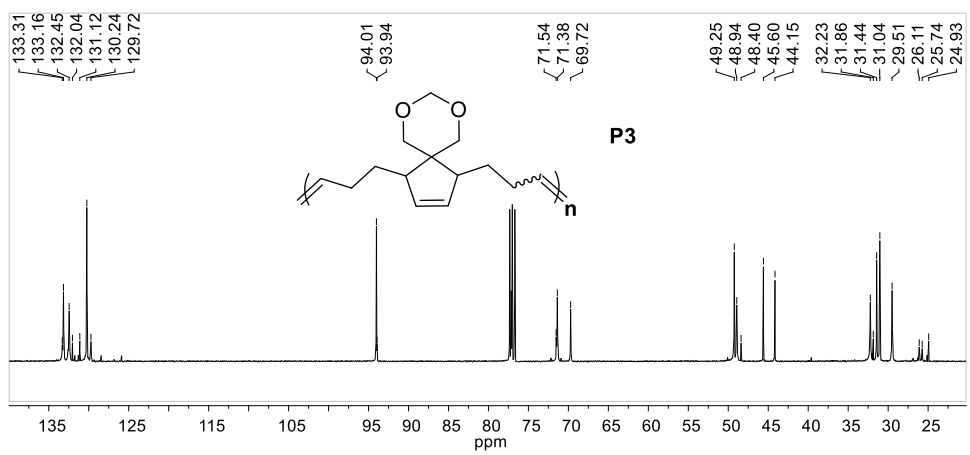

Figure S2.17-2. ^{13}C NMR of carbon type tandem RO/RCM polymer

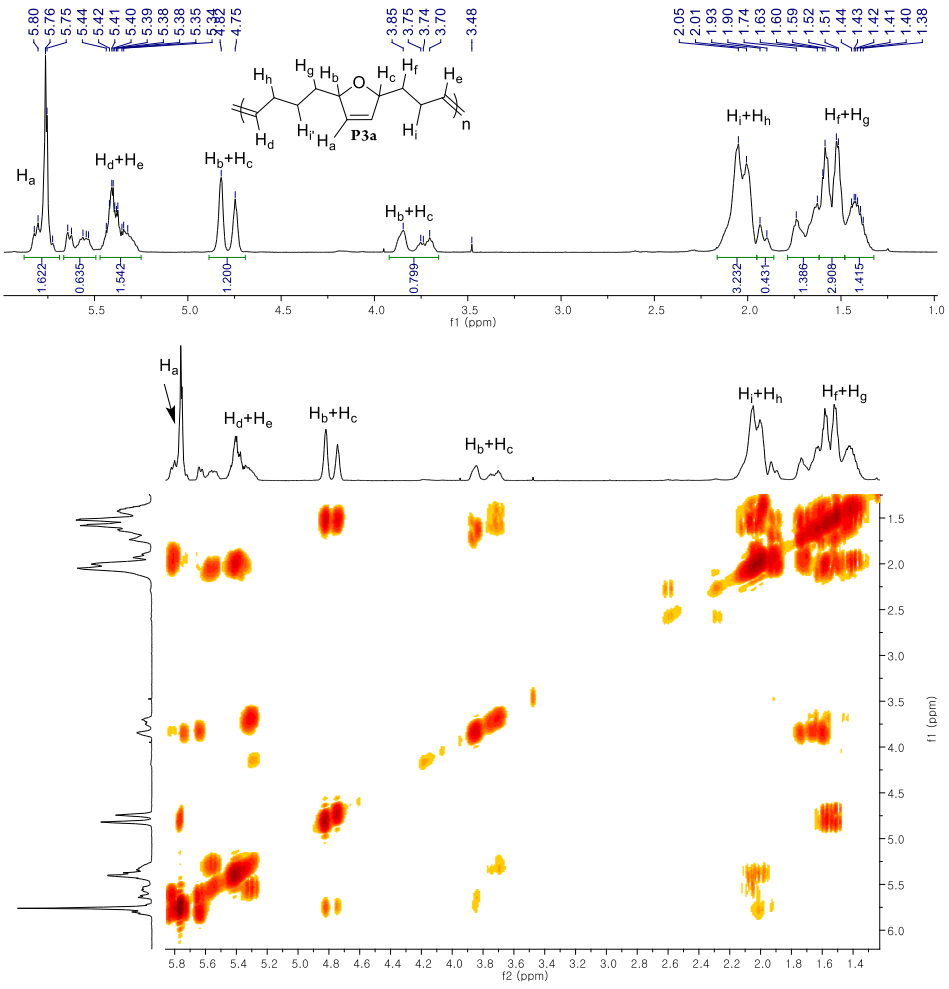

Figure S2.18-1. 1D and 2D COSY Proton NMR spectra of **P3a**.

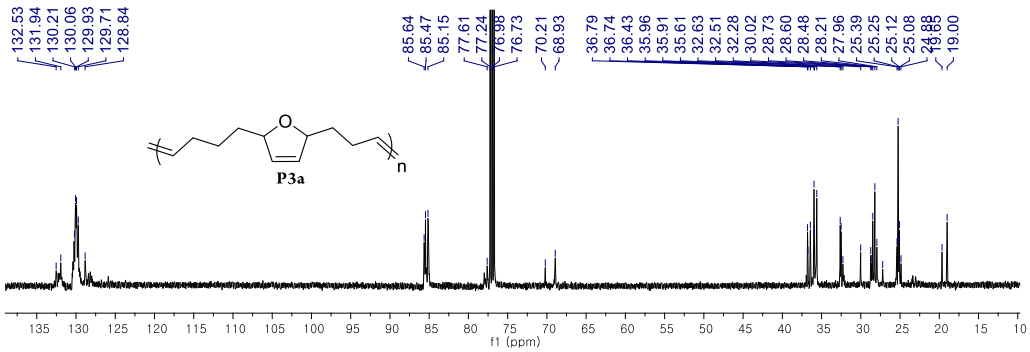

Figure S2.18-2. Carbon NMR spectrum of **P3a**.

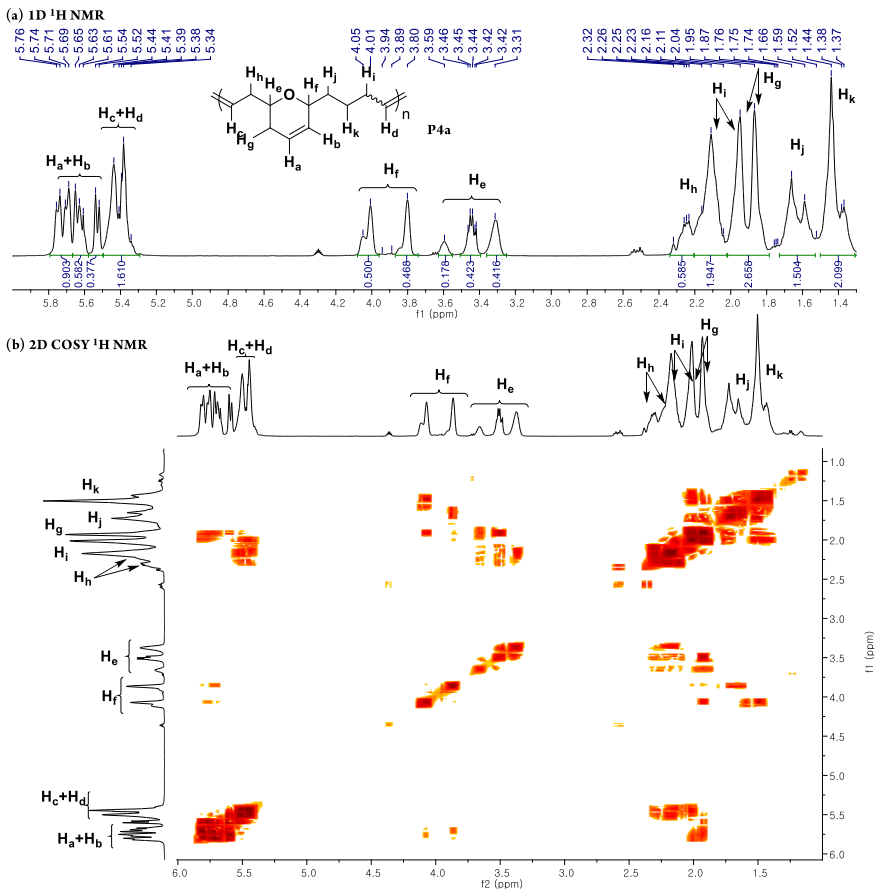

Figure S2.19-1. 1D and 2D COSY Proton NMR spectra of **P4a**.

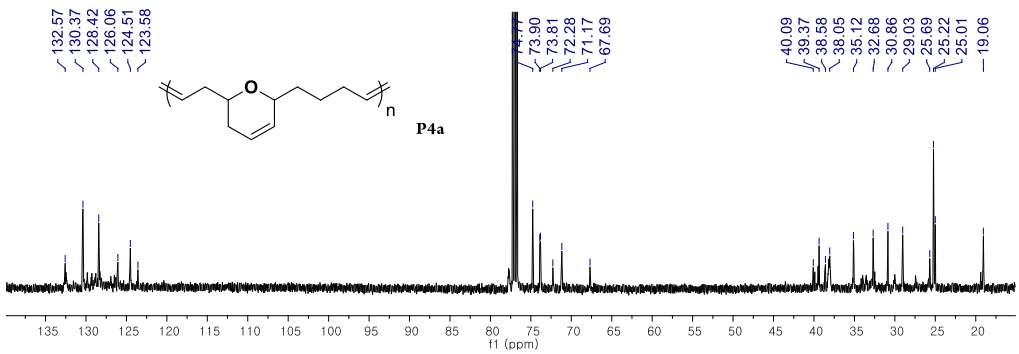

Figure S2.19-2. Carbon NMR spectrum of **P4a**.

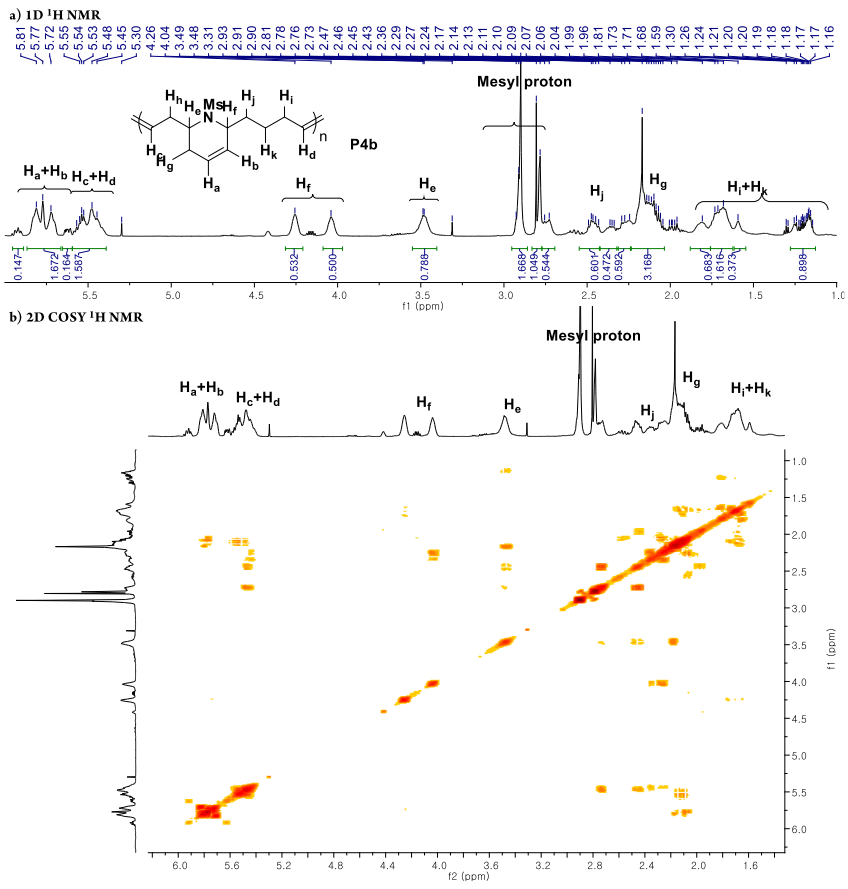

Figure S2.20-1. 1D and 2D COSY Proton NMR spectra of **P4b**.

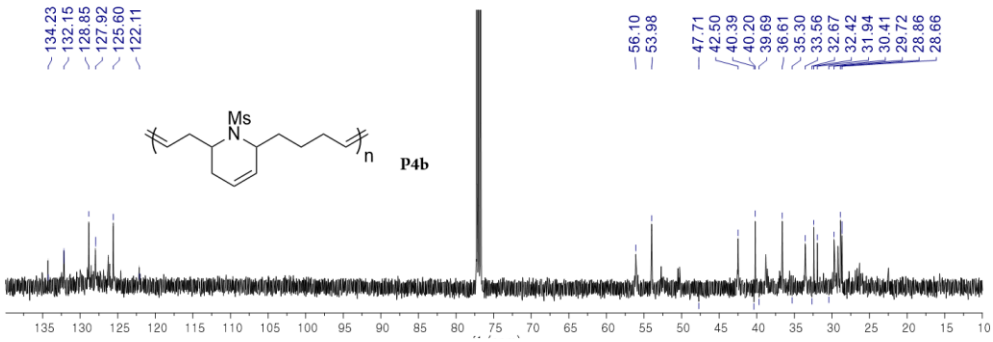

Figure S2.20-2. Carbon NMR spectrum of **P4b**.

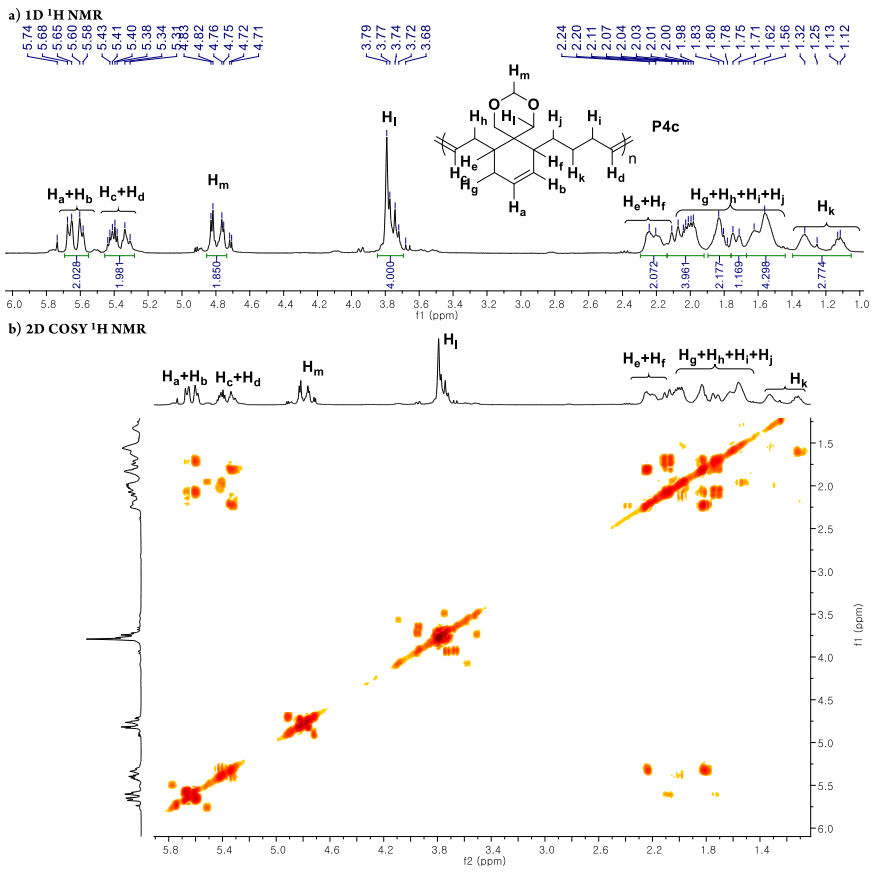

Figure S2.21-1. 1D and 2D COSY Proton NMR spectra of **P4c**.

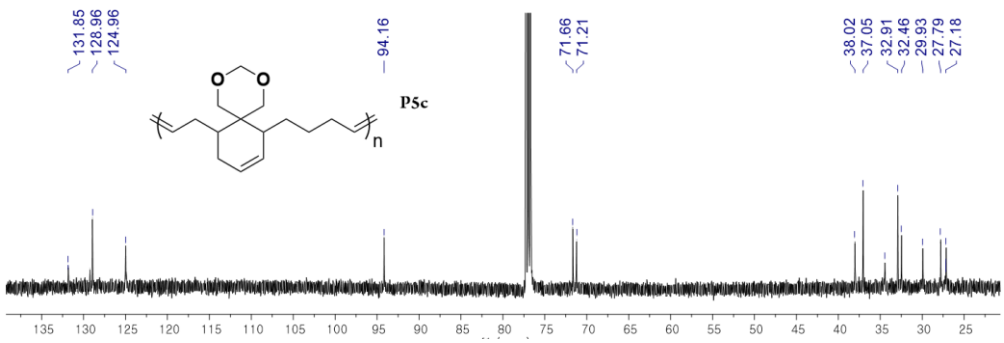

Figure S2.21-2. Carbon NMR spectrum of **P4c**.

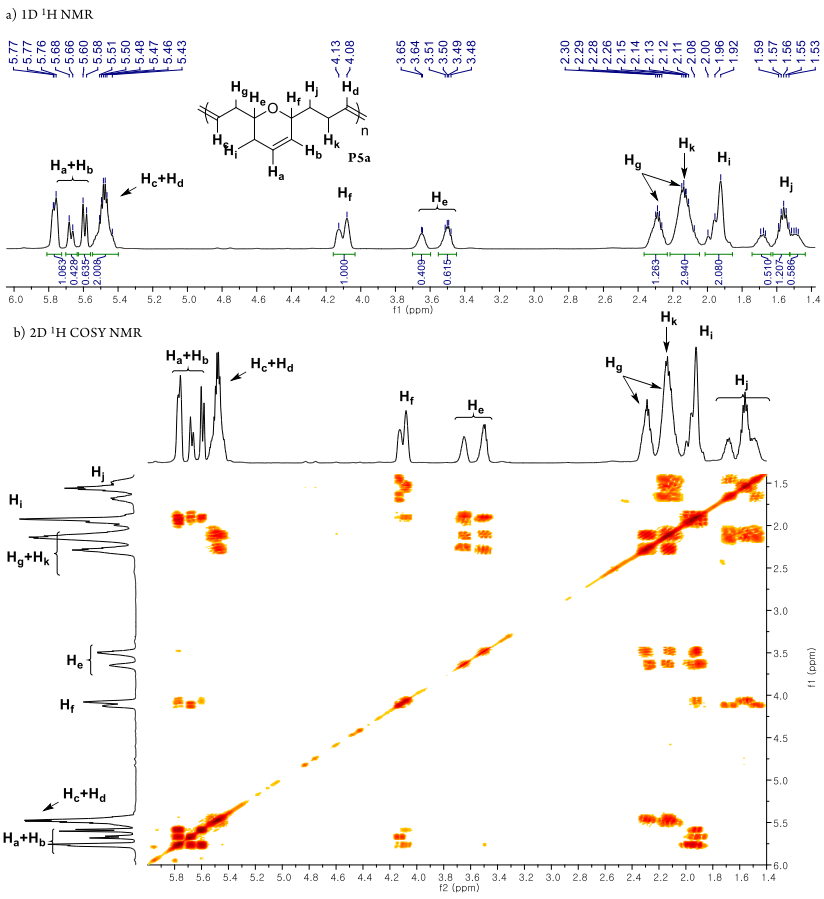

Figure S2.22-1. 1D and 2D COSY Proton NMR spectra of **P4a**.

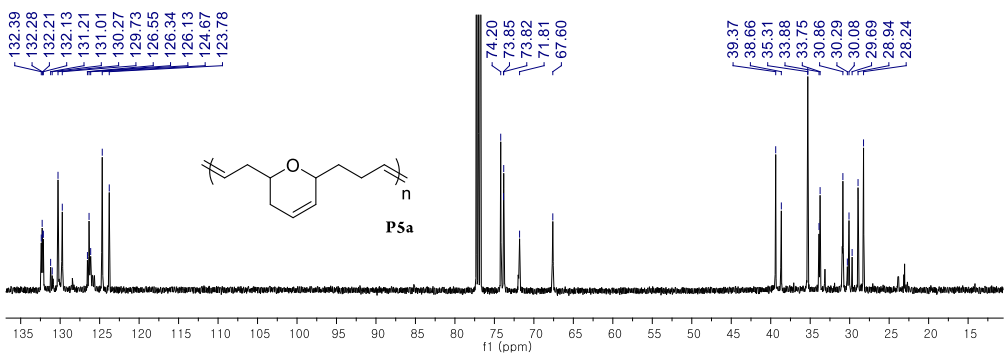

Figure S2.22-2. Carbon NMR spectrum of **P4a.**

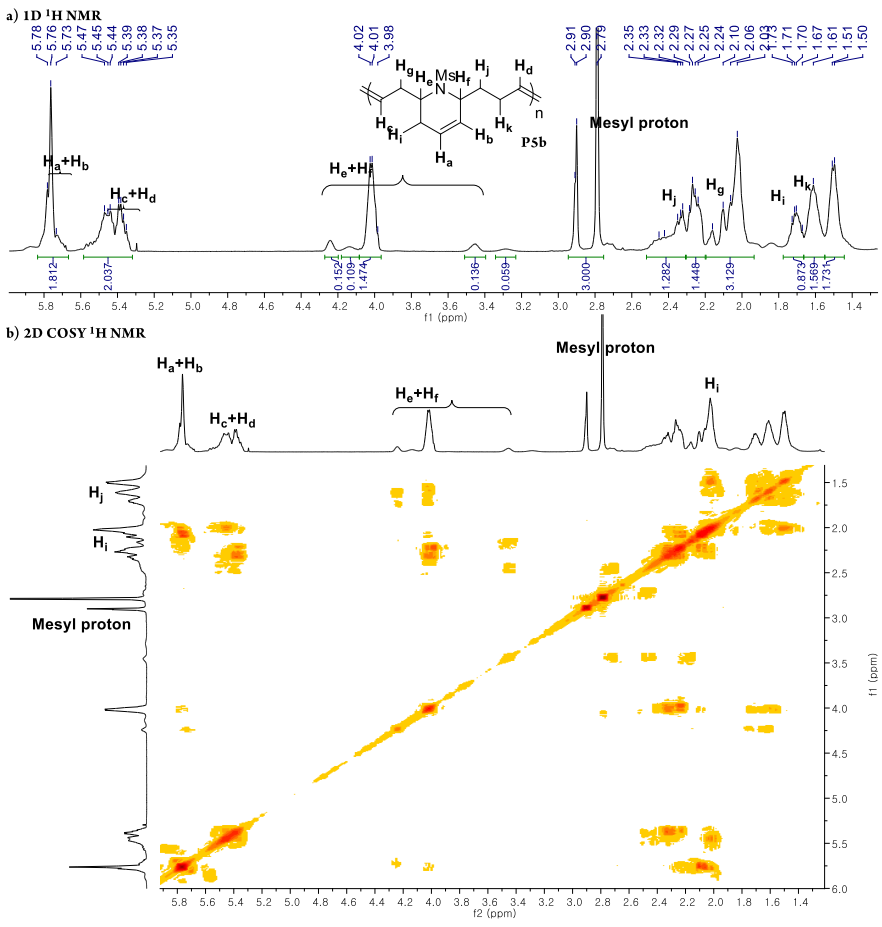

Figure S2.23-1. 1D and 2D COSY Proton NMR spectra of **P4b**.

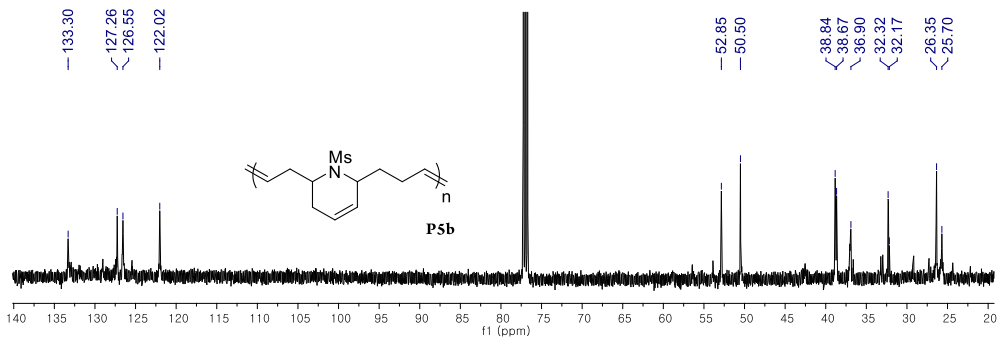

Figure S2.23-2. Carbon NMR spectrum of **P4b**.

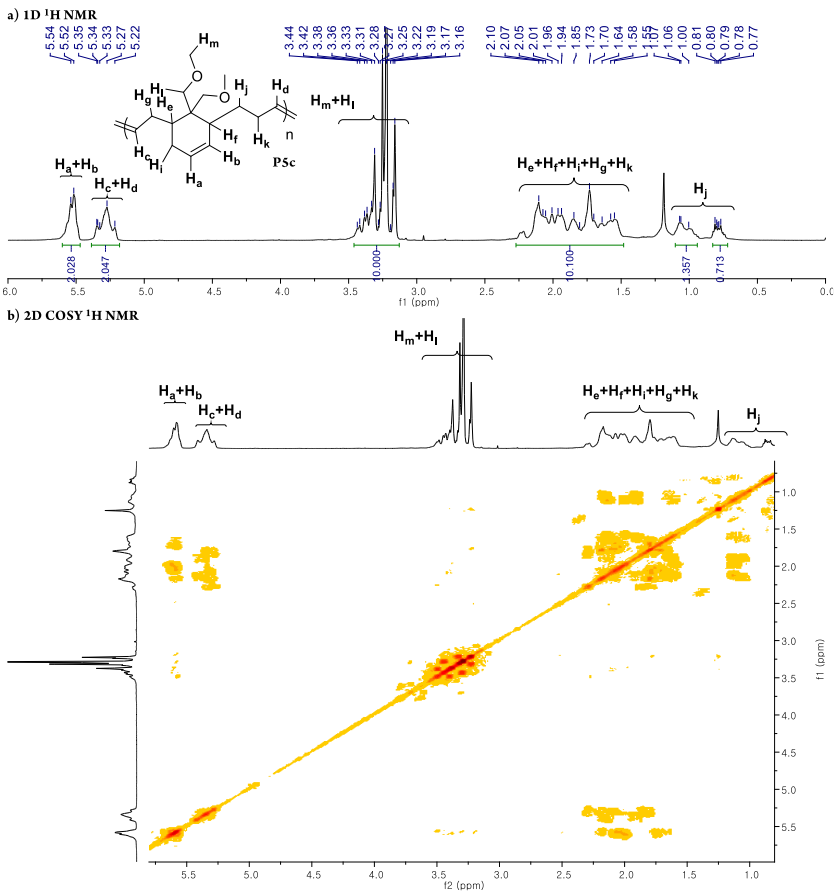

Figure S2.24-1. 1D and 2D COSY Proton NMR spectra of **P4c**.

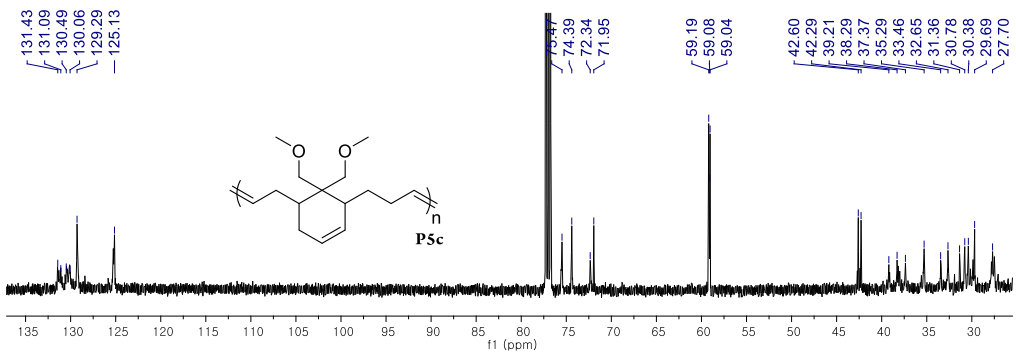

Figure S2.24-2. Carbon NMR spectrum of **P4c**

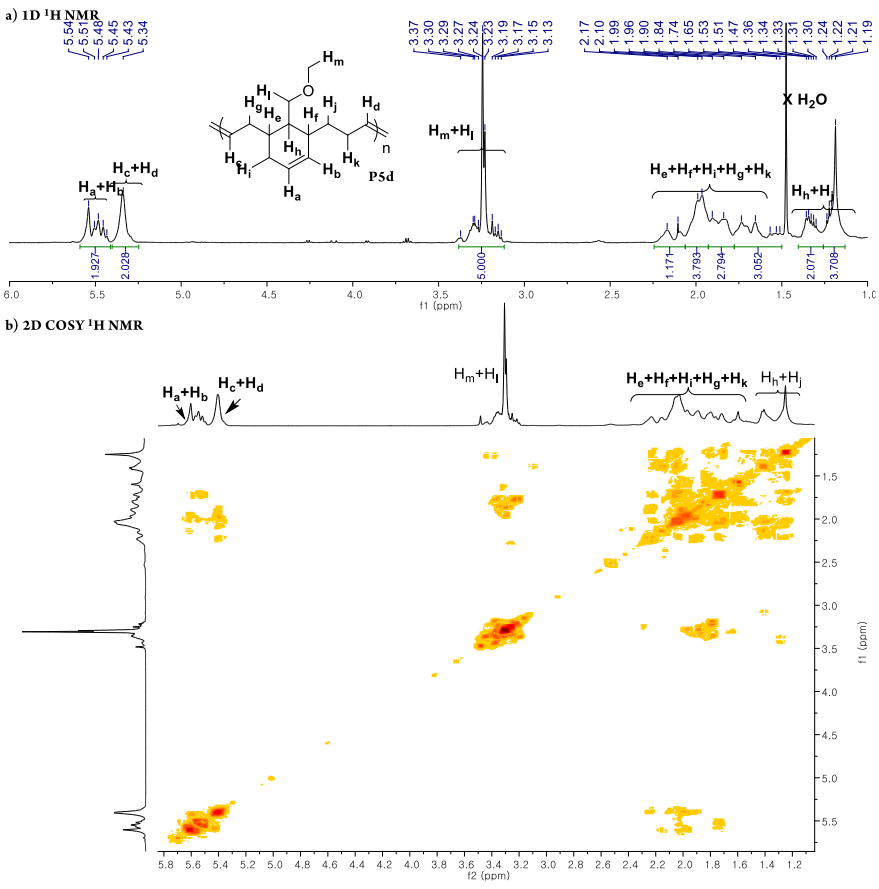

Figure S2.25-1. 1D and 2D COSY Proton NMR spectra of **P4d**.

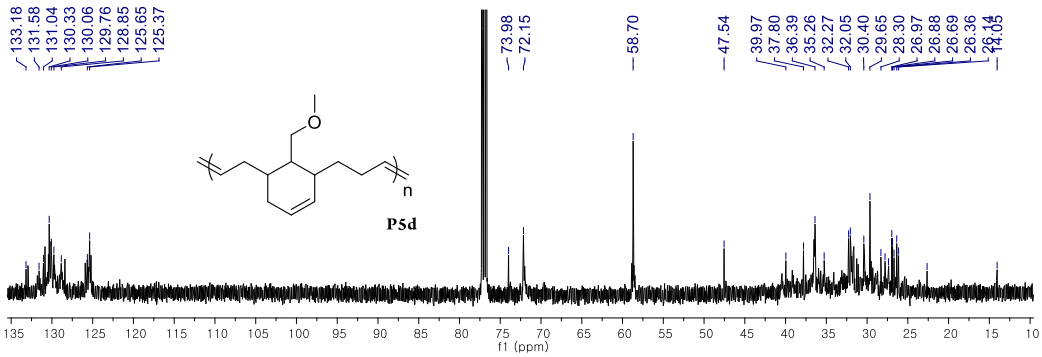

Figure S2.25-2. Carbon NMR spectrum of **P4d**

4. SEC traces of cascade polymers

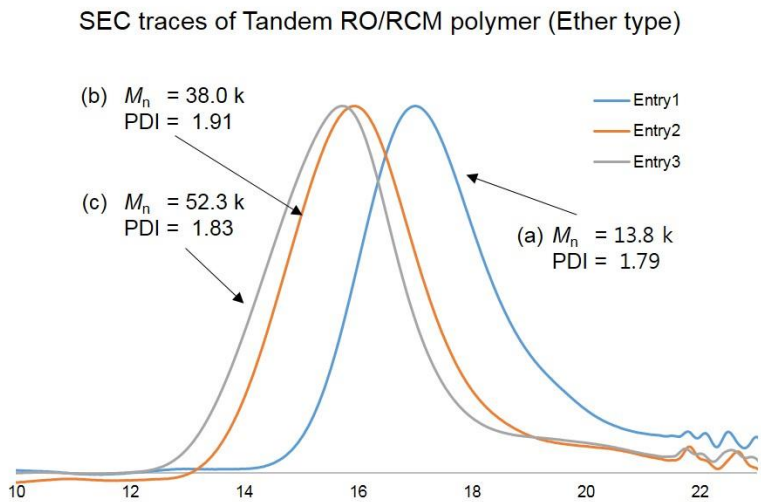

Figure S2.26. THF SEC traces for the tandem RO/RCM ether type polymer. Molecular weights and PDIs are listed in the figure. (a) SEC trace of Table1-Entry1. (b) SEC trace of Table1-Entry2. (c) SEC trace of Table1-Entry3.

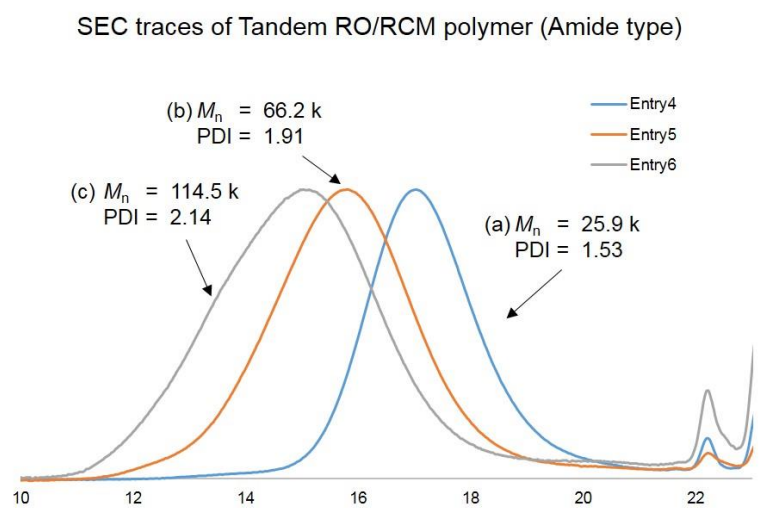

Figure S2.27. THF SEC traces for the tandem RO/RCM amide type polymer. Molecular weights and PDIs are listed in the figure. (a) SEC trace of Table1-Entry4. (b) SEC trace of Table1-Entry5. (c) SEC trace of Table1-Entry6.

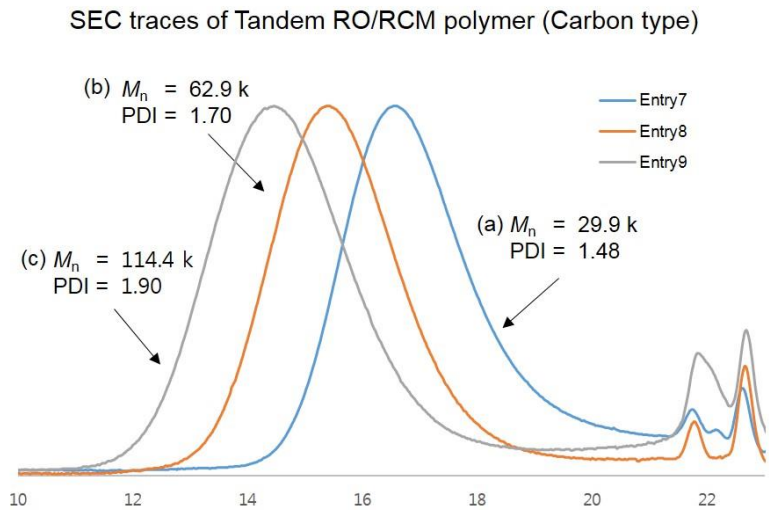

Figure S2.28. THF SEC traces for the tandem RO/RCM carbon type polymer. Molecular weights and PDIs are listed in the figure. (a) SEC trace of Table1-Entry7. (b) SEC trace of Table1-Entry8. (c) SEC trace of Table1-Entry9.

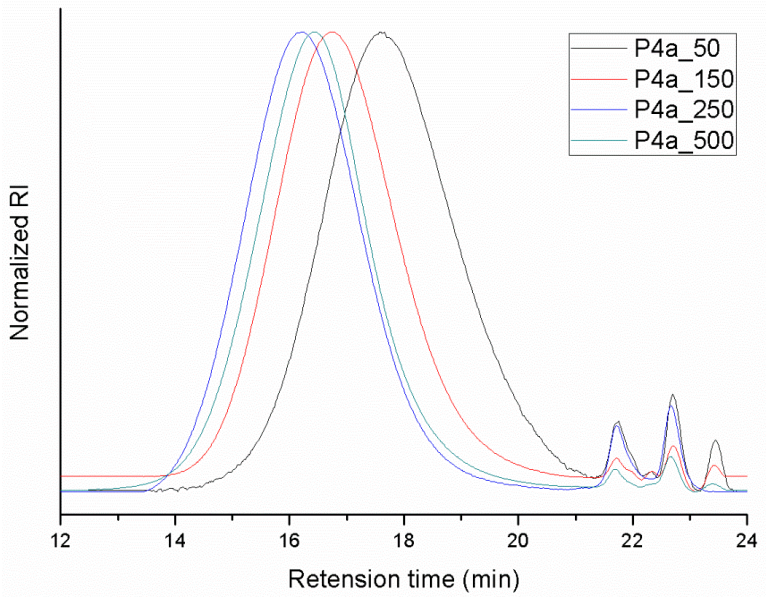

Figure S2.29. THF SEC traces for the cascade polymer of **P4a** (**Table2**, Entries 1-4).

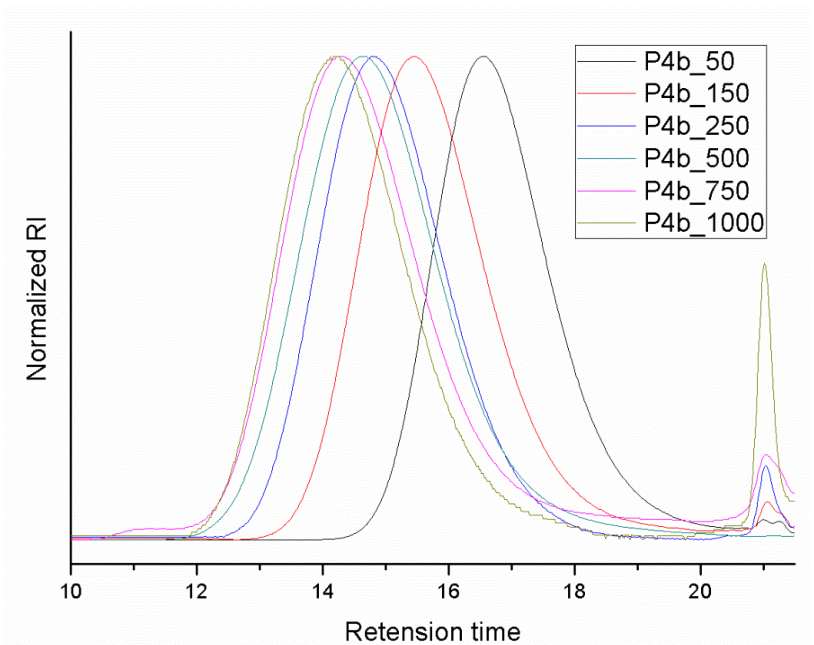

Figure S2.30. THF SEC traces for the cascade polymer of **P4b** (**Table2**, Entries 5-10).

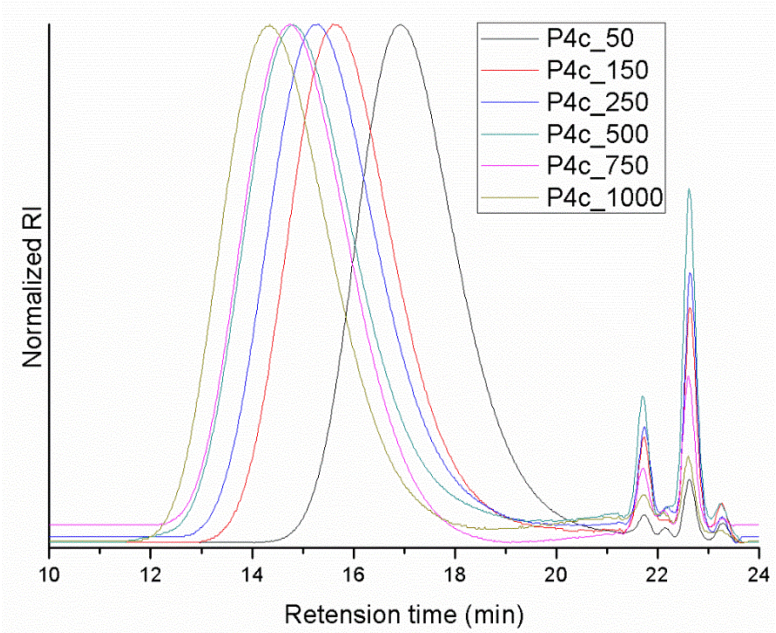

Figure S2.31. THF SEC traces for the cascade polymer of **P4c** (**Table2**, Entries 11-16).

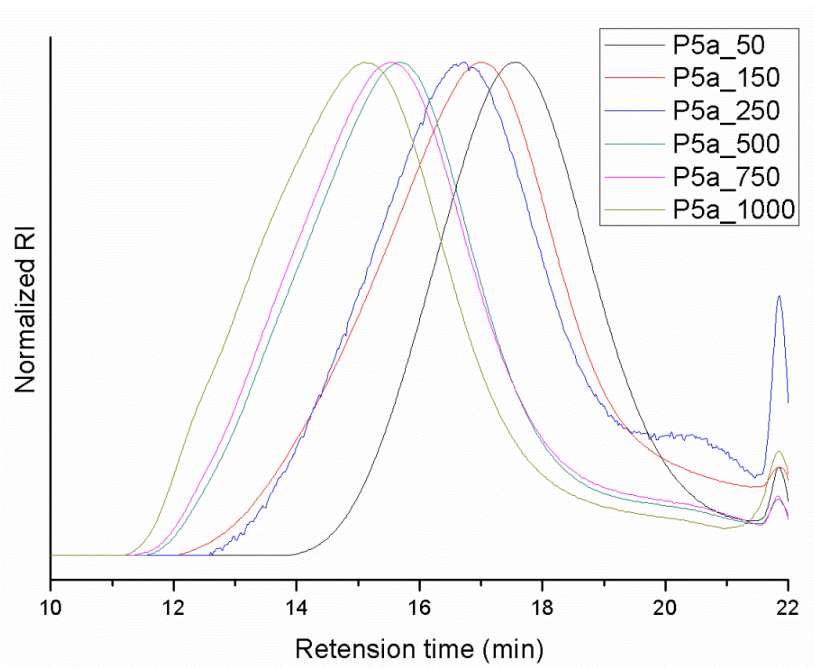

Figure S2.32. THF SEC traces for the cascade polymer of **P5a** (**Table3**, Entries 1-6).

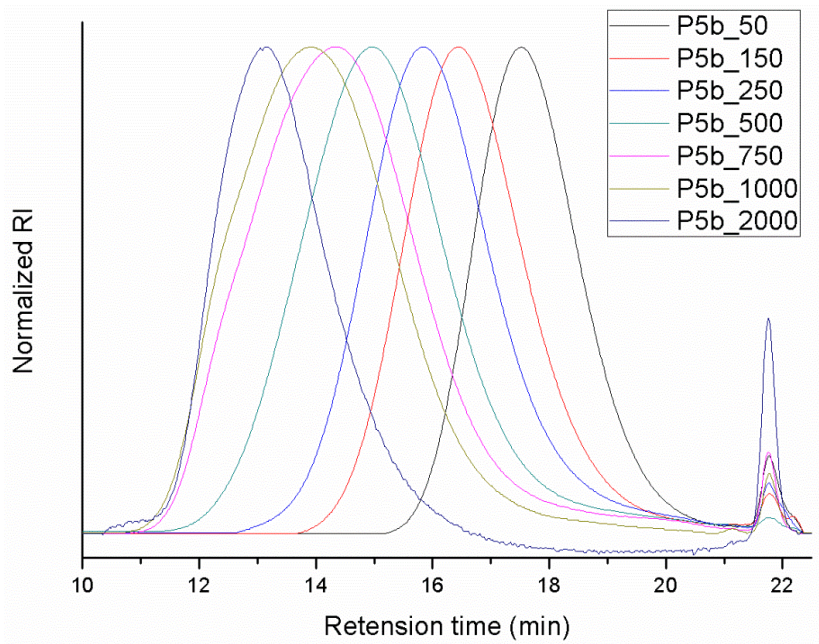

Figure S2.33. THF SEC traces for the cascade polymer of **P5b** (**Table3**, Entries 7-13)

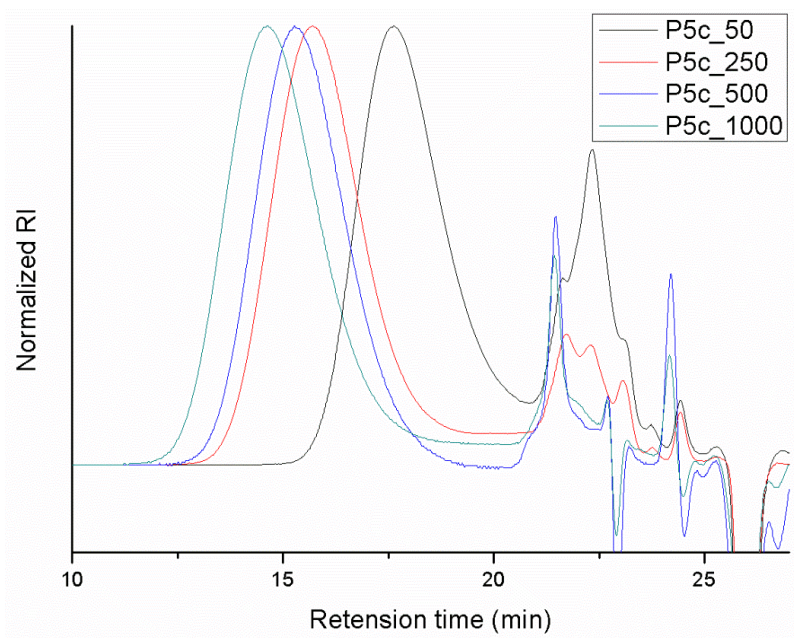

Figure S2.34. THF SEC traces for the cascade polymer of **P5c** (**Table3**, Entries 14-17).

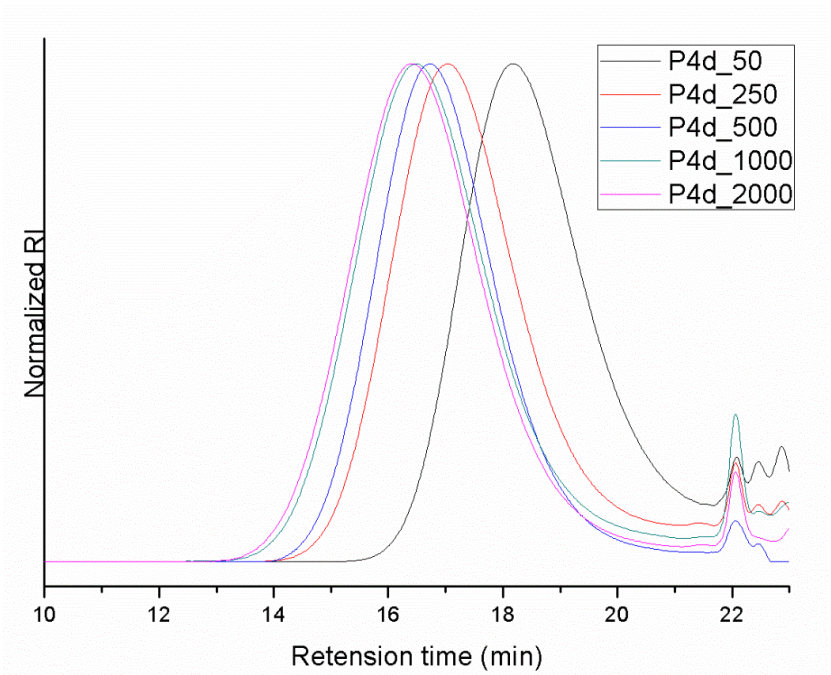

Figure S2.35. THF SEC traces for the cascade polymer of **P5d** (**Table3**, Entries 18-22).

5. MALDI-TOF of Cascade polymer

MALDI-TOF data of cascade polymer

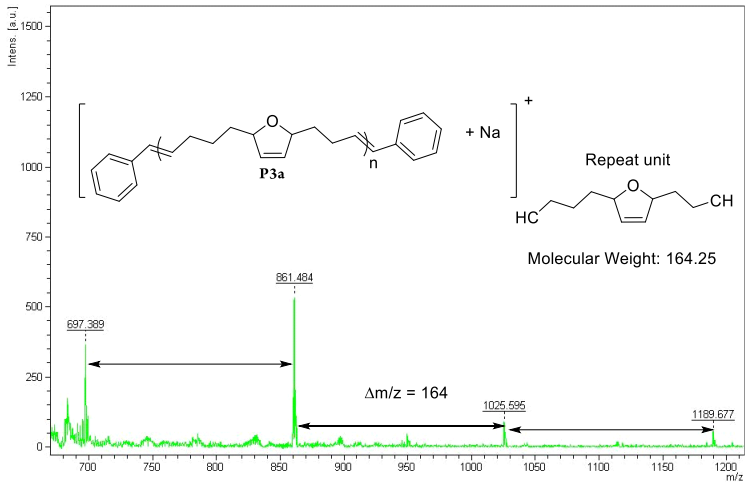

Figure S2.36. MALDI-TOF of **P3a,**

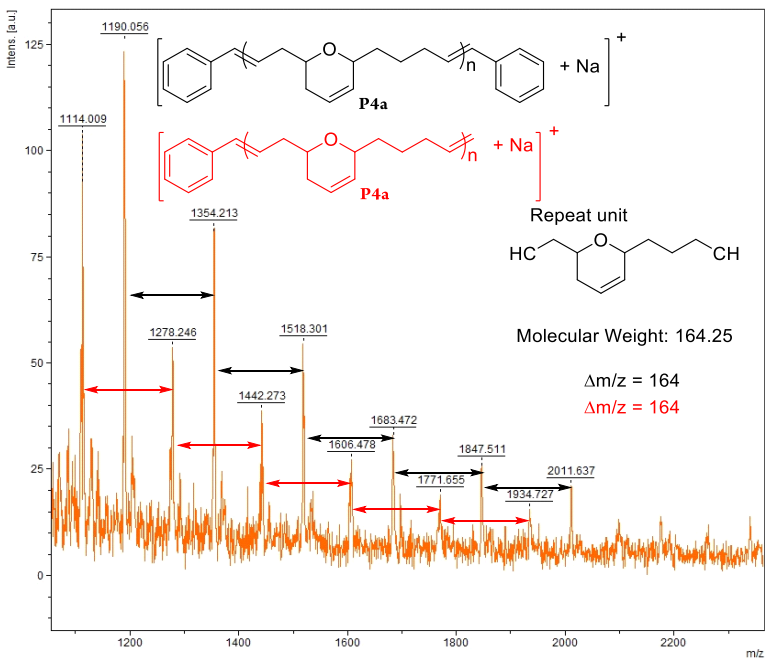

Figure S2.37. MALDI-TOF of **P4a**

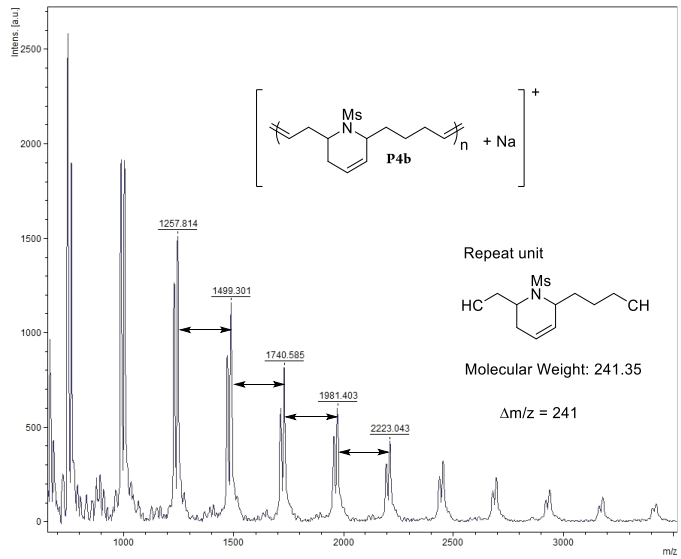

Figure S2.38. MALDI-TOF of **P4b**

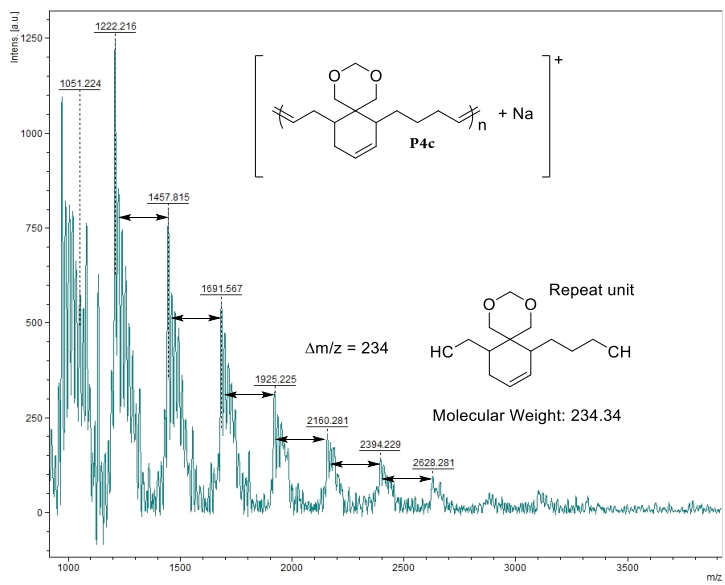

Figure S2.39. MALDI-TOF of **P4c**

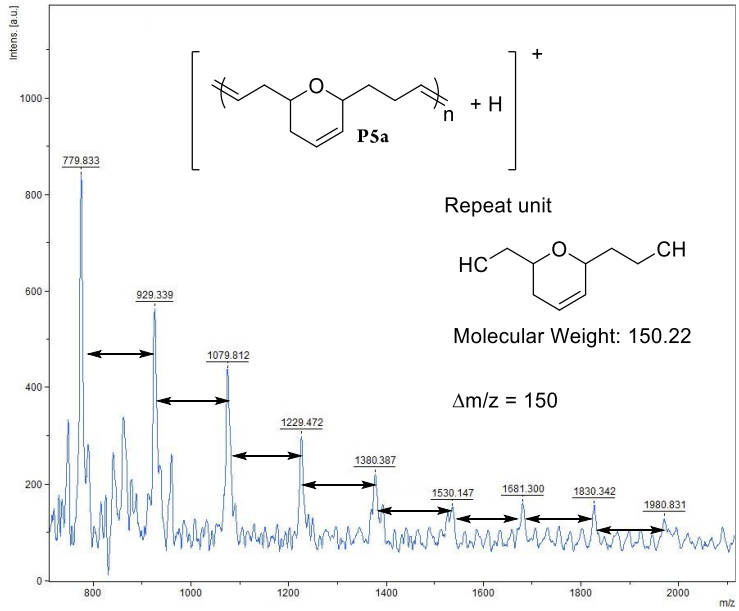

Figure S2.40. MALDI-TOF of **P5a**

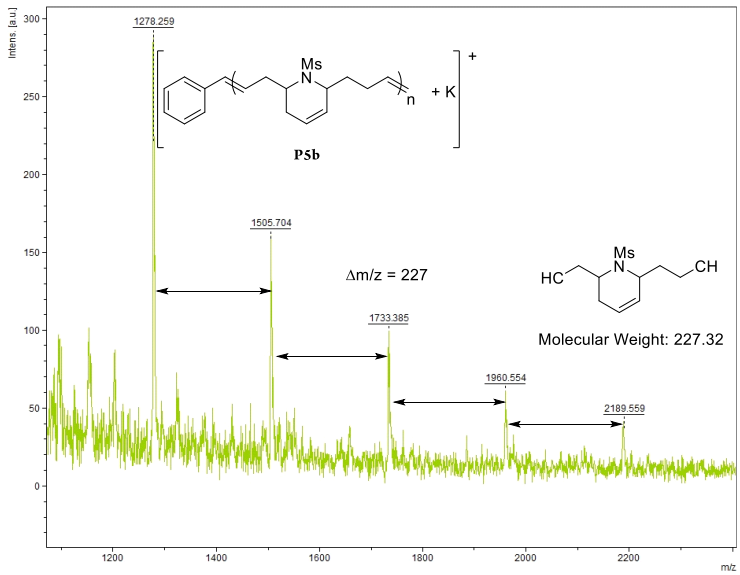

Figure S2.41. MALDI-TOF of **P5b**

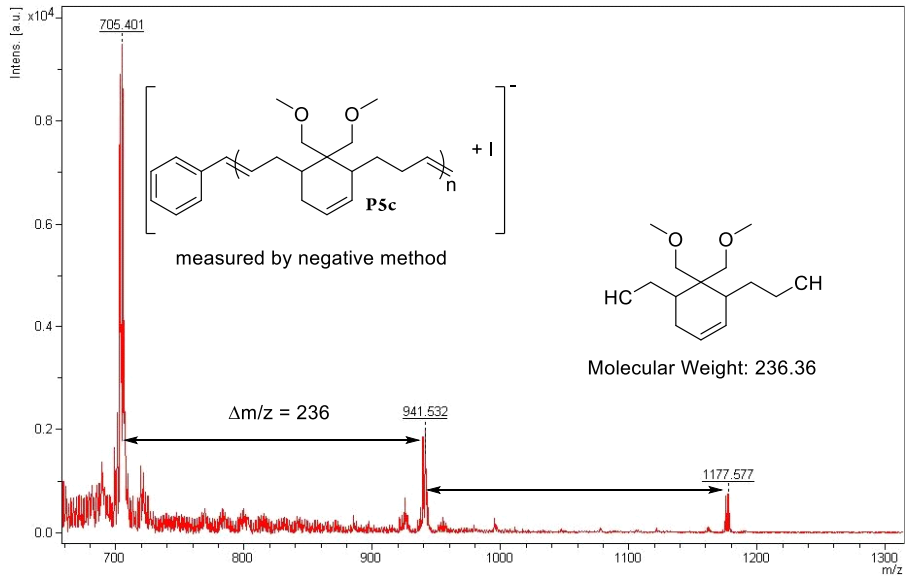

Figure S2.42. MALDI-TOF of **P5c**

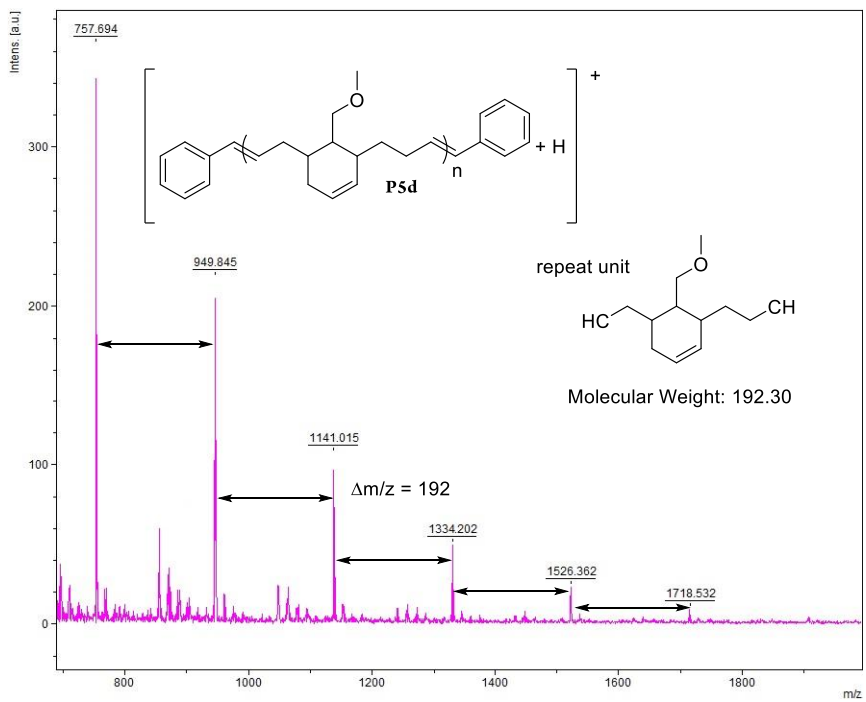

Figure S2.43. MALDI-TOF of **P5d**

2.6 REFERENCES

(1) (a) Grubbs, R. H.; Chang, S. *Tetrahedron* **1998**, *54*, 4413. (b) Fürstner, A. *Angew. Chem., Int. Ed*. **2000**, *39*, 3013. (c) Grubbs, R. H. *Handbook of Metathesis*, Wiley-VCH: Weinheim, **2003**, *1*, 2. (d) Grubbs, R. H. *Tetrahedron* **2004**, *60*, 7117.

(2) (a) Novak, B. M.; Grubbs, R. H. *J. Am. Chem. Soc*. **1988** *110*, 960. (b) Nguyen, S. T.; Johnson, L. K.; Grubbs, R. H. *J. Am. Chem. Soc.* **1992**, *114*, 3974. (c) Nguyen, S. T.; Grubbs, R. H. *J. Am. Chem. Soc*. **1993**, *115*, 9858. (d) Schwab, P.; France, M. B.; Ziller, J. W.; Grubbs, R. H. *Angew. Chem. Int. Ed.* **1995**, *34*, 2039. (e) Schwab, P.; Grubbs, R. H.; Ziller, J. W. *J. Am. Chem. Soc.* **1996**, *118*, 100. (f) Scholl, M.; Ding, S.; Lee, C. W.; Grubbs, R. H. *Org. Lett*. **1999**, *1*, 953. (g) Trnka, T. M.; Grubbs, R. H. *Acc. Chem. Res*. **2001**, *34*, 18.

(3) (a) Schrock, R. R.; Murdzek, J. S.; Bazan, G, C.; Robibins, J.; DiMare, M.; O'Regan, M. *J. Am. Chem. Soc.* **1990**, *112*, 3875. (b) Bazan, G. C.; Oskam, J. H.; Cho, H.-N.; Park, L. Y.; Schrock, R. R. *J. Am. Chem. Soc.* **1991**, *113*, 6899. (c) Feldman, J.; Schrock, R. R. *Prog. Inorg, Chem.* **1991**, *39*, 1.

(4) For reviews, see: (a) Novak, B. M.; Risse, W.; Grubbs, R. H. *Adv. Polym. Sci*. **1992**, *102*, 47-72. (b) Grubbs, R. H.; Khosaravi, E. *Material Science and Technology*, **1999**, *20*, 65. c) Buchmeiser, M. R. *Chem. Rev*. **2000**, *100*, 1565.

(5) For reviews, see: (a) Gruubs, R. H.; Miller, S. J.; Fu, G. C. *Acc. Chem. Res.* **1995**, *28*, 446. (b) Deiters, A.; Martin, S. F. *Chem. Rev*. **2004**, *104*, 2199. (c) Schmidt, B.; Hermanns, J. *Curr. Org. Chem*. **2006**, *10*, 1363.

(6) For recent reviews, see: (a) Schuster, M.; Blechert, S. *Angew. Chem. Int. Ed*. **1997**, *36*, 2036. (b) Connon, S. J.; Blechert, S. *Angew. Chem. Int. Ed.* **2003**, *42*, 1900. (c)

Grubbs, R. H. *Handbook of Metathesis*, 2nd ed.; Wiley-VCH: Weinheim, **2015**; Vols. 2, 3.

(7) (a) Novak, B. M.; Grubbs, R. H. *J. Am. Chem. Soc*. **1988**, *110*, 960. (b) Schrock, R. R. *Acc. Chem. Res*. **1990**, *23*, 158. (c) Bielawski, C. W.; Grubbs, R. H. *Angew. Chem., Int. Ed*. **2000**, *39*, 2903.

(8) (a) For a review on olefin metathesis cyclopolymerization, see: Choi, S.-K.; Gal, Y.-S.; Jin; S.-H.; Kim, H. K. *Chem. Rev.* **2000**, *100*, 1645. For examples of olefin metathesis cyclopolymerization, see: (b) Fox, H. H.; Wolf, M. O.; Odell, R.; Lin, B. L.; Schrock, R. R.; Wrington, M. S. *J. Am. Chem. Soc*. **1994**, *116*, 2827. (c) Anders, U.; Nuyken, O.; Buchmeiser, M. R.; Wurst, K. *Angew. Chem., Int. Ed*. **2002**, *41*, 4044. (d) Anders, U., Nuyken, O.; Buchmeiser, M. R.; Wurst, K. *Macromolecules* **2002**, *35*, 9029. (e) Mayershofer, M. G.; Nuyken, O.; Buchmeiser, M. R. *Macromolecules* **2006**, *39*, 3484. (f) Kang, E.-H.; Lee, I. S.; Choi, T.-L. *J. Am. Chem. Soc*. **2011**, *133*, 11904. (g) Kim, J.; Kang, E.-H.; Choi, T.-L. *ACS Macro Lett.* **2012**, *1*, 1090. (h) Kang, E.-H.; Lee, I.-H.; Choi, T.-L. *ACS Macro Lett.* **2012**, *1*, 1098. (i) Lee, I. S.; Kang, E.-H.; Choi, T.-L. *Chem. Sci*. **2012**, *3*, 761. (j) Kang, E.-H.; Yu, S.-Y; Lee, I.-H.; Park S.-E.; Choi, T.-L. *J. Am. Chem. Soc.* **2014**, *136*, 10508.

(9) (a) Wagener, K. B.; Boncella, J. M.; Nel, J. G. *Macromolecules* **1991**, *24*, 2649. (b) Patton, J. T.; Boncella, J. M.; Wagener, K. B. *Macromolecules* **1992**, *25*, 3862. (c) Brzezinska, K.; Wolfe, P. S.; Watson, M. D.; Wagener, K. B. *Macromol. Chem. Phys.* **1996**, *197*, 2065. (d) Mutlu, H.; Montero de Espinosa, L.; Meier, M. A. R. *Chem. Soc. Rev.* **2011**, *40*, 1404.

(10) Choi, T.-L.; Rutenberg, I. M.; Grubbs, R. H. *Angew. Chem. Int. Ed*. **2002**, *41*, 3839.

(11) Ding, L.; Xie, M.; Yang, D.; Song, C. *Macromolecules* **2010**, *43*, 10336.

(12) (a) Park, H.; Choi, T.-L. *J. Am. Chem. Soc.* **2012**, *134*, 7270. (b) Park, H.; Lee, H.-K; Choi, T.-L. *J. Am. Chem. Soc.* **2013**, *135*, 10769. (c) Park., H.; Kang, E.-H.; Müller., L.; Choi, T.-L. *J. Am. Chem. Soc.* **2016**, *138*, 2244.

(13) Gutekunst, W. R.; Hawker, C. J. *J. Am. Chem. Soc.* **2015**, *137*, 8038.

(14) Kang, C.; Park, H.; Lee, J.-K.; Choi, T.-L. *J. Am. Chem. Soc.* **2017***, 139,* 11309.

(15) (a) Lee, H.-K.; Bang, K.-T.; Hess, A.; Grubbs, R. H.; Choi, T.-L. *J. Am. Chem. Soc.* **2015**, *137*, 9262. (b) Lee, H.-K.; Choi, T.-L. *ACS Macro Lett.* **2018**, *7*, 531.

(16) (a) Kanaoka, S.; Grubbs, R. H. *Macromolecules* **1995**, 28, 4707. (b) Weck, M.; Schwab, P.; Grubbs, R. H. *Macromolecules* **1996**, 29, 1789.

(17) Garber, S. B.; Kingsbury, J. S.; Gray, B. L.; Hoveyda, A. H. *J. Am. Chem. Soc*. **2000**, 122, 8168.

(18) Nelson, D. J.; Ashworth, I. W.; Hillier, I. H.; Kyne, S. H.; Pandian, S.; Parkinson, J. A.; Percy, J. M.; Rinaudo, G.; Vincent, M. A. *Chem. Eur. J.* **2011**, *17*, 13087.

(19) Hejl, A.; Scherman, O. A.; Grubbs, R. H. *Macromolecules* **2005**, 38, 7214.

(20) Chatterjee, A. K.; Choi, T.-L.; Sanders, D. P.; Grubbs, R. H. *J. Am. Chem. Soc.* **2003**, *125*, 11360.

Chapter 3: Unusual Superior Activity of the First Generation Grubbs Catalyst in Cascade Olefin Metathesis Polymerization

3.1. Abstract

We reported a new cascade ring-opening/closing metathesis polymerization of monomers containing two cyclopentene moieties (Chapter 2). Several Ru catalysts were tested, but the best polymerization results were unexpectedly obtained using the first-generation Grubbs catalyst (**G1**). This was puzzling since the second- and third-generation Grubbs catalysts are well known for their higher activity compared to **G1**. In order to explain the unique and superior activity of **G1**, we conducted a series of kinetics experiments for the polymerization of 3,3'-oxydicyclopent-1-ene, a representative monomer of this cascade polymerization, as well as the competition polymerization with cycloheptene using the various Grubbs catalysts. Based on our results, we propose a model in which the differences in the steric hindrance between the different ligands and the monomer determine the selectivity of the catalyst approach to the monomer and, therefore, the extent to which the productive pathway leads to successful cascade polymerization. In short, **G1** with the smaller ligand showed a high preference for the productive pathway.

3.2 Introduction

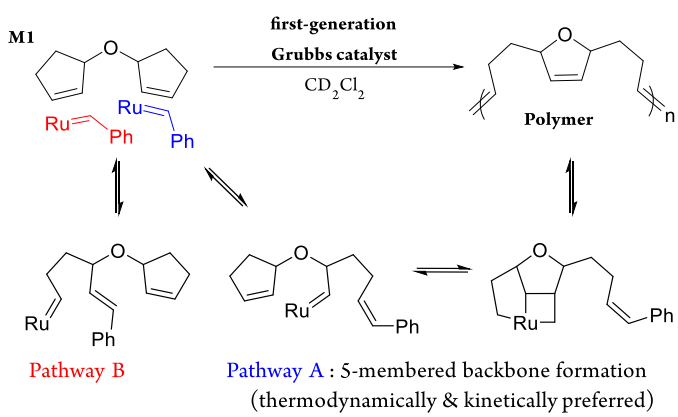

Scheme 3.1. Cascade ring-opening/ring-closing olefin metathesis polymerization

Over the past several decades, olefin metathesis reactions have been widely used as an efficient method to form new carbon-carbon double bonds[1] via three fundamental transformations, namely, ring-opening metathesis (ROM)[2], ring-closing metathesis (RCM)[3], and cross metathesis (CM)[4]. Owing to the continuous development of the Schrock catalysts[5] based on W and Mo metals, and the Grubbs catalysts[6] based on Ru metal, the field of olefin metathesis has greatly expanded in terms of both organic and polymer synthesis. In the case of the user-friendly Grubbs catalyst, the first-generation Grubbs catalyst (**G1**), which has two phosphine ligands,[7] was frequently used because of its wide functional group tolerance and high stability. However, **G1** suffered from significantly lower activity compared to the Schrock catalysts. This diminished its utility. To increase its activity, Grubbs' group exchanged one of the phosphine ligands with a strong σ-donating *N*-heterocyclic carbene (NHC) to give the well-known second-generation Grubbs catalyst (**G2**).[6f,8] With this catalyst, more challenging olefin metathesis reactions using electron-deficient or bulky olefins became possible, thus broadening the scope and utility of olefin metathesis reactions.[9] A representative example in polymer synthesis is the ring-opening insertion metathesis polymerization of diacrylates and cycloalkene monomers to give A,B-alternating copolymers and this was not possible with **G1**.[10] The highly active third-generation Grubbs catalyst (**G3**) was subsequently developed by replacing the phosphine ligand of **G2** with a more labile pyridine ligand. As a result of its significantly increased initiation rate, the highly active **G3** has become the most popular catalyst for numerous living ring-opening metathesis polymerizations (ROMP)[12] of bulky monomers[13] and living cyclopolymerizations[14] to give block copolymers with narrow dispersity from a wider range of monomers. With this catalyst, our group and others have demonstrated several cascade polymerizations via interesting tandem reactions[15] which were unsuccessful with **G1**. In contrast, we recently reported another unique cascade ring-opening/ring-closing metathesis polymerization of monomers containing two cyclopentene moieties using **G1** to give well-defined polymers containing new rings via a rearrangement reaction. (**Scheme 3.1**)[15d] One surprising and puzzling feature was that the intrinsically less active **G1**

outperformed **G3,** which should be generally more active.[15] Herein, we describe our efforts to mechanistically understand this unique tendency of the cascade metathesis polymerization using various Ru catalysts. We have monitored the kinetics of the polymerization of 3,3'-oxydicyclopent-1-ene **(M1)** and its competition reactions with cycloheptene. From the results, we have developed a model to show that the size of the ligand determines the preference between two competing pathways; indeed, **G1** which possessed the smaller ligand proceeded with a productive pathway to give superior efficiency in this cascade polymerization.

3.3. Results and Discussion

Previously, we compared the conversion of **M1** during the cascade polymerization (**M1** concentration of 0.5 M and catalyst loading of 2 mol%) using three Grubbs catalysts: **G1**, the second-generation Hoveyda-Grubbs catalyst (**HG2**), and **G3**.[15d] After 6 h, the conversions for **G1** and **HG2** were 100% and 45%, respectively, while that of **G3** could not be determined due to unknown side reactions. (**Figure S2**) In order to understand this ironic superiority of **G1** over the supposedly more active catalysts containing the NHC ligand, we used NMR experiments to monitor the kinetics of the cascade polymerization of **M1** over 25 min (**M1** concentration of 0.33 M in CD_2Cl_2 and monomer/initiator ratio of 10:1) with three different catalysts: **G1**, **HG2**, and **G3**.

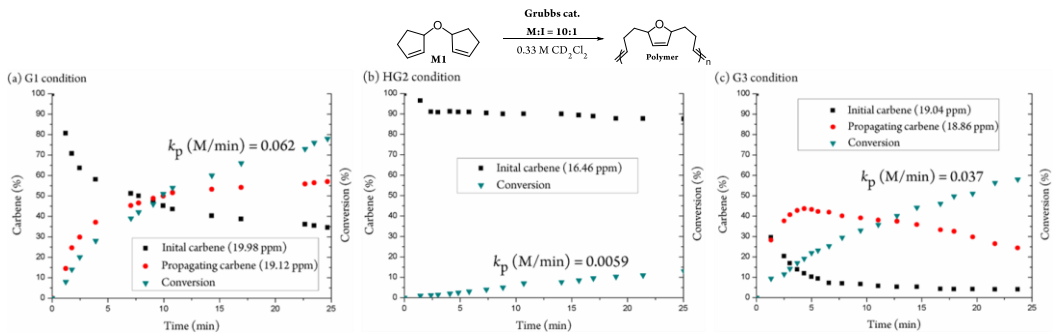

Figure 3.1. Kinetic plots of cascade polymerization of M1. Carbene % and polymerization conversion were determined by ^{1}H NMR.

The result using **G1** (**Figure 3.1(a)**) showed that the initiation rate was moderate; the initial carbene at 19.98 ppm decreased to 35% while a new propagating carbene at 19.12 ppm increased proportionately up to 55%. The polymerization proceeded well with conversion up to 75% and the corresponding propagating rate was 0.062 M/min. Next, **HG2** (**Figure 3.1(b)**), both initiation and polymerization were much slower than **G1**. For **HG2**, the propagating carbene from the 14 electron Ru species was impossible to observe by ^{1}H NMR.[16] Notably, the k_p of **HG2** was about 10 times lower than that of **G1** (k_p of 0.062 vs 0.0059 M/min, respectively). Despite possessing a stronger σ-donation NHC ligand, one could initially attribute this very slow propagation to the slow initiation of **HG2**. For **G3** (**Figure 3.1(c)**), the rapid dissociation of the 3-chloropyridine ligand led to the fastest initiation (90% initiation in 5 min). A new peak at 18.86 ppm corresponding to the propagating carbene increased up to 45% in 5 min, gradually decreasing over time. In spite of the fastest initiation of **G3**, however, its k_p was about 1.7 times slower than the intrinsically less active **G1** (0.062 M/min vs 0.037 M/min). In particular, after 3 min, although the population of the propagating carbene was higher for **G3** than **G1** (38% vs 30%), the conversion was higher for **G1** than **G3** (20% vs 13%) (**Figure 3.1(a)**, **(c)**). In other words, even with lower activity and a lower amount of propagating species, the cascade polymerization worked best with **G1,** which is in contrast with the general order of the Grubbs catalysts' activities.[17]

To understand this puzzle, we focused on the mechanism of the polymerization and the structural differences between the ligands of **G1** and **G3**. As shown in **Scheme 3.2**, the Grubbs catalysts can approach **M1** via two pathways: the productive pathway A (**Scheme 3.2(a)**), and the unproductive pathway B (**Scheme 3.2(b)**). In pathway A, the Ru metal faces the oxygen linker such that it ring-opens two cyclopentenes to form a thermodynamically stable 5-membered heterocycle repeat unit. In pathway B, however, the Ru metal approaches from the opposite direction and the cascade reaction does not occur because the first ring-opened cyclopentene rapidly undergoes ring-closure to reform the

monomer instead of producing the thermodynamically and kinetically unfavored 7-membered ring.

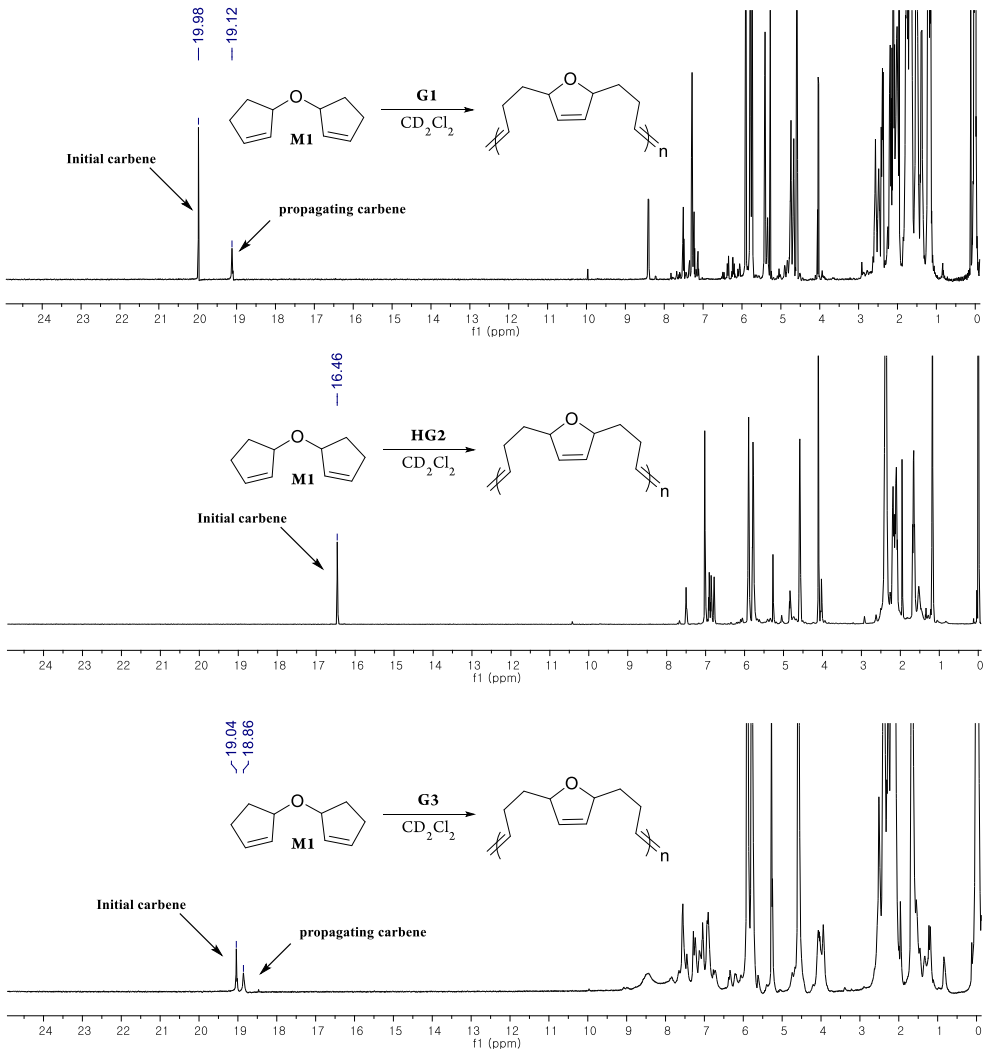

Figure S3.2. Quantitative analysis of remaining initial carbene and generating propagating carbene with M1 using Grubbs catalysts (^{1}H NMR in CD_2Cl_2)

Scheme 3.2. Plausible modeling of cascade metathesis polymerization with M1 and ROMP with cycloheptene

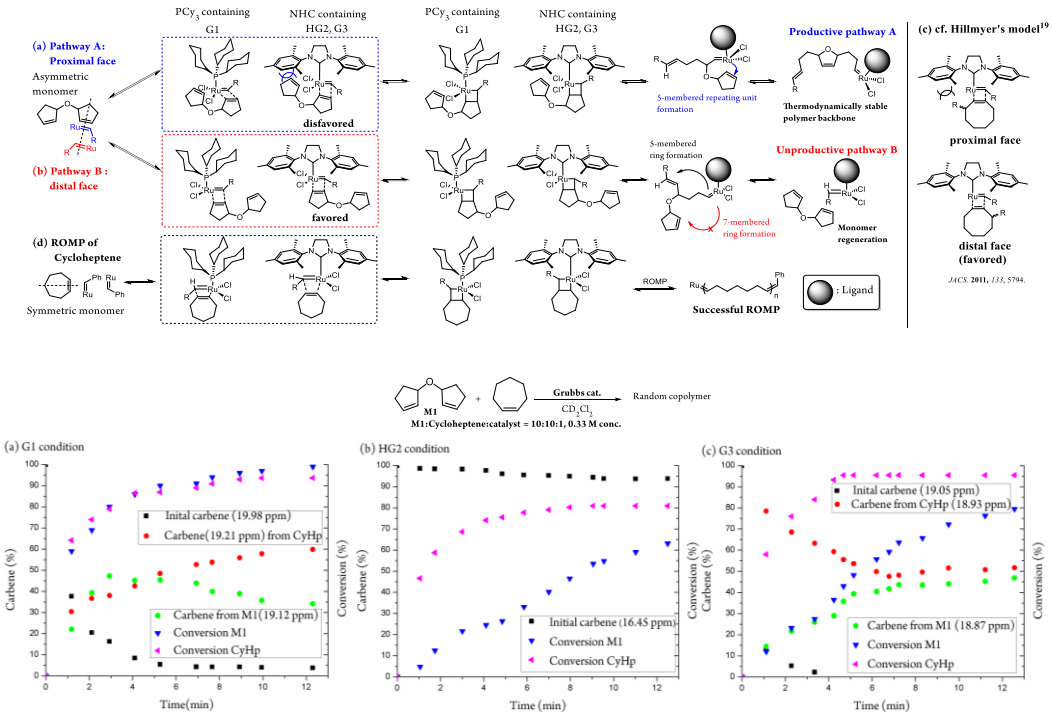

Figure 3.3. Kinetic plots of competitive polymerization between M1 and cycloheptene. Carbene % and polymerization conversion were determined by ^{1}H NMR. CyHp : cycloheptene.

Thus, the efficiency of the polymerization in this system should depend not only on the intrinsic activity of the catalyst but also on its selectivity towards the productive pathway. According to crystallographic studies from the Peterson group[18], the phosphine ligand on **G1** is cone-shaped, with a PCy_3-Ru angle of 96°, whereas the more active NHC-containing catalysts form a fence-type geometry with angles of 150.7° in the horizontal direction and 115.3° in the perpendicular direction. This results in higher steric congestion in the NHC-containing catalysts. Based on these arguments, therefore the sterically demanding NHC-Ru catalysts would favor the unproductive pathway B over the productive cascade polymerization pathway A due to the steric repulsion between the 3-substituted

cyclopentene of **M1** and the NHC ligand of the catalyst (**Scheme 3.2**). Thus, a low efficiency of the polymerization will occur, as were our observations. On the other hand, both pathways are accessible for **G1** which contains a relatively smaller ligand, so that even with its decreased activity, the cascade polymerization proceeds smoothly and efficiently via the productive pathway. This model is in good agreement with the model used by Hillmyer's group (**Scheme 3.2(c)**) to describe the regioselectivity of the ROMP of 3-substituted cyclooctene using **G2** and **G3**.[19] Similarly, they argued that due to steric repulsion between the substituent at the 3-position of cyclooctene and the NHC ligand, distal face led to head-to-tail regioregular ROMP polymers for **G2** and **G3** (**Scheme 3.2(d)**). On the other hand, the smaller ligand of **G1** allowed both the proximal and distal faces to form a random polymer. Very recently, Kennemur's group also reported a similar regioregular ROMP polymer from 3-substituted cyclopentene and **HG2** via an analogous distal face mechanism.[20] By applying the same rationale of ligand sizes directing the preference in the accessibility of the monomer to our results, we could explain how the same size-preference (distal face) led to the regioselective ROMP of 3-substituted cyclooctene in the literature,[19] but to the poor cascade polymerization using NHC-containing catalysts in our instance.

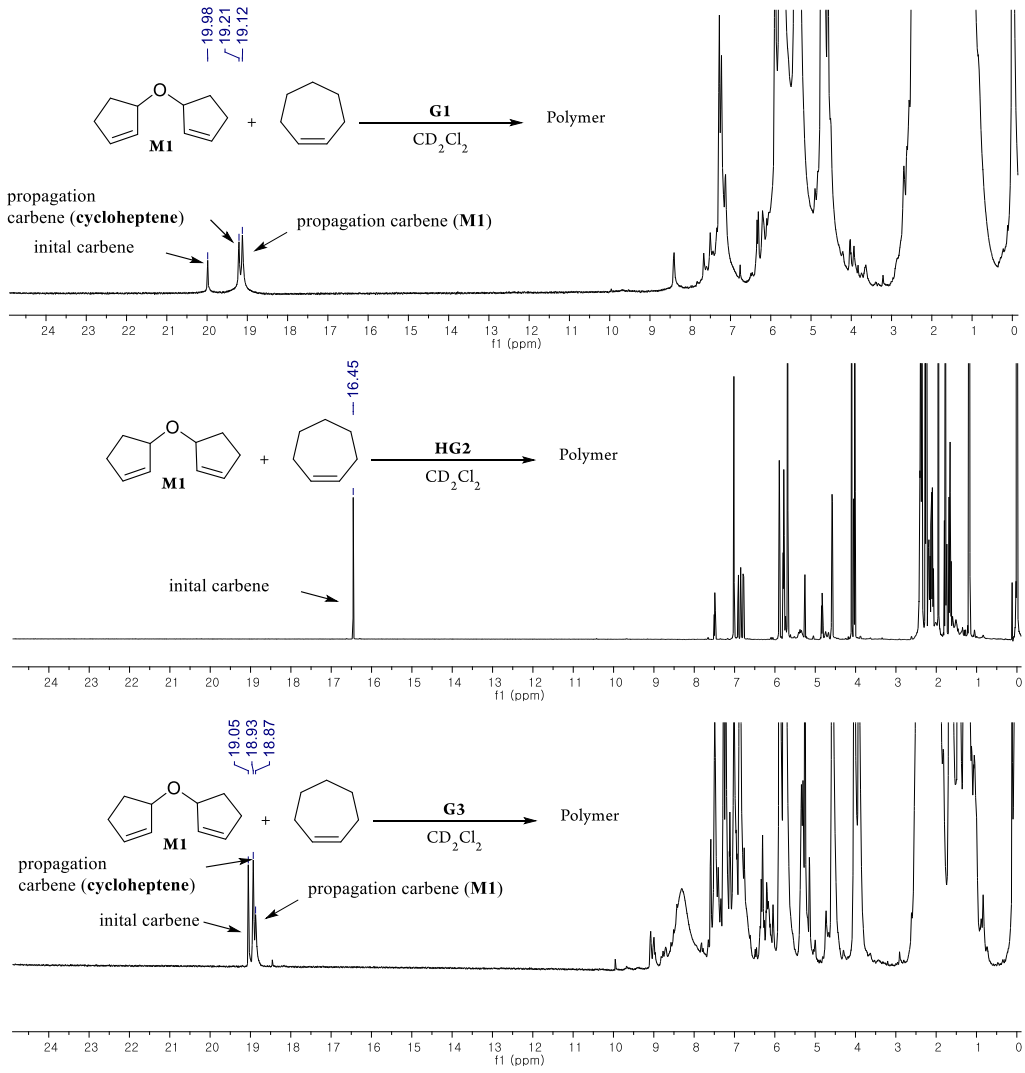

Figure 3.4. Quantitative analysis of remaining initial carbene and generating propagating carbene with M1, cycloheptene using Grubbs catalysts (^{1}H NMR in CD_2Cl_2)

Table 3.1. Rates of competition polymerization with M1 and cycloheptene (unit: s^{-1})

Entry	catalyst	k_{M1}	$k_{cycloheptene}$	$k_{M1} : k_{cycoheptene}$
1	**G1**	0.52	0.54	1 : 1.04
2	**HG2**	0.073	0.38	1 : 5.60
3	**G3**	0.11	0.61	1 : 5.90

In order to confirm this assumption, we designed a competition experiment in which **M1** and cycloheptene were copolymerized. Cycloheptene has a ring strain energy similar to cyclopentane but undergoes ROMP at this dilute concentration. Furthermore, symmetric cycloheptene is a good candidate for this competition experiment since either pathway of the catalyst's approach would give successful and identical ROMP products[21], thus allowing the polymerization rate of each catalyst to be compared (**Scheme 2(d)**). The ^{1}H NMR experiments were conducted with 10 equivalents of **M1** and cycloheptene using the different catalysts (**G1**, **HG2,** and **G3**), and the kinetic plots were monitored for the first 12 min. First, with **G1**, complete initiation occurred within 6 min, and two types of propagating carbenes corresponding to the carbene reacted with cycloheptene and **M1** appeared simultaneously at 19.21 ppm and 19.12 ppm, respectively. Also, a random copolymerization of both **M1** and cycloheptene proceeded at high rates with higher than 90% conversion in 10 minutes (**Figure 3.2(a)**). The initial rate of polymerization during the first 4 min was almost the same for both; 0.52 M/min and 0.54 M/min for **M1** and cycloheptene, respectively (**Table 3.1, Entry 1**). This result implied that even with the competition, the cascade polymerization using **G1** proceeded well via the productive pathway A. In the case of **HG2** (**Figure 3.2(b)**), the ROMP of cycloheptene was quite fast (0.38 M/min), despite a slow initiation, but cascade polymerization of **M1** was much slower with a rate of 0.073 M/min. The polymerization of cycloheptene was 5.6 times faster than **M1** (**Table 3.1, Entry 2**). Finally, the competition experiment using **G3** (**Figure 3.2(c)**), showed the fastest initiation, with completion within 4 min. After 1 min, the propagating carbene from cycloheptene (at 18.93 ppm) reached 80% while that from **M1** (at 18.87 ppm) was 15%. This translated to the fastest reactivity; the ROMP of cycloheptene was 0.61 M/min (**Table 3.1, Entry 4**), reaching 95% conversion in 5 min, but the cascade polymerization rate for **M1** was 0.11 M/min, about 5.2 times slower than that of **G1**. Likewise, cycloheptene polymerized 5.9 times faster than **M1** using **G3**, suggesting that the Ru catalysts containing the large NHC ligand reacted faster with cycloheptene (about 6-fold increase), while the Ru catalyst containing the smaller PCy_3 ligand (**G1**) showed no

preference at all. This also supports the model in which the low reactivity of the NHC-containing catalysts was attributed not to their intrinsic low activity, but to their strong preference for the unproductive pathway B (distal face) to reform the monomer, **M1,** over the productive pathway A that would have led to the cascade polymerization (**Scheme 3.2**). As such, **G1** was shown to be the best catalyst for this system given its excellent selectivity for the productive pathway in the cascade polymerization with **M1**.

From these results, we could predict that cross-linking formation using **M1a** in **chapter 2** could proceed depending on the different type of Grubbs catalysts.

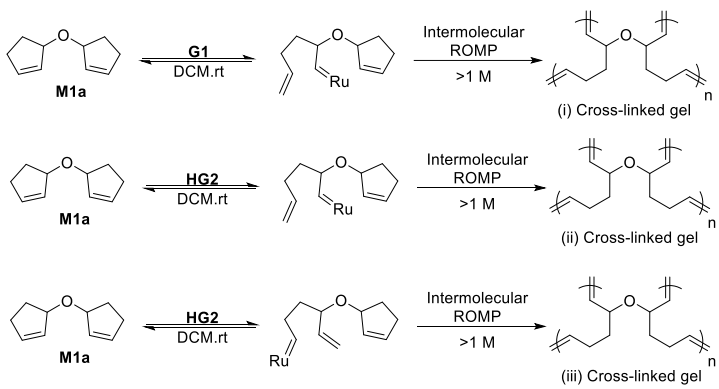

Scheme 3.3. Cross-linking formation using different Grubbs catalysts

In order to determine which of the two cross-linking catalysts occurred more rapidly, the following experiment was carried out. The reaction conditions were to cross-link the 2 mol% catalyst at 1.5 M concentration. In the experiment using **HG2**, cross-linking was formed in about 50 seconds and cross-linking was formed in about 3 minutes and 36 seconds using **G1**. Cross-linking is about four times slower in **G1** conditions.

Considering the cross-linking process, the cross-linking gel can be formed faster in **HG2** because cross-linking formation is performed irrespective of the approach direction of the catalyst, unlike cascade polymerization. In cascade polymerization, only **pathway A** (**Scheme 3.2.**) is the only pathway for polymer formation, but in cross-linked gel formation, both **pathways A** and **B** can form cross-linked gels. Therefore, cross-linking through ring-closing metathesis with other monomers seems to accelerate using **HG2**.

3.4 Conclusion

In conclusion, we have disclosed how **G1**, which has an intrinsically lower activity, is able to promote superior performance in the cascade polymerization of **M1**. We conducted polymerization kinetics experiment with **M1** and its competition experiments with cycloheptene using various Ru catalysts. Based on our results, we propose a plausible model in which the size of the ligand determines the preference for the productive polymerization pathway. As a result, more active catalysts containing bulky NHC ligand favor unproductive pathways which leads to retarded polymerization. On the other hand, **G1**, with smaller PCy_3 ligands, could more easily proceed to the productive pathway, resulting in superior polymerization efficiency. This work provides a deeper understanding of the olefin metathesis mechanism process, accounting for a unique observation that was different from the general reactivity order of Grubbs catalysts.

3.5 Experimental Section

General experimental

All reagents which are commercially available were used without further purification. For polymerization, DCM ample was used. DCM was just opened and used before using on polymerization. Thin-layer chromatography (TLC) was carried out on MERCK TLC silica gel 60 F254 and flash column chromatography was performed using MERCK silica gel 60 (0.040~0.063 mm). ^{1}H-NMR was recorded by Varian/Oxford As-500 (500 MHz) spectrometers.

Monomer & polymer preparation for experiment and analysis

Preparation of M1

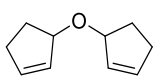

Ether formation from allylic alcohols catalyzed by samarium trichloride by Ouertani, Mohsen; Collin, Jacqueline; Kagan, Henri B. From

Tetrahedron **1985**, 41(18), 3689-93.

^{1}H-NMR and ^{13}C-NMR analysis data are available in the same literature.

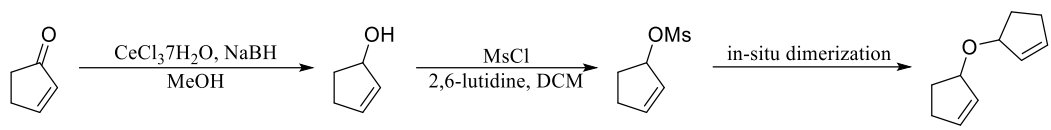

To a solution of 2-cyclopentenone (2.49 g, 30 mmol) and cerium trichloride heptahydrate (12.30 g, 33 mmol) in MeOH (60 ml), $NaBH_4$ (2.0 g,36 mmol) was added slowly with an ice bath and stirred for 15 min. The reaction mixture was extracted with diethyl ether and water and dried with $MgSO_4$. Cyclopentenol is purified by silica gel column chromatography (Ethyl Acetate /Hexane = 1/1) to yield corresponding alcohol with 60-80 % yield. With cyclopentenol (0.87 g, 10 mmol) and DCM (25 ml) solution, 2,6-lutidine (1.3 ml, 12 mmol) was added to solution. After 5 mins, Mesyl chloride (0.41 ml, 5 mmol) is added slowly. During the reaction, not only Mesylate but also Monomer1 was synthesized by in-situ dimerization. The yield of Corresponding ether is 40 %.

Polymer Characterization

P1, H 1H NMR 1H NMR (500 MHz, $CDCl_3$, ppm): 5.79-5.76 (s, 2H, Hd), 5.44-5.37(m, 2H, Ha), 4.83(s, 1H, Hc), 4.75(s, 1H, Hc), 2.07 (s, 4H, Hb), 1.58 (s, 4H, H3)

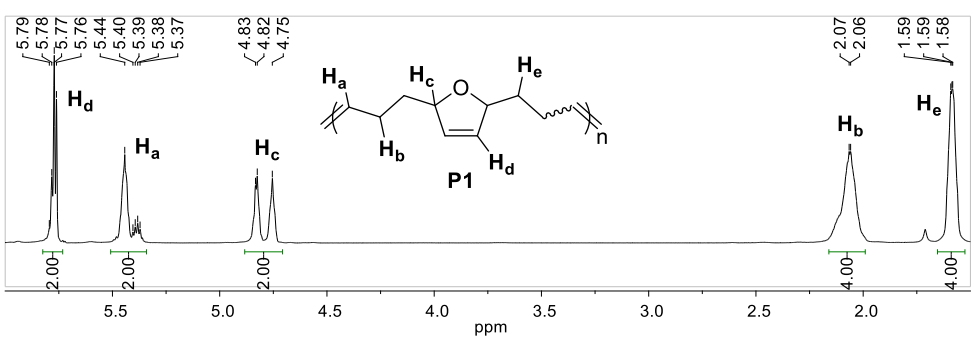

Figure S3.1. ^{1}H NMR spectrum of P1 (^{1}H NMR in $CDCl_3$)

Ref: Lee, H.-K.; Bang, K.-T.; Hess, A.; Grubbs, R. H.; Choi, T.-L. *J. Am. Chem. Soc.*

2015, *137*, 9262.

Poly(cycloheptene), H. 1H NMR (500 MHz, CDCl3, δ): 5.41- 5.31 (m, 2H, Ha), 2.08-1.90 (m, 4H, Hb), 1.40-1.22 (m, 6H, Hc/Hd).

Ref: Hejl, A., Scherman, O.A., and Grubbs, R.H. *Macromolecules.* **2005**, *38*, 7214.

Observation of the carbene for the reactions

To a 2-mL vial was a monomer (0.200 mmol) magnetic bar added and purged with Ar. 300 μL of CD_2Cl_2 was added to dissolve the monomer. After preparing a stock solution of initiator (0.02 mmol) using 300 μL of CD_2Cl_2 with a drop of hexamethyldisilane as an internal standard under the inert atmosphere, all of the solutions was ejected by microsyringe and transferred to Ar-filled NMR tube with septa cap.(The sample is first checked for the number of initial carbene species by NMR measurement before the monomer is injected, and then the process proceeds.) ^{1}H NMR spectrum of it was obtained to check the initial ratio between the initiator and internal standard. To a solution of NMR tude, 300 μL of the stock solution of monomer was added (M1: catalyst = 10: 1), then the total volume of the reaction mixture (600 μL) was rapidly transferred to Ar-filled NMR tube with a septa cap by syringe. ^{1}H NMR spectrum of the mixture was obtained with a scan number of 16, and the remaining and changing carbene signals were quantified by the internal standard. (In the competition experiment, cycloheptene was added to achieve a ratio of M1: cycloheptene: catalyst = 10: 10: 1.)

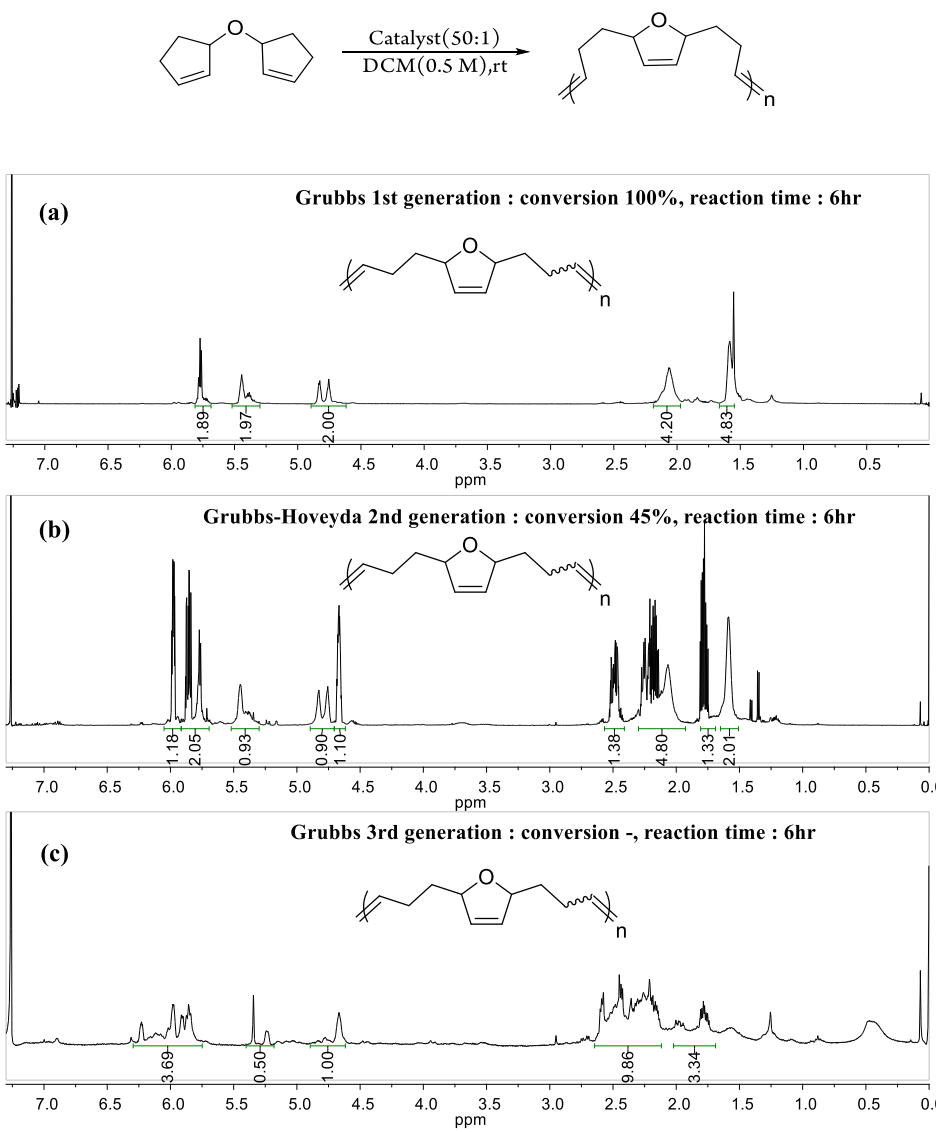

Figure S3.2. Unknown side reaction of cascade polymerization using G3 (a) G1 (b) HG2 (c) G3 (^{1}H NMR in $CDCl_3$)

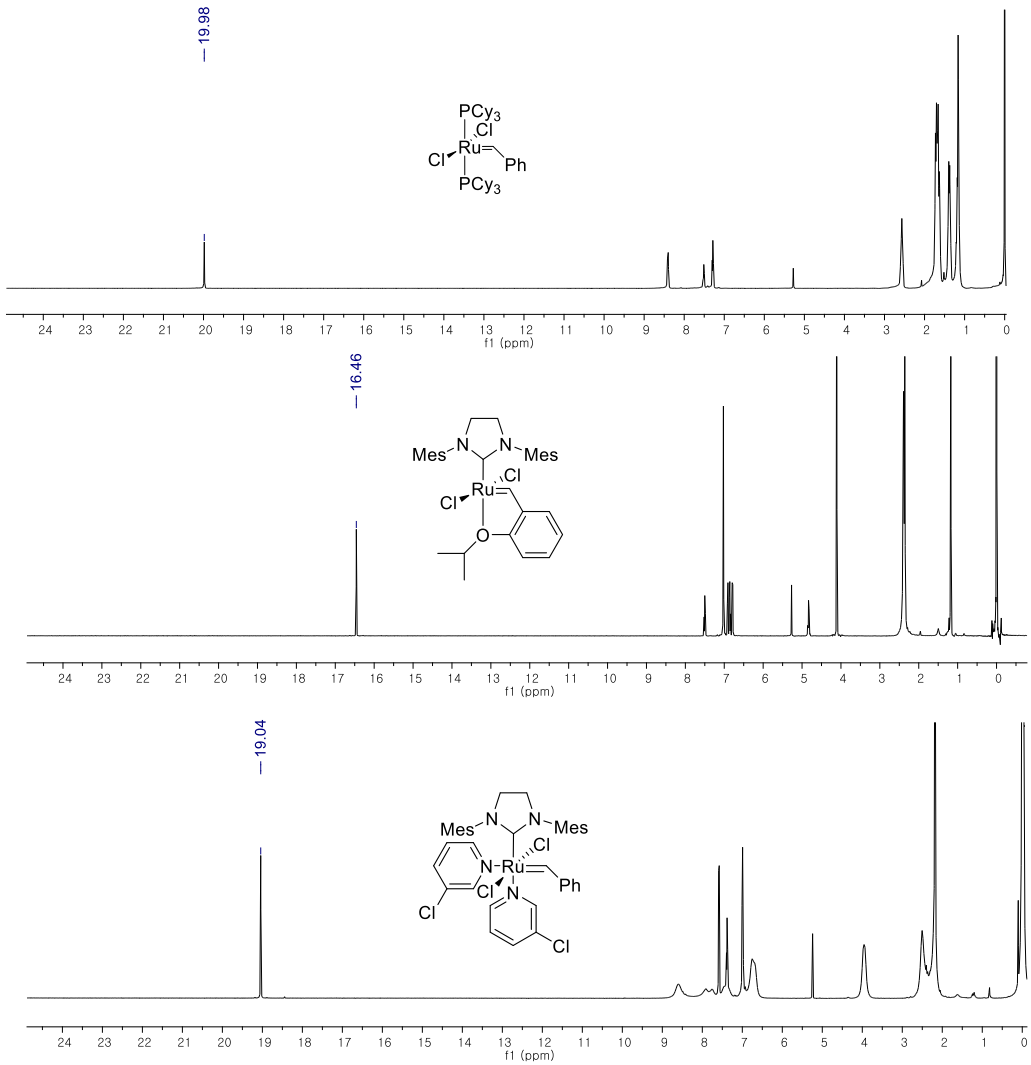

Figure S3.3. Quantitative analysis of initial carbene of corresponding Grubbs catalyst (CD_2Cl_2)

The initial carbene signals observed in the above spectrums were measured. These were used as a reference for the change of carbene produced after monomer injection.

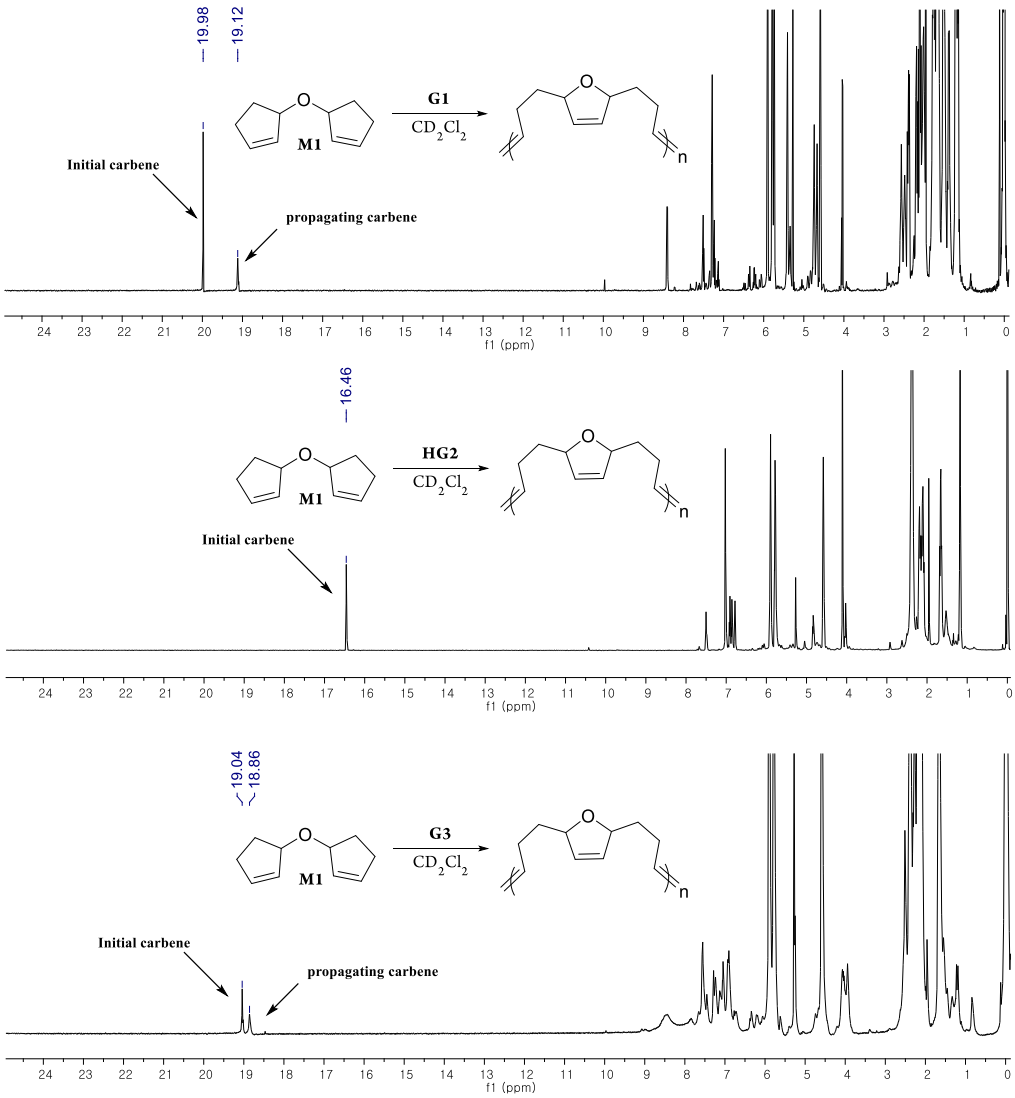

Figure S3.4. Quantitative analysis of remaining initial carbene and generating propagating carbene with M1 using Grubbs catalysts (^{1}H NMR in CD_2Cl_2)

The above spectrums show where and how the newly formed or changing carbene signals were observed according to each Grubbs catalyst during homopolymerization with **M1**.

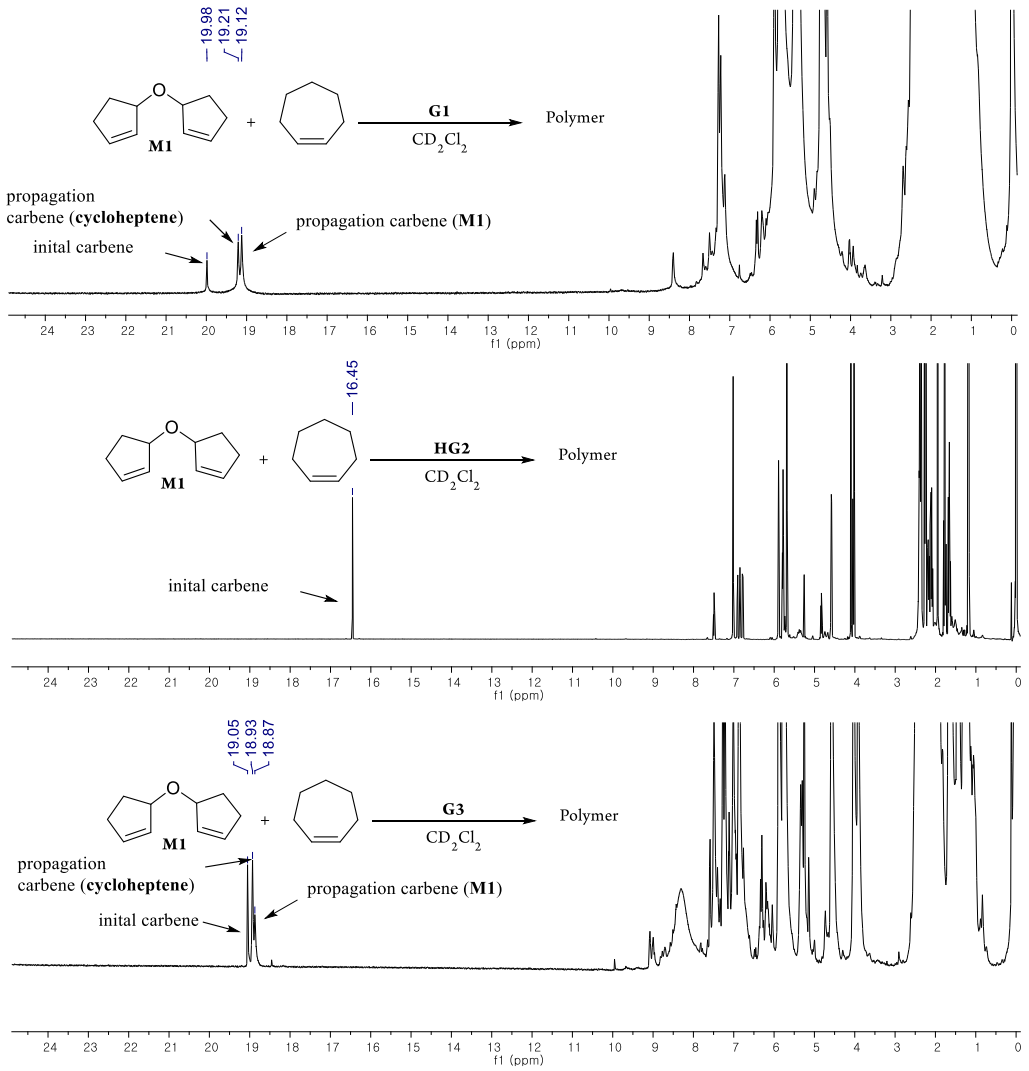

Figure S3.5. Quantitative analysis of remaining initial carbene and generating propagating carbene with M1, cycloheptene using Grubbs catalysts (^{1}H NMR in CD_2Cl_2)

The above spectrums show where and how to observe newly formed or changing carbene signals according to each Grubbs catalyst during random copolymerization through competitive polymerization experiments with **M1** and cycloheptene.

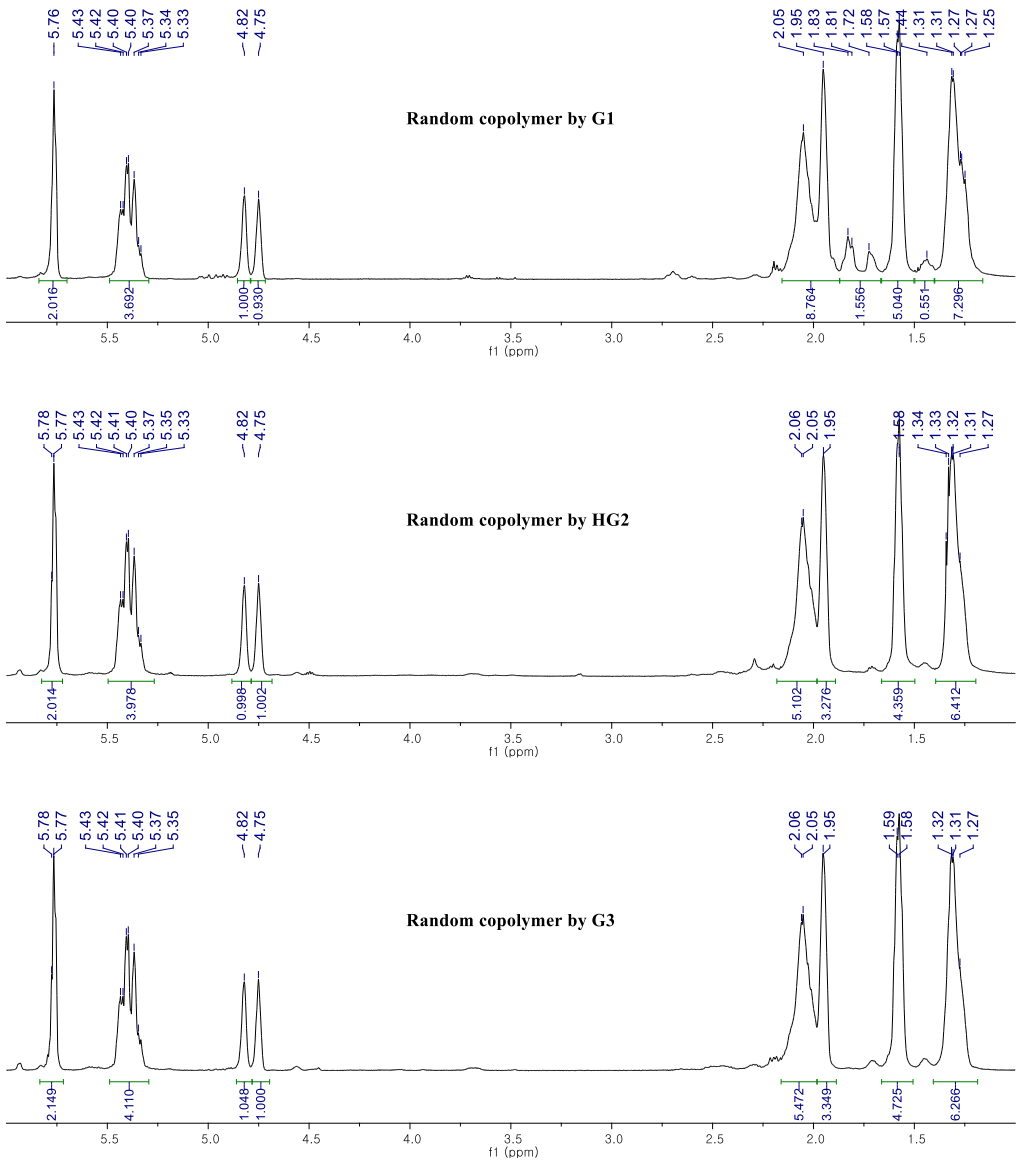

Figure S3.6. ^{1}H NMRs of purified and isolated random copolymer (^{1}H NMR in $CDCl_3$)

The above each polymerization experiments were carried out in the same manner as the experimental conditions in the text. (**M1 : cycloheptene : cat** = 10 : 10 : 1) The above NMR data were obtained by vacuum drying the precipitate obtained after the polymerization experiment under the same conditions as in the text.

In these NMR spectrums, random copolymerization was observed when compared with

peaks of reported homopolymer.

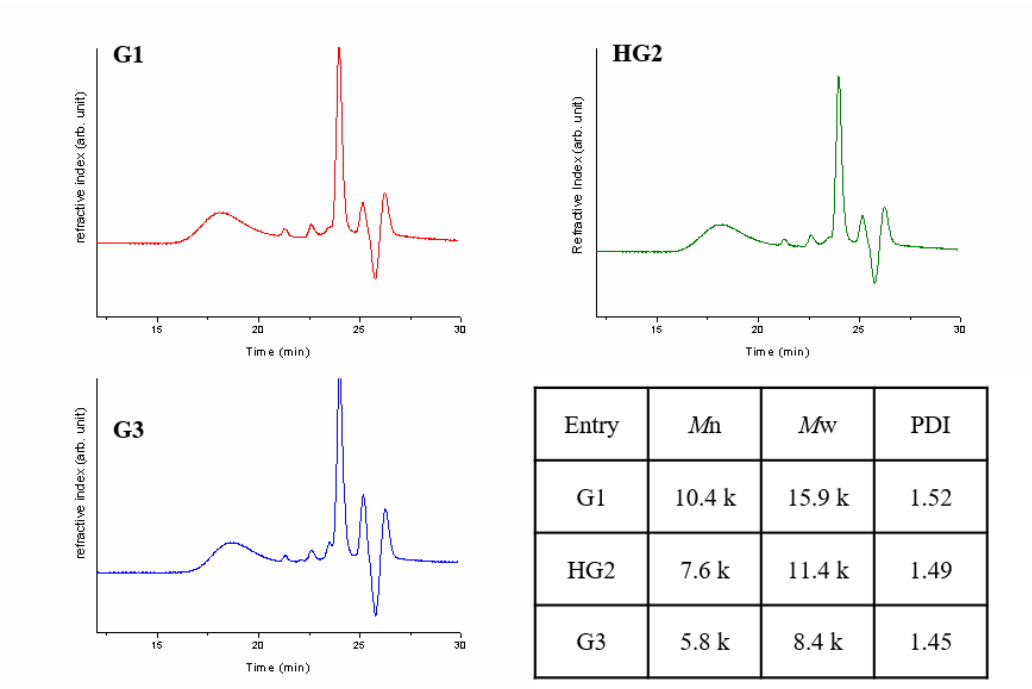

Entry	*M*n	*M*w	PDI
G1	10.4 k	15.9 k	1.52
HG2	7.6 k	11.4 k	1.49
G3	5.8 k	8.4 k	1.45

Figure S3.7. SEC traces of purified and isolated random copolymer (THF SEC)

The results of each SEC traces were measured with the same polymer as the NMR obtained above.

No bimodal distribution can be observed in all the SEC traces. This means that this polymerization proceeds in the form of a random copolymer.

Reactivity ratio: To determine reactivity ratio, we used Fineman-Ross method. Mixed monomers with the ratios of [**M1**]:[**cycloheptene**] = 90:10, 75:25, 60:40, 45:55, and 30:70 were prepared, then the catalyst was injected at 0 ℃ (ice bath). To obtain the ratio of incorporated monomers at an early stage, the reaction was quenched after 30 seconds by ethyl vinyl ether, and the incorporated ratios were obtained from 1H NMR analysis.

Arranged Fineman-Ross equation : $G = H\gamma_1 - \gamma_2$ ($\frac{f_1(2F_1-1)}{(1-f_1)F_1} = G$, $\frac{f_1^2(1-F_1)}{(1-f_1)^2F_1} = H$)

Table S3.1. The reactivity ratio between **M1** and cycloheptene with **G1**

[M1]:[G1]	**[cycloheptene] : [G1]**	*f*1	F1	$\frac{f_1(2F_1-1)}{(1-f_1)F_1}$ (G)	$\frac{f_1^2(1-F_1)}{(1-f_1)^2F_1}$ (H)
90	10	0.9	0.893	9.705487	7.921613
75	25	0.75	0.732	3.295082	1.901639
60	40	0.6	0.573	1.676702	0.382199
45	55	0.45	0.432	0.880165	-0.25758
30	70	0.3	0.284	0.463064	-0.65191

Figure S3.8. The linear plot for reactivity ratio between M1 and cycloheptene with G1

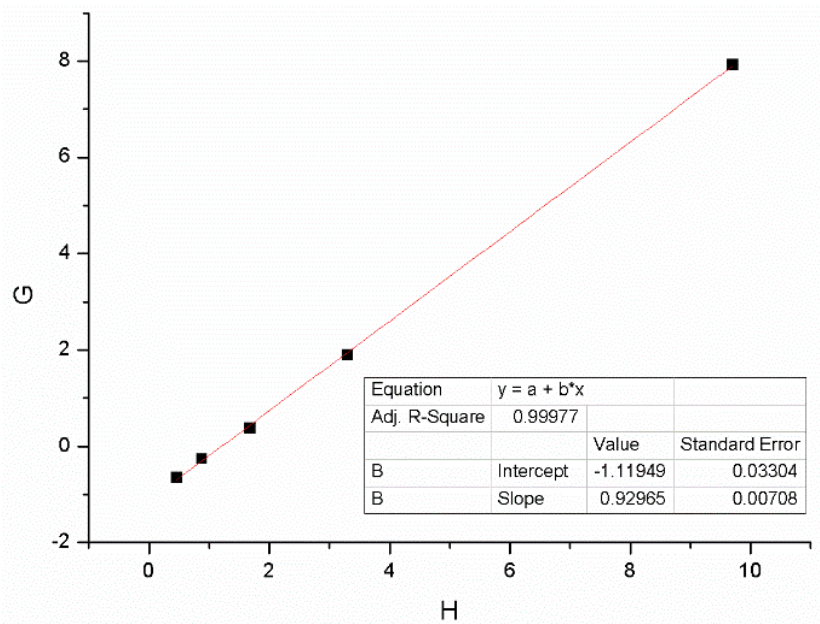

$\gamma_1 = 0.9297$ $\gamma_2 = 1.1195$

both ratios around 1, M1 will react as fast with M1 or cycloheptene and a random copolymer is formed

Table S3.2. The reactivity ratio between **M1** and cycloheptene with **HG2**

[M1]:[HG2]	**[cycloheptene] : [HG2]**	*f*1	F1	$\frac{f_1(2F_1-1)}{(1-f_1)F_1}$ (G)	$\frac{f_1^2(1-F_1)}{(1-f_1)^2F_1}$ (H)
90	10	0.9	0.856	13.62617	7.485981
75	25	0.75	0.68	4.235294	1.588235
60	40	0.6	0.512	2.144531	0.070313
45	55	0.45	0.379	1.096862	-0.52243
30	70	0.3	0.283	0.465349	-0.65724

Figure S3.9. The linear plot for reactivity ratio between M1 and cycloheptene with HG2

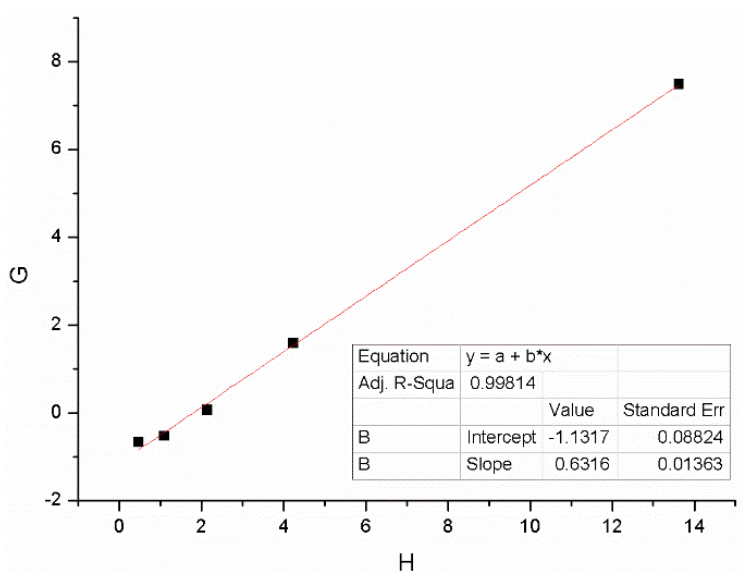

$\gamma_1 = 0.6316$ $\gamma_2 = 1.1317$

In the initial stage of the copolymerization, cycloheptene is incorporated faster and the copolymer is rich in M1. When this monomer gets depleted, more M1 segments are added.

Table S3.3. The reactivity ratio between **M1** and cycloheptene with **G3**

[M1]:[G3]	**[cycloheptene] : [G3]**	*f*1	F1	$\frac{f_1(2F_1-1)}{(1-f_1)F_1}$ (G)	$\frac{f_1^2(1-F_1)}{(1-f_1)^2F_1}$ (H)
90	10	0.9	0.887	10.31905	7.853439
75	25	0.75	0.738	3.195122	1.934959
60	40	0.6	0.584	1.60274	0.431507
45	55	0.45	0.424	0.909403	-0.29331
7	70	0.3	0.272	0.491597	-0.71849

Figure S3.10. The linear plot for reactivity ratio between M1 and cycloheptene with G3

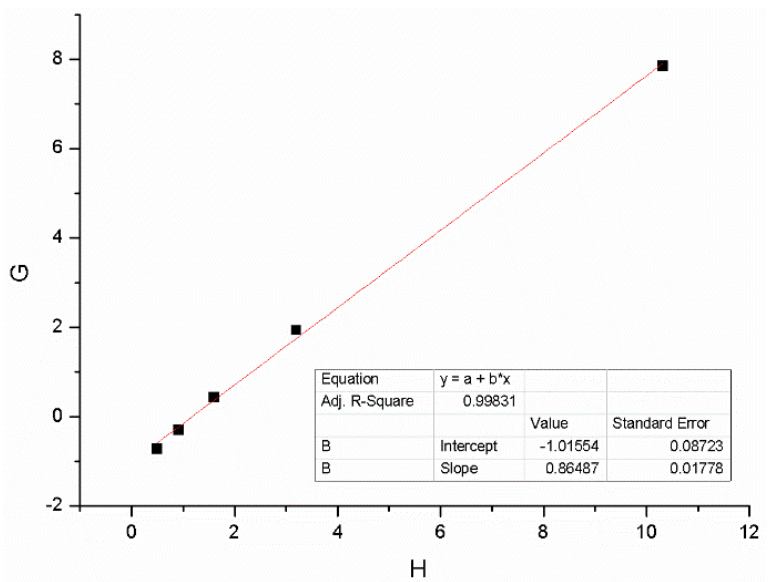

$\gamma_1 = 0.8649$ $\gamma_2 = 1.0155$

The result of G3 shows moderate results for the results of G1 and HG2.

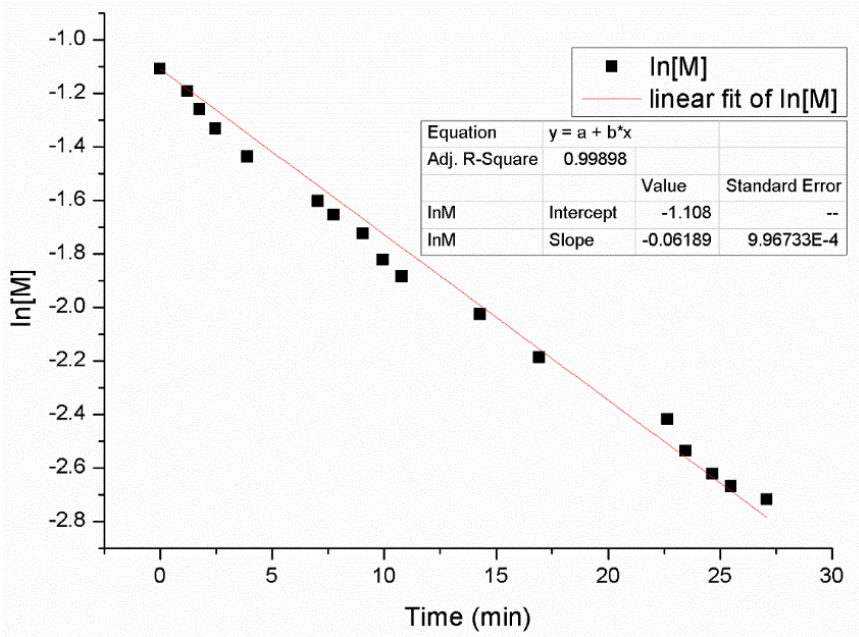

Figure S3.11. (a) Plots of ln([M]) vs. time of M1 (homopolymerization) with G1

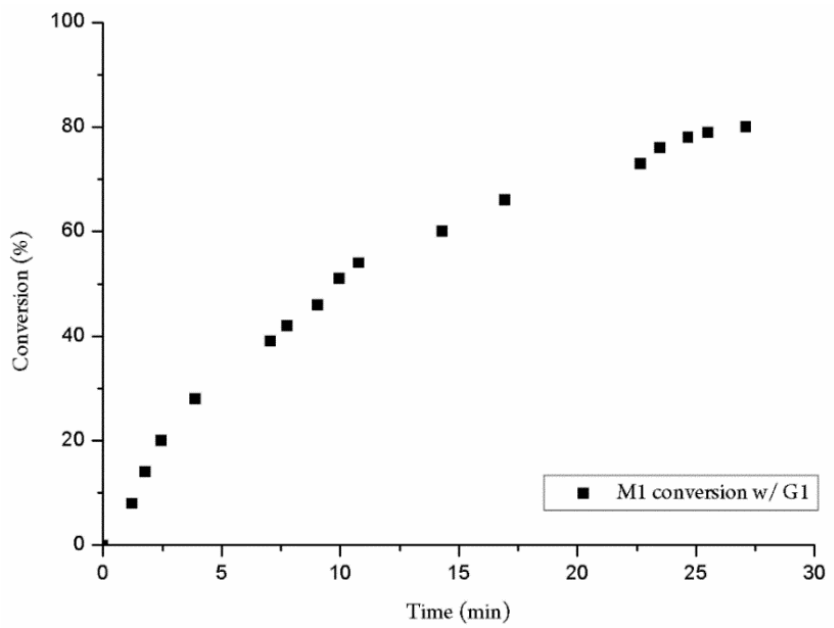

Figure S3.11. (b) Plots of Conversion vs. time of M1 (homopolymerization) with G1

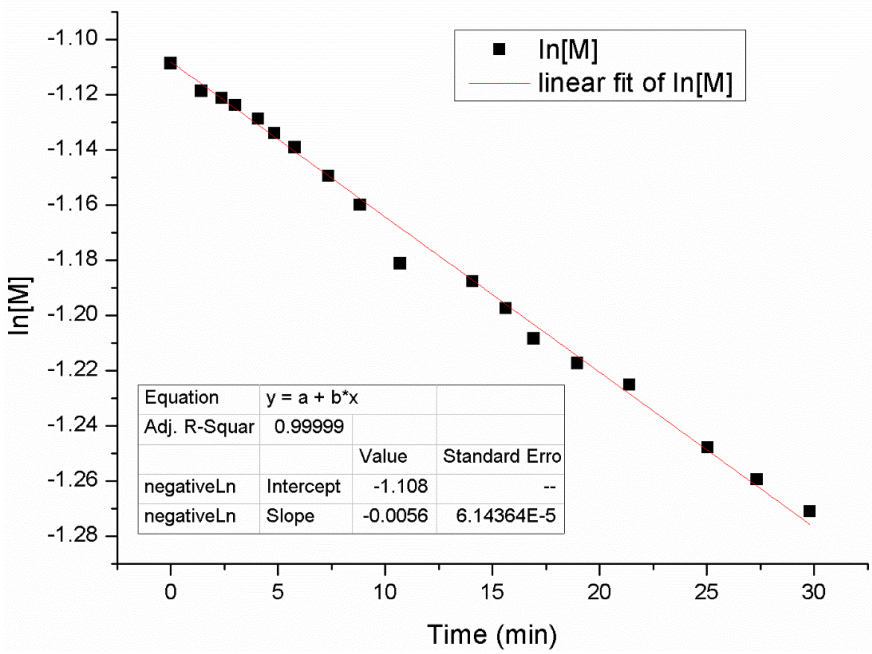

Figure S3.12. (a) Plots of ln([M]) vs. time of M1 (homopolymerization) with HG2

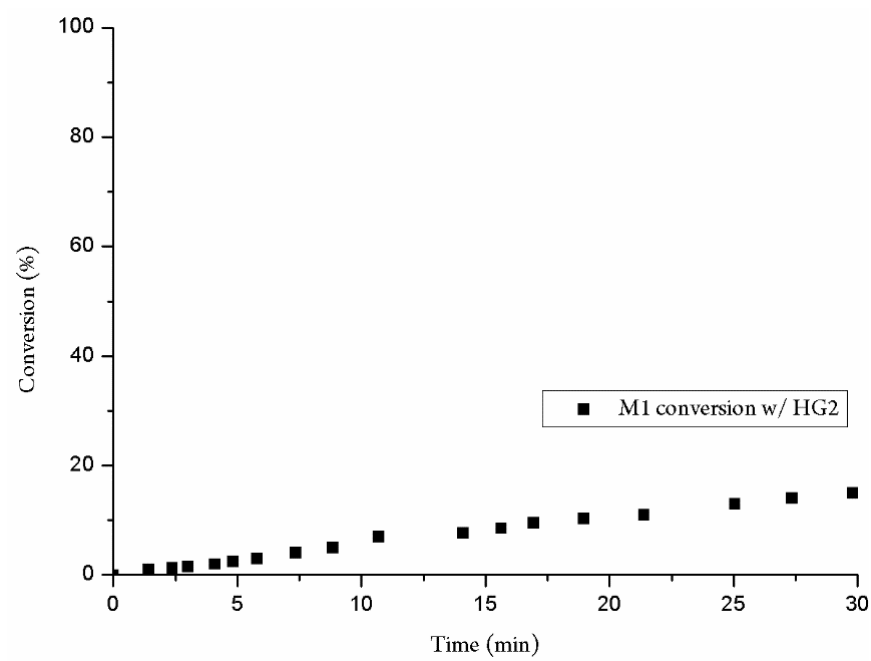

Figure S3.12. (b) Plots of ln([M]) vs. time of M1 (homopolymerization) with HG2

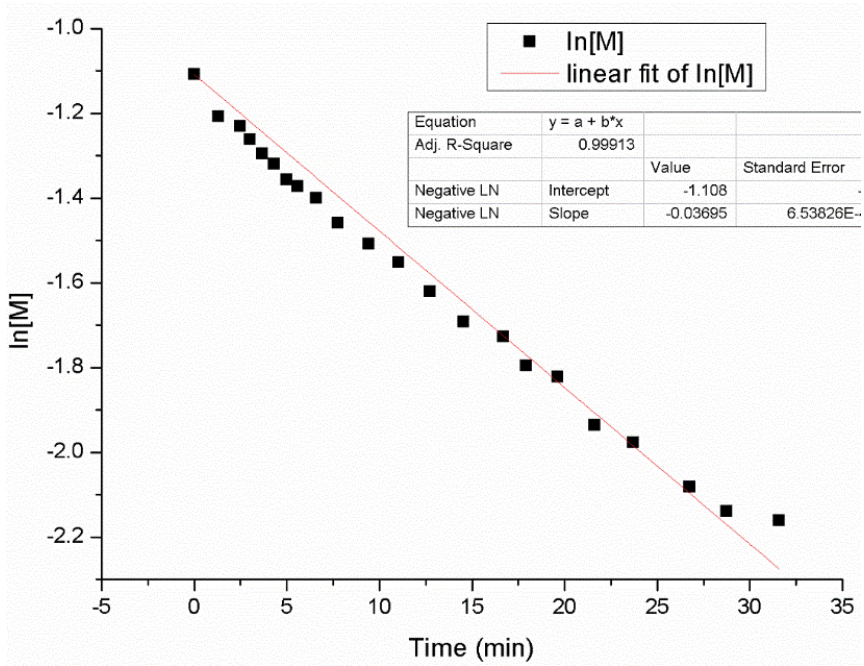

Figure S3.13. (a) Plots of ln([M]) vs. time of M1 (homopolymerization) with G3

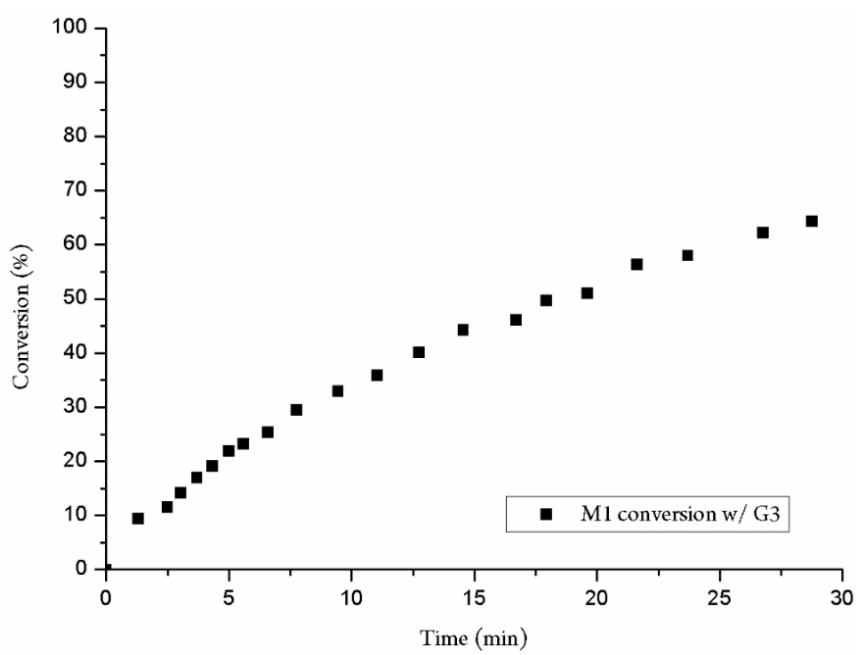

Figure S3.13. (b) Plots of Conversion vs. time of M1 (homopolymerization) with G3

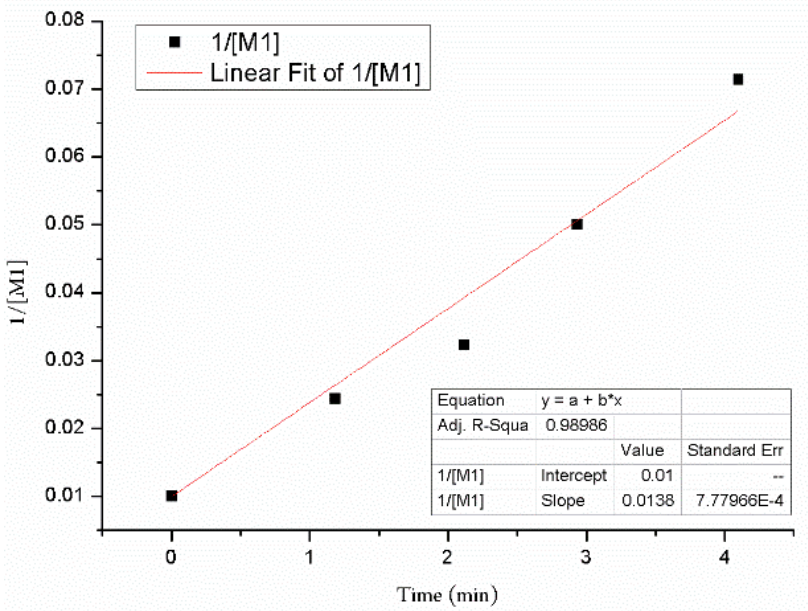

Figure S3.14. (a) Plots of [1/M1] vs. time of M1 (competition polymerization) with G1

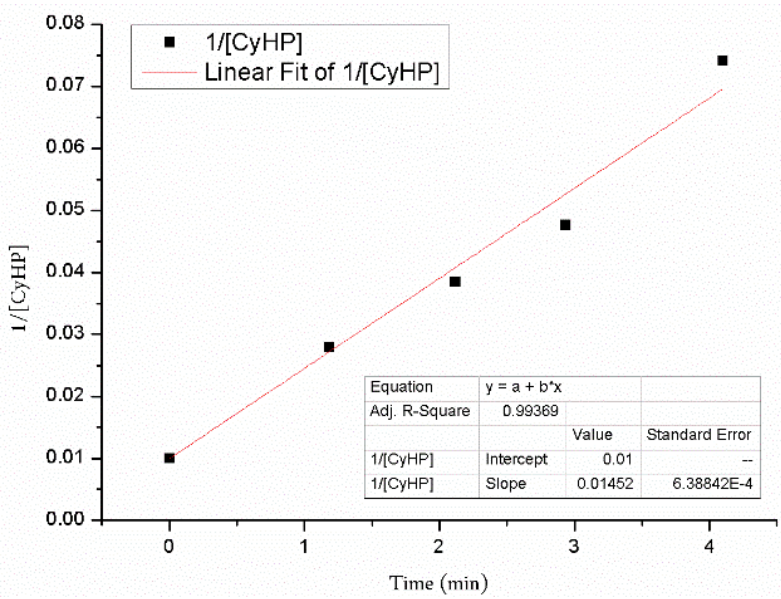

Figure S3.14. (b) Plots of [1/cyHP] vs. time of cycloheptene (competition polymerization) with G1

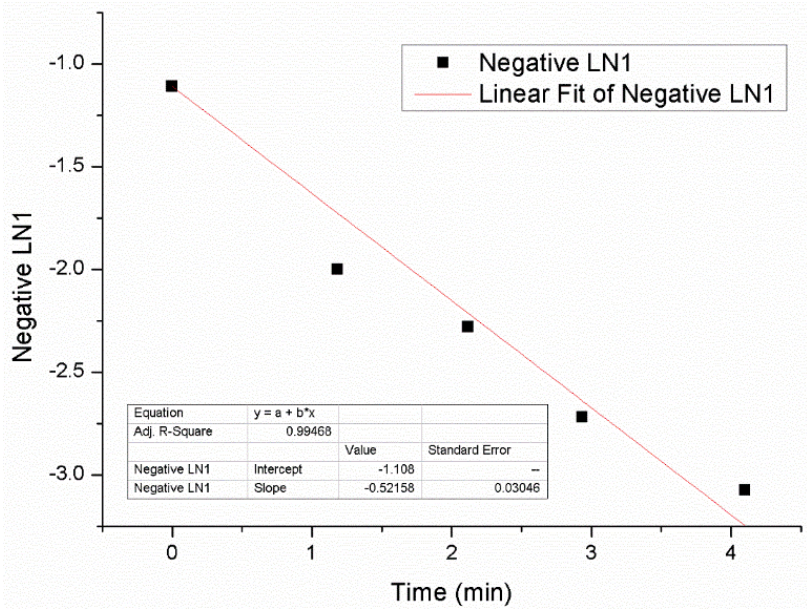

Figure S3.14. (c) Plots of ln([M]) vs. time of M1 (competition polymerization) with G1

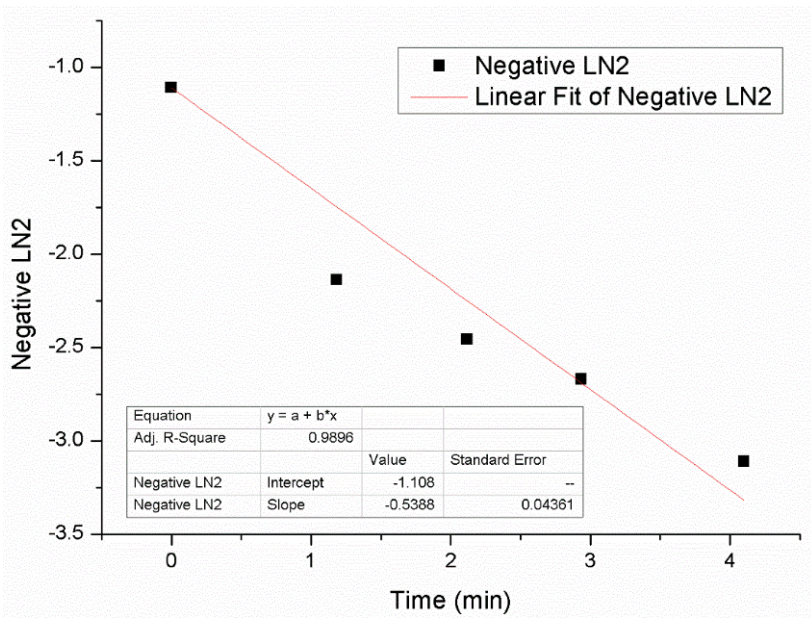

Figure S3.14. (d) Plots of ln([M]) vs. time of cycloheptene (competition copolymerization) with G1

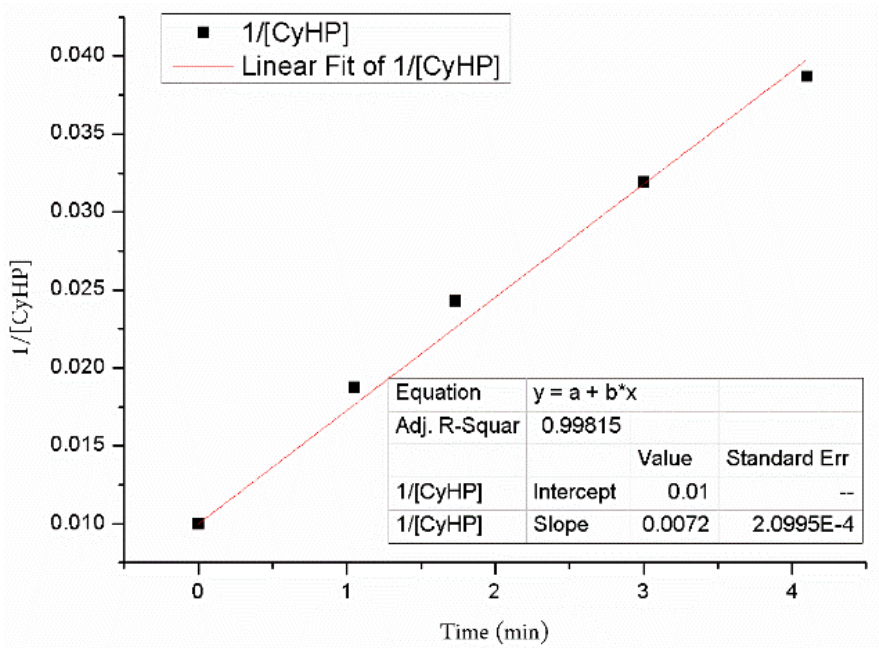

Figure S3.15. (a) Plots of [1/M1] vs. time of M1 (competition polymerization) with HG2

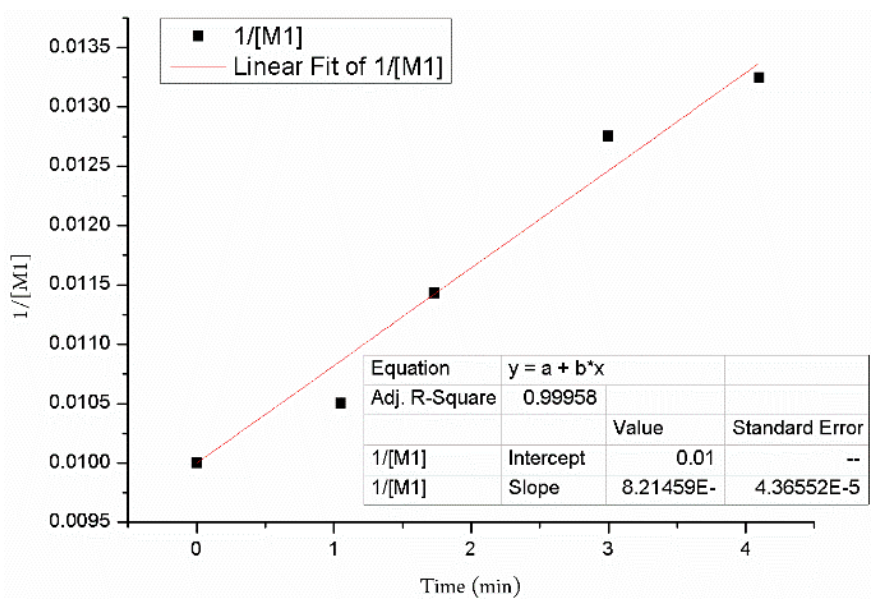

Figure S3.15. (b) Plots of [1/cyHP] vs. time of cycloheptene (competition polymerization) with HG2

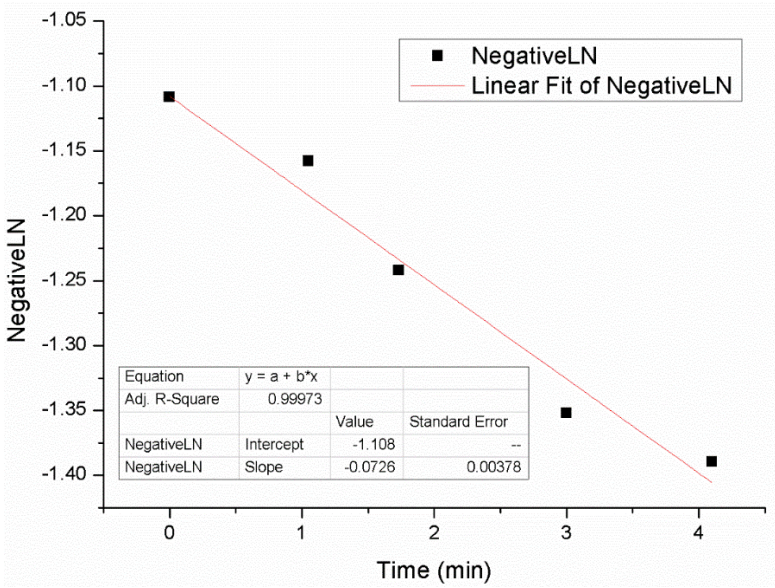

Figure S3.15. (c) Plots of ln([M]) vs. time of M1 (competition copolymerization) with HG2

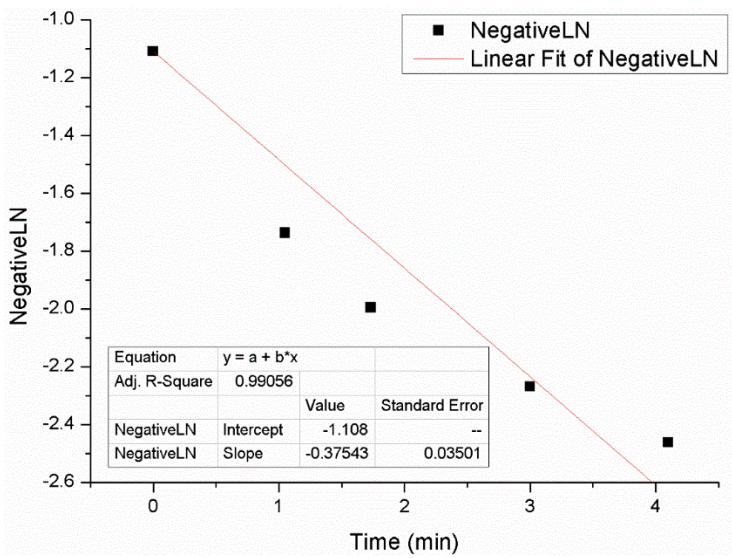

Figure S3.15. (d) Plots of ln([M]) vs. time of cycloheptene (competition copolymerization) with HG2

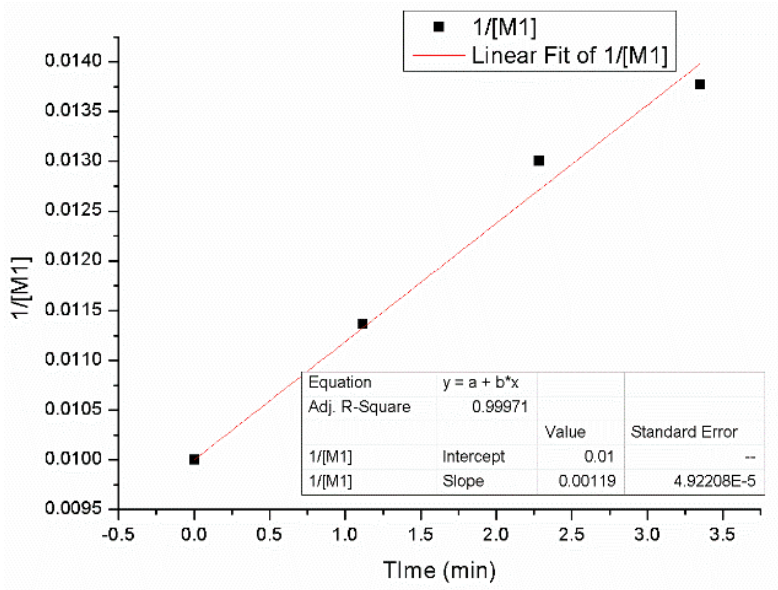

Figure S3.16. (a) [1/M1] vs. time of M1 (competition polymerization) with G3

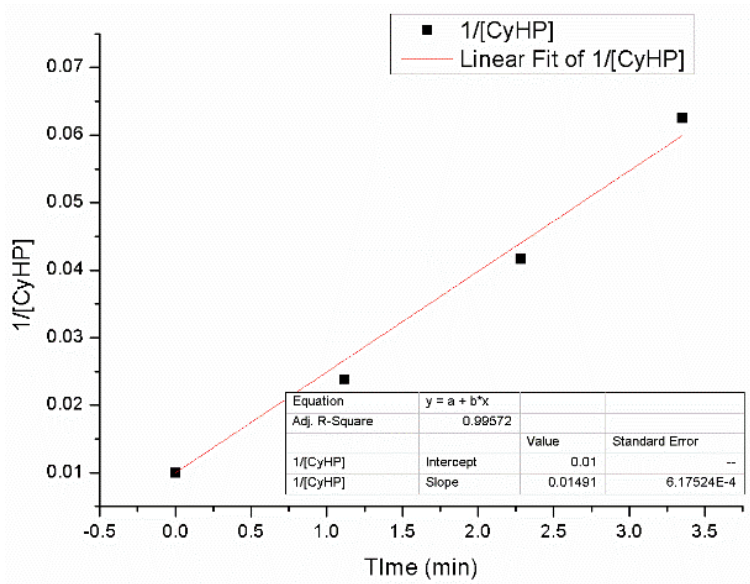

Figure S3.16. (b) [1/cyHP] vs. time of cycloheptene (competition polymerization) with G3

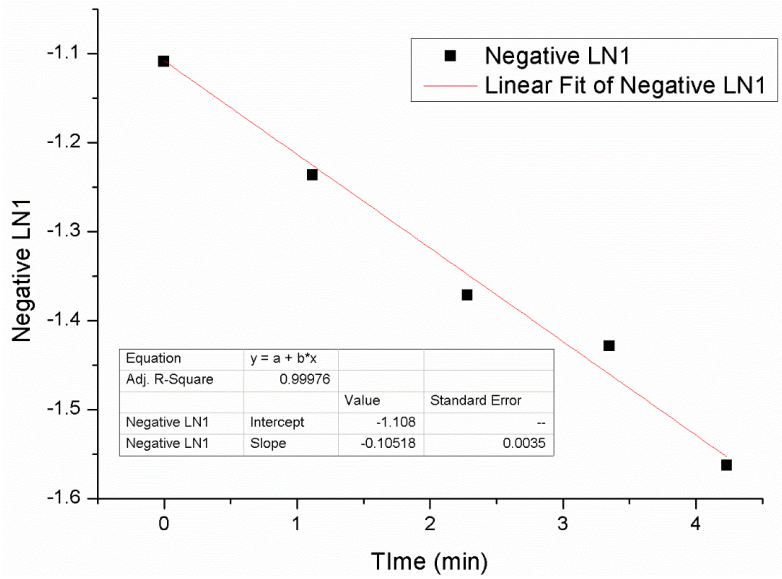

Figure S3.16. (c) Plots of ln([M]) vs. time of M1 (competition copolymerization) with G3

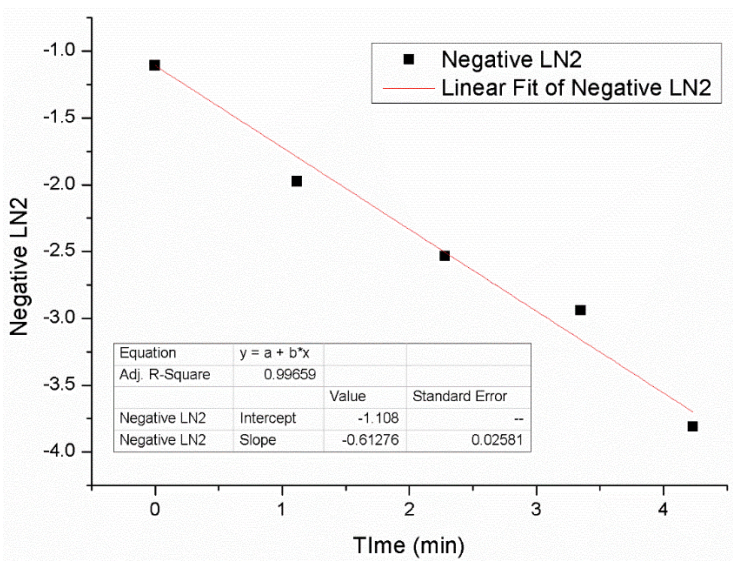

Figure S3.16. (d) Plots of ln([M]) vs. time of cycloheptene (competition copolymerization) with G3

TableS3.4. Rates of competition polymerization with M1 and cycloheptene (unit : $M^{-1} \cdot s^{-1}$: 2nd order)

Entry	catalyst	k_{M1}	$k_{cycloheptene}$	k_{M1} : $k_{cycoheptene}$
1	**G1**	0.014	0.015	1 : 1.07
2	**HG2**	0.00082	0.0073	1 : 8.90
3	**G3**	0.0012	0.015	1 : 12.5

TableS3.5. Rates of competition polymerization with M1 and cycloheptene (unit: s^{-1} :1st order)

Entry	catalyst	k_{M1}	$k_{cycloheptene}$	k_{M1} : $k_{cycoheptene}$
1	**G1**	0.52	0.54	1 : 1.04
2	**HG2**	0.073	0.38	1 : 5.60
3	**G3**	0.11	0.61	1 : 5.90

It is difficult to conclude that this reaction itself is precisely a 1st order reaction or 2nd order reaction, as it is not irreversible, as in general reactions, but also as a partially reversible process. Therefore, both data are provided, there is no significant difference in overall priority trends of Grubbs catalyst trends in the cascade polymerization.

3.6 References

(1) (a) Grubbs, R. H.; Chang, S. Recent advances in olefin metathesis and its application in organic synthesis. *Tetrahedron* **1998**, *54*, 4413-4450. (b) Fürstner, A. Olefin Metathesis

and Beyond A list of abbreviations can be found at the end of this article. *Angew. Chem., Int. Ed*. **2000**, *39*, 3013-3043. (c) Grubbs, R. H. *Handbook of Metathesis*, Wiley-VCH: Weinheim, **2003**, *1*, 2. (d) Grubbs, R. H. Olefin metathesis. *Tetrahedron* **2004**, *60*, 7117-7140.

(2) For reviews, see: (a) Novak, B. M.; Risse, W.; Grubbs, R. H. The development of well-defined catalysts for ring-opening olefin metathesis polymerizations (ROMP). *Adv. Polym. Sci.* **1992**, *102*, 47-72. (b) Grubbs, R. H.; Khosaravi, E. Ring-Opening Metathesis Polymerization (ROMP) and Related Processes. *Material Science and Technology*, **1999**, *20*, 65-101. c) Buchmeiser, M. R. Homogeneous Metathesis Polymerization by Well-Defined Group VI and Group VIII Transition-Metal Alkylidenes: Fundamentals and Applications in the Preparation of Advanced Materials. *Chem. Rev*. **2000**, *100*, 1565-1604.

(3) For reviews, see: (a) Gruubs, R. H.; Miller, S. J.; Fu, G. C. Ring-Closing Metathesis and Related Processes in Organic Synthesis. *Acc. Chem. Res.* **1995**, *28*, 446-452. (b) Deiters, A.; Martin, S. F. Synthesis of Oxygen- and Nitrogen-Containing Heterocycles by Ring-Closing Metathesis. *Chem. Rev*. **2004**, *104*, 2199-2238. (c) Schmidt, B.; Hermanns, J. Ring closing metathesis of substrates containing more than two C-C-double bonds: rapid access to functionalized heterocycles. *Curr. Org. Chem*. **2006**, *10*, 1363-1396.

(4) For recent reviews, see: (a) Schuster, M.; Blechert, S. Olefin Metathesis in Organic Chemistry. *Angew. Chem. Int. Ed*. **1997**, *36*, 2036-2056. (b) Connon, S. J.; Blechert, S. Recent developments in olefin cross-metathesis. *Angew. Chem. Int. Ed.* **2003**, *42*, 1900-1923. (c) Grubbs, R. H. *Handbook of Metathesis*, 2nd ed.; Wiley-VCH: Weinheim, **2015**; Vols. 2, 3.

(5) (a) Schrock, R. R.; Murdzek, J. S.; Bazan, G, C.; Robibins, J.; DiMare, M.; O'Regan, M. Synthesis of molybdenum imido alkylidene complexes and some reactions involving acyclic olefins. *J. Am. Chem. Soc.* **1990**, *112*, 3875-3886. (b) Bazan, G. C.; Oskam, J. H.; Cho, H.-N.; Park, L. Y.; Schrock, R. R. Living ring-opening metathesis polymerization of

2,3-difunctionalized 7-oxanorbornenes and 7-oxanorbornadienes by Mo(CHCMe$_2$R)(NC$_6$H$_3$-iso-Pr$_2$-2,6)(*O*-tert-Bu)*2* and Mo(CHCMe$_2$R)(NC$_6$H$_3$-iso-Pr$_2$-2,6)(OCMe$_2$CF$_3$)$_2$. *J. Am. Chem. Soc.* **1991**, *113*, 6899-6907. (c) Feldman, J.; Schrock, R. R. Recent Advances in the Chemistry of "d^0" Alkylidene and Metallacyclobutane Complexes. *Prog. Inorg, Chem.* **1991**, *39*, 1-74.

(6) (a) Novak, B. M.; Grubbs, R. H. The ring opening metathesis polymerization of 7-oxabicyclo[2.2.1]hept-5-ene derivatives: a new acyclic polymeric ionophore. *J. Am. Chem. Soc.* **1988** *110*, 960-961. (b) Nguyen, S. T.; Johnson, L. K.; Grubbs, R. H. Ring-opening metathesis polymerization (ROMP) of norbornene by a Group VIII carbene complex in protic media. *J. Am. Chem. Soc.* **1992**, *114*, 3974-3975. (c) Nguyen, S. T.; Grubbs, R. H. Syntheses and activities of new single-component, ruthenium-based olefin metathesis catalysts. *J. Am. Chem. Soc.* **1993**, *115*, 9858–9859. (d) Schwab, P.; France, M. B.; Ziller, J. W.; Grubbs, R. H. A Series of Well-Defined Metathesis Catalysts–Synthesis of [RuCl$_2$(=CHR′)(PR$_3$)$_2$] and Its Reactions. *Angew. Chem., Int. Ed.* **1995**, *34*, 2039–2041. (e) Schwab, P.; Grubbs, R. H.; Ziller, J. W. Synthesis and Applications of RuCl2(=CHR‘)(PR$_3$)$_2$: The Influence of the Alkylidene Moiety on Metathesis Activity. *J. Am. Chem. Soc.* **1996**, *118*, 100-110. (f) Scholl, M.; Ding, S.; Lee, C. W.; Grubbs, R. H. Synthesis and Activity of a New Generation of Ruthenium-Based Olefin Metathesis Catalysts Coordinated with 1,3-Dimesityl-4,5-dihydroimidazol-2-ylidene Ligands. *Org. Lett.* **1999**, *1*, 953-956. (g) Trnka, T. M.; Grubbs, R. H. The Development of L$_2$X$_2$Ru=CHR Olefin Metathesis Catalysts: An Organometallic Success Story. *Acc. Chem. Res*. **2001**, *34*, 18-29.

(7) (a) Kanaoka, S.; Grubbs, R. H. Synthesis of Block Copolymers of Silicon-Containing Norbornene Derivatives via Living Ring-Opening Metathesis Polymerization Catalyzed by a Ruthenium Carbene Complex. *Macromolecules* **1995**, 28, 4707-4713. (b) Weck, M.; Schwab, P.; Grubbs, R. H. Synthesis of ABA Triblock Copolymers of Norbornenes and 7-Oxanorbornenes via Living Ring-Opening Metathesis Polymerization Using Well-Defined,

Bimetallic Ruthenium Catalysts. *Macromolecules* **1996**, 29, 1789-1793.

(8) Bielawski, C. W.; Grubbs, R. H. Highly Efficient Ring-Opening Metathesis Polymerization (ROMP) Using New Ruthenium Catalysts Containing N-Heterocyclic Carbene Ligands. *Angew. Chem., Int. Ed*. **2000**, *39*, 2903-2906.

(9) Chatterjee, A. K.; Choi, T.-L.; Sanders, D. P.; Grubbs, R. H. A General Model for Selectivity in Olefin Cross Metathesis. *J. Am. Chem. Soc.* **2003**, *125*, 11360-11370.

(10) Love, J. A.; Morgan, J. P.; Trnka, T. M.; Grubbs, R. H. A Practical and Highly Active Ruthenium-Based Catalyst that Effects the Cross Metathesis of Acrylonitrile. *Angew. Chem., Int. Ed.* **2002**, *41*, 4035-4037.

(11) Choi, T.-L.; Rutenberg, I. M.; Grubbs, R. H. Synthesis of A,B-alternating copolymers by ring-opening-insertion-metathesis polymerization. *Angew. Chem. Int. Ed*. **2002**, *41*, 3839-3841.

(12) Choi, T.-L.; Grubbs, R. H. Controlled Living Ring-Opening-Metathesis Polymerization by a Fast-Initiating Ruthenium Catalyst. *Angew. Chem. Int. Ed.* **2003**, *42*, 1743-1746.

(13) (a) Kim, K.-O.; Choi, T.-L. Synthesis of Rod-Like Dendronized Polymers Containing G4 and G5 Ester Dendrons via Macromonomer Approach by Living ROMP. *ACS Macro Lett.* **2012**, *1*, 445-448. (b) Park, H.; Lee, H.-K; Kang, E.-H.; Choi, T.-L. Controlled cyclopolymerization of 4,5-disubstituted 1,7-octadiynes and its application to the synthesis of a dendronized polymer using Grubbs catalyst. *J. Polym. Sci. Part A: Polym. Chem.* **2015**, *53*, 274-279 (c) Park., H.; Kang, E.-H.; Müller., L.; Choi, T.-L. Versatile Tandem Ring-Opening/Ring-Closing Metathesis Polymerization: Strategies for Successful Polymerization of Challenging Monomers and Their Mechanistic Studies. *J. Am. Chem. Soc.* **2016**, *138*, 2244-2251(d) Dutertre. F; Bang.K.-T.; Loppinet. B.; Choi. I.-H.; Choi, T.-L.; Fytas.G. Structure and Dynamics of Dendronized Polymer Solutions: Gaussian Coil or Macromolecular Rod? *Macromolecules.* **2016**, *49*, 2731-2740.

(14) (a) Kang, E.-H.; Lee, I. S.; Choi, T.-L. Ultrafast Cyclopolymerization for Polyene Synthesis: Living Polymerization to Dendronized Polymers. *J. Am. Chem. Soc*. **2011**, *133*, 11904-11907. (b) Kang, E.-H.; Lee, I.-H.; Choi, T.-L. Brush Polymers Containing Semiconducting Polyene Backbones: Graft-Through Synthesis via Cyclopolymerization and Conformational Analysis on the Coil-to-Rod Transition. *ACS Macro Lett.* **2012**, *1*, 1098-1101. (c) Park, H.; Lee, H.-K; Choi, T.-L Faster cyclopolymerisation of 4,4-disubstituted 1,7-octadiynes through an enhanced Thorpe–Ingold effect. *Polym. Chem.* **2013**, *4*, 4676-4681 (d) Kang, E.-H.; Yu, S.-Y; Lee, I.-H.; Park S.-E.; Choi, T.-L. Strategies to Enhance Cyclopolymerization using Third-Generation Grubbs Catalyst. *J. Am. Chem. Soc.* **2014**, *136*, 10508-10514.

(15) (a) Park, H.; Choi, T.-L. Fast Tandem Ring-Opening/Ring-Closing Metathesis Polymerization from a Monomer Containing Cyclohexene and Terminal Alkyne. *J. Am. Chem. Soc.* **2012**, *134*, 7270−7273. (b) Park, H.; Lee, H.-K; Choi, T.-L. Tandem Ring-Opening/Ring-Closing Metathesis Polymerization: Relationship between Monomer Structure and Reactivity. *J. Am. Chem. Soc.* **2013**, *135*, 10769-10775. (c) Gutekunst, W. R.; Hawker, C. J. A General Approach to Sequence-Controlled Polymers Using Macrocyclic Ring Opening Metathesis Polymerization. *J. Am. Chem. Soc.* **2015**, *137*, 8038-8041. (d) Lee, H.-K.; Bang, K.-T.; Hess, A.; Grubbs, R. H.; Choi, T.-L. Multiple Olefin Metathesis Polymerization That Combines All Three Olefin Metathesis Transformations: Ring-Opening, Ring-Closing, and Cross Metathesis. *J. Am. Chem. Soc.* **2015**, *137*, 9262-9265. (e*)* Park., H.; Kang, E.-H.; Müller., L.; Choi, T.-L. Versatile Tandem Ring-Opening/Ring-Closing Metathesis Polymerization: Strategies for Successful Polymerization of Challenging Monomers and Their Mechanistic Studies. *J. Am. Chem. Soc.* **2016**, *138*, 2244-2251. (f) Kang, C.; Park, H.; Lee, J.-K.; Choi, T.-L. Cascade Polymerization via Controlled Tandem Olefin Metathesis/Metallotropic 1,3-Shift Reactions for the Synthesis of Fully Conjugated Polyenynes. *J. Am. Chem. Soc.,***2017***, 139,* 11309-11312.

(16) (a) Sanford, M. S.; Henling, L. M.; Day, M. W.; Grubbs, R. H. Ruthenium-Based Four-Coordinate Olefin Metathesis Catalysts The authors thank the NSF for generous support of this research. *Angew. Chem., Int. Ed*. **2000**, *39*, 3451-3453. (b) For another example of stable 14e⁻-Ru carbene having carbene signal, see: Coalter, J. N., III; Bollinger, J. C.; Eisenstein, O.; Caulton, K. G. R-Group reversal of isomer stability for $RuH(X)L_2(CCHR)$ vs. $Ru(X)L_2(CCH_2R)$: access to four-coordinate ruthenium carbenes and carbynes. *New J. Chem.* **2000**, *24*, 925-927. (c) Direct detection of 14e⁻-Ru intermediate by ESI-MS was reported, see: Wang, H.; Metzger, R. ESI-MS Study on First-Generation Ruthenium Olefin Metathesis Catalysts in Solution: Direct Detection of the Catalytically Active 14-Electron Ruthenium Intermediate. *Organometallics* **2008**, *27*, 2761-2766.

(17) Ritter,T.; Hejl,A.; Wenzel,A.G.; Funk,T.W.; Grubbs, R.H. A Standard System of Characterization for Olefin Metathesis Catalysts. *Organometallics*, **2006**, 25, 5743-5745.

(18) Huang, J.; Stevens, E. D.; Nolan, S. P.; Petersen, J. L. Olefin Metathesis-Active Ruthenium Complexes Bearing a Nucleophilic Carbene Ligand. *J. Am. Chem. Soc.* **1999**, *121*, 2674-2678.

(19) (a) Kobayashi, S.; Pitet, L. M.; Hillmyer, M. A. Regio- and Stereoselective Ring-Opening Metathesis Polymerization of 3-Substituted Cyclooctenes. *J. Am. Chem. Soc.* **2011**, *133*, 5794-5797. (b) Martinez, H.; Miró, P.; Charbonneau, P.; Hillmyer, M.A.; Cramer, C.J. Selectivity in Ring-Opening Metathesis Polymerization of Z-Cyclooctenes Catalyzed by a Second-generation Grubbs Catalyst. *ACS Catal.*, **2012,** *2*, 2547-2556. (c) Martinez, H.; Zhang, J.; Kobayashi, S.; Xu, Y.; Pitet, L.; Matta, M. E.; Hillmyer, M. A. Functionalized regio-regular linear polyethylenes from the ROMP of 3-substituted cyclooctenes *Appl. Petrochem. Res.* **2015**, *5*, 19-25. (d) Radlauer, M. R.; Matta, M. E.; Hillmyer, M. A. Regioselective cross metathesis for block and heterotelechelic polymer synthesis. *Polym. Chem.* **2016**, *7*, 6269-6278. (e) Kobayashi. S.; Fukuda. K.; Kataoka. M.; Tanaka. M. Regioselective Ring-Opening Metathesis Polymerization of 3-Substituted

Cyclooctenes with Ether Side Chains. *Macromolecules*, **2016**, *49*, 2493-2501.

(20) Brits. S.; Neary. W. J.; Palui. G.; Kennemur. J. G. A new echelon of precision polypentenamers: highly isotactic branching on every five carbons. *Polym. Chem.,* **2018**, DOI:10.1039/C7PY01922J.

(21) Hejl, A.; Scherman, O.A.; Grubbs, R.H. Ring-Opening Metathesis Polymerization of Functionalized Low-Strain Monomers with Ruthenium-Based Catalysts. *Macromolecules.* **2005**, *38*, 7214-7218.

Chapter 4:

Multiple Olefin Metathesis Polymerization

4.1. Abstract

In general, when two or more metathesis transformations are used at the same time to successfully carry out the metathesis polymerization, the polymerization process must be very precise to form the desired polymer structure. Otherwise, only polymers of the ill-defined microstructure can be obtained. Many previous examples have shown polymerization using two metathesis transformations. However, none of the three metathesis transformations were used at the same time. We will now talk about multiple olefin metathesis polymerization using all three metathesis transformations simultaneously. Previously, we successfully developed new polymerization methodologies for monomers containing two cycloalkene moieties. Using this monomer, multiple olefin metathesis polymerization method yielded well-defined polymers via a combination of ring-opening, ring-closing, and cross-metathesis (multiple olefin metathesis polymerization (MOMP) using the second monomer, diacrylate. However, one-shot MOMP showed a very narrow monomer scope because of certain undesired side reactions. To overcome this limitation, we designed various types of newly modified monomers containing cyclopentene and even more challenging ring-strain free cyclohexene moieties, so that polymerization would produce a thermodynamically favored six-membered ring backbone repeat unit. With this enhanced driving force for polymerization, these new monomers successfully underwent that one-shot MOMP, which uses all three types of metathesis transformations in a single step, was possible with these monomers and gave highly A,B-alternating copolymers with high selectivity as well. This was possible because the newly designed monomers with the appropriate thermodynamic and kinetic preferences suppressed undesired polymerization pathways and reduced defects in the polymer microstructures. In short, we present our strategies for achieving superior MOMP using these new monomers.

4.2. Introduction

Olefin metathesis reaction is a powerful method for preparing various molecules that involve the exchange of carbon-carbon double bonds.[1] This field has rapidly advanced over

the last two decades, with the development of highly active Grubbs[2] and Schrock catalysts.[3] Organic chemists have developed ring-opening metathesis (ROM),[4] ring-closing metathesis (RCM),[5] and cross-metathesis (CM)[6] for the synthesis of complex organic compounds such as natural products and drugs. Furthermore, polymer chemists have developed polymerizations, such as ring-opening metathesis polymerization (ROMP),[7] cyclopolymerization (CP),[8] and acyclic diene metathesis polymerization (ADMET)[9] using CM reactions. However, most examples of metathesis polymerization methodologies rely on only one of the three types of olefin metathesis reactions to produce simple polymer structures. In order to synthesize well-defined polymers with complex microstructures, tandem polymerization, where more than two types of olefin metathesis transformations are combined in one-shot or one-pot reactions, has been developed successfully, analogous to cascade reactions in organic synthesis.[10-15]

The first representative example of using more than two types of olefin metathesis processes was ring-opening-insertion metathesis polymerization (ROIMP) using the second-generation Grubbs catalyst, which was used to synthesize well-defined A,B-alternating copolymers in a one-shot method.[10] The high degree of alternation of this copolymer was due to enthalpically driven selective CM to form α,β-unsaturated carbonyl olefins with the in-situ generated polymers via fast ROMP of cycloalkene using the second-generation Grubbs catalyst. Another example is the two-pot polymerization using two olefin metathesis reactions sequentially (ROMP followed by ADMET) to produce branched polymers in an independent manner.[11] Recently, a new concept of cascade polymerization via cascade ring-opening/ring-closing polymerization of monomers containing cycloalkene and terminal alkyne moieties[12] has attracted much attention because this selective cascade polymerization proceeded in a living manner, using the fast-initiating third-generation Grubbs catalyst to produce even sequence-specific polymers.[13] The most recently reported living polymerization combining olefin metathesis and metallotropic shift occurred in a perfectly alternating cascade manner to produce unique conjugated polyeneynes. [14] Lastly, we have reported cascade ring-opening/ring-closing polymerization (chapter 2) using

monomers containing two

Scheme 4.1. Cascade ring-opening/ring-closing metathesis polymerization in Chapter 2 and Multiple Olefin Metathesis Polymerization with M1 derivatives

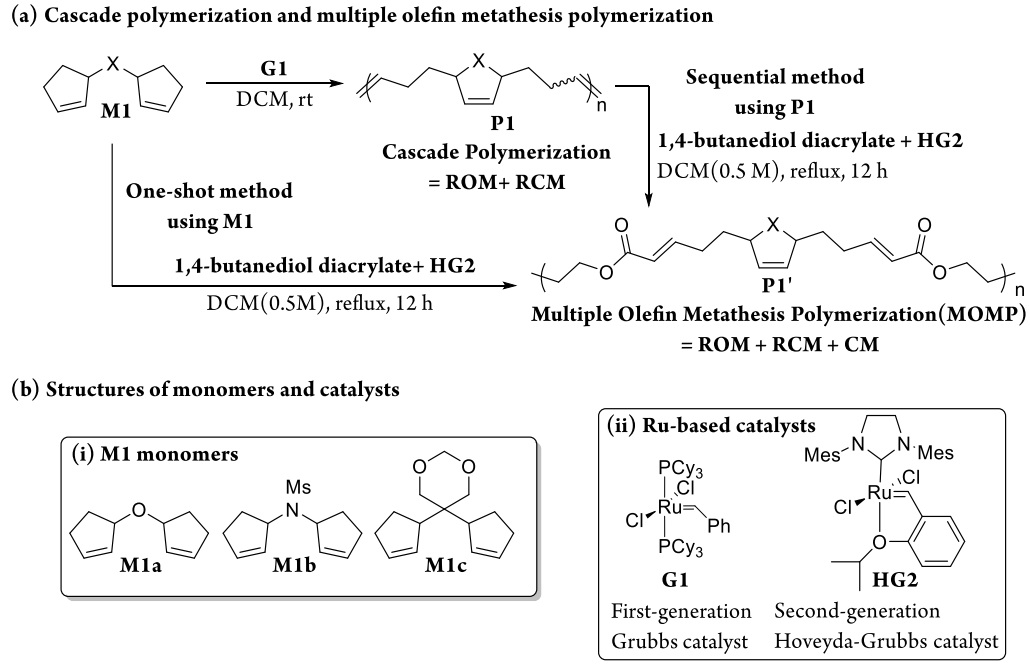

cyclopentene moieties and multiple olefin metathesis polymerization (MOMP), where all three types of olefin metathesis transformations occurred simultaneously to produce well-defined A,B-alternating copolymers using the same monomers[15a] (**Scheme 1a**). Although these two types of polymerization methods were mechanistically unique, the monomer scopes for MOMP were very narrow and they have limitation for getting defect-free polymer structure [15]. When one-shot MOMP was performed using a monomer containing symmetric dicyclopentene moieties, undesired side structures (seven-membered ring) could be formed and trapped by diacrylate insertion so that the structure of the polymer could be ruined. To avoid this problem, further improvement of the reactivity and selectivity of the MOMP were needed and expansion of their polymerization scopes was also needed. One needs to investigate the origins of the low reactivity and narrow monomer scope and to develop a new strategy to overcome these limitations. Herein, we report a new

design of bis-cycloalkene monomers towards achieving highly efficient cascade polymerization with a broad monomer scope with defect-free MOMP polymer structure. Since these polymerizations using the newly designed monomers produced kinetically and thermodynamically preferred six-membered ring backbone structures, we were able to broaden the monomer scope for the MOMP, by suppressing the generation of side products that caused significant defects in the previous one-shot MOMP method.

4.3 Results & Discussion

For the first time, to broaden the utility of cascade polymerization in chapter 2, we experimented to determine if the resulting polymers could undergo post-modification with a second-generation Grubbs catalyst. If the coupling between internal olefins on **P1a-c** and α,β-unsaturated carbonyl olefins on diacrylate monomers proceeded with high conversion and high selectivity, as in the case of CM,[13] the diacrylates could be selectively inserted into the polymers to yield A,B-alternating copolymer containing α,β-unsaturated carbonyl olefins. To test this idea, the purified polymers (**P1a-c**) were treated with 1,4-butandiol-diacrylate and **HG2** under optimized conditions (**Scheme 4.2.**).

After the back-biting of the catalyst into the acyclic olefins on the polymers, a series of exclusive CMs occurred selectively with the diacrylate,[13] and this process converted **P1a**, **P1b**, and **P1c** into thermodynamically more stable **P1a'**, **P1b'**, and **P1c'**, respectively, containing α,β-unsaturated carbonyl olefin with moderate molecular weights (**Table 4.1**).

Scheme 4.2. Multiple olefin metathesis polymerization (MOMP) with P1a-c.

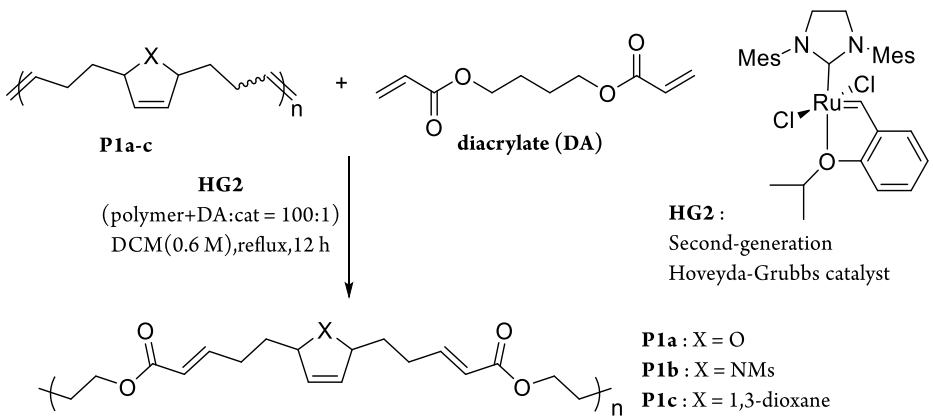

Table 4.1. Analysis of MOMP products

polymer	A,B-alt. [%][a]	M_n[b] (kDa)	M_w[b](kDa)	PDI[b]
P1a	97.5	10.6	22.0	2.09
P1b	94.3	7.3	13.5	1,82
P1c	94.2	16.4	30.7	1.87
P1a (one-shot)	95.5	9.3	19.8	2.11

[a]Determined by ^{1}H NMR spectroscopic analysis. [b] Determined by THF SEC calibrated using polystyrene standards.

The structural features of these well-defined A,B-alternating copolymers (**P1a-c**) were explicitly confirmed with ^{1}H NMR analysis (**Figure 4.1**). First, the internal olefins near 5.5 ppm on **P1** disappeared (**Figure 4.1**, **P1a** Ha), and new peaks corresponding to the α,β-unsaturated carbonyl olefins appeared at 7.0 ppm and 5.8 ppm (**Figure 4.1**, **P1a'** Ha and Hb, respectively). In particular, the newly formed olefin was 100% E isomer with a coupling constant of 16 Hz (Figure S13-1). Furthermore, the signal from the cyclic olefin (**Figure 4.1.**, **P1a'** Hd) still remained at 5.8 ppm (**Figure 4.1.**, **P1a'** Hc). A,B-alternations of the polymers were calculated by comparing the ratio of newly formed α,β-carbonyl olefins and the remaining internal olefins on the original homopolymers; in all cases,

significant alternations were observed (97.5% for **P1a**, 94.3% for **P1b**, and 94.2% for **P1c**, **Table 4.1.**). These structural analyses demonstrated the successful preparation of well-defined A,B-alternating copolymers via the sequential CM reaction.

Scheme 4.3. MOMP via a one-shot method.

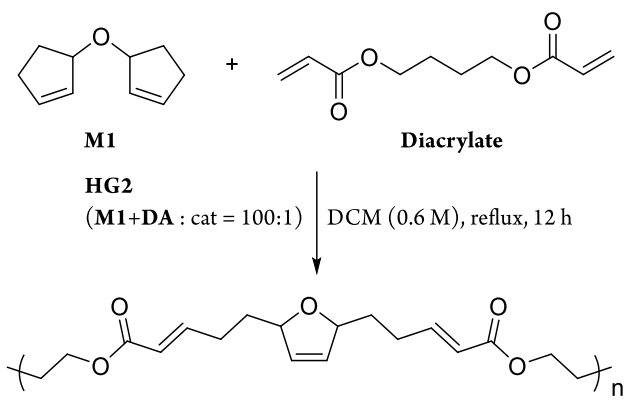

We expected that it would also be possible to obtain the identical A,B-alternating copolymer via the one-shot polymerization method instead of the two-step sequential method described above. M1 with the diacrylate was polymerized with **HG2** under the same conditions as those of the previous sequential method (**Scheme 4.1**). After 12 h of polymerization, the identical A,B-alternating copolymer **P1a** (one-shot) was obtained and confirmed with ^{1}H NMR (**Table 4.1.**). This result provides the first example of multiple olefin metathesis polymerization (MOMP), wherein all three types of olefin metathesis transformations (ring-opening, ring-closing, and cross metathesis) were combined in an orderly manner to produce just one uniform polymer microstructure via precisely controlled pathways.

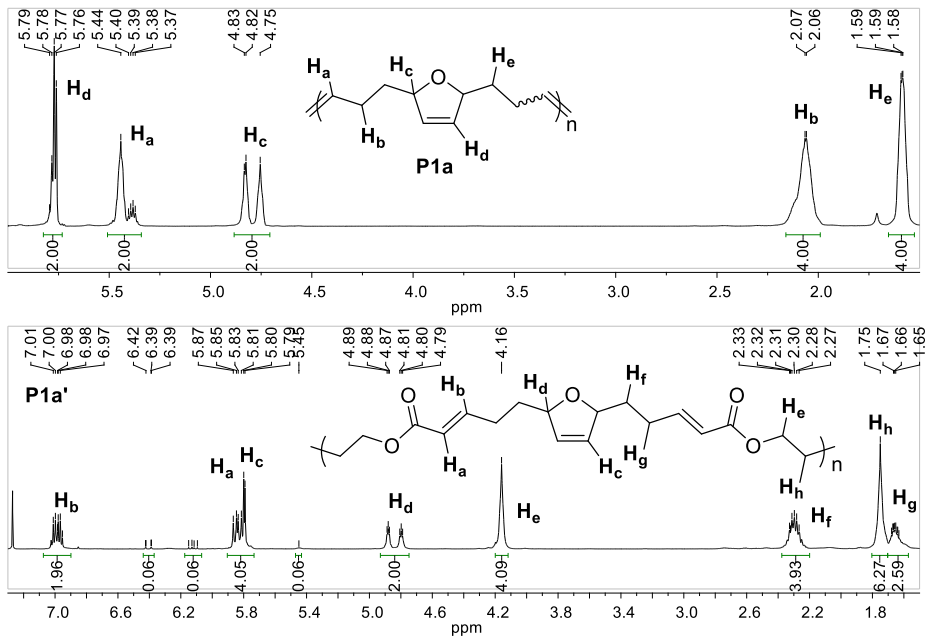

Figure 4.1. ^{1}H NMR spectra of P1a and P1a'

Next, we envisioned that these new monomers which gave successful cascade polymerization would undergo MOMP that uses all three types of olefin metathesis transformations (ROM, RCM, and CM). For MOMP, we used another monomer, 1,4-butanediol diacrylate as a coupling partner and instead of **G1**, more active second-generation Hoveyda–Grubbs catalyst **(HG2)**[16] that promote selective CM with electron deficient olefins such as acrylates (**Scheme 4.5**). The MOMP proceeds by the initial ring-opening/closing cascade reaction of the monomer having bis-cycloalkene followed by consecutive and selective CM with 1,4-butanediol diacrylate by one-shot manner19 to form A,B-alternating copolymers having thermodynamically stable α,β-unsaturated carbonyl olefins. However, in our previous report on MOMP, only **M1a** with the ether linkage underwent successful one-shot MOMP while **M1b** and **M1c** produced A,B-alternating copolymer only by sequential MOMP. The sequential MOMP consisted of two step processes: the initial cascade polymerization of **M1b** and **M1c** followed by inserting

Scheme 4.4. A New Strategy for Improving Polymerization Efficiency and Selectivity of M4 derivatives by Forming a Six-membered Ring in the Polymer

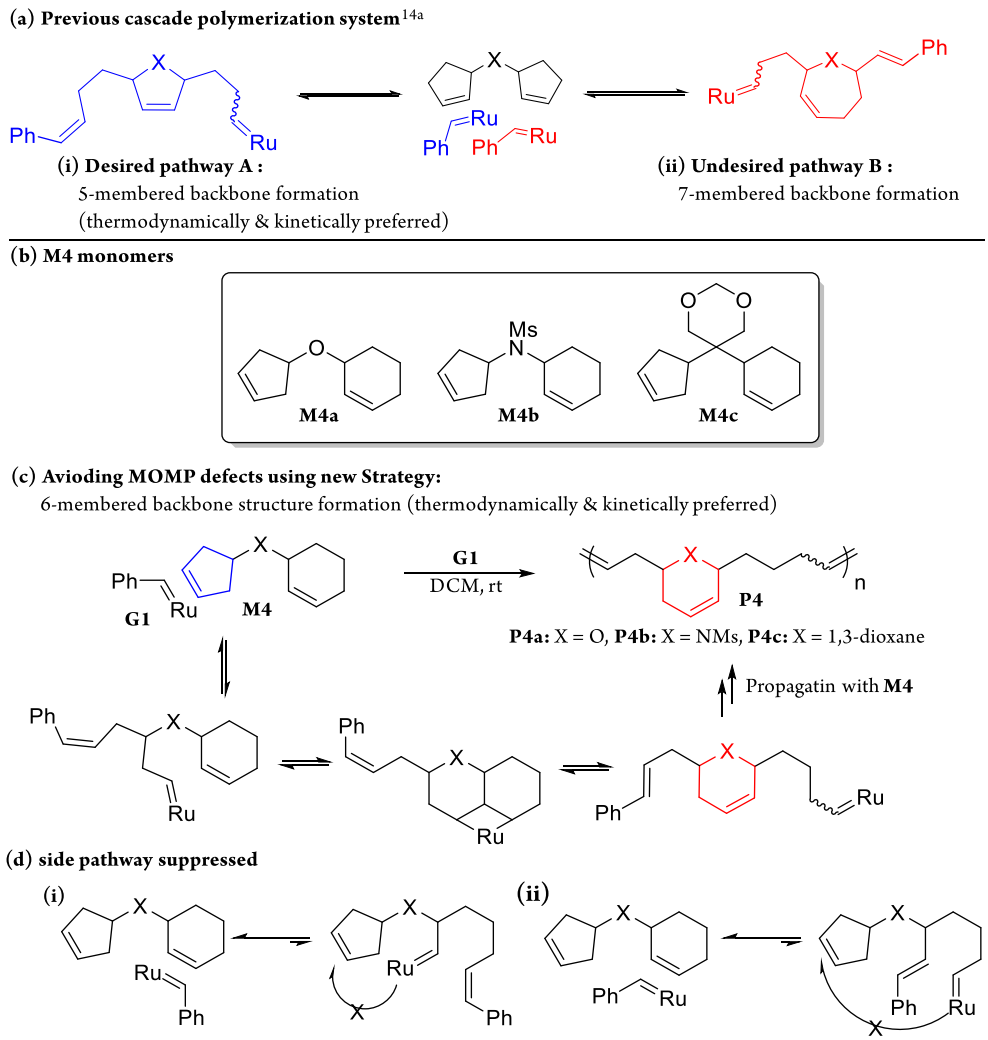

the diacrylate via selective CM on the isolated polymers, **P1b**, **P1c**. In other words, one-shot MOMP of **M1b** and **M1c** with the diacrylate was less than satisfactory because some side reactions such as undesired seven-membered ring formation trapped by the irreversible CM process with the diacrylate, significantly lowered the desired A,B-alternating microstructures. Here, we reasoned that these new monomers would undergo MOMP with enhanced selectivity. Because the six-membered ring backbone formation during the

polymerization is both thermodynamically and kinetically preferred so that the undesired side pathway such as more challenging and slow eight-membered ring formation would be completely suppressed.

Several new monomers such as **M3a** and **M4a**, and **M5a-c** were tested for MOMP by both one-shot and sequential methods and the results were compared. First, all the internal olefins should undergo selective cross metathesis with the diacrylate to obtain well-defined A,B-alternating copolymers and this alternation can be simply calculated from the integration by monitoring disappearance of the internal olefin at 5.5ppm and appearance of new α,β-unsaturated carbonyl olefin at 7.0 and 5.8 ppm by ^{1}H NMR. In the case of **M3a** showing structural similarity to **M1a**, one-shot and sequential MOMP methods were carried out. With both MOMP methods, using **M3a** and **P3a**, we obtained the identical polymer showing alternation over 92% and M_n of 6-8 kDa respectively (**Table 4.2. Entries 1-2**). In the cases of one-shot MOMP using M4a and M5a, both showed high alternation over 94% and M_n over 7 kDa (**Table 4.2. Entries 3,5**). Moreover, the analogous sequential MOMP using **P4a** and **P5a** via the sequential method produced the same copolymer with almost identical A,B-alternation although their M_n were slightly lower than the one-shot method(**Table 4.2. Entries 4,6**). Lastly, we also conducted one-shot MOMP using **M5b** and **M5c** containing sulfonamide and carbon linkage, as well as sequential MOMP using **P5b** and **P5c**, and both methods gave a very similar copolymer showing almost the same structural features by ^{1}H NMR with the alternation over 92% and M_n ranging between 7 kDa and 11 kDa (**Table 4.2. Entries 7–10**).

Scheme 4.5. MOMP results with M3, M4 and M5 derivatives

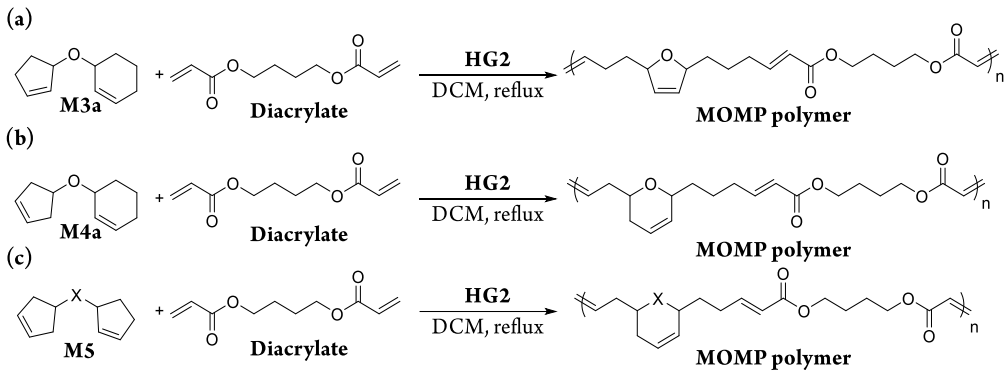

M5a: X = O, **M5b:** X = NMs, **M5c:** X = 1,3-dimethoxypropane
Diacrylate = 1,4-butanediol diacrylate

Table 4.2. One-shot MOMP with M3-5 monomers and sequential MOMP with P3-5 polymers

Entries	Monomer	Method	M(P):D:C	Conc. (M)	Time (h)	Mna (kDa)	PDI[a]	Alternation[b] (%)	Yield (%)
1	**M3a**	One-shot	50:50:1	0.5	12	7.8	1.53	92	74
2	**P3a**	Sequential	50:50:1	0.5	12	5.7	1.36	95	73
3	**M4a**	One-shot	50:50:1	0.5	12	7.3	1.61	97	85
4	**P4a**	Sequential	50:50:1	0.5	12	4.8	1.49	95	72
5	**M5a**	One-shot	50:50:1	0.5	4	7.4	2.24	94	78
6	**P5a**	Sequential	50:50:1	0.5	4	6.4	1.36	94	82
7	**M5b**	One-shot	50:50:1	0.5	8	11.0	1.57	94	78
8	**P5b**	Sequential	50:50:1	0.5	12	9.9	1.23	95	72
9	**M5c**	One-shot	50:50:1	0.5	12	7.5	1.76	92	81
10	**P5c**	Sequential	50:50:1	0.5	12	7.7	1.31	92	84

[a] Determined by THF SEC calibrated using polystyrene standards. [b] Conversion was determined by crude 1H NMR analysis

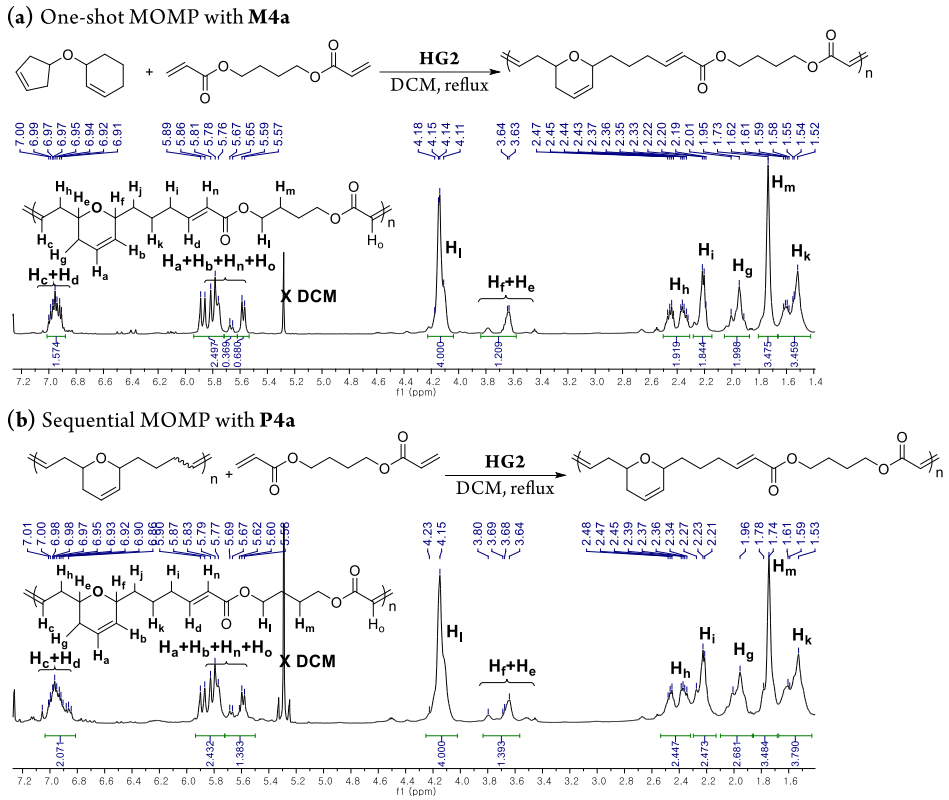

Figure 4.3. Proton spectra of one-shot MOMP with M4a (a) and sequential MOMP with P4a (b)

Next, we also wanted to test and increase the diversity of MOMP using a variety of monomers. In total 15 monomers were used to perform MOMP. Unfortunately, unlike the monomers mentioned above, each had problems. The details are as follows. In the case of **1**,**14**,**15**, the steric factor in monomers was too large, so that the olefin and the binding itself became difficult so that the color of the Grubbs catalyst did not change at all and the MOMP did not proceed at all after long reaction time (> 48 h). On the other hand, in the case of other monomers **2-13**, the conversions of each MOMP were relatively low due to the difference in the reactivity between the diastereomers of the monomer, but the MOMP proceeded. Using these monomers, it was difficult to obtain a perfect form of MOMP. So we tried to think of another way to increase the diversity of MOMP.

Scheme 2.5. Various monomer scopes of MOMP

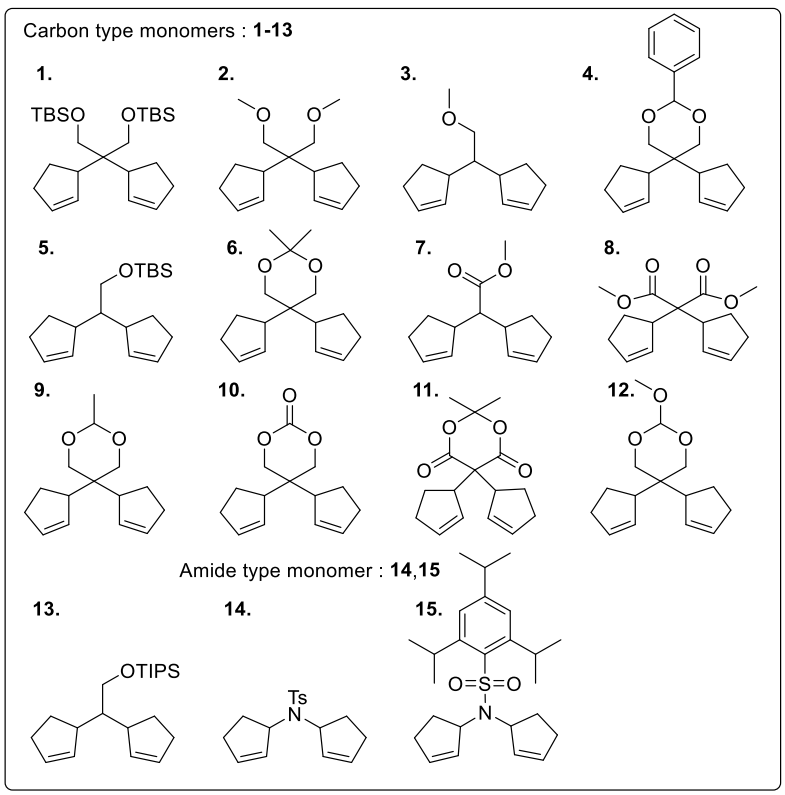

Thus, we carried out the further MOMP reactions using three additional diacrylates (1,4-phenylene diacrylate, propane-2,2-diylbis(4,1-phenylene) diacrylate, 2,2-dimethylpropane-1,3-diyl diacrylate) with **M1a** and **M4b** to confirm that the other acrylates are also able to use for the MOMP. In these cases, we also could get A,B-alternating copolymer with high alternation and high molecular weight using a one-shot MOMP method. However, when using 1,4-butanediol diacrylate, proton NMR assignment for the polymeric structure was simple and much clearer than with other diacrylates. Therefore, 1,4-butanediol diacrylate was chosen as the best candidate for MOMP. The difference in polymerization efficiency is not significant even with any diacrylates as we could observe in NMR and data in **Table 4.3.** Using other diacrylates, we also could get alternating copolymer efficiently using MOMP.

Scheme 4.6. one-shot MOMP with other diacrylates.

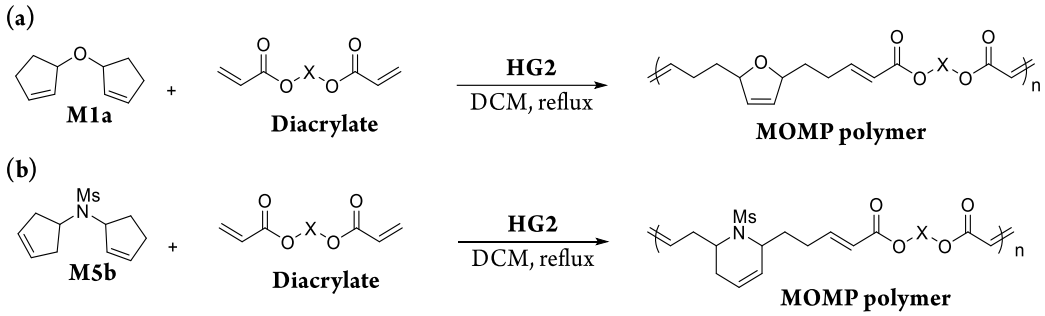

Diacrylate = 1,4-phenylene diacrylate, propane-2,2-diylbis(4,1-phenylene) diacrylate, 2,2-dimethylpropane-1,3-diyl diacrylate

Table 4.3. one-shot MOMP results with other diacrylates.

Entry	Monomer	Diacrylate	M:D:C	Time (h)	M_n[a] (kDa)	$Đ_M$[a]	A,B-alt.[b] (%)	Yield (%)
1	**M1a**	1,4-phenylene diacrylate	50:50:1	12	11.9	1.90	98	78
2	**M1a**	propane-2,2-diylbis(4,1-phenylene) diacrylate	50:50:1	12	13.9	1.96	97	82
3	**M1a**	2,2-dimethylpropane-1,3-diyl diacrylate	50:50:1	12	9.1	1.84	95	92
4	**M5b**	1,4-phenylene diacrylate	50:50:1	12	10.2	1.79	98	83
5	**M5b**	propane-2,2-diylbis(4,1-phenylene) diacrylate	50:50:1	12	9.7	1.88	94	92
6	**M5b**	2,2-dimethylpropane-1,3-diyl diacrylate	50:50:1	12	11.2	1.82	96	86

[a] Molecular weight and dispersity ($Đ_M$) were determined using THF SEC calibrated using polystyrene standards. [b] Alternation was determined using ^{1}H NMR analysis. Reaction concentration: 0.5 M.

Scheme 2.6. Possible intermediates in Pathway B in one-shot MOMP.

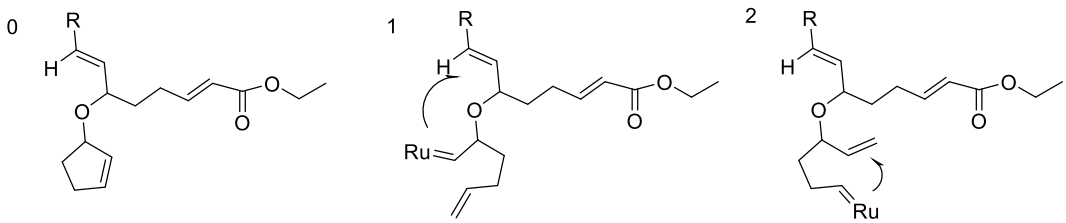

In addition, from the conclusions in **Chapter 3**, we can consider the difference between the sequential method and the one-shot method mechanism in MOMP using **HG2** catalysts. If One-shot MOMP is carried out at a low concentration (< 0.8 M) which cross-linking does not occur, then **Pathway A** and **B** (**Scheme 3.2**) could be considered as a possible pathway unlike cascade polymerization which could form polymer using **Pathway A**. If polymerization underwent to **pathway A** first in one-shot MOMP, resulting the polymer will proceed following cascade polymerization first and cross-metathesis sequentially. In case of **Pathway B** (**Scheme 3.2**.), which did not form a polymer in cascade polymerization, there are two cases in one-shot MOMP. The first is to return to the monomer, and the second, to form a Ru species, which, in conjunction with the DA, is opened back to one side. (If the monomer is attached with **1** or **2** in **scheme 2.6.**, it can be considered. But, in these cases, if cascade polymer proceeds with low probability, it will be final structure through CM or it will be a defect in cascade polymer form.) This second case is irreversibly formed **1**, **2**. In other words, no matter which catalyst is attached to the generated (**0**), the result of pathway A, 1, will eventually form a cascade polymer. And the output of **Pathway B**, in the case of **2**, it will return to **0** again. Again, cyclopentene can form a cascade polymer as a result. In other words, considering the progress of the reaction as a whole, the conversion of ether monomer in MOMP is faster than the conversion of homopolymerization, cascade polymerization because MOMP contributes to forming the final structure in both **Pathway A** and **B**. However, all these predicted results are only possible if the specific concentration of MOMP is well maintained. It is important to note that the concentration is very important in MOMP as well as cascade polymerization because there is a possibility that cross-linked gels or other defects may form if the concentration becomes too high in the middle of

reaction. In other words, the most important factor in the overall system is concentration.

Finally, it can be concluded that **Pathway B** as well as **Pathway A** in MOMP act as a key step to form a resulting MOMP polymer in the whole polymerization process.

4.4. Conclusion

In short, we could expand the scope of one-shot MOMP using these new monomers and understand the design principle of these new monomers thereby suppress defects promoted by the undesired pathways. Futhermore newly designed monomers were used for MOMP system and these new monomers successfully underwent one-shot MOMP, which combined all three olefin metathesis processes, to give A,B-alternating copolymers with higher selectivity than those in the previous studies. This high selectivity was due to the novel monomer design that promoted thermodynamically and kinetically preferred six-membered ring cyclization, thereby suppressing the formation of defects caused by the undesired side-reactions. This taught an important lesson that novel monomer design based on an understanding of thermodynamic parameters can not only broaden the polymerization scope but also greatly improved the polymerization efficiency

4.5. Experimental Section

2) MOMP polymer

The general procedure of multiple olefin metathesis polymerization

The sequential process by cross metathesis

To a flask charged with the isolated polymer (0.32 mmol) and 1,4-butanediol diacrylate (62.5 mg, 0.32 mmol) in 1 ml of DCM, Grubbs Hoveyda second generation catalyst (3.5 mg). Quick degassing by dynamic vacuum was conducted and the flask was fitted with a condenser and refluxed under argon for 6 hours. The product was precipitated by cooled hexane.

The one-shot process

To a flask charged with dicyclopentene monomer (0.32 mmol) and 1,4-butanediol diacrylate (62.5 mg, 0.32 mmol) in 1 ml of DCM, Grubbs Hoveyda second generation catalyst (3.5 mg). Quick degassing by dynamic vacuum was conducted and the flask was fitted with a condenser and refluxed under argon for 6 hours. The product was precipitated by hexane.

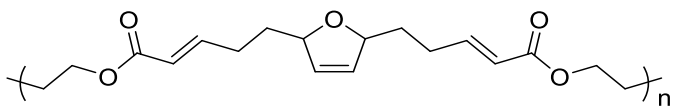

^{1}H NMR (500 MHz, $CDCl_3$, ppm) δ 7.01 – 6.97 (2H, m), 5.79 - 5.87 (4H, m), 4.79 - 4.98 (2H, d), 4.16 (4H, s), 2.27 – 2.33 (4H, m), 1.75 (6H, s), 1.65-1.67 (2H, s)

^{13}C NMR (500 MHz, $CDCl_3$, ppm) δ 166.40, 166.36, 148.93, 148.80, 130.59, 130.43, 130.05, 129.87, 121.28, 121.12, 84.88, 84.75, 63.59, 34.81, 33.97, 28.13, 27.72, 25.29

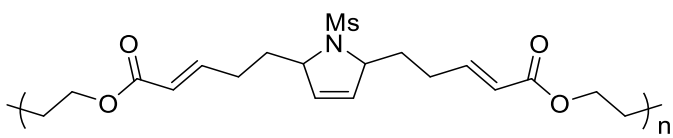

^{1}H NMR (500 MHz, $CDCl_3$, ppm) δ 6.91 – 7.00 (2H, m), 5.79 - 5.88 (4H, m), 4.63 (1H, s), 4.39 (1H, s), 4.16 (4H, s) 2.96 (1.5H, s), 2.74 (1.5H, s), 2.13-2.33 (2H, br), 1.89 (4H, m), 1.75 (4H, s)

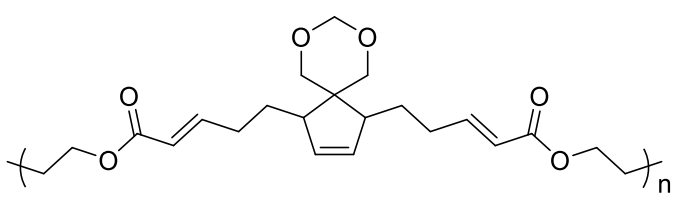

^{1}H NMR (500 MHz, $CDCl_3$, ppm) δ 6.94 – 6.99 (2H, m), 5.74 - 5.87 (4H, m), 4.83 (2H, d), 4.16 (4H, s), 3.48 -3.87 (4H), 2.20 - 2.53 (6H, broad), 1.76 (6H, s), 1.24-1.28 (2H, broad)

^{13}C NMR (500 MHz, $CDCl_3$, ppm) δ 131.16, 132.45, 130.24, 94.01, 71.54, 71.38, 68.72, 49.25, 48.94, 48.40, 45.60, 44.15, 32.23, 31.86, 31.44, 31.04, 29.51

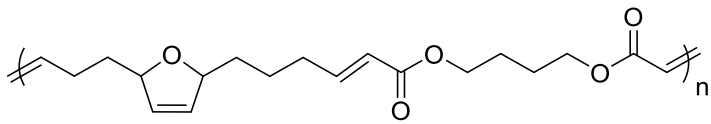

^{1}H NMR (500 MHz, $CDCl_3$, ppm) δ 7.01 (2H, s), 5.77-5.86 (4H, m), 4.77-4.87 (2H, d), 4.15 (4H, s), 2.29 (3H, s), 1.95-2.04(1H, d), 1.74(6H, s), 1.54-1.65(5H, s*2)

^{13}C NMR (500 MHz, CDCl3, ppm) δ 166.56, 149.08, 130.29, 129.98, 129.50, 85.40, 84.76, 63.67, 36.12, 35.33, 34.89, 34.11, 32.15, 32.04, 29.64, 29.16, 27.80, 25.39, 23.94, 23.54, 22.60, 22.21, 21.04

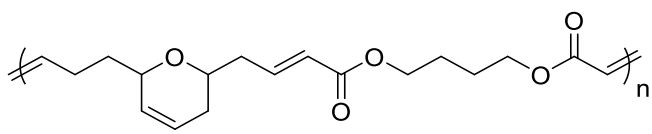

^{1}H NMR (500 MHz, $CDCl_3$, ppm) δ 7.00 (2H, m), 5.57-5.89 (4H, m), 4.18 (4H, s), 3.63 (1H, s), 2.33-2.47 (2H, d), 2.19 (2H, s), 1.95 (2H, s), 1.73 (3H, s), 1.52 (4H, s)

^{13}C NMR (500 MHz, $CDCl_3$, ppm) δ 168.19, 167.98, 150.90, 146.94, 131.66,131.07, 125.94, 125.02, 124.75, 124.55, 122.93, 122.82, 122.21, 76.08, 73.97, 68.17, 65.31, 65.24, 40.21, 39.43, 36.34, 34.83, 33.76, 33.71, 33.49, 32.43, 26.94, 26.92, 25.00

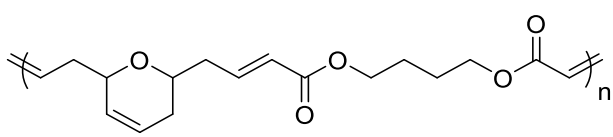

^{1}H NMR (500 MHz, $CDCl_3$, ppm) δ 7.00 (2H, m), 5.58-5.91 (4H, m), 4.24 (4H, s), 3.46-3.79 (1H, s), 2.30-2.57 (4H, m), 2.03 (2H, s), 1.66-1.75 (5H, s)

^{13}C NMR (500 MHz, $CDCl_3$, ppm) δ 167.96, 150.85, 146.66, 142.14, 138.02, 136.02, 131.57, 131.32, 126.36, 125.44, 124.62, 122.75, 75.35, 73.92, 68.15, 65.35, 40.17, 39.43, 35.15, 32.39, 29.25, 26.92, 26.00, 22.61

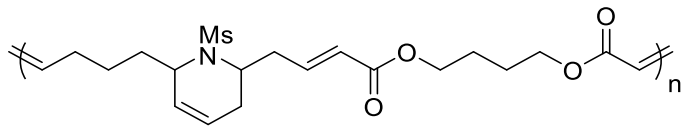

^{1}H NMR (500 MHz, $CDCl_3$, ppm) δ 6.90-6.99 (2H, m), 5.73-5.93 (4H, m), 4.10-4.26 (6H, m), 2.80-2.93 (3H, d), 2.22-2.49 (7H, m), 1.31-1.58 (3H, d), 1.58 (3H, s), 1.27 (4H, s)

^{13}C NMR (500 MHz, $CDCl_3$, ppm) δ 167.93, 167.62, 167.41, 149.47, 146.98, 146.32, 130.42, 130.18, 129.60, 127.89, 127.19, 125.53, 125.15, 123.78, 123.37, 123.26, 65.45, 65.41,65.28, 57.70, 55.13, 54.42, 53.89, 50.91, 43.67, 37.60, 33.33, 30.90, 30.80, 29.97, 28.39, 27.82, 26.88, 26.85

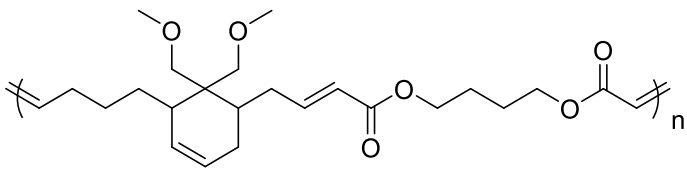

^{1}H NMR (500 MHz, $CDCl_3$, ppm) δ 7.00 (2H, m), 5.81-5.88 (2H, s), 5.53-5.63 (2H, m), 4.18 (4H, s), 3.19-3.55 (10H, m), 2.04-2.52 (8H, m), 1.77 (7H, s)

^{13}C NMR (500 MHz, $CDCl_3$, ppm) δ 168.23, 168.16, 168.12, 168.09, 151.65, 151.30, 151.17, 150.81, 130.25, 130.14, 127.20, 126.94, 123.49, 123.31, 122.79, 122.64, 122.03, 76.67, 76.50, 75.54, 73.39, 73.13, 72.42, 65.25, 60.72, 60.71, 60.67, 60.61, 44.26, 43.96, 39.61, 35.09, 34.31, 32.41, 32.41,31.93, 29.91, 29.71, 26.95, 23.62

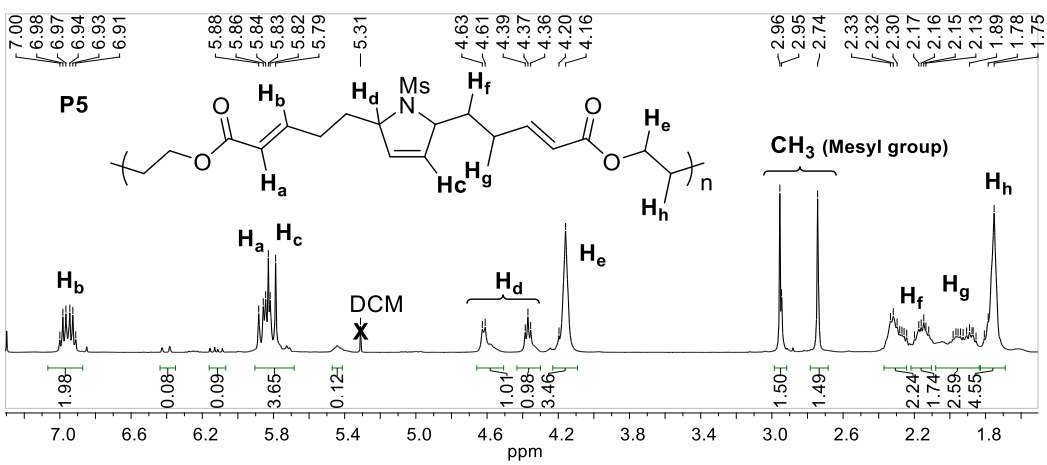

Figure S4.1-1. ^{1}H NMR of Mesyl amide type multiple olefin metathesis polymer

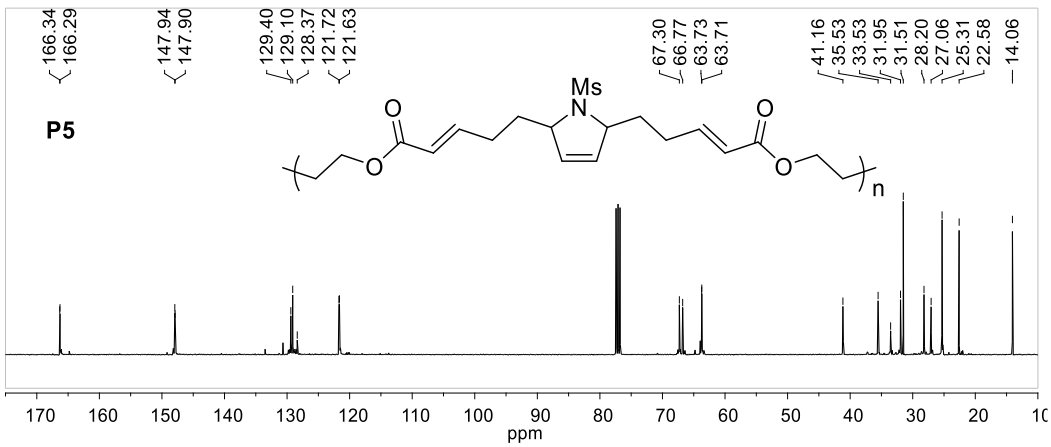

Figure S4.1-2. ^{13}C NMR of Mesyl amide type multiple olefin metathesis polymer

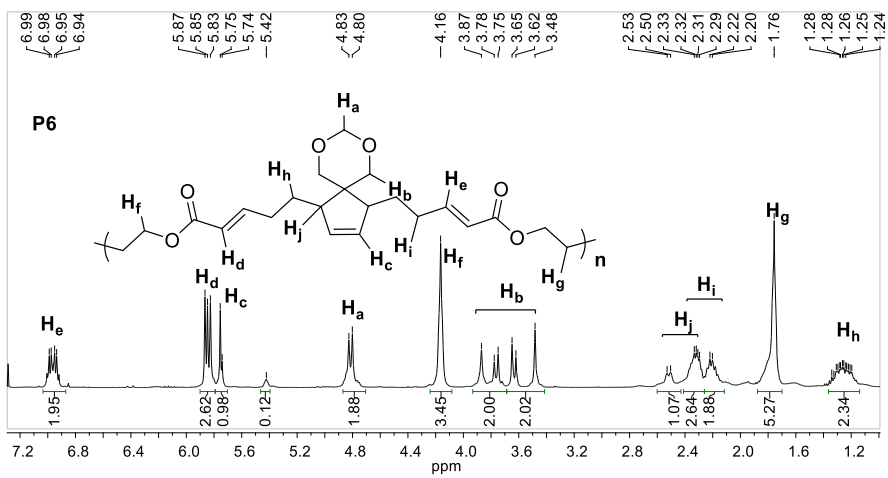

Figure S4.2-1. ^{1}H NMR of carbon type multiple olefin metathesis polymer

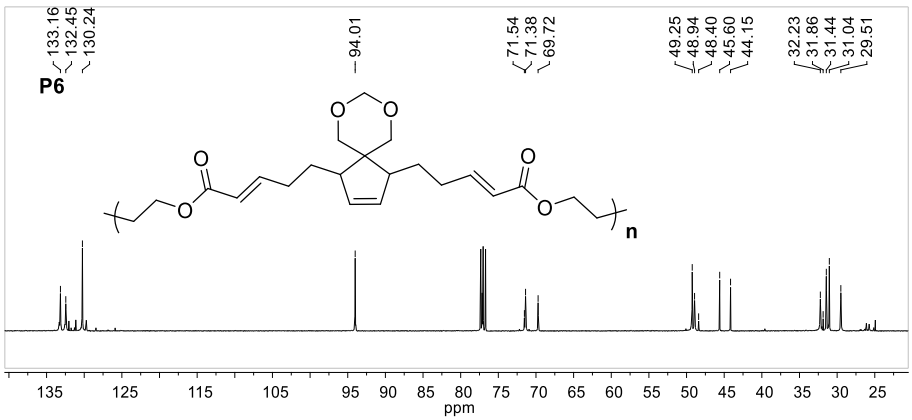

Figure S4.2-2. ^{13}C NMR of carbon type multiple olefin metathesis polymer

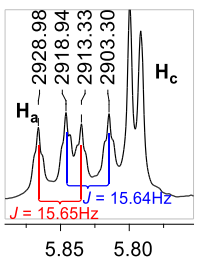

Figure S4.3. ^{1}H NMR of P4 of magnified H_a signal with its coupling constants.

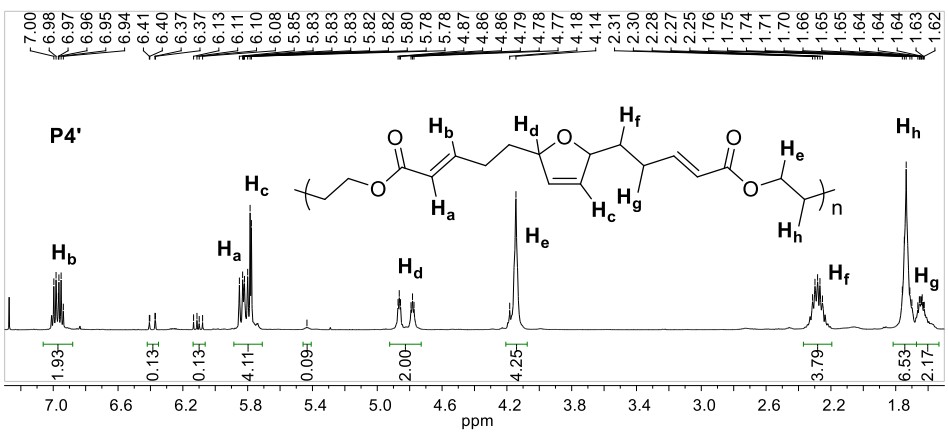

Figure S4.3-2. ^{1}H NMR of ether type multiple olefin metathesis polymer (one-pot

method)

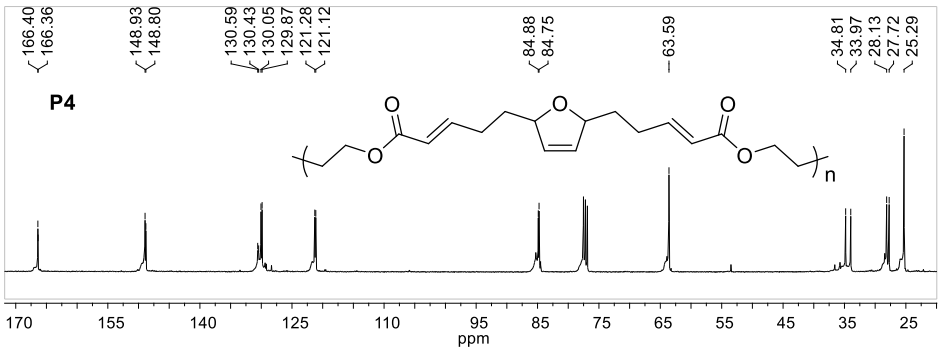

Figure S4.3-3. ^{13}C NMR of ether type multiple olefin metathesis polymer

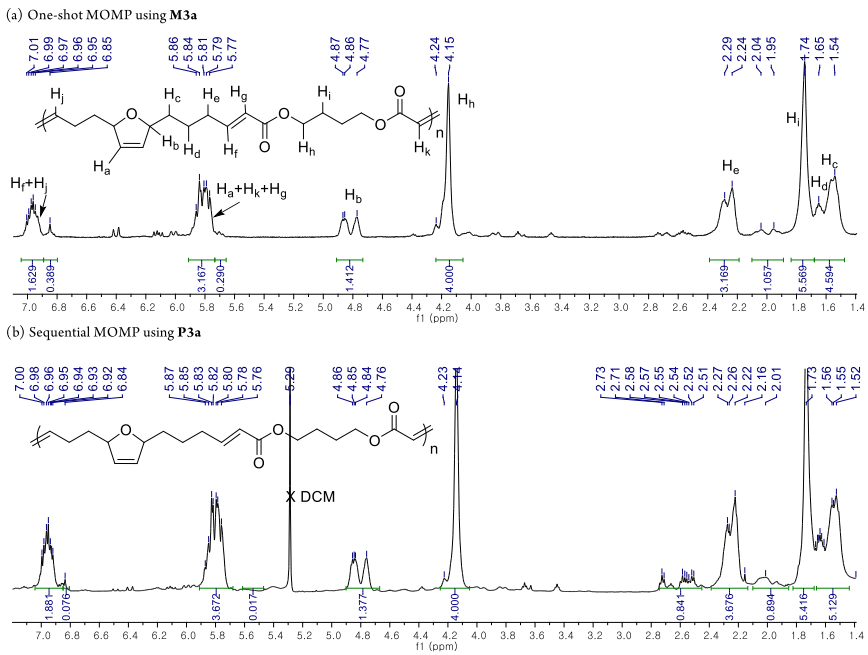

Figure S4.4-1. Proton NMR spectra of MOMP polymer using **M3a** and **P3a**.

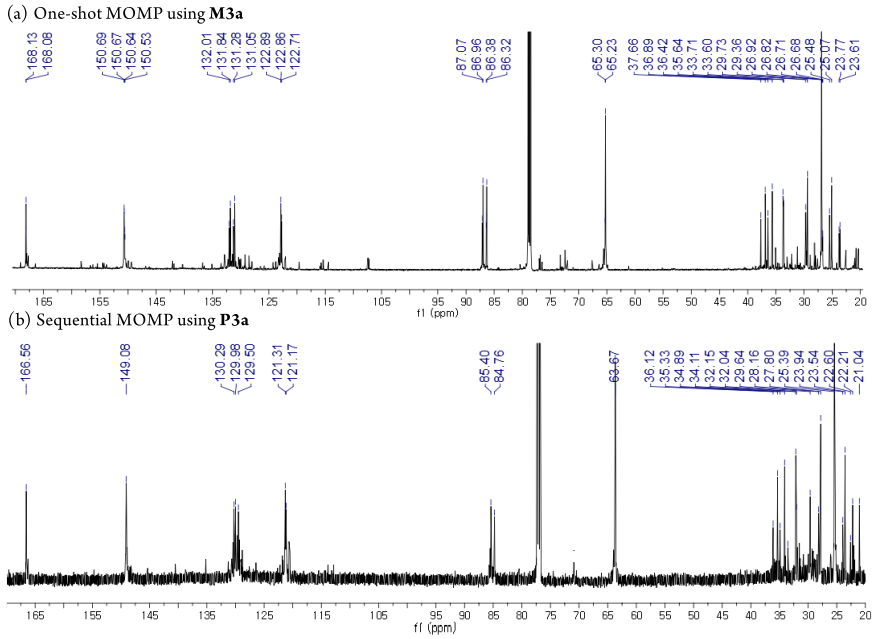

Figure S4.4-2. Carbon NMR spectra of MOMP polymers using **M3a** and **P3a**.

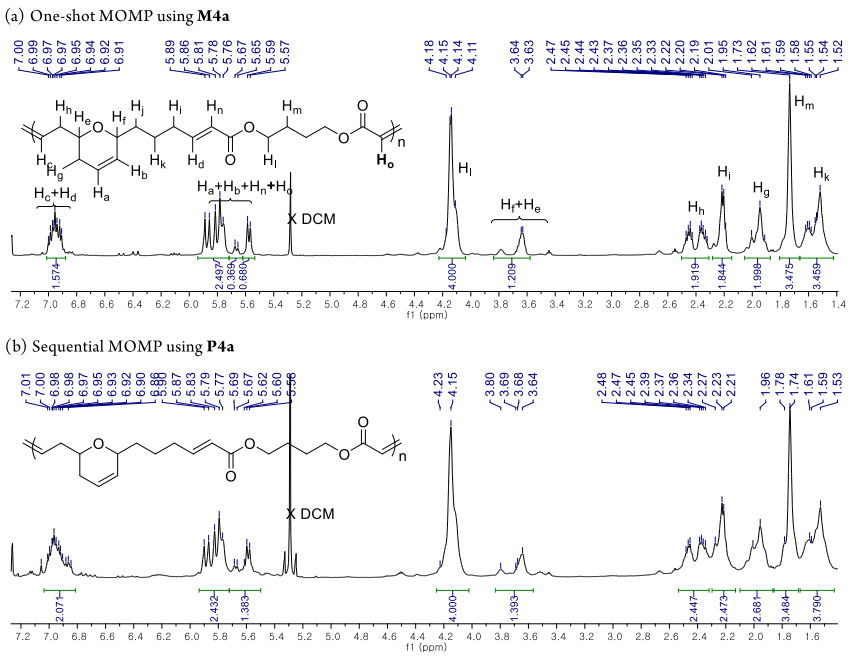

Figure S4.5-1. Proton NMR spectra of MOMP polymer using **M4a** and **P4a**.

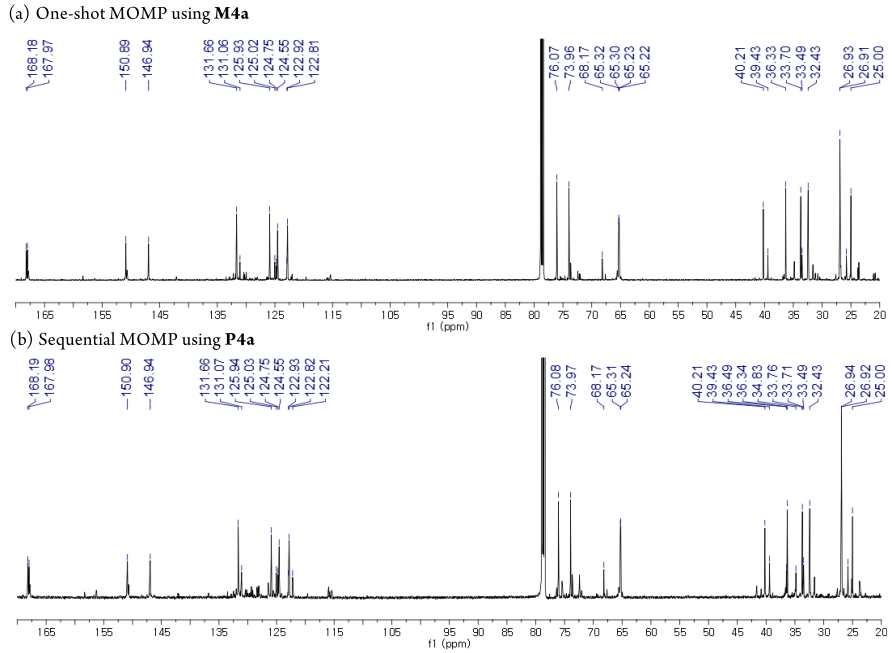

Figure S4.5-2. Carbon NMR spectra of MOMP polymers using **M4a** and **P4a**.

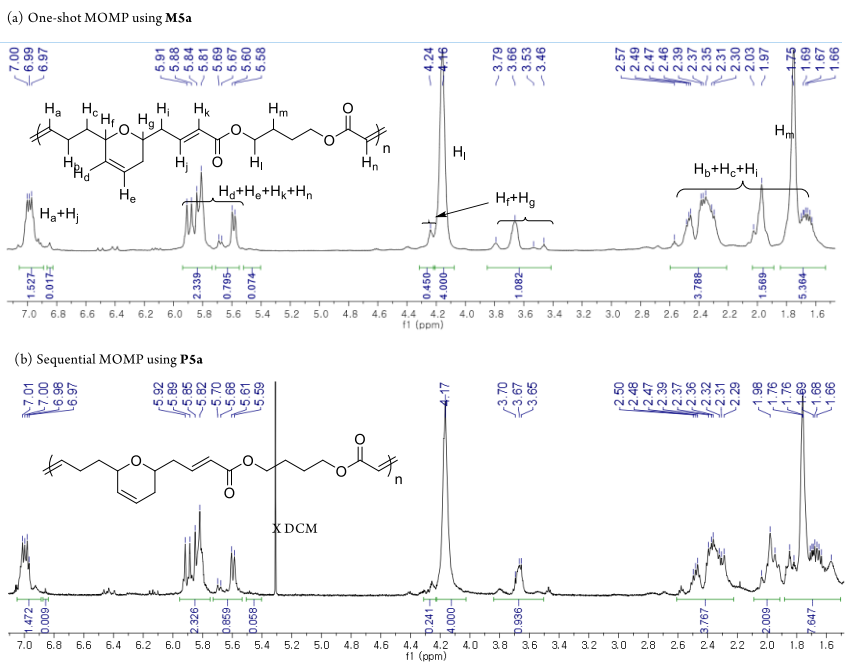

Figure S4.6-1. Proton NMR spectra of MOMP polymer using **M5a** and **P5a**.

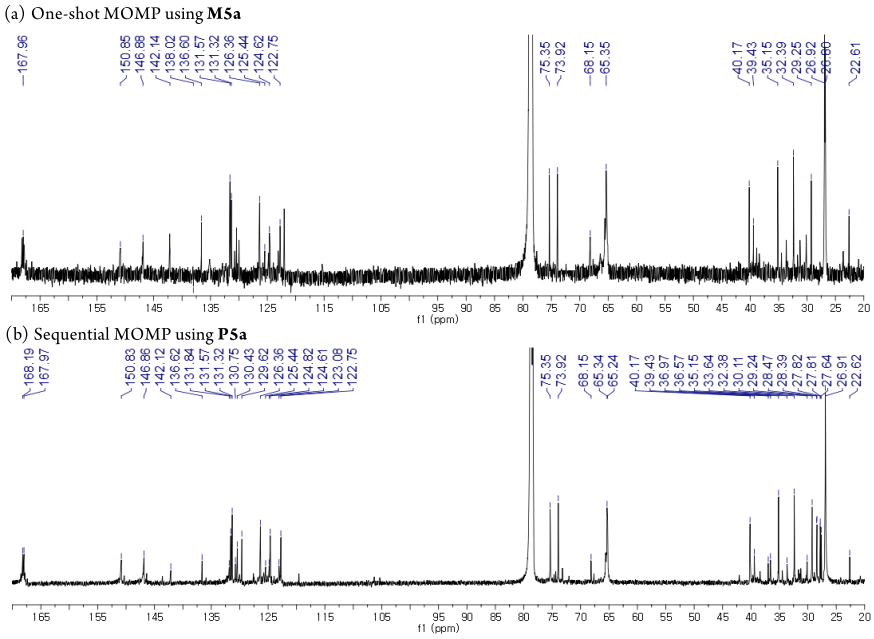

Figure S4.6-2. Carbon NMR spectra of MOMP polymers using **M5a** and **P5a**.

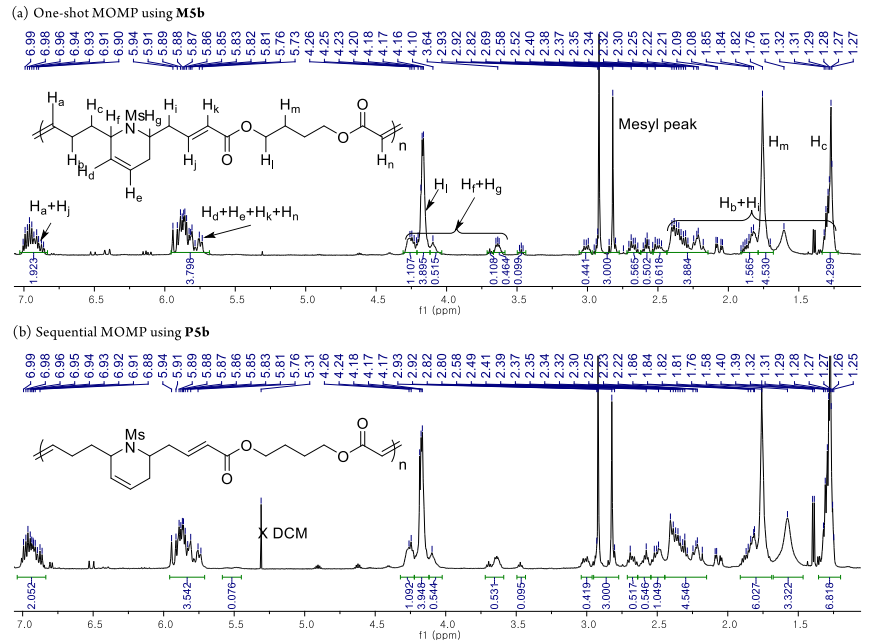

Figure S4.7-1. Proton NMR spectra of MOMP polymer using **M5b** and **P5b**.

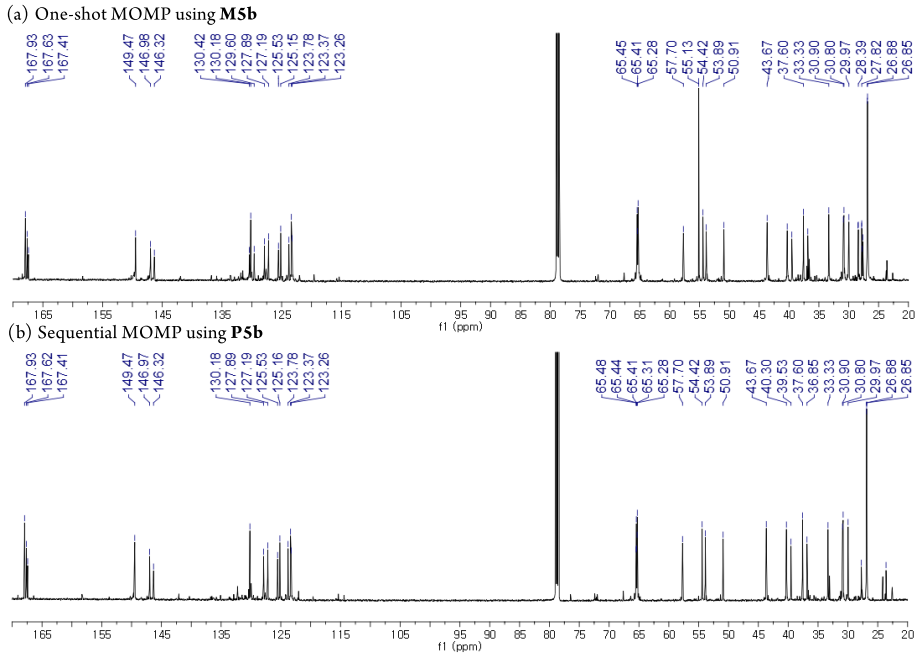

Figure S4.7-2. Carbon NMR spectra of MOMP polymers using **M5b** and **P5b**.

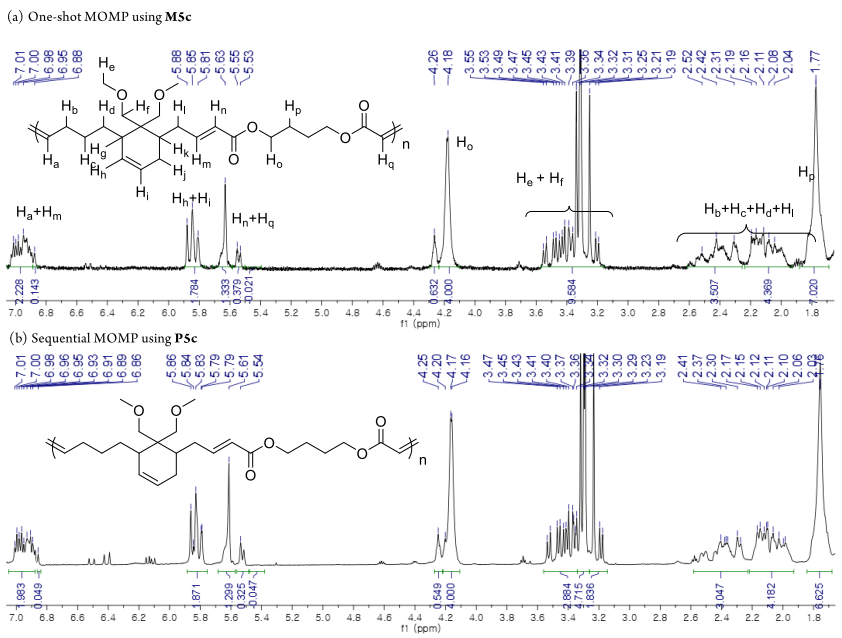

Figure S4.8-1. Proton NMR spectra of MOMP polymer using **M5c** and **P5c**.

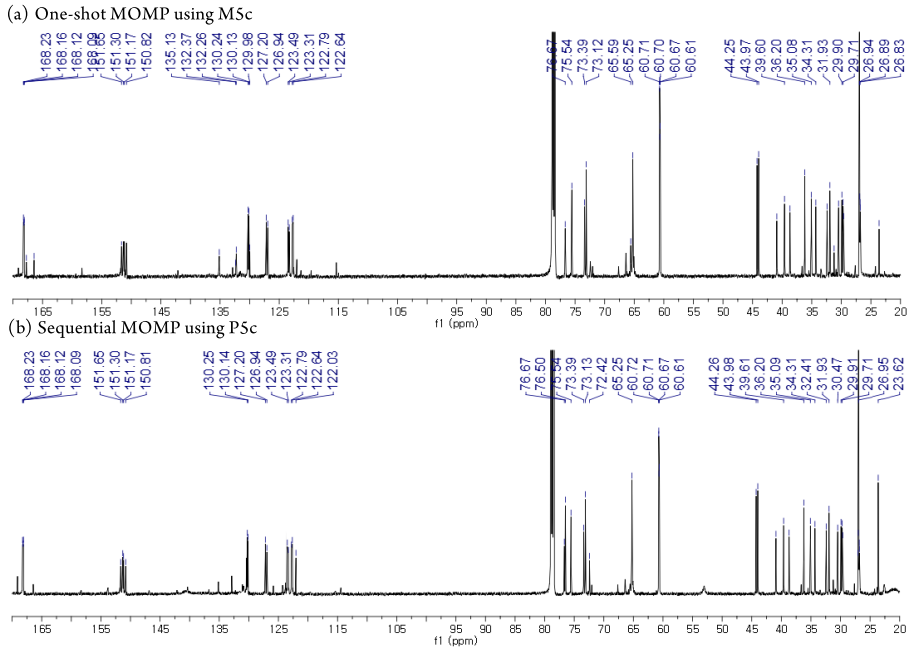

Figure S4.8-2. Carbon NMR spectra of MOMP polymers using **M5c** and **P5c**.

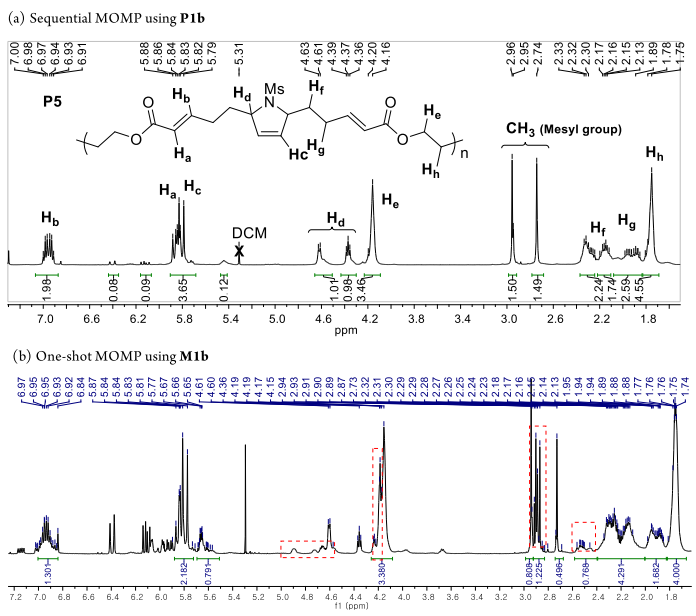

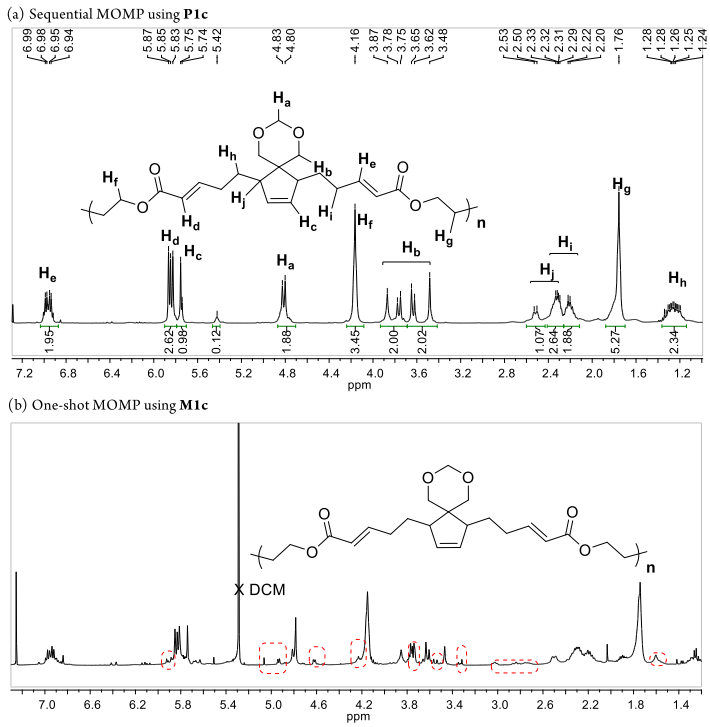

Figure S4.9. Comparison between defect-free Sequential MOMP and One-shot MOMP using **P1b**, **M1b** and **P1c**, **M1c**.

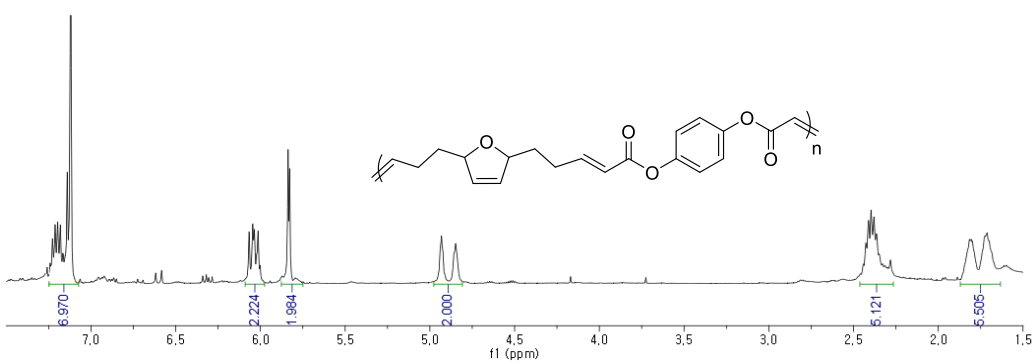

Figure S4.10. One-shot MOMP with M1a and 1,4-phenylene diacrylate

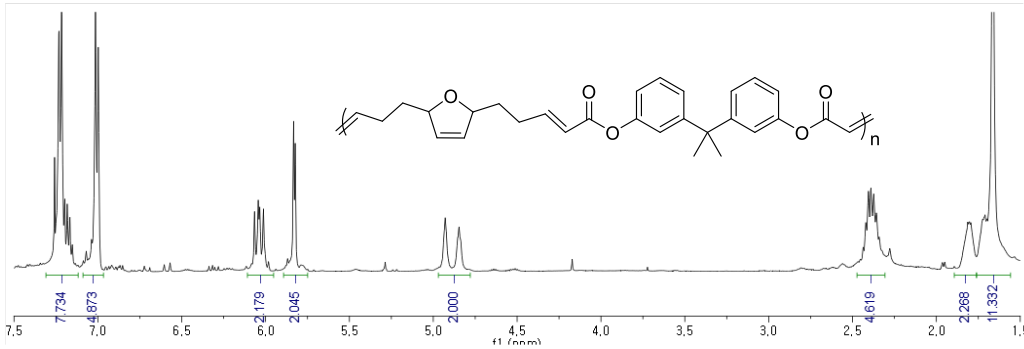

Figure S4.11. One-shot MOMP with M1a and propane-2,2-diylbis(4,1-phenylene) diacrylate

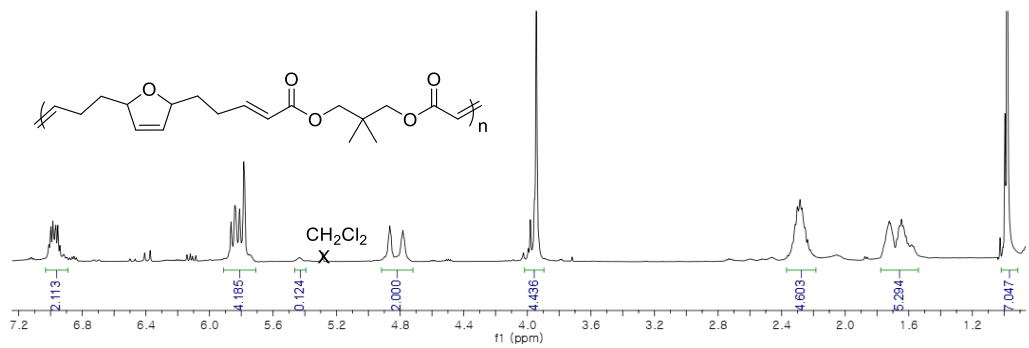

Figure S4.12. One-shot MOMP with M1a and 2,2-dimethylpropane-1,3-diyl diacrylate

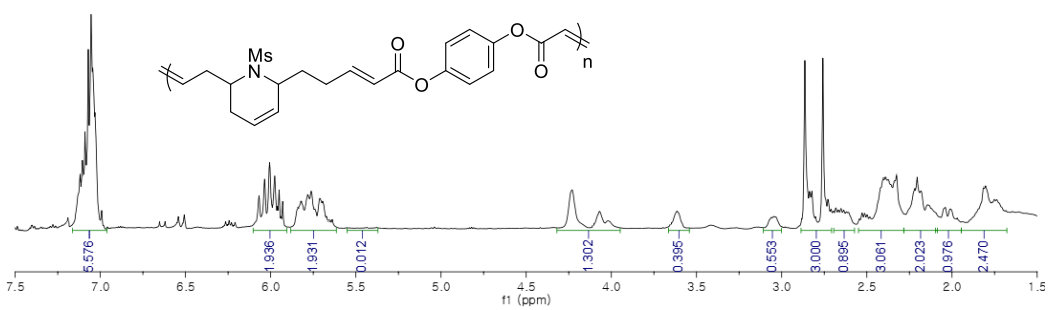

Figure S4.13. One-shot MOMP with M5b and 1,4-phenylene diacrylate

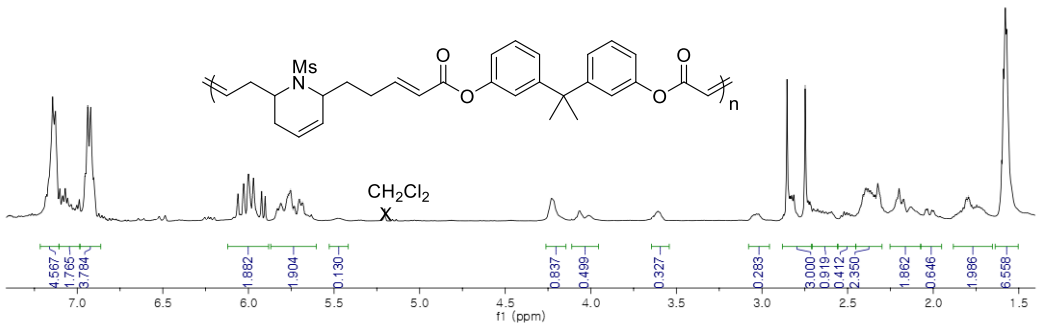

Figure S4.14. One-shot MOMP with M5b and propane-2,2-diylbis(4,1-phenylene) diacrylate

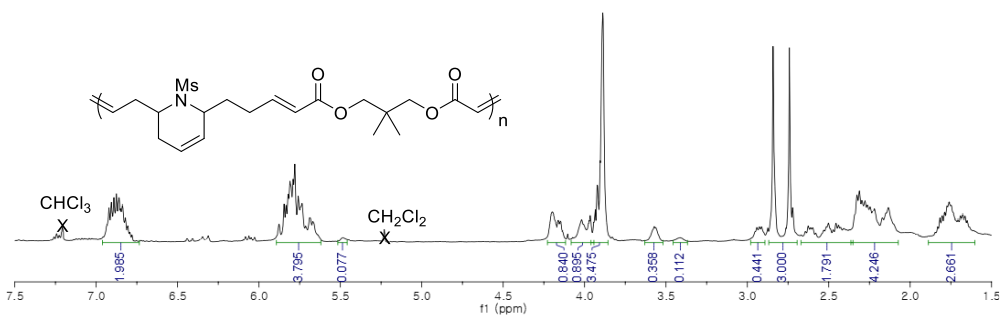

Figure S4.15. One-shot MOMP with M5b and 2,2-dimethylpropane-1,3-diyl diacrylate

4.6 References

(1) (a) Grubbs, R. H.; Chang, S. *Tetrahedron* **1998**, *54*, 4413. (b) Fürstner, A. *Angew. Chem., Int. Ed*. **2000**, *39*, 3013. (c) Grubbs, R. H. *Handbook of Metathesis*, Wiley-VCH: Weinheim, **2003**, *1*, 2. (d) Grubbs, R. H. *Tetrahedron* **2004**, *60*, 7117.

(2) (a) Novak, B. M.; Grubbs, R. H. *J. Am. Chem. Soc.* **1988** *110*, 960. (b) Nguyen, S. T.; Johnson, L. K.; Grubbs, R. H. *J. Am. Chem. Soc.* **1992**, *114*, 3974. (c) Nguyen, S. T.; Grubbs, R. H. *J. Am. Chem. Soc.* **1993**, *115*, 9858. (d) Schwab, P.; France, M. B.; Ziller, J. W.; Grubbs, R. H. *Angew. Chem. Int. Ed.* **1995**, *34*, 2039. (e) Schwab, P.; Grubbs, R. H.; Ziller, J. W. *J. Am. Chem. Soc.* **1996**, *118*, 100. (f) Scholl, M.; Ding, S.; Lee, C. W.; Grubbs, R. H.

Org. Lett. **1999**, *1*, 953. (g) Trnka, T. M.; Grubbs, R. H. *Acc. Chem. Res*. **2001**, *34*, 18.

(3) (a) Schrock, R. R.; Murdzek, J. S.; Bazan, G, C.; Robibins, J.; DiMare, M.; O'Regan, M. *J. Am. Chem. Soc.* **1990**, *112*, 3875. (b) Bazan, G. C.; Oskam, J. H.; Cho, H.-N.; Park, L. Y.; Schrock, R. R. *J. Am. Chem. Soc.* **1991**, *113*, 6899. (c) Feldman, J.; Schrock, R. R. *Prog. Inorg, Chem.* **1991**, *39*, 1.

(4) For reviews, see: (a) Novak, B. M.; Risse, W.; Grubbs, R. H. *Adv. Polym. Sci.* **1992**, *102*, 47-72. (b) Grubbs, R. H.; Khosaravi, E. *Material Science and Technology*, **1999**, *20*, 65. c) Buchmeiser, M. R. *Chem. Rev*. **2000**, *100*, 1565.

(5) For reviews, see: (a) Gruubs, R. H.; Miller, S. J.; Fu, G. C. *Acc. Chem. Res.* **1995**, *28*, 446. (b) Deiters, A.; Martin, S. F. *Chem. Rev*. **2004**, *104*, 2199. (c) Schmidt, B.; Hermanns, J. *Curr. Org. Chem*. **2006**, *10*, 1363.

(6) For recent reviews, see: (a) Schuster, M.; Blechert, S. *Angew. Chem. Int. Ed*. **1997**, *36*, 2036. (b) Connon, S. J.; Blechert, S. *Angew. Chem. Int. Ed.* **2003**, *42*, 1900. (c) Grubbs, R. H. *Handbook of Metathesis*, 2nd ed.; Wiley-VCH: Weinheim, **2015**; Vols. 2, 3.

(7) (a) Novak, B. M.; Grubbs, R. H. *J. Am. Chem. Soc*. **1988**, *110*, 960. (b) Schrock, R. R. *Acc. Chem. Res*. **1990**, *23*, 158. (c) Bielawski, C. W.; Grubbs, R. H. *Angew. Chem., Int. Ed*. **2000**, *39*, 2903.

(8) (a) For a review on olefin metathesis cyclopolymerization, see: Choi, S.-K.; Gal, Y.-S.; Jin; S.-H.; Kim, H. K. *Chem. Rev.* **2000**, *100*, 1645. For examples of olefin metathesis cyclopolymerization, see: (b) Fox, H. H.; Wolf, M. O.; Odell, R.; Lin, B. L.; Schrock, R. R.; Wrington, M. S. *J. Am. Chem. Soc*. **1994**, *116*, 2827. (c) Anders, U.; Nuyken, O.; Buchmeiser, M. R.; Wurst, K. *Angew. Chem., Int. Ed*. **2002**, *41*, 4044. (d) Anders, U., Nuyken, O.; Buchmeiser, M. R.; Wurst, K. *Macromolecules* **2002**, *35*, 9029. (e) Mayershofer, M. G.; Nuyken, O.; Buchmeiser, M. R. *Macromolecules* **2006**, *39*, 3484. (f) Kang, E.-H.; Lee, I. S.; Choi, T.-L. *J. Am. Chem. Soc*. **2011**, *133*, 11904. (g) Kim, J.; Kang, E.-H.; Choi, T.-L. *ACS Macro Lett.* **2012**, *1*, 1090. (h) Kang, E.-H.; Lee, I.-H.; Choi, T.-L.

ACS Macro Lett. **2012**, *1*, 1098. (i) Lee, I. S.; Kang, E.-H.; Choi, T.-L. *Chem. Sci*. **2012**, *3*, 761. (j) Kang, E.-H.; Yu, S.-Y; Lee, I.-H.; Park S.-E.; Choi, T.-L. *J. Am. Chem. Soc.* **2014**, *136*, 10508.

(9) (a) Wagener, K. B.; Boncella, J. M.; Nel, J. G. *Macromolecules* **1991**, *24*, 2649. (b) Patton, J. T.; Boncella, J. M.; Wagener, K. B. *Macromolecules* **1992**, *25*, 3862. (c) Brzezinska, K.; Wolfe, P. S.; Watson, M. D.; Wagener, K. B. *Macromol. Chem. Phys.* **1996**, *197*, 2065. (d) Mutlu, H.; Montero de Espinosa, L.; Meier, M. A. R. *Chem. Soc. Rev.* **2011**, *40*, 1404.

(10) Choi, T.-L.; Rutenberg, I. M.; Grubbs, R. H. *Angew. Chem. Int. Ed*. **2002**, *41*, 3839.

(11) Ding, L.; Xie, M.; Yang, D.; Song, C. *Macromolecules* 2010, *43*, 10336.

(12) (a) Park, H.; Choi, T.-L. *J. Am. Chem. Soc.* **2012**, *134*, 7270. (b) Park, H.; Lee, H.-K; Choi, T.-L. *J. Am. Chem. Soc.* **2013**, *135*, 10769. (c) Park., H.; Kang, E.-H.; Müller., L.; Choi, T.-L. *J. Am. Chem. Soc.* **2016**, *138*, 2244.

(13) Gutekunst, W. R.; Hawker, C. J. *J. Am. Chem. Soc.* **2015**, *137*, 8038.

(14) Kang, C.; Park, H.; Lee, J.-K.; Choi, T.-L. *J. Am. Chem. Soc.* **2017***, 139,* 11309.

(15) (a) Lee, H.-K.; Bang, K.-T.; Hess, A.; Grubbs, R. H.; Choi, T.-L. *J. Am. Chem. Soc.* **2015**, *137*, 9262. (b) Lee, H.-K.; Choi, T.-L. *ACS Macro Lett.* **2018**, *7*, 531.

(16) (a) Kanaoka, S.; Grubbs, R. H. *Macromolecules* **1995**, 28, 4707. (b) Weck, M.; Schwab, P.; Grubbs, R. H. *Macromolecules* **1996**, 29, 1789.

Chapter 5:

Sequence Specific Olefin Metathesis Polymerization

5.1 Abstract

We proposed and developed a new strategy for the synthesis of sequence-specific polymers that employs two type of cascade metathesis. Central to this research is the development of newly designed monomer which combined with two-types of monomer which were used for cascade metathesis polymerization, directional synthesis of sequence-specific polymers.

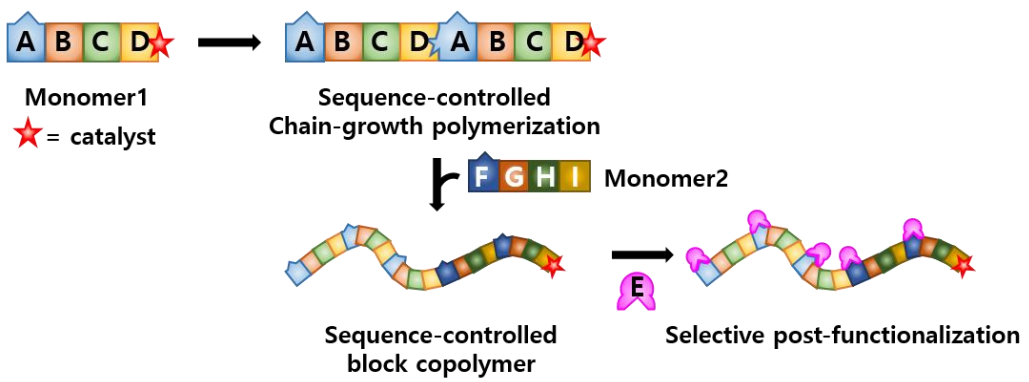

Figure 5.1. The concept of sequence-specific living polymerization

5.2 Introduction

Previously, we reported the selective tandem polymerization from monomers containing alkynes and cycloalkenes.[1] We found that monomer which has alkyne and cycloalkene was able to achieve living polymerization and the cascade processes always started from alkynes with alkyne selectivity.[1] Based on this previous results, we newly proposed that new monomer designs with more than two ring system. The second two ring system is originated from cascade polymerization using a monomer containing two cyclopentene moieties in its structure. These polymerization methods yielded well-defined polymers via a combination of ring-opening and ring-closing metathesis. Newly designed monomer, **M1** contains four repeating units, A-B-C-D, but the initial polymerization would always occur from the alkyne because of its alkyne-first selectivity with Grubbs 3rd generation catalyst. Because of thermodynamically and kinetically controlled cascade reactions, we are also

able to control how to start the polymerization and end up the polymerization. Following this assumption, sequence-specific polymerization (SSP) would be able to form a polymer in our desired pathway. More interestingly, the resulting polymers contain diene which can undergo post-modification by Diels-Alder reaction to put the fifth element of the SS P to give poly(ABCDE)$_n$ without any defects. (**Scheme 5.1**)

Using Grubbs ultra-fast initiating catalysts, Grubbs 3rd generation catalyst, we expect living polymerization with these monomers because there should be no chain-transfer reaction to disturb molecular weight distribution. To this living end of Ru carbene, we can add other monomers with a different sequence such as **M2** containing FGHI repeat unit. This would give us poly(ABCD)-*b*-poly(FGHI). (Scheme 2)

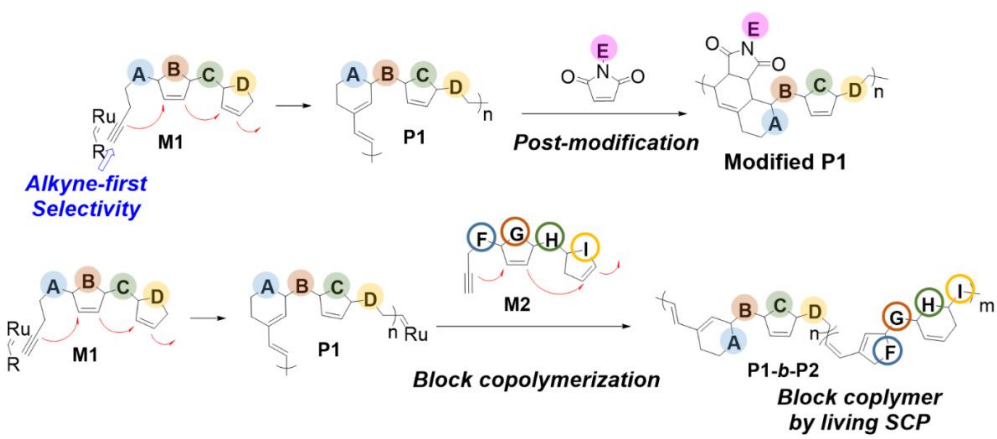

Scheme 5.1. Examples of the sequence-controlled living polymerization

Furthermore, we can control the length of the linkers in the monomers and this precisely controls the ring sizes on the products. This would not only give us the control of the functional group sequences, but also the sequence control on the ring sizes as well. Lastly, we can easily install oxygen and nitrogen in the monomers and resulting polymers should contain various well-defined heterocycles with precise ring sizes, which are often found in the natural products and synthetic drugs. Surely, to these unprecedented block copolymers, we can add dienophile E again to further flourish the richness of the SCP. These new

complex block copolymers can become interesting materials showing vastly different self-assembly and phase separation behaviors. Their polymer physics and nanostructures would attract many of scientists from other fields and bring fruitful collaboration opportunities.

5.3 Results & Discussion

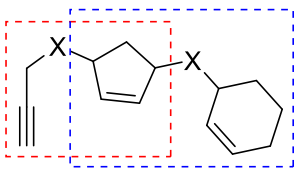

Chemically, this system consists of a combination of two cascade polymerization systems. The red part is tandem RO / RCM polymerization[1] and the blue part has a moiety of cascade RO / RCM polymerization[2]. Each system has an optimized reaction concentration. This is an important point in sequence specific polymerization. Each system has an optimized reaction concentration. This is an important point in polymer polymerization. In the case of tandem RO / RCM polymerization, polymerization is optimized under the condition of 0.3-0.05 M concentration. On the other hand, cascade RO / RCM polymerization is optimized for reaction at relatively high concentration. Therefore, it is necessary to investigate the progress of the reaction at the polymer concentration condition after the monomer synthesis. We synthesized two kinds of monomers through organic synthesis as follows.

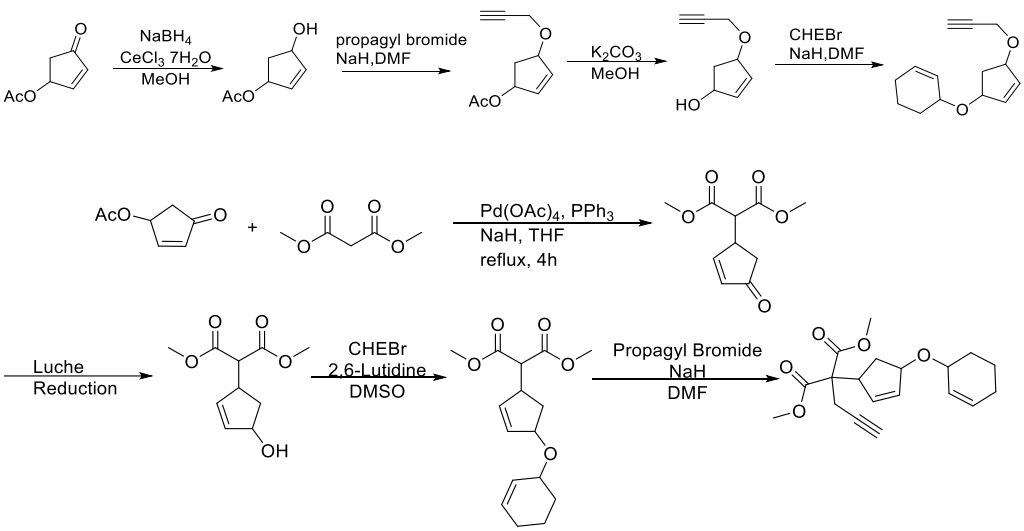

Scheme 5.2 Monomer synthesis for sequence specific metathesis polymerization

Sequence specific metathesis polymerization was carried out using the monomers completed by a series of simple organic syntheses as follows. The initial stage of this study was focused on what concentration and how it progressed.

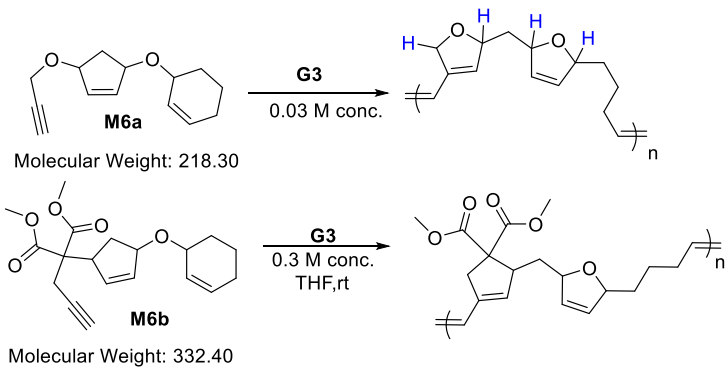

Scheme 5.3 Sequence specific metathesis polymerization using M6a, M6b

We could find the specific condition for this polymerization: the concentration optimized for the polymerization reaction follows the optimized concentration of the first red box. The monomer of the ether group is known to proceed well at a dilute concentration (0.03 M) and is optimized at a relatively high (0.3 M) for the malonate type. However, the reaction did not proceed under the cascade metathesis polymerization conditions (blue box).

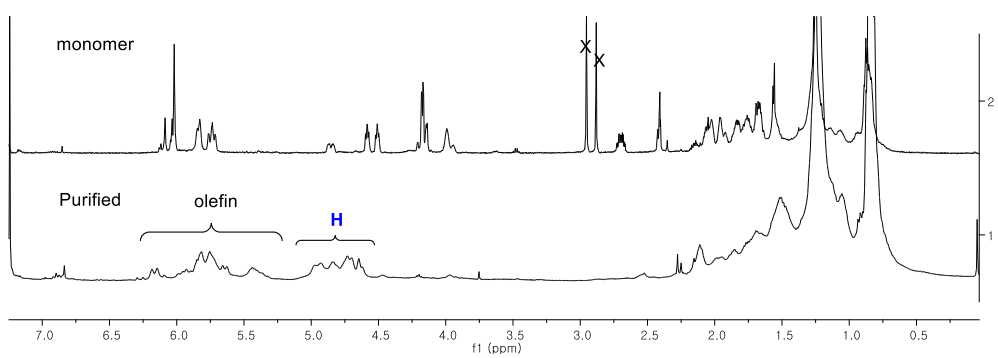

Figure 5.1 proton NMR of M6a and P6a

We obtained high conversion results through various reaction conditions and confirmed the change through NMR. It is possible to observe the change of the ether type monomer to the

polymer (**Figure 5.1**). However, it is difficult to assign easily due to the diastereomeric moieties. It is necessary to confirm the structural characteristics surely through the future research. In the case of the malonate type monomer, the conversion itself was able to proceed with a very high polymer reaction. Similarly, the complexity of the structure was inevitable due to the diastereomer. However, with the existing results, rough assignments were possible (**Figure 5.2**).

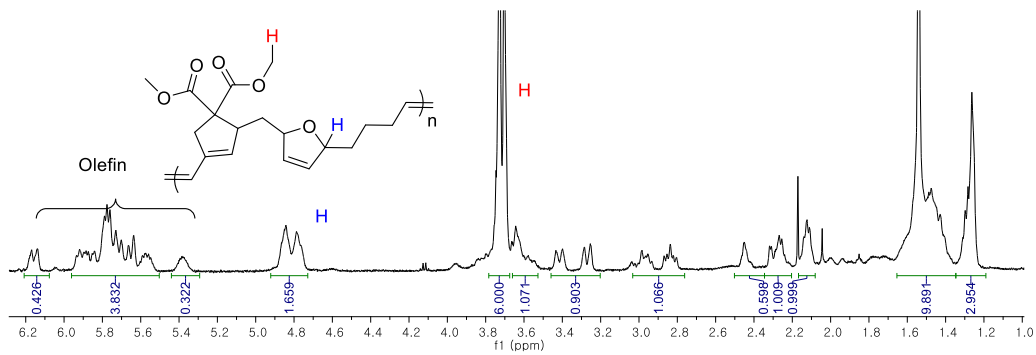

Figure 5.2 proton NMR of P6b

However, there is a problem that the molecular weight is too small to be a successful polymer in terms of the molecular weight of the polymer. In fact, when considering the molecular weight of the monomer, it may be an oligomer. (**Table5.1**) At low M: I ratio like 30:1, the conversion itself was high. Conversely, when the ratio was increased to about 100: 1, the conversion was also lowered. This means that the reactivity of the monomer itself is not excellent. Since it is predictable that the amide series monomer can have good reactivity as revealed in previous studies, it is a priority to complete the monomer of the new candidate.

Table 5.1 Polymerization results of M6a, M6b

Entry	Monomer	Monomer:cat, (Temp)	Conv. (%)	M_n (kDa)	PDI
1	**M6a**	50:1, rt	58.8	-	-
2	**M6a**	30:1, 0°C	98	0.74 k	1.18
3	**M6a**	100:1, 0°C	58	-	-
4	**M6b**	50:1, rt	98	-	-
5	**M6b**	30:1, 0	95	1.3	1.31
6	**M6b**	100:1, 0	45	-	-

5.5 Conclusion

In conclusion, we have combined sequence cascade polymerization with sequence cascade polymerization to complete sequence specific metathesis polymerization. At present, the lack of monomer candidates and high molecular weight are not enough for good polymerization system and these problems should be improved to get better results. However, we could predict the polymerization through the desired pathway. Through further research, we will finally establish a new system that can polymerize more complex but well-structured polymers.

5.6 Reference

(1) (a) Park, H.; Choi, T.-L. *J. Am. Chem. Soc.* **2012**, *134*, 7270. (b) Park, H.; Lee, H.-K; Choi, T.-L. *J. Am. Chem. Soc.* **2013**, *135*, 10769. (c) Park., H.; Kang, E.-H.; Müller., L.; Choi, T.-L. *J. Am. Chem. Soc.* **2016**, *138*, 2244.

(2) (a) Lee, H.-K.; Bang, K.-T.; Hess, A.; Grubbs, R. H.; Choi, T.-L. *J. Am. Chem. Soc.* **2015**, *137*, 9262. (b) Lee, H.-K.; Choi, T.-L. *ACS Macro Lett.* **2018**, *7*, 531.

국문 초록

올레핀 메타테시스 반응은 탄소간 이중결합의 위치를 변경하는 반응으로 이를 통해 다양한 종류의 유기화합물의 합성은 물론 고분자 중합에도 널리 사용되어왔다. 특히 작용기에 대해서 안정성이 높고 반응성 또한 우수한 루테늄 금속을 기반으로 한 그럽스 촉매가 개발되면서 올레핀 메타테시스 반응은 현대 유기화학에 있어 주요한 반응으로 손 꼽히게 된다. 이 논문에서는 이러한 메타테시스를 이용한 새로운 고분자 중합법의 개발에 대한 연구를 서술하였다. 이 연구는 두 개의 씨클로알켄을 가지고 있는 단량체를 이용하여 정교하면서도 잘 정립된 구조의 고분자를 성공적으로 중합할 수 있게끔 만들어 주었다.

제 1장에서는 메타테시스 반응과 메타테시스 고분자 반응에 대한 전반적인 개요를 살펴보았다.

제 2장에서는 두 개의 씨클로알켄을 가지고 있는 단량체의 단계적 연쇄 고리 열림/고리 닫음 메타테시스 중합에 대해서 서술하였다. 이 시스템은 일반적인 메타테시스를 이용한 중합보다는 복잡성과 정교함에 있어서 개선된 시스템이다. 일반적인 메타테시스 고분자 중합이 한번에 한 종류의 메타테시스를 사용할 수 밖에 없는 반면 우리는 이 방법을 통하여 매우 복잡하면서도 정교한 구조의 고분자를 2가지 종류의 메타테시스를 결합하여

중합 할 수 있었다.

3장에서는 2장에서 완성한 중합법이 일반적으로 알려진 2세대 이상 그럽스 촉매의 높은 반응성을 고려할 때 상대적으로 반응성이 낮은 그럽스 1세대 촉매가 이 시스템에서 가장 좋은 효율의 촉매인 이유를 명확히 설명할 수 없었다. 그래서 우리는 이 시스템에서만 관찰되는 그럽스 1세대 촉매에 대한 독특한 선택성에 대하여 설명하고자 본 시스템의 대표적인 이터 단량체와 다양한 그럽스 촉매를 이용한 단일 고분자 중합의 반응속도 실험와 더불어 대칭한 씨클로헵텐과의 경쟁 반응을 통한 반응속도 실험도 함께 실시하였다. 이 결과들을 토대로 그럽스 촉매의 서로 다른 리간드에 따라 발생하는 스터릭 효과의 차이가 단량체와 촉매 접근의 선택성 차이를 만들어 고분자 중합 반응경로의 진행에 영향을 준다는 것을 확인하였다. 이처럼 다른 세대의 Grubbs 촉매에 따라 달라지는 고분자 중합 반응 경로에 미치는 영향은 독특한 그럽스 촉매의 선호도가 왜 발생하는지 그리고 어떻게 고분자 중합의 효율에 영향을 주는가에 대한 메커니즘에 대한 통찰력을 얻을 수 있었다

4장에서는 멀티플 올레핀 메타테시스 중합에 대해서 서술하였다 앞서 이야기한 것과 같이 메타테시스를 이용한 중합은 총 3종류의 메타테시스 방법 중 2가지를 결합한 경우는 고분자 구조를 정교하게 만들기 어렵다는 점에서 매우 어려운 중합법이라 할 수 있다. 하지만 이 연구를 통해서 우리는

처음으로 모든 종류의 메타테시스 방법을 한번에 사용하여 정교한 구조의 고분자를 합성할 수 있는 고분자 중합법을 완성하였다. 완성된 고분자는 매우 정교한 교차블럭 공중합체를 성공적으로 완성하였다.

마지막 장에서는 순서 특정 올레핀 메타테시스 중합에 대해서 기술하였다. 기존에 연구된 알카인에 선택성을 가지고 있는 그럽스 3세대 촉매를 이용하여 2장에서 소개된 단량체와 결합하여 새로운 종류의 올레핀 중합법을 완성할 있었다. 새로운 형태의 단량체의 구조는 형성된 고분자에 다양한 순서를 포함할 수 있는 가능성을 가지고 있다.